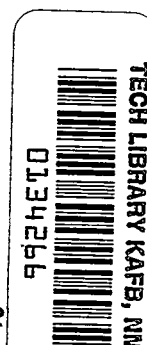NASA Technical Paper 1102

Longitudinal Aerodynamic Characteristics at Mach 0.60 to 2.86 of a Fighter Configuration With Strut Braced Wing

Samuel M. Dollyhigh, William J. Monta,
and Giuliana Sangiorgio

DECEMBER 1977

NASA

NASA Technical Paper 1102

Longitudinal Aerodynamic Characteristics at Mach 0.60 to 2.86 of a Fighter Configuration With Strut Braced Wing
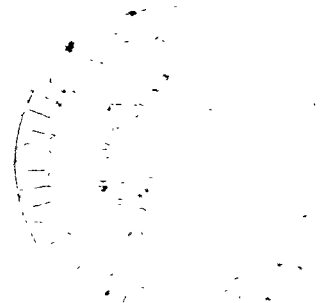
Samuel M. Dollyhigh, William J. Monta, and Giuliana Sangiorgio

Langley Research Center
Hampton, Virginia

NASA

National Aeronautics
and Space Administration

Scientific and Technical Information Office

1977

SUMMARY

An investigation has been made in the Mach number range from 0.60 to 2.86 to determine the effects on longitudinal aerodynamic characteristics of utilizing struts to brace the wing to allow the wing thickness to be reduced on the LFAX-8 fighter configuration. Structural and load analysis indicated that the maximum airfoil thickness could be reduced from 4.5 to 3.1 percent with the strut brace concept. Wave drag analysis indicated that reducing the wing maximum thickness on the LFAX-8 from 4.5 percent to 3.1 percent would yield a significant reduction in zero-lift wave drag of about 28 percent at the design Mach number of 1.60. Three strut arrangements were designed and tested: a single straight strut, a single swept strut, and a set of tandem straight struts. In addition, a wire of approximately the same cross-sectional area replaced the single straight strut on one series of runs. Also, the original LFAX-8 with the 4.5-percent-thick wing was retested to serve as a base line for this investigation.

Reducing the wing thickness increased subsonic drag and reduced transonic and supersonic drag as expected. The total zero-lift drag coefficient at Mach 1.60 was reduced by approximately 8 percent. Neither reducing the wing thickness nor adding struts changed the pitching-moment or lift-curve characteristics appreciably. Further, adding the single unswept strut had no effect on the horizontal tail control characteristics. The most advantageous of the strut arrangements in terms of drag at all test Mach numbers was, first, the single straight strut, followed by the single swept strut, and then the tandem struts. Zero-lift drag reductions at Mach 1.60 of approximately 6, 5, and 4 percent were achieved with the single unswept strut, single swept strut, and tandem struts, respectively. The tandem struts incurred a severe drag penalty at transonic speeds, probably because of adverse interference between them. Also, as expected, the cylindrical strut or wire with cross-sectional area approximately the same as the single straight strut had severe drag penalties across the test Mach number range.

INTRODUCTION

The National Aeronautics and Space Administration, in keeping with its charter to investigate innovative concepts with potential aerodynamic payoffs, has conducted a study of the aerodynamic trade-offs of incorporating a strut-braced thin wing on a supersonic fighter airplane concept. Preliminary structural and load analysis indicated that the

incorporation of strut braces would allow a reduction in maximum airfoil thickness ratio from 4.5 percent to 3.1 percent (a 31-percent reduction) for a contemporary fighter configuration. Subsequent wave drag estimates indicated that reducing wing thickness by 31 percent would reduce zero-lift wave drag about 28 percent at the design Mach number of 1.60. The configuration, designated LFAX-8, resulted from a previous NASA design study, and the results of the wind-tunnel test program on the model have been reported in references 1 and 2. The configuration employed a cranked-leading-edge wing to reduce the rearward aerodynamic-center shift with Mach number while providing good lift-drag characteristics at both subsonic and supersonic speeds. The wing had a camber surface designed to have minimum drag due to lift at the design lift coefficient of 0.10 at a Mach number of 1.60. The wing camber also provided a substantial positive pitching-moment increment at zero lift and thus lower trimmed drag at high lift coefficients. The original airfoil section was an NACA 65A004.5.

Three strut arrangements were designed and tested: a single straight strut, a single swept strut, and a set of tandem straight struts. In addition, the single straight strut was replaced by a wire of approximately equivalent cross-sectional area on a series of runs. Wind-tunnel tests of the LFAX-8 with the different strut arrangements were conducted over a Mach number range from 0.60 to 2.86. Also, the original LFAX-8 with the 4.5-percent-thick wing was retested to serve as a base line for this investigation. The results of the wind-tunnel tests along with a theoretical analysis of some of the supersonic data are reported herein.

SYMBOLS

The force and moment coefficients are referenced to the stability-axis system. The moment reference point is located at fuselage station (F.S.) 55.852 cm, which corresponds to 41 percent of $\bar{c}$.

A   aspect ratio

b   span, cm

c   aerodynamic chord, cm

$\bar{c}$ mean aerodynamic chord, cm

C_D drag coefficient, $\dfrac{\text{Drag}}{qS}$

2

$C_{D,b}$ base-drag coefficient, $\dfrac{\text{Base drag}}{qS}$

$C_{D,c}$ chamber-drag coefficient, $\dfrac{\text{Chamber drag}}{qS}$

$C_{D,i}$ internal-drag coefficient, $\dfrac{\text{Internal drag}}{qS}$

$C_{D,o}$ drag coefficient at zero lift

C_L lift coefficient, $\dfrac{\text{Lift}}{qS}$

C_m pitching-moment coefficient, $\dfrac{\text{Pitching moment}}{qS\bar{c}}$

L/D lift-drag ratio

M free-stream Mach number

q free-stream dynamic pressure, Pa

S reference area of wing including fuselage intercept, cm^2

t local wing thickness, cm

x distance along X axis, positive rearward from nose of fuselage

y distance along Y axis, positive left

z distance along Z axis, positive up

α angle of attack, deg

Γ dihedral angle, deg

$\Delta C_{D,o}$ $= \left(C_{D,o} \text{ of modified LFAX-8}\right) - \left(C_{D,o} \text{ of original LFAX-8}\right)$

δ_h horizontal-tail deflection angle, positive when trailing edge is down, deg

Λ leading-edge sweep angle, deg

DESCRIPTION OF THE MODEL

The model utilized for the strut-braced wing concept was the 0.047-scale model of the LFAX-8 which was reported in references 1 and 2. A three-view drawing of the complete model configuration with single unswept strut is shown in figure 1(a) and details of the wing, horizontal tail, vertical tail, ventral fin, and struts are shown in figures 1(b) to 1(g). Some geometric characteristics are given in table I. A photograph of the model with the single unswept strut is shown in figure 2. The configuration incorporates a fuselage; a cranked-leading-edge wing with horizontal-ramp-type inlets located ahead of the wing; twin horizontal tails, twin vertical tails, and twin ventral fins mounted on booms; and lateral strakes on the forebody. Four strut arrangements were tested in the configuration.

The wing planform had a cranked leading edge; the inboard section had a leading-edge sweep angle of 56.5^O; and the outboard section had a sweep angle of 37°. The original airfoil section was an NACA 65A004.5, with the thickness distributed about the theoretical camber surface. The second wing had the original thickness distribution scaled by 0.6889 to give a maximum thickness of 3.1 percent. Both wings were designed to have minimum drag due to lift at a design lift coefficient of 0.10 at a Mach number of 1.60. Camber surface ordinates for both wings are presented in table II.

The configuration employed low twin horizontal tails with an airfoil section that was 4 percent biconvex. The horizontal tails had a negative dihedral angle of 8.7^O and could be deflected. The twin vertical tails were canted inboard at an angle of 12° with respect to the vertical and had an airfoil section that was 3.5 percent half-biconvex with the flat side outboard. The ventral fins were made from a 0.318-cm-thick flat plate with a beveled-edge total angle of 30°. The forebody strakes were 12.50 cm long and 0.48 cm wide and were made from 0.16-cm-thick flat plate with a beveled-edge total angle of 20°. The single struts (fig. 1(g)) had chords normal to the leading edge of 1.280 cm and were made from a 0.051-cm-thick flat plate. The tandem struts had chords of 1.016 cm and were made from 0.041-cm-thick flat plate. Both single and tandem struts had beveled-edge total angles of 30°. A wire with a 0.248-cm diameter was also tested in place of the single unswept strut. Small pod-type fairings that would be necessary to carry the loads on the airplane were simulated on the fuselage and wing at the strut juncture.

TESTS AND CORRECTIONS

The tests were conducted in the Langley 8-foot transonic pressure tunnel and the Langley Unitary Plan wind tunnel at Mach numbers 0.60 to 2.86. The conditions under which the tests were conducted are as follows:

Mach number	Reynolds number per meter	Stagnation pressure, kPa	Stagnation temperature, K
0.60	10.30×10^6	100.55	322
.80	10.50	86.18	
.90	11.06	86.18	
.95	11.25	86.18	
.98	11.19	86.18	
1.20	11.74	86.18	
1.60	6.56	54.63	339
2.00	6.56	63.54	
2.50	6.56	81.30	
2.86	6.56	98.44	

The dew points were maintained sufficiently low to prevent measurable condensation effects in the test sections. The angle-of-attack range was from approximately -6° to 20°. In order to assure boundary-layer transition to turbulent conditions at Mach numbers from 0.60 to 1.20, 0.0160-cm-wide transition strips of No. 90 carborundum grit were placed on the body 3.05 cm aft of the nose and strips of No. 100 carborundum grit were placed 1.02 cm streamwise on the wings, tails, ventral fins, inlet ramps, and external ramps. For the Mach number range from 1.60 to 2.86, the strips were changed to No. 50 carborundum grit at the same locations. The method of reference 3 was used to determine transition-strip size and location. Aerodynamic forces and moments on the model were measured by means of a six-component strain-gage balance which was housed within the model. The balance was attached to a 3.49-cm-diameter sting which in turn was rigidly fastened to the tunnel support system. Balance-chamber pressures were measured by means of pressure tubes located in the vicinity of the balance. The internal flow correction utilized data from reference 1 which were obtained by means of a rake in each duct consisting of 13 total-pressure tubes and 5 static-pressure tubes; the rakes were placed 0.25 cm ahead of the exit plane of the ducts. The base pressure was measured by means of two pressure tubes which were fastened to the sting and held approximately 0.16 cm from the base of the model. No internal-flow pressure rakes were installed for the present investigation. The drag data presented herein have been adjusted to the condition of free-stream static pressure at the model base and in the balance chamber. Figures 3 to 5 show the coefficients of base, chamber, and internal drag which were used to correct the drag data. Values of internal and base drag for Mach numbers from 1.60 to 2.86 are different from those used previously to correct the drag data in references 1 and 2. Those values in references 1 and 2 contained an error in data reduction which resulted in corrections to the data which were 47 percent too

large. The data were corrected for this report. Corrections to the model angles of attack have been made for both tunnel-airflow misalinement and deflection of the balance and sting under load.

PRESENTATION OF RESULTS

The results of this investigation are presented in the following figures:

DISCUSSION OF RESULTS

The effects on longitudinal aerodynamic characteristics of reducing the wing maximum thickness from 4.5 percent to 3.1 percent for the LFAX-8 wind-tunnel model are shown in figure 6. References 1 and 2 report the results of wind-tunnel test programs on the original LFAX-8 with the 4.5-percent-thick wing. Reducing the wing thickness has negligible effect on pitching-moment and lift-curve characteristics throughout the Mach number and angle-of-attack range of the tests. As would be expected, the thinner wing had higher drag coefficients and a lower maximum lift-drag ratio over the subsonic speed range. Reducing the wing maximum thickness decreases the leading-edge radius which in turn results in a loss of leading-edge suction. However, starting at Mach 0.95 and for the supersonic speed regime, supersonic flow and the resulting wave drag dominate, and reducing the wing thickness reduces the wave drag. Theoretical calculations indicated that at the design Mach number of 1.60, reducing wing thickness would provide a 28-percent reduction in wave drag which resulted in an experimentally realized 8-percent reduction in zero-lift drag coefficient.

Since the reduction of wing thickness was brought about by utilizing a strut, figures 7 to 11 present the effects of adding various strut arrangements to the configuration

with the thinner wing. Figure 7 shows the effects on longitudinal aerodynamic characteristics of adding a single unswept strut of 4 percent maximum thickness. The strut has negligible effect on pitching-moment and lift-curve characteristics. Drag effects are practically nil at subsonic speeds, and at transonic and supersonic speeds a small drag penalty is incurred by adding the strut. The zero-lift drag penalty is less than 2 percent at Mach 1.60. The effect of the strut on the horizontal tail control characteristics is presented in figure 8. There are no observable differences in the control characteristics of the configuration with and without the strut.

Figure 9 shows the effect on longitudinal aerodynamic characteristics of a single strut of 4 percent maximum thickness swept back at an angle of 20°. The same comments about insignificant increments in pitching moments and lift curves still apply. However, the swept strut has more wetted area and produces a little greater drag across the test Mach number range. The zero-lift drag penalty increases to approximately 3 percent at Mach 1.60. In addition to the single strut on each side, tandem struts were investigated. The tandem strut arrangement relieves chordwise bending moments as well as spanwise bending moments. Figure 10 shows the effects of adding tandem struts, which also had a maximum thickness of 4 percent but with reduced chord length. Again there are no significant effects on the pitching-moment or lift curves. The drag increase is more severe than that associated with the increase in wetted area of the tandem struts, particularly at transonic speeds where evidently there is adverse interference between the struts. Zero-lift drag coefficient increases approximately 5 percent at Mach 1.60.

As a check case, a cylindrical strut (wire) of equivalent cross-sectional area was tested in place of the single unswept strut and the data are presented in figure 11. The cylindrical strut did have some small effects on pitching-moment and lift-curve characteristics. However, as expected, the cylindrical strut had severe drag penalties across the test Mach number range. The zero-lift drag penalty at Mach 1.60 was approximately 12 percent, which resulted in the configuration with thin wing and cylindrical strut having more drag than the original LFAX-8 with the 4.5-percent-thick wing.

A summary comparison of experimental zero-lift drag coefficient increments attributable to modifications of the original LFAX-8 configuration is shown in figure 12.

Figure 13 shows theoretical and experimental zero-lift drag increments at supersonic speeds attributable to modification of the original LFAX-8 configuration. The theoretical drag increment is composed of a wave drag increment and a skin friction increment calculated by methods of references 4 and 5, respectively. The theoretical and experimental increments due to reducing the wing thickness are in excellent agreement at the two lower Mach numbers, but agreement falls off at Mach 2.5 as the wave drag calculation methods start to violate the assumptions of linear theory for a configuration with low fineness ratio. Agreement is still excellent for the configuration with

single unswept strut but becomes only fair when the single strut is swept. The agreement between theory and experiment is poor for the tandem struts. This poor agreement is not surprising since the theory does not account for interference between the struts.

CONCLUDING REMARKS

An investigation has been made in the Mach number range from 0.60 to 2.86 to determine the effects on longitudinal aerodynamic characteristics of utilizing struts to brace the wing to allow the wing thickness to be reduced on the LFAX-8 fighter configuration. Structural and load analysis indicated that the maximum airfoil thickness could be reduced from 4.5 to 3.1 percent with the strut brace concept. Wave drag theory indicated that reducing the wing thickness on the LFAX-8 from 4.5 percent to 3.1 percent would yield a significant reduction in zero-lift wave drag of 28 percent at the design Mach number of 1.60. Three strut arrangements were designed and tested: a single straight strut, a single swept strut, and a set of tandem straight struts. In addition, a wire of approximately the same cross-sectional area replaced the single straight strut on one series of runs. The original LFAX-8 with the 4.5-percent-thick wing was retested to serve as a base line for this investigation.

Reducing the wing thickness increased subsonic drag and reduced transonic and supersonic drag as expected. The total zero-lift drag coefficient at Mach 1.60 was reduced by approximately 8 percent. Neither reducing the wing thickness nor adding struts changed the pitching-moment or lift-curve characteristics appreciably. Further, adding the single unswept strut had no effect on the horizontal tail control characteristics. The most advantageous of the strut arrangements in terms of drag at all test Mach numbers was the, first, single straight strut, followed by the single swept strut, and then the tandem struts. Zero-lift drag reductions at Mach 1.60 of approximately 6, 5, and 4 percent were achieved with the single unswept strut, single swept strut, and tandem struts, respectively. The tandem struts incurred a severe drag penalty at transonic speeds, probably because of adverse interference between them. Also, as expected, the cylindrical strut with cross-sectional area approximately the same as the single straight strut had severe drag penalties across the test Mach number range.

Langley Research Center
National Aeronautics and Space Administration
Hampton, VA 23665
November 2, 1977

REFERENCES

1. Dollyhigh, Samuel M.; and Hallissy, James B.: Longitudinal Stability and Control Characteristics at Mach 0.30 to 2.86 of a Fighter Configuration With a Cranked-Leading-Edge Wing Planform. NASA TM X-3039, 1974.

2. Dollyhigh, Samuel M.: Stability and Control Characteristics of a Fighter Configuration With a Cranked-Leading-Edge Wing Planform at Mach Numbers 1.60 to 2.86. NASA TM X-2695, 1973.

3. Braslow, Albert L.; Hicks, Raymond M.; and Harris, Roy V., Jr.: Use of Grit-Type Boundary-Layer-Transition Trips on Wind-Tunnel Models. Conference on Aircraft Aerodynamics, NASA SP-124, 1966, pp. 19-36. (Also available as NASA TN D-3579.)

4. Harris, Roy V., Jr.: An Analysis and Correlation of Aircraft Wave Drag. NASA TM X-947, 1964.

5. Sommer, Simon C.; and Short, Barbara J.: Free-Flight Measurements of Turbulent-Boundary-Layer Skin Friction in the Presence of Severe Aerodynamic Heating at Mach Numbers From 2.8 to 7.0. NACA TN 3391, 1955.

TABLE I.- GEOMETRIC CHARACTERISTICS

(a) Component geometry

Wing:

A 2.64

Λ, deg . . . . 56.5 and 37

$\bar{c}$, cm 28.913

b, cm 62.453

S, including fuselage intercept, cm^2 . . . . 1476.784

Airfoil section distributed about theoretical camber . . . . NACA 65A004.5

Horizontal tail (exposed):

A 2.418

Λ, deg 42

Γ, deg . . . . -8.7

$\bar{c}$, cm 12.502

Span, cm 28.875

Area, cm^2 . . . . 344.780

Airfoil section . . . . 4% biconvex

Vertical tail (each):

A 0.862

Λ, deg 57

$\bar{c}$, cm 12.621

Span, cm 9.652

Area, cm^2 . . . . 108.032

Airfoil section . . . . 3.5% half-biconvex

Cant-in, deg 12

Inlet area (one duct), cm^2 . . . . 11.613

Exit area (one duct), cm^2 . . . . 17.039

Chamber area, cm^2 . . . . 15.619

Base area (excluding chamber and exit areas), cm^2 . . . . 9.213

(b) Wetted areas and reference lengths

Component	Wetted area, cm^2	Reference length, cm
Wing	1768.990	28.913
Fuselage	2975.065	96.520
Vertical tails	425.193	12.621
Horizontal tails	694.734	12.502
Ventral fins	122.980	12.443

TABLE II.- CAMBER SURFACE ORDINATES FOR WINGS

x/c, percent	$\Delta z/c$, percent from leading edge, at —								
	$\frac{y}{b/2} = 0.236$	$\frac{y}{b/2} = 0.300$	$\frac{y}{b/2} = 0.500$	$\frac{y}{b/2} = 0.600$	$\frac{y}{b/2} = 0.645$	$\frac{y}{b/2} = 0.750$	$\frac{y}{b/2} = 0.850$	$\frac{y}{b/2} = 0.950$	$\frac{y}{b/2} = 1.000$
0	0	0	0	0	0	0	0	0	0
.5	0	.004	.016	.029	.010	-.017	-.019	-.023	-.017
2.5	0	.009	.082	.122	.048	-.094	-.091	-.132	-.095
5.0	-.004	.015	.131	.182	.087	-.184	-.185	-.233	-.229
10.0	-.039	.015	.153	.224	.135	-.295	-.361	-.428	-.402
20.0	-.271	-.152	.120	.241	.193	-.446	-.671	-.723	-.624
30.0	-.595	-.411	-.022	.171	.203	-.593	-.934	-1.021	-.791
40.0	-.962	-.746	-.175	.076	.193	-.719	-1.123	-1.327	-.900
50.0	-1.346	-1.050	-.350	-.048	.116	-.852	-1.325	-1.620	-.974
60.0	-1.698	-1.340	-.591	-.179	-.048	-.988	-1.506	-1.935	-1.033
80.0	-2.449	-1.979	-1.050	-.467	-.434	-1.254	-1.837	-2.626	-1.009
100.0	-3.146	-2.618	-1.510	-.761	-.579	-1.508	-2.172	-3.505	-.905

25.438

13.853

F. S. 96. 520

F. S. 55. 852

F. S. 0

1.250   12.497

Moment reference center
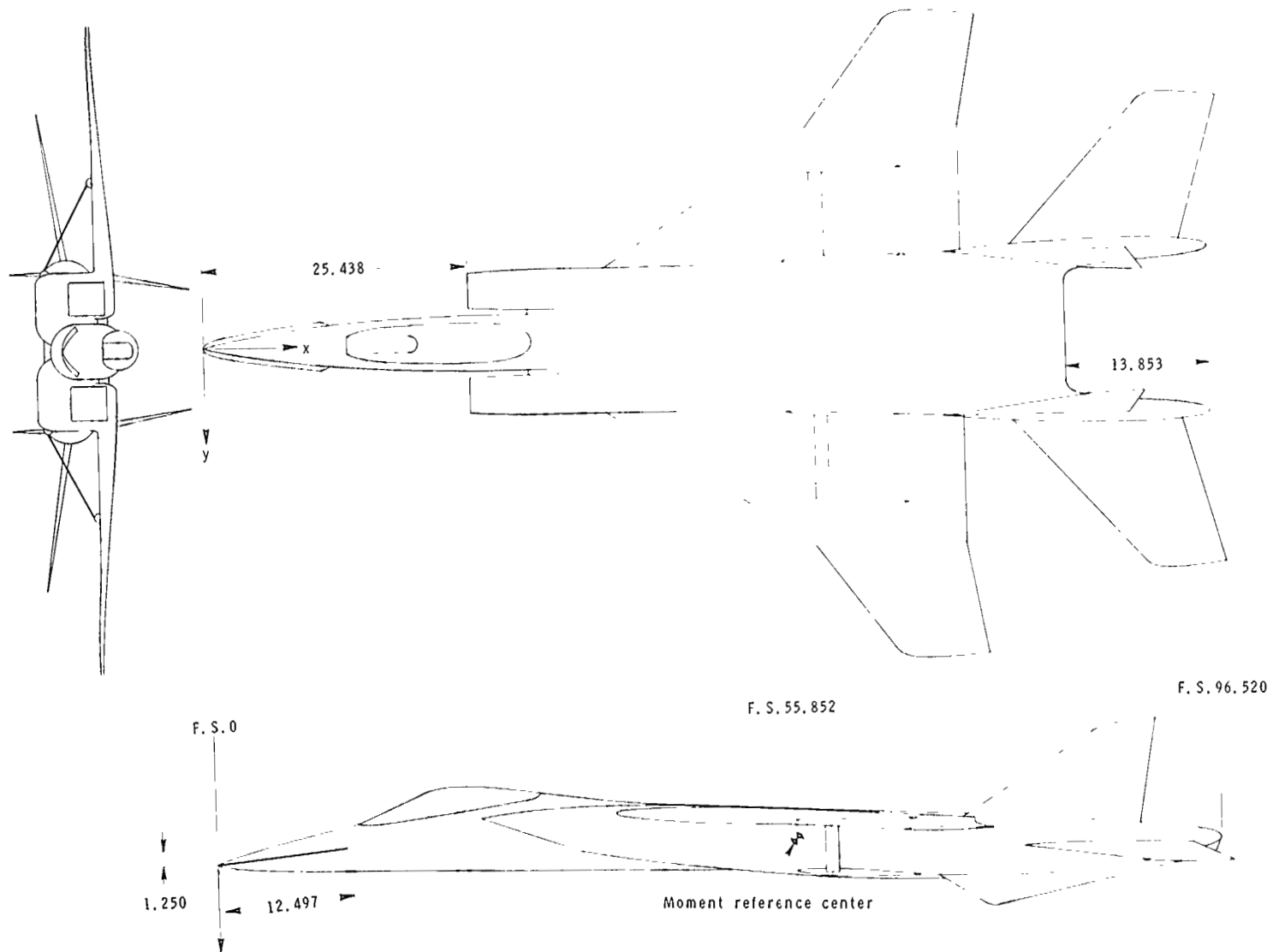
(a) Complete model with single unswept struts.

Figure 1.- Model drawings.   All dimensions are in centimeters, except as noted.

(b) Wing.

Figure 1.- Continued.

F. S. 77.432

Model ℄

8.412

16.429

42°

14.437

3°

13.050

7.452
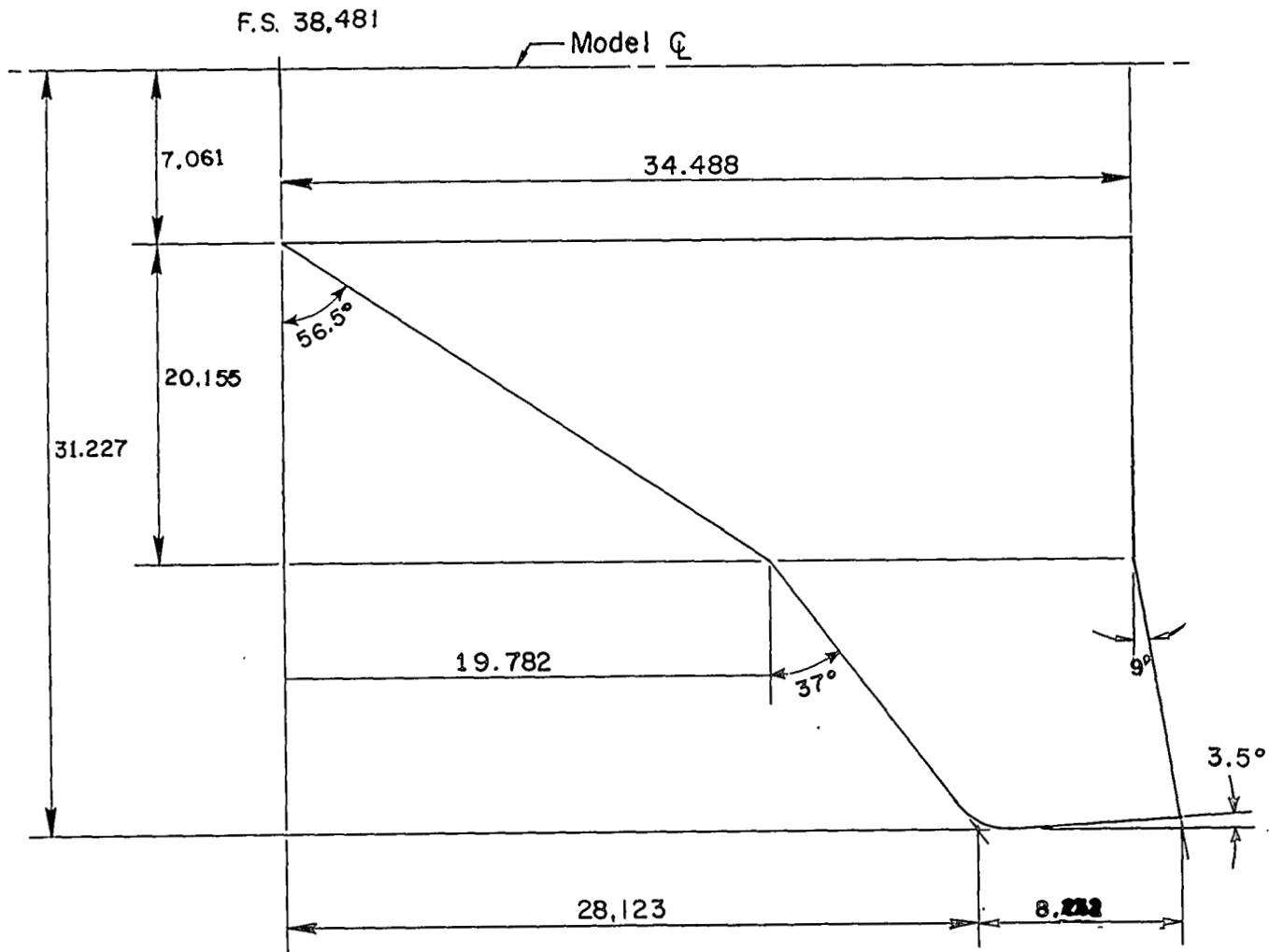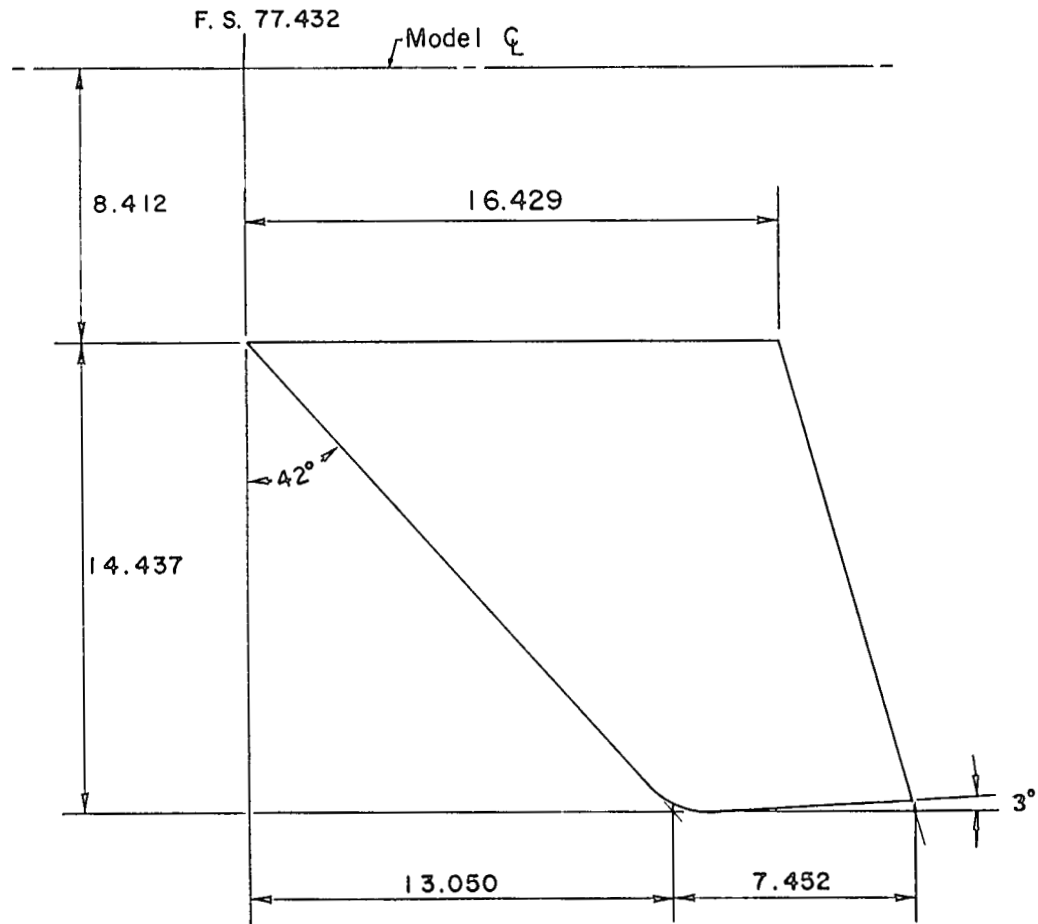
(c) Horizontal tail.

Figure 1.- Continued.
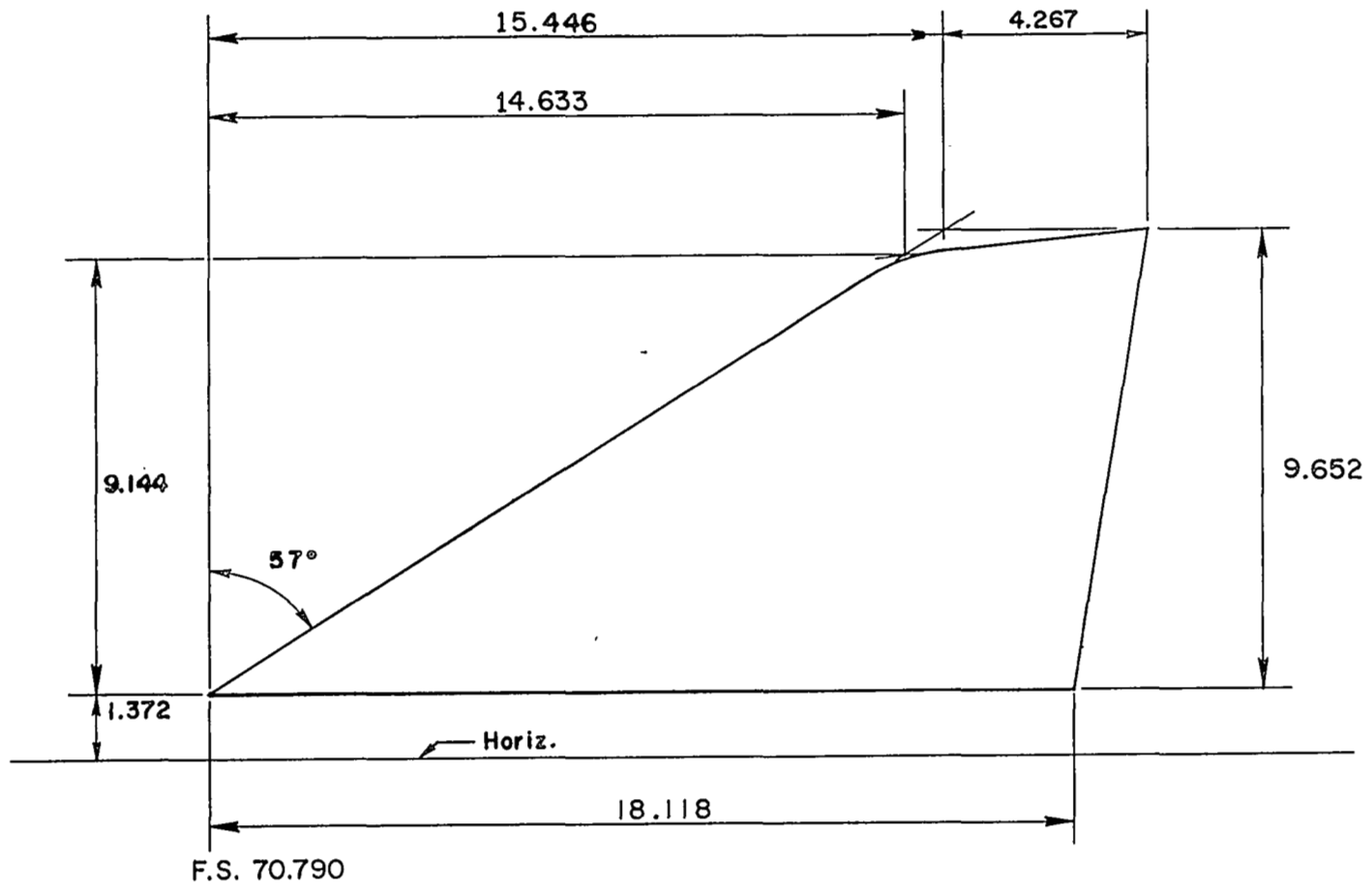
(d) Vertical tail.

Figure 1.- Continued.

27.231

Horizontal ref. line

1.046

1.194

3.810

3.038

4.862

21.681

F.S. 69.215
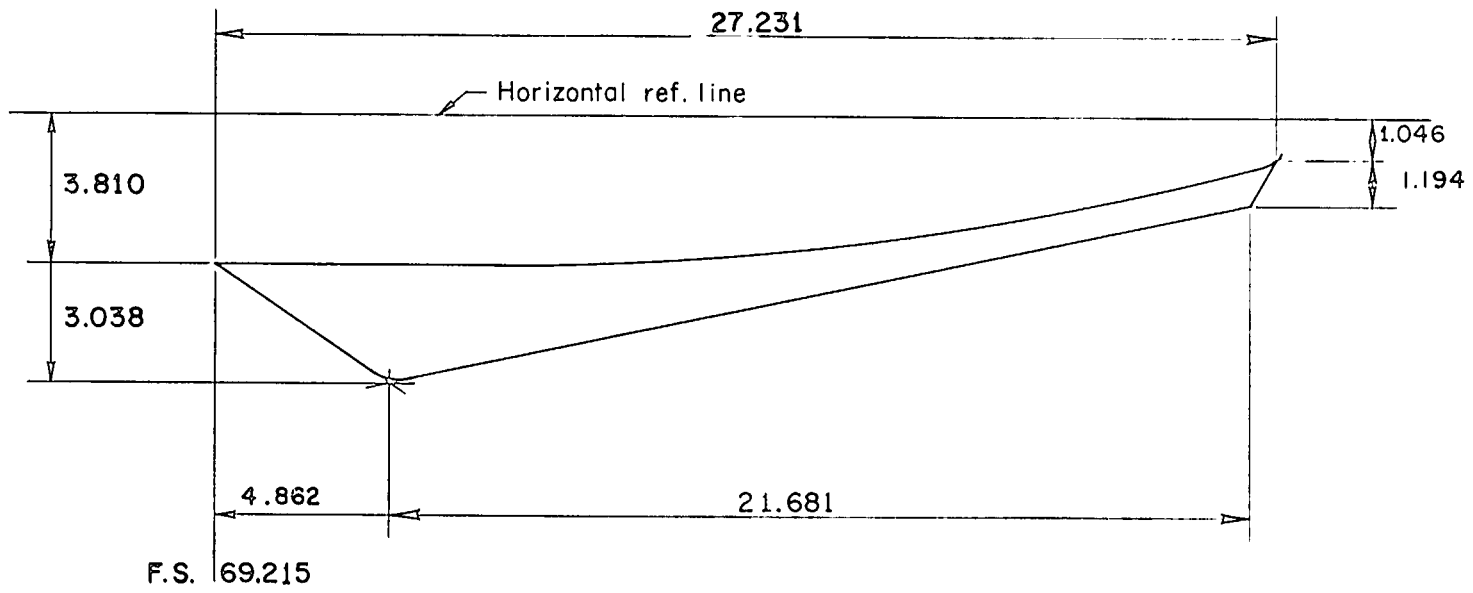
(e) Ventral fin.

Figure 1.- Continued.

Sta. 55.63   Sta. 58.93   Sta. 66.80

4.09

8.31

Single unswept   Tandem
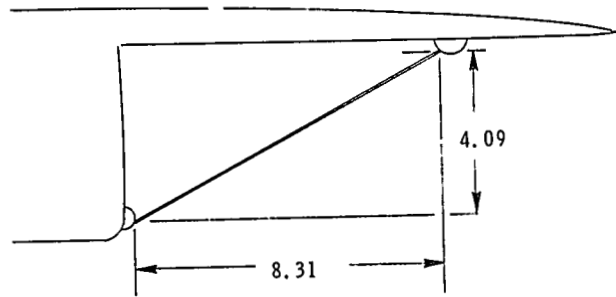
Unswept and tandem struts

Sta. 55.63   Sta. 58.93

Sta. 52.14   Sta. 55.44
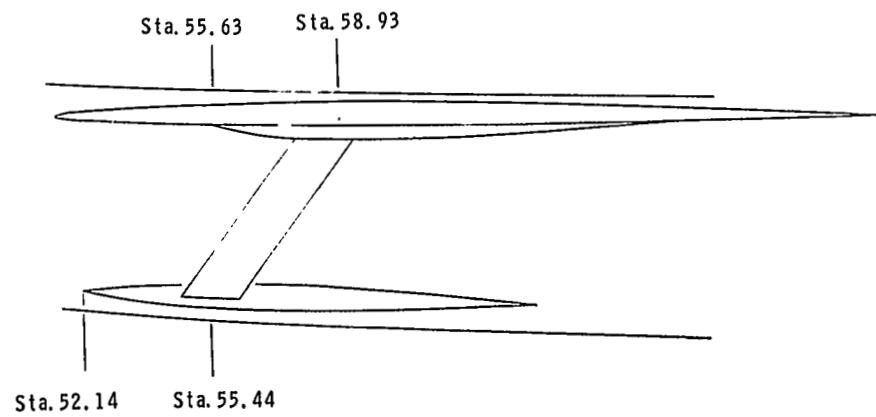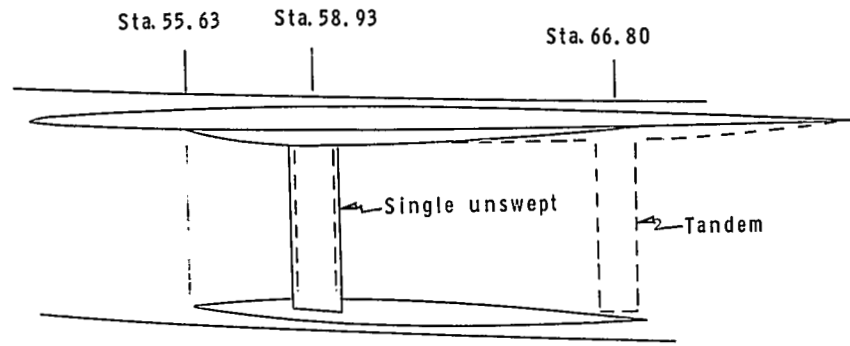
Swept strut

(f) Strut configuration.

Figure 1.- Continued.

20°

t

20°

Struts	c	t
Single	1.28	.051
Tandem	1.02	.041

9.25

c

.61

3.30

11.79

Fuselage fairing

30°

.051

30°

18.1°

9.80

1.28

Swept struts

.86

3.30

11.79

Small wing fairing

9.25

Circular struts

.248 diam.

.86

.86

3.30

17.27

6.10

Large wing fairing
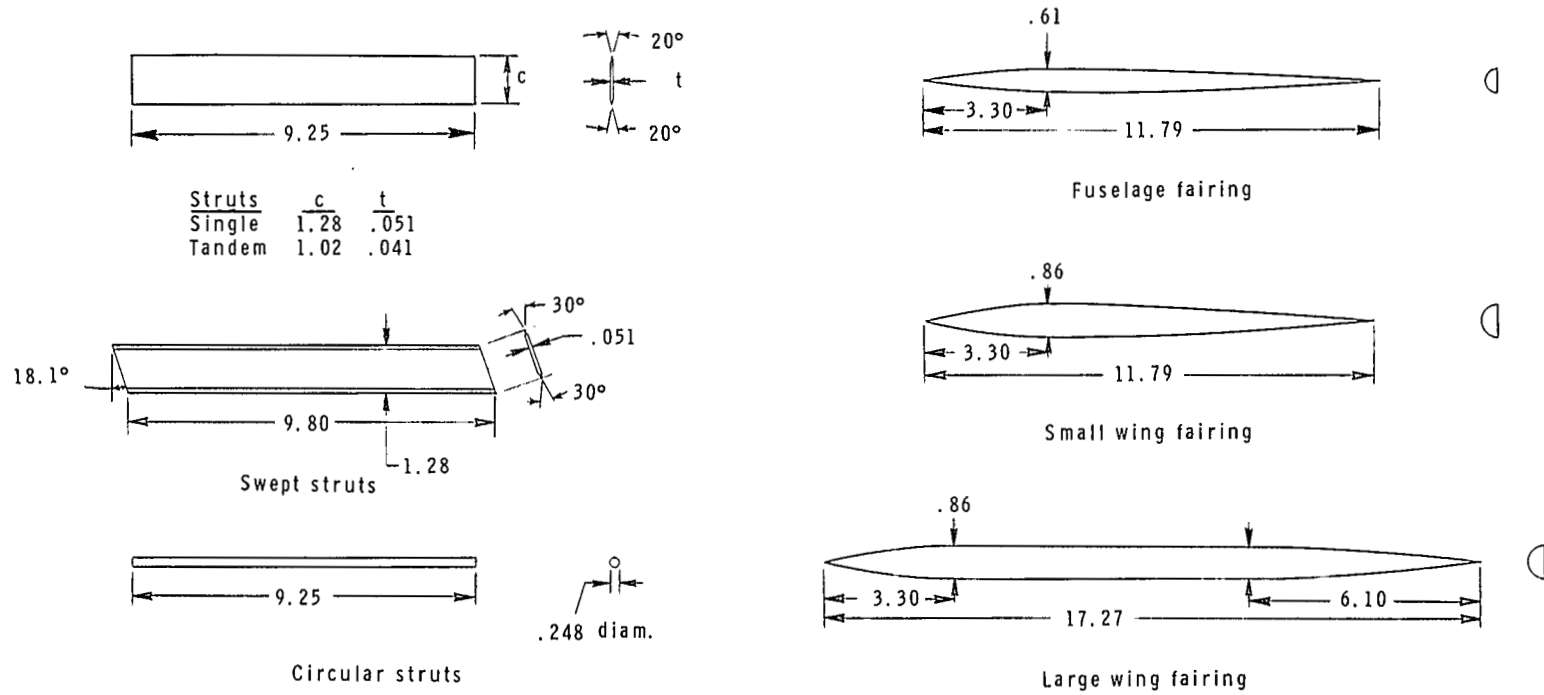
(g) Struts and fairings.

Figure 1.- Concluded.

L-77-1005

Figure 2.- The LFAX-8 model with single unswept strut configuration.
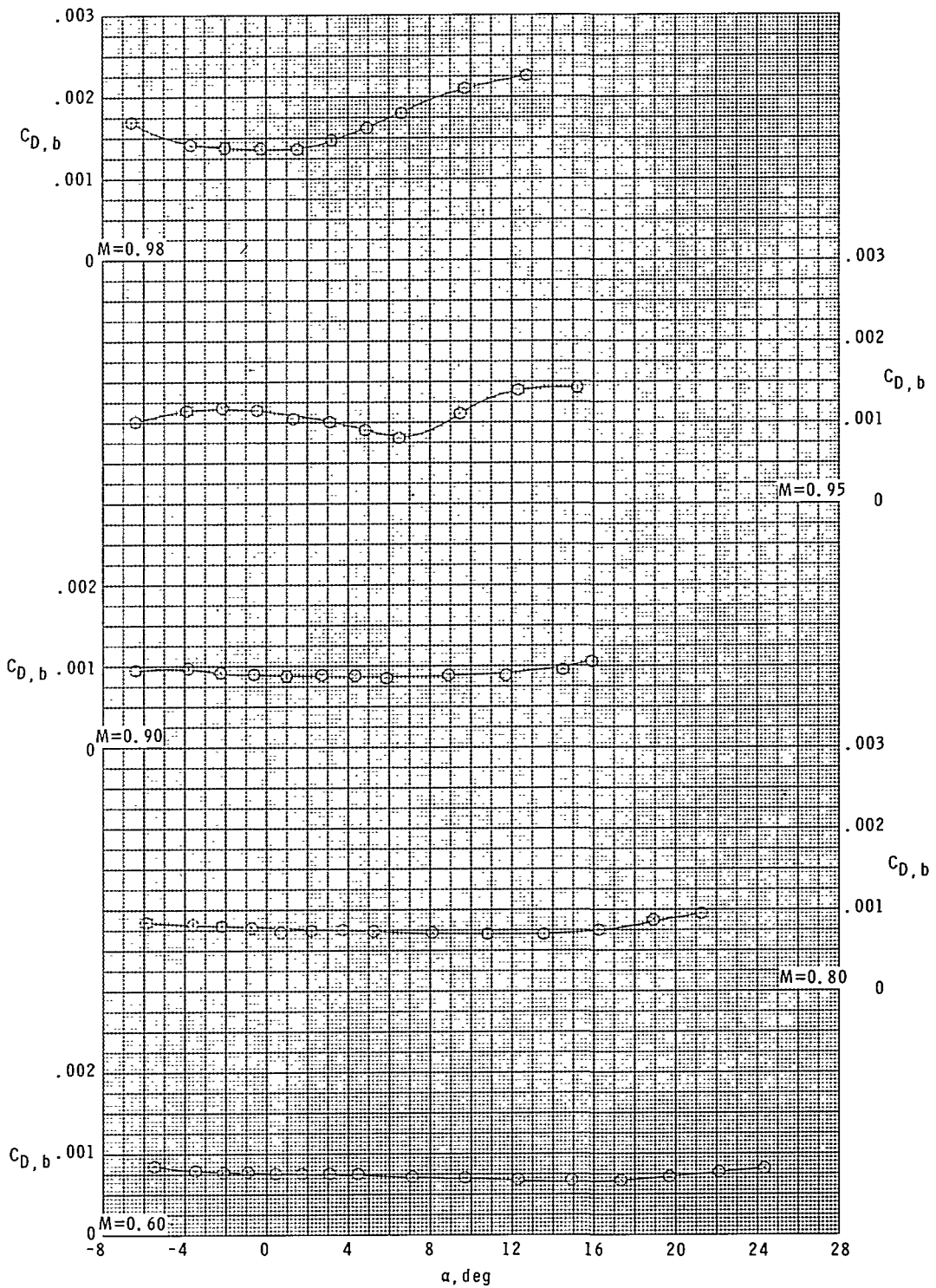
Figure 3.- Base-drag coefficient.
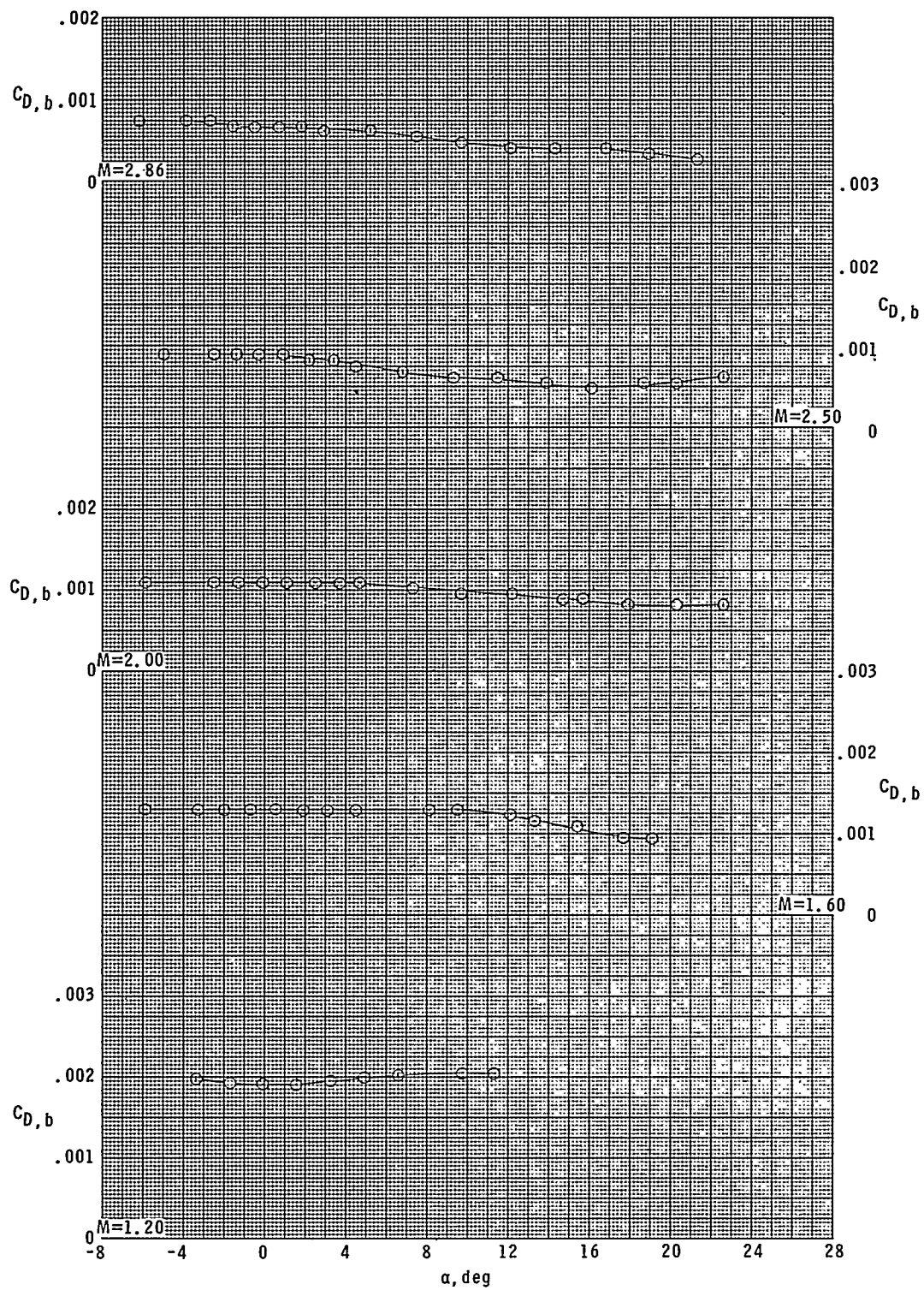
Figure 3.- Concluded.
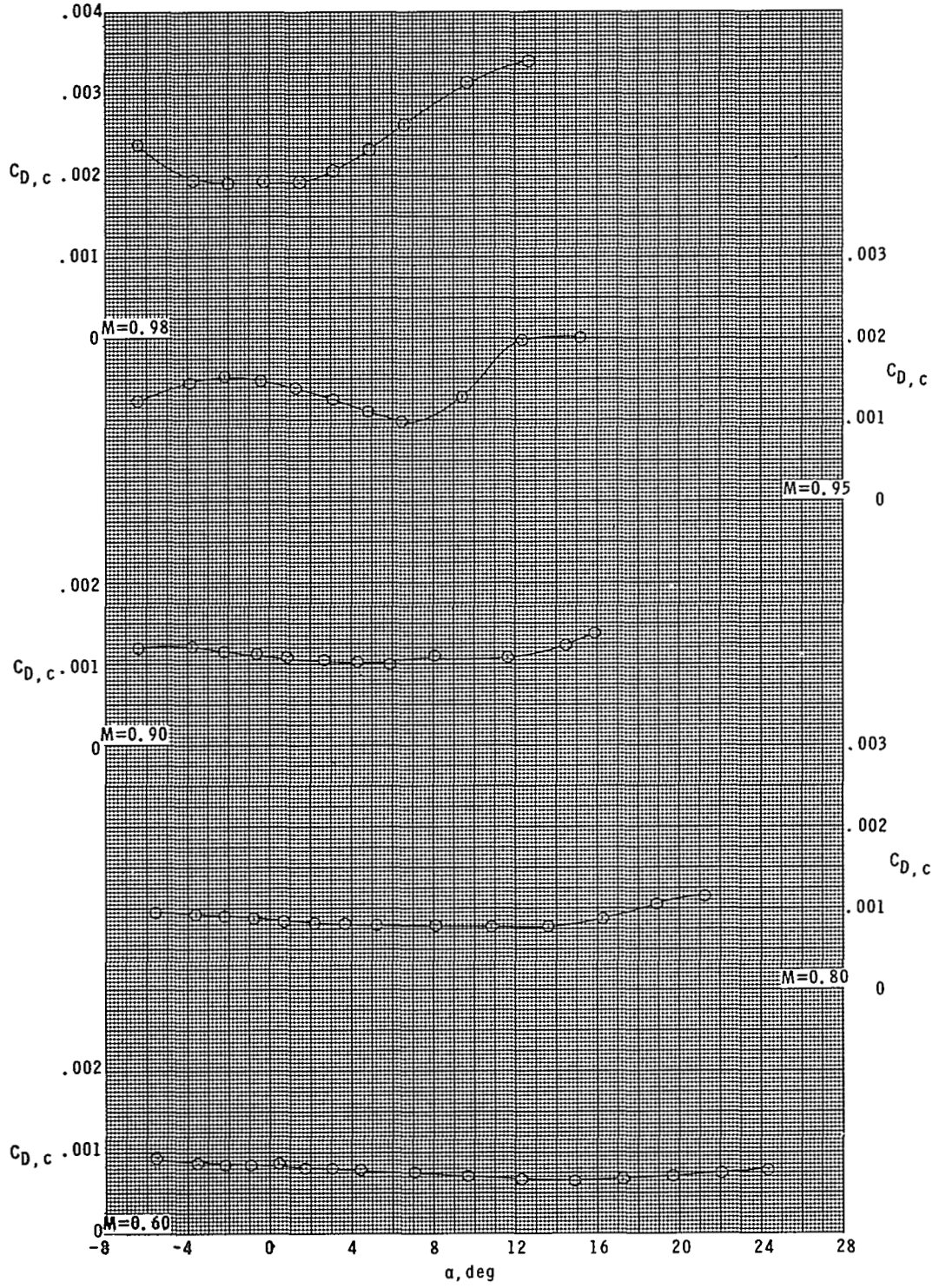
Figure 4.- Chamber-drag coefficient.
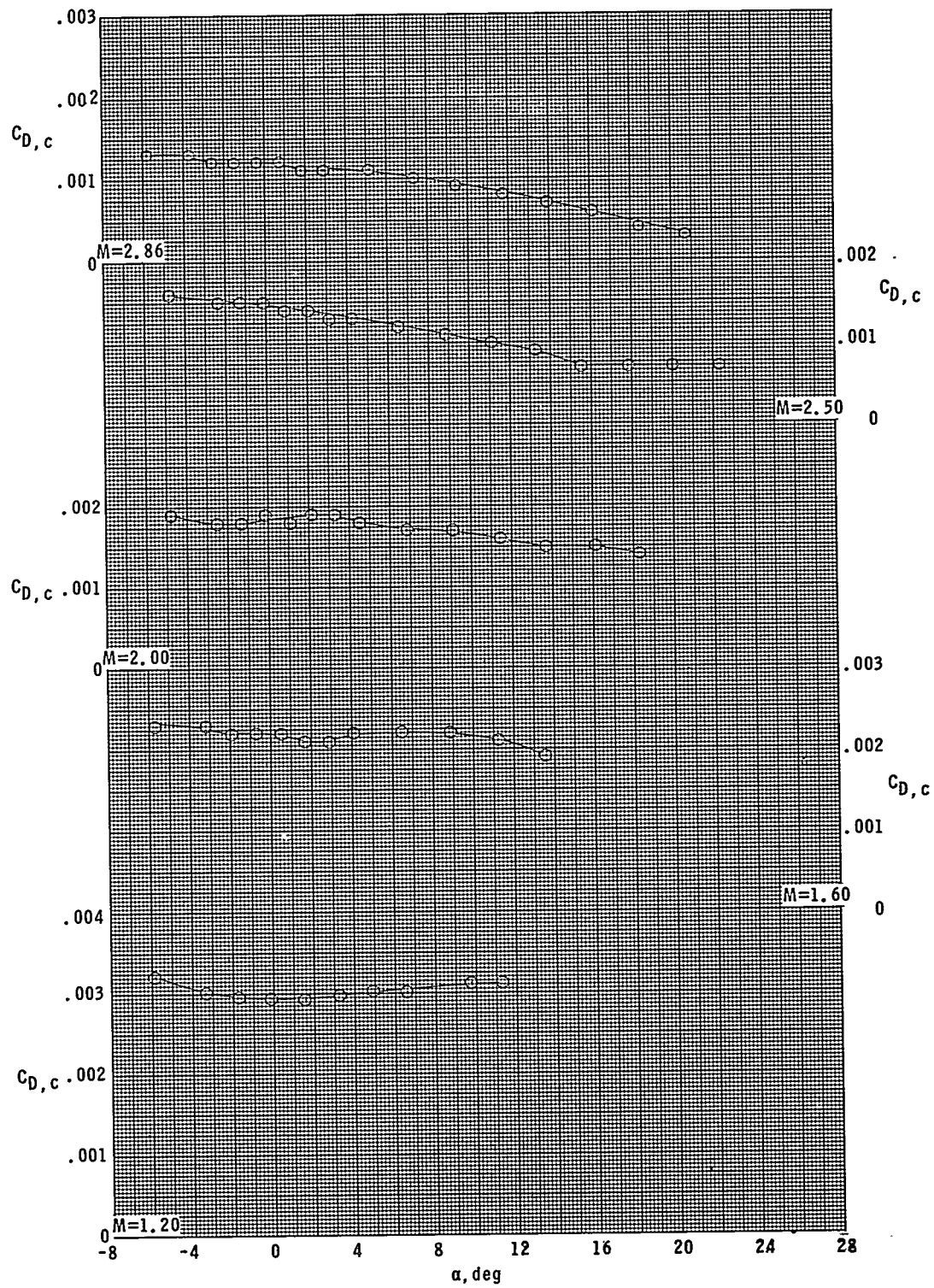
Figure 4.- Concluded.
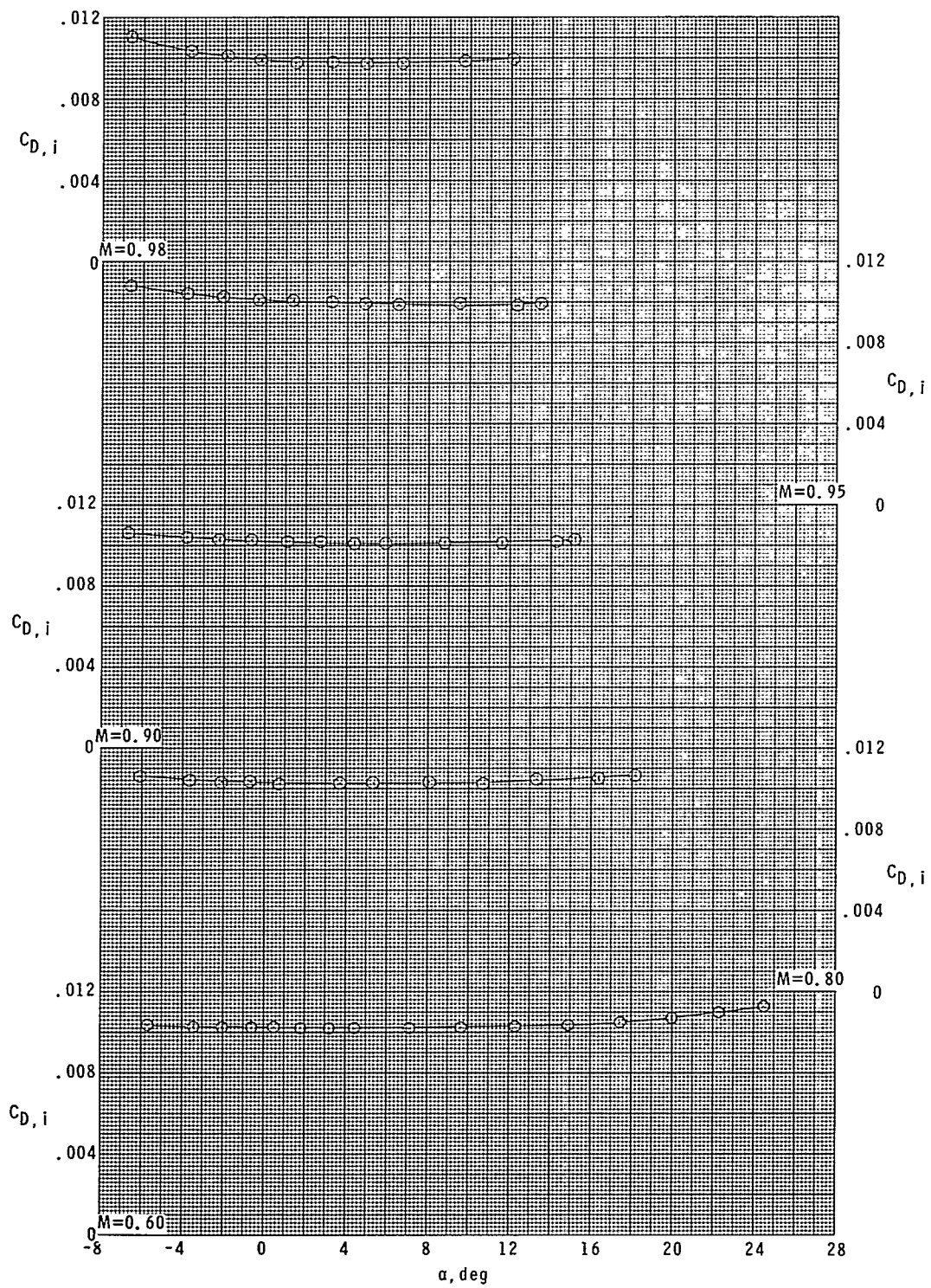
Figure 5.- Internal-drag coefficient.
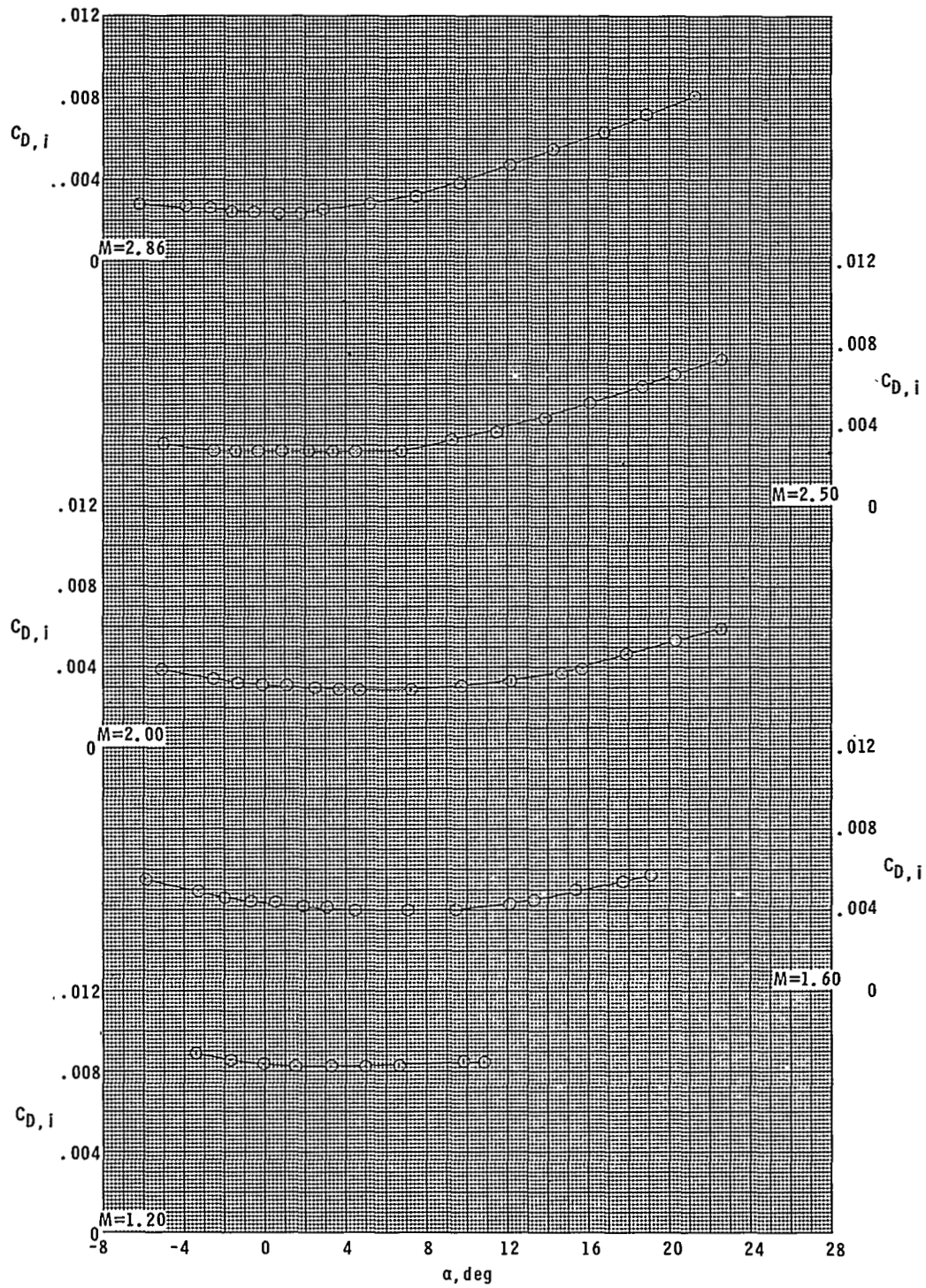
Figure 5.- Concluded.
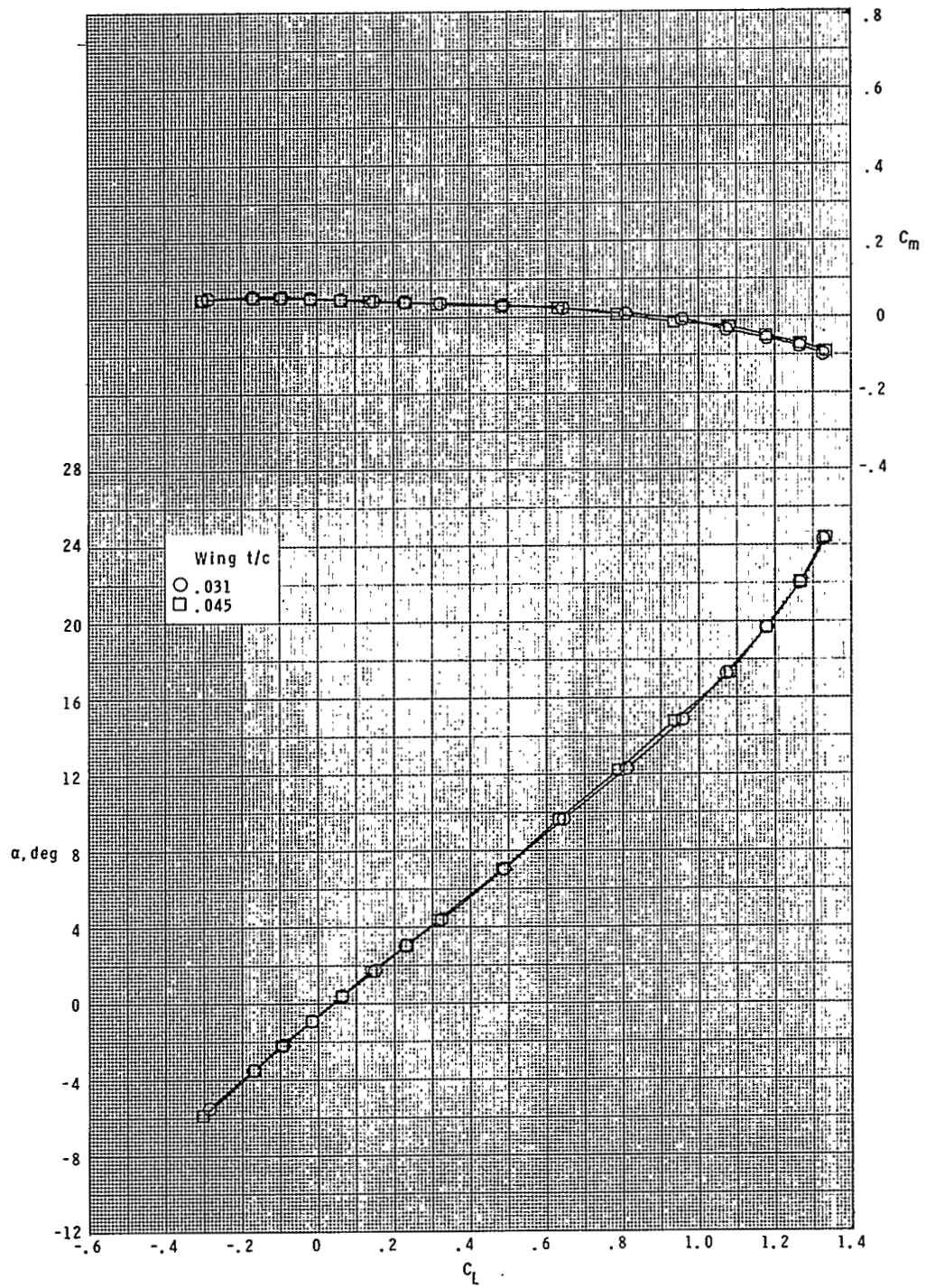
(a) M = 0.60.

Figure 6.- Effect of wing thickness on longitudinal aerodynamic characteristics
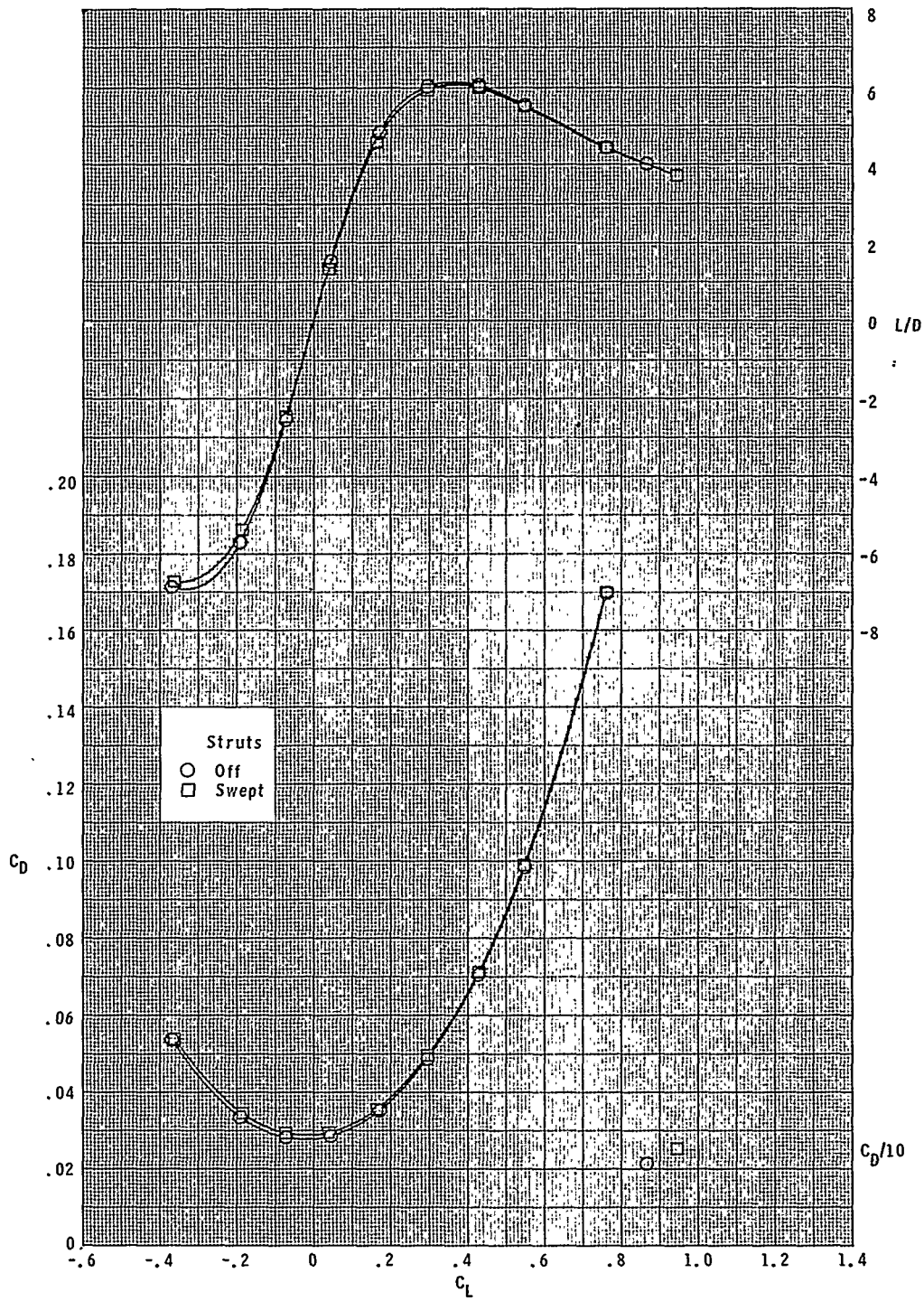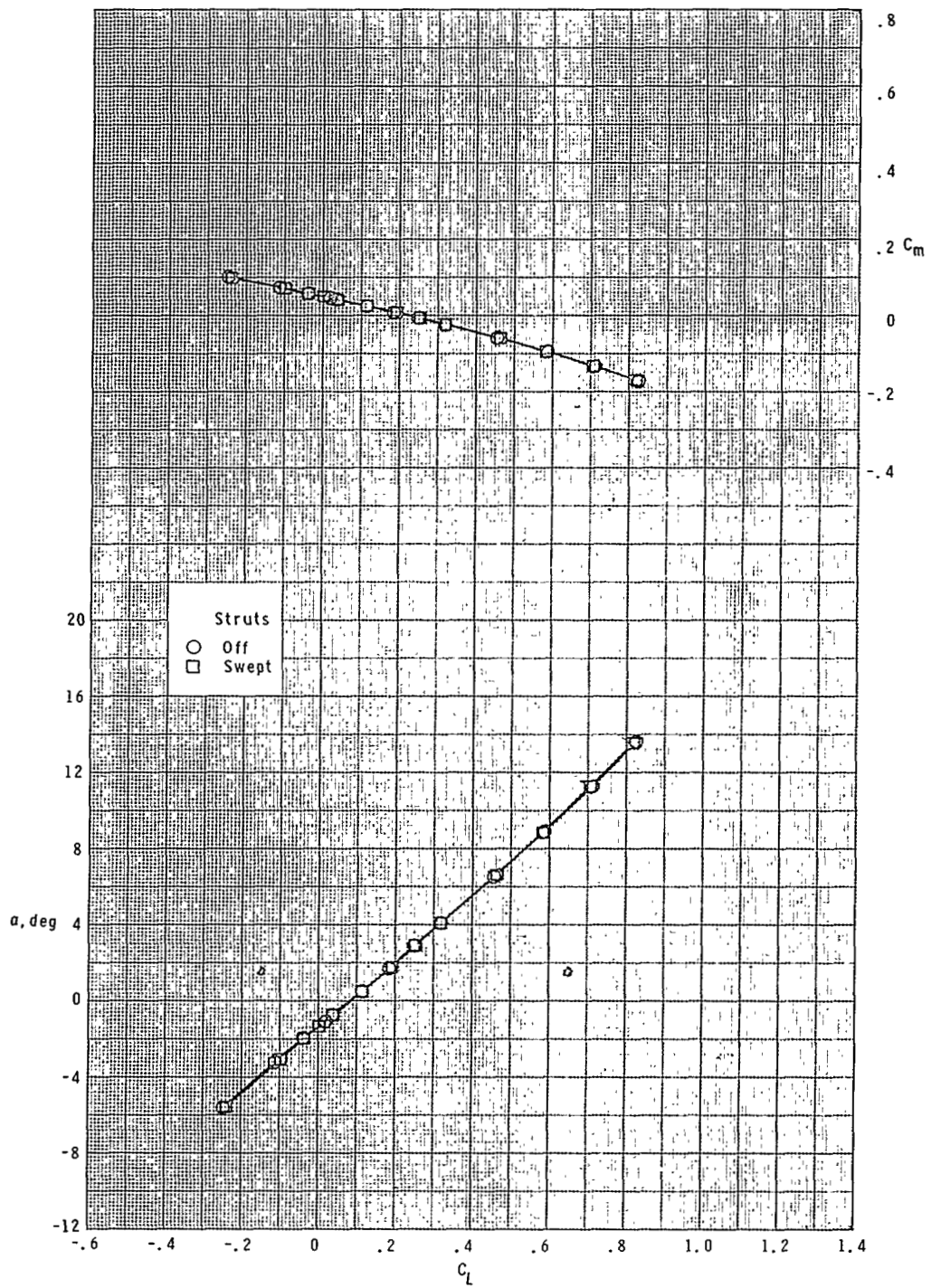for $\delta_h = 0^o$.
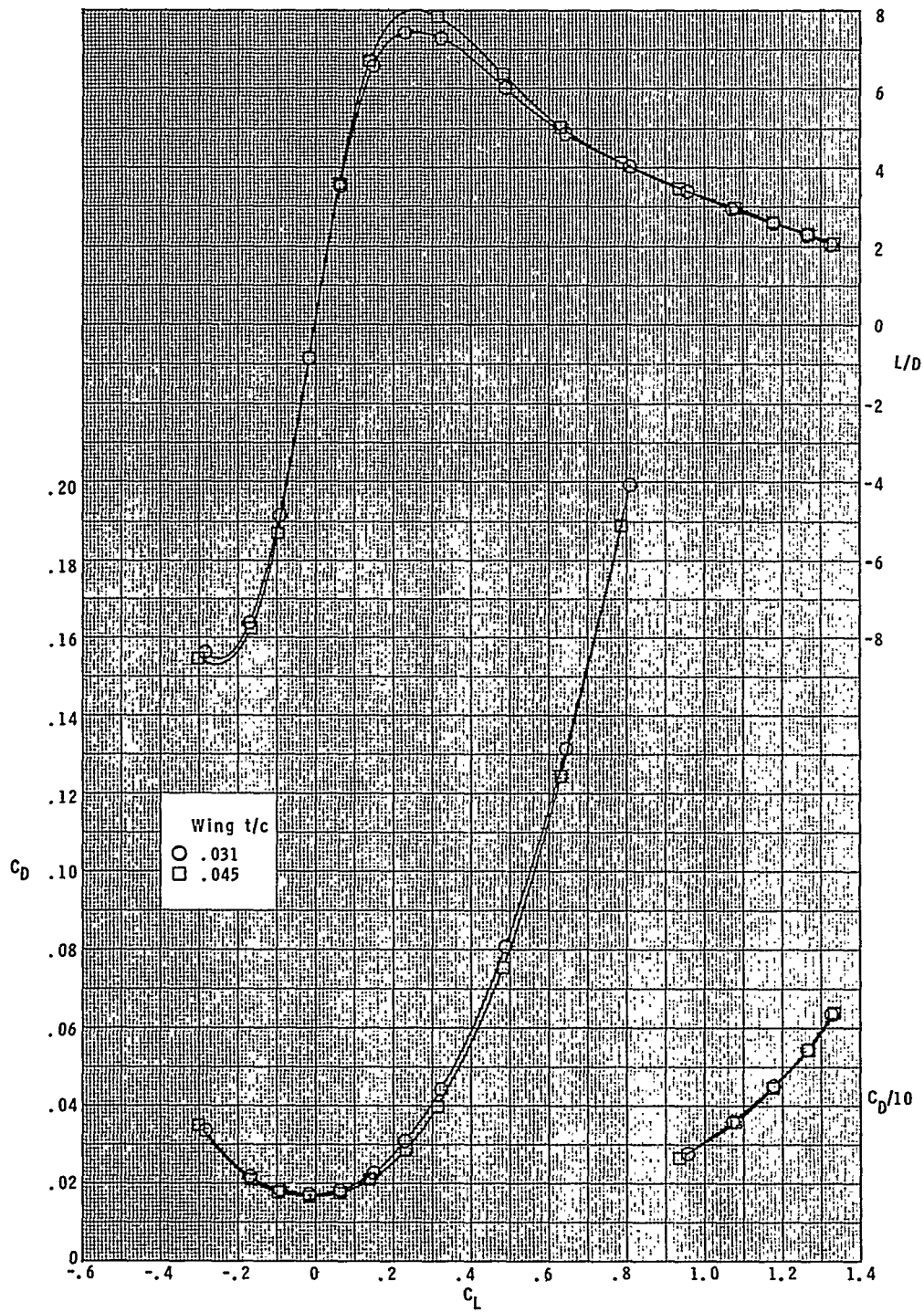
(a) Concluded.
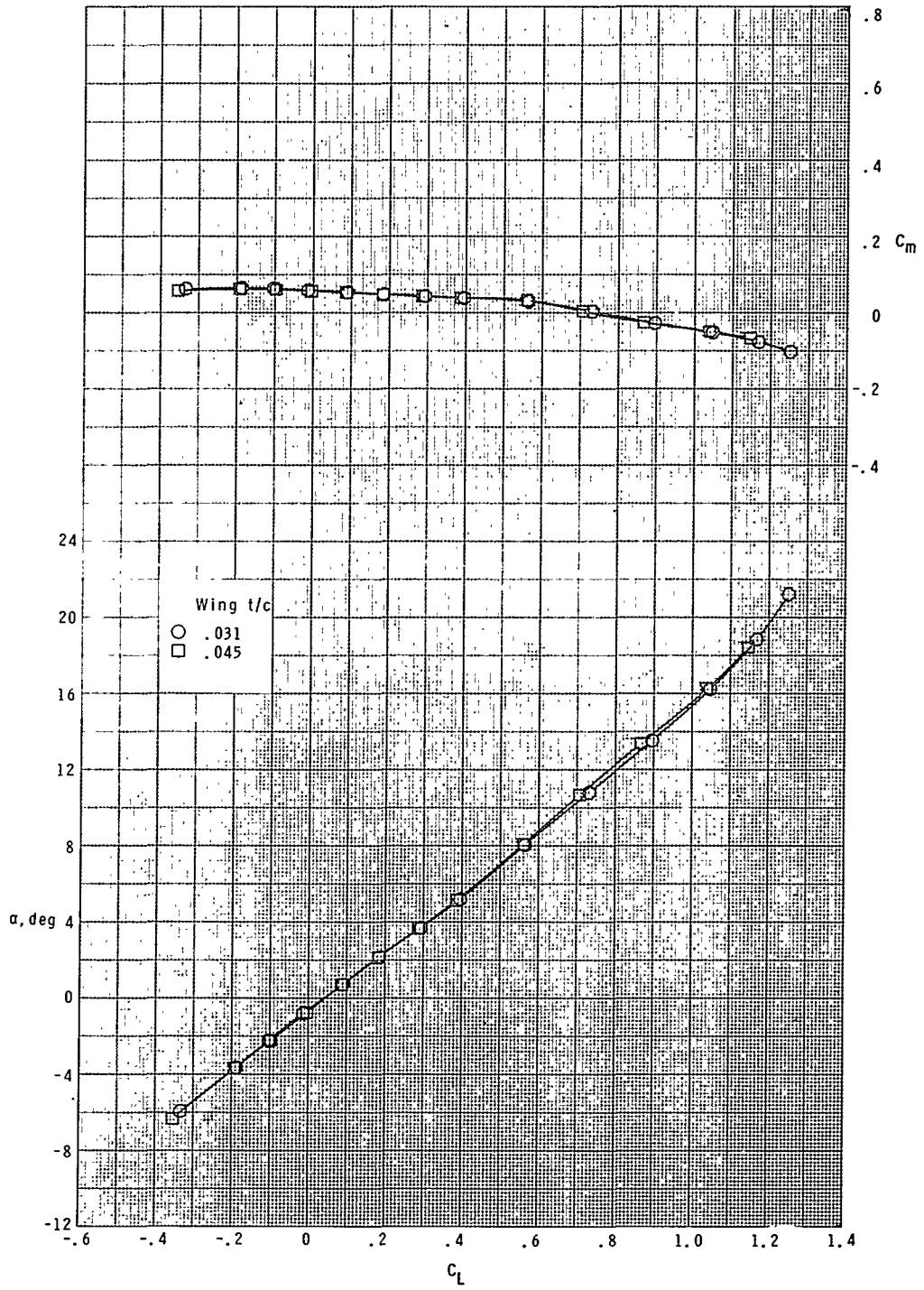
Figure 6.- Continued.

(b)   M = 0.80.

Figure 6.- Continued.
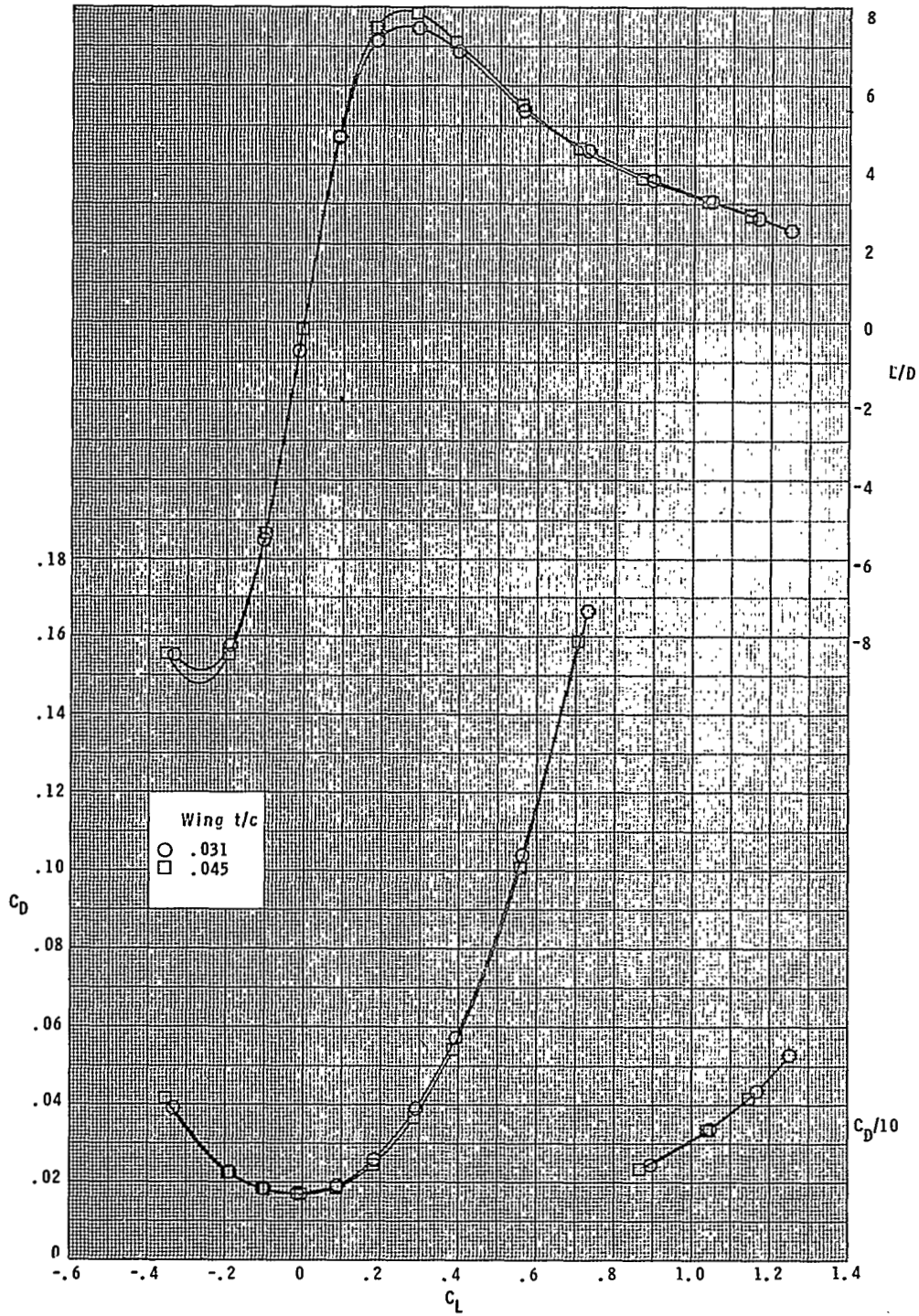
(b) Concluded.
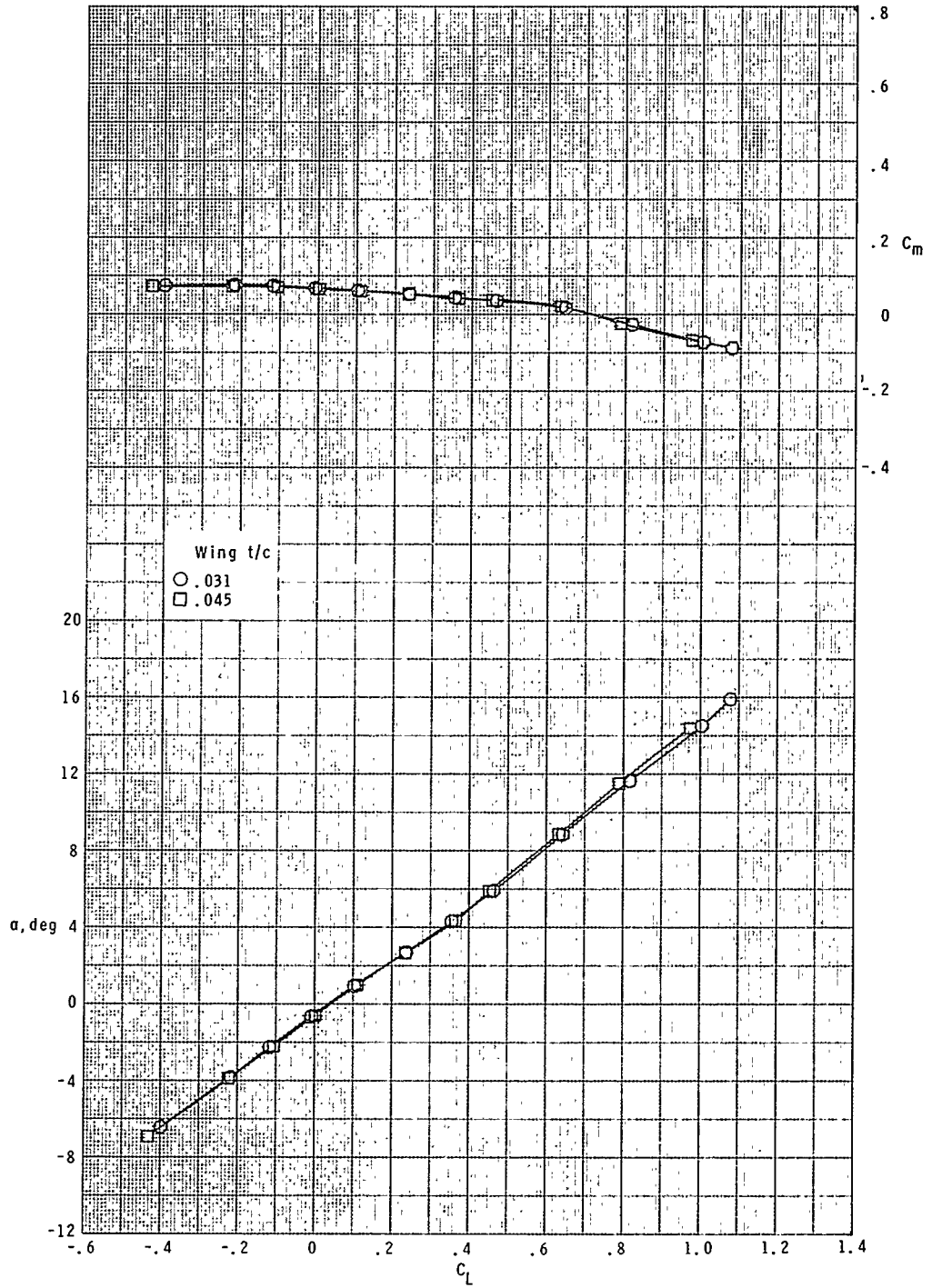
Figure 6.- Continued.

(c) M = 0.90.

Figure 6.- Continued.
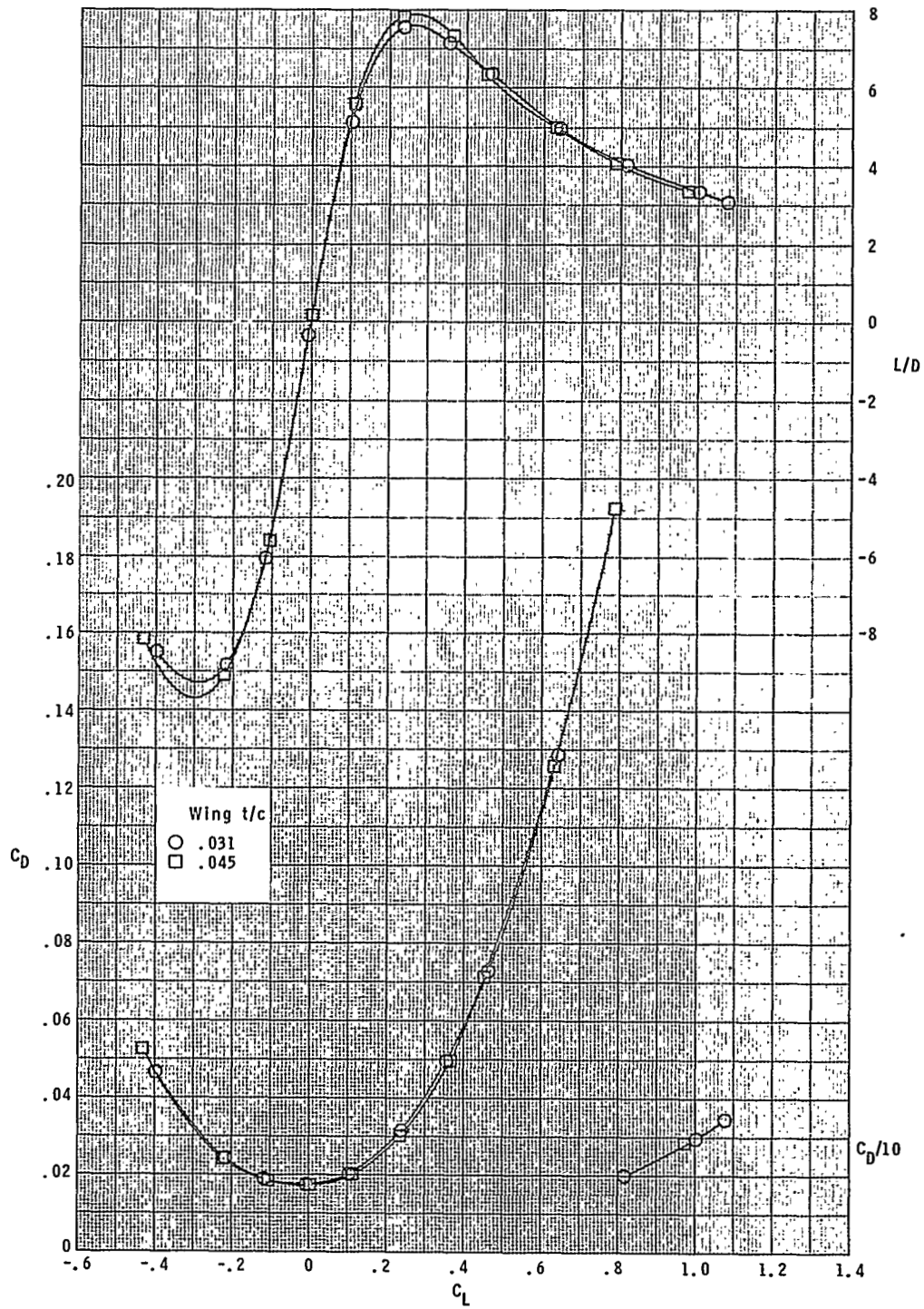
(c) Concluded.
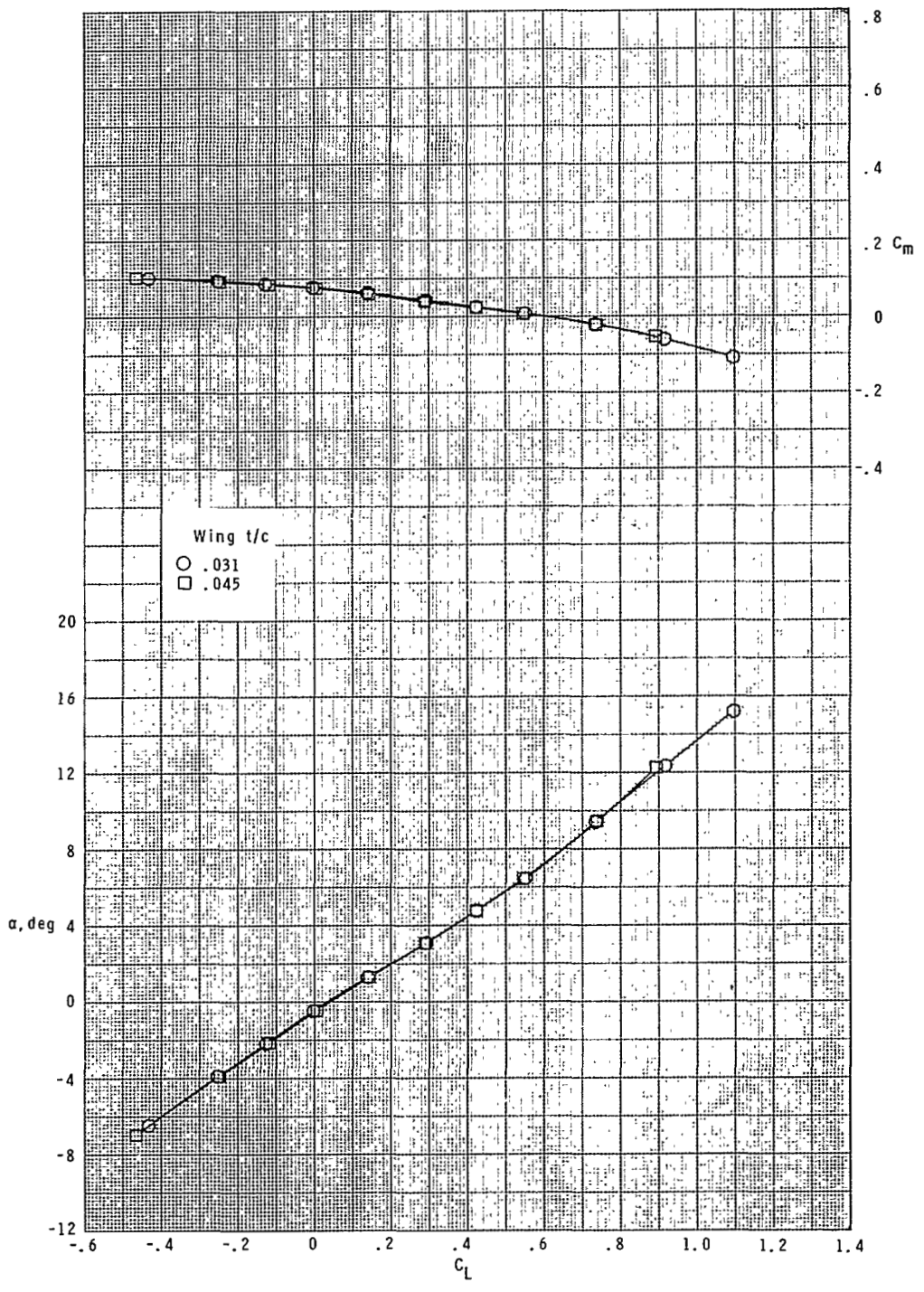
Figure 6.- Continued.

(d)   M = 0.95.

Figure 6.- Continued.
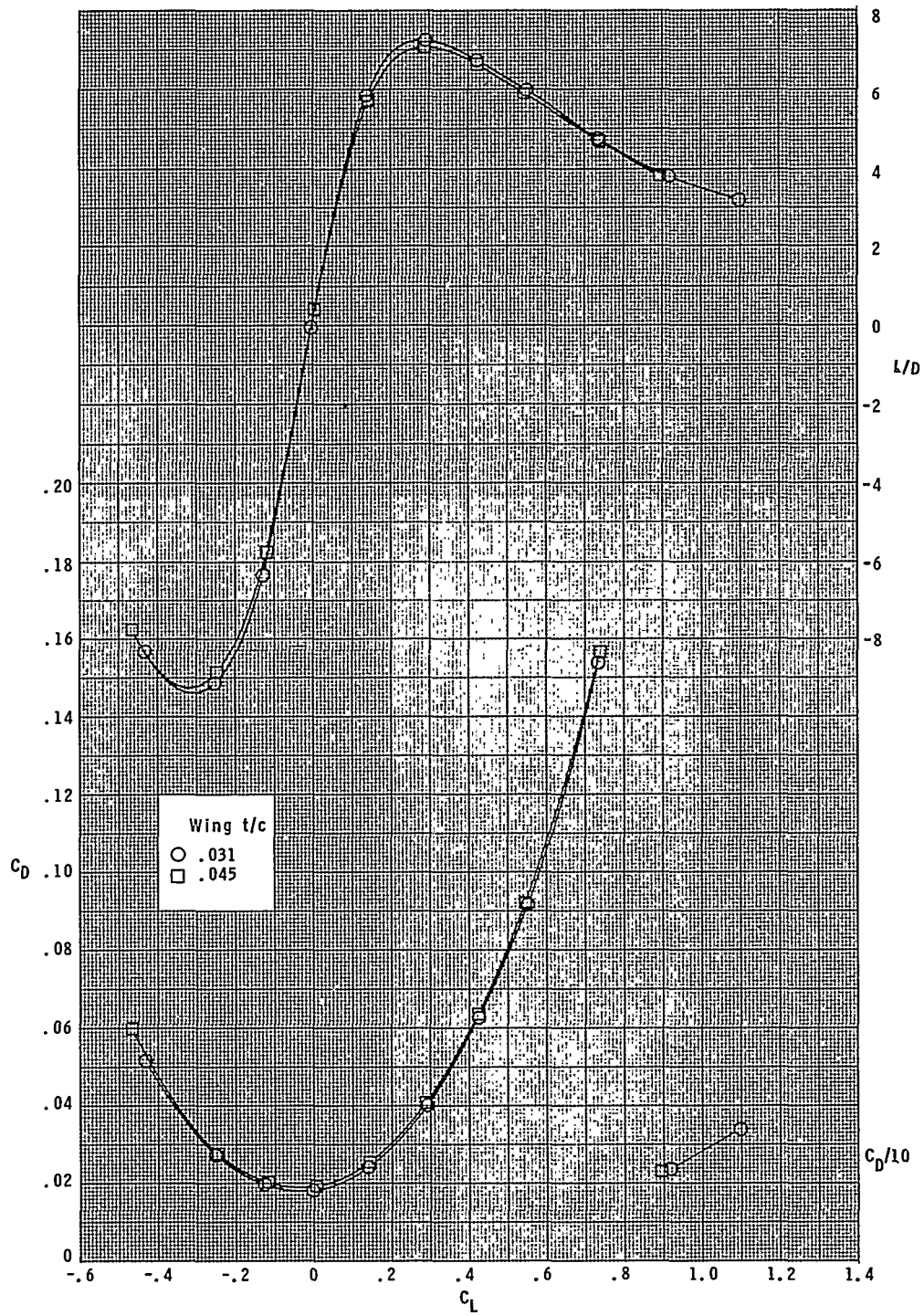
(d) Concluded.
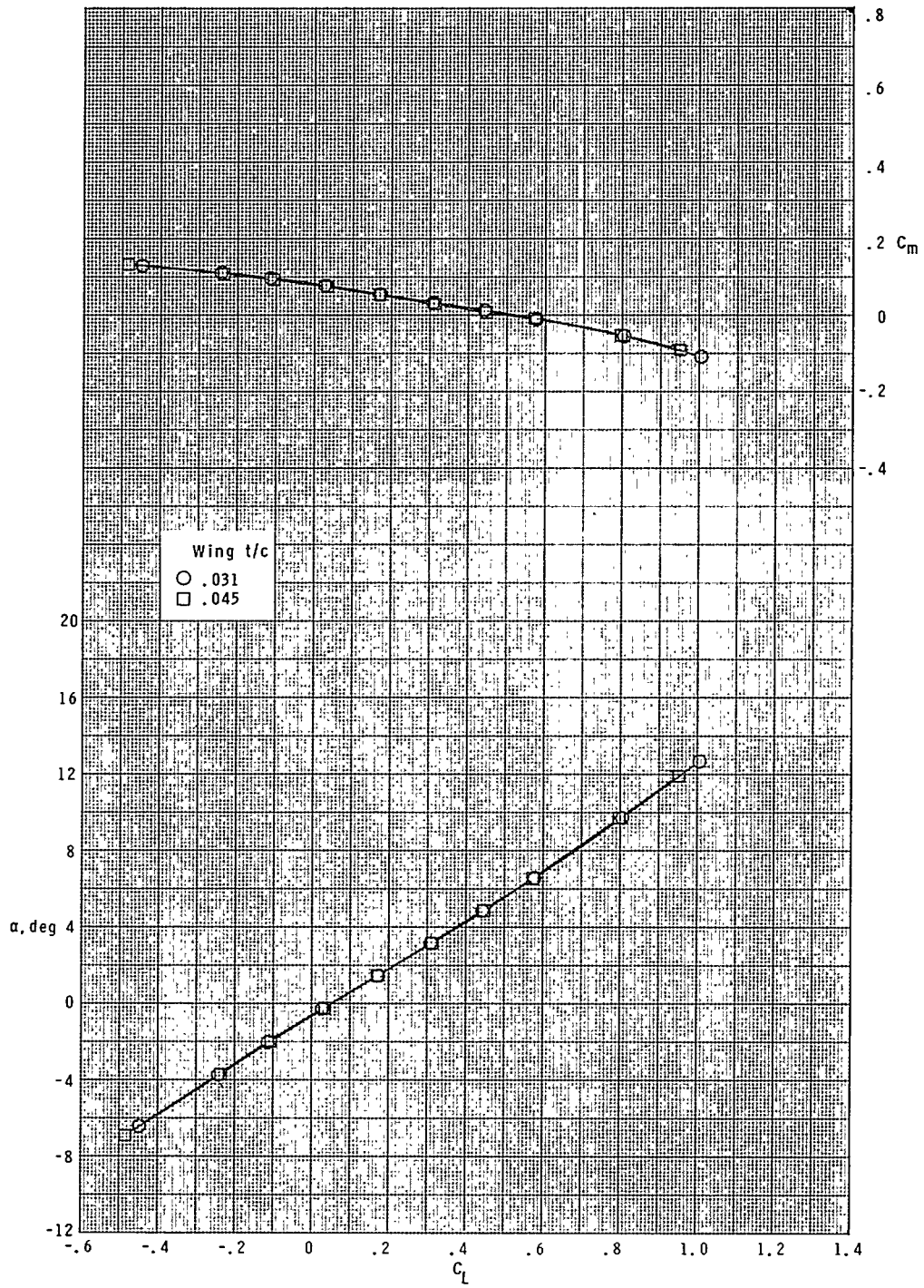
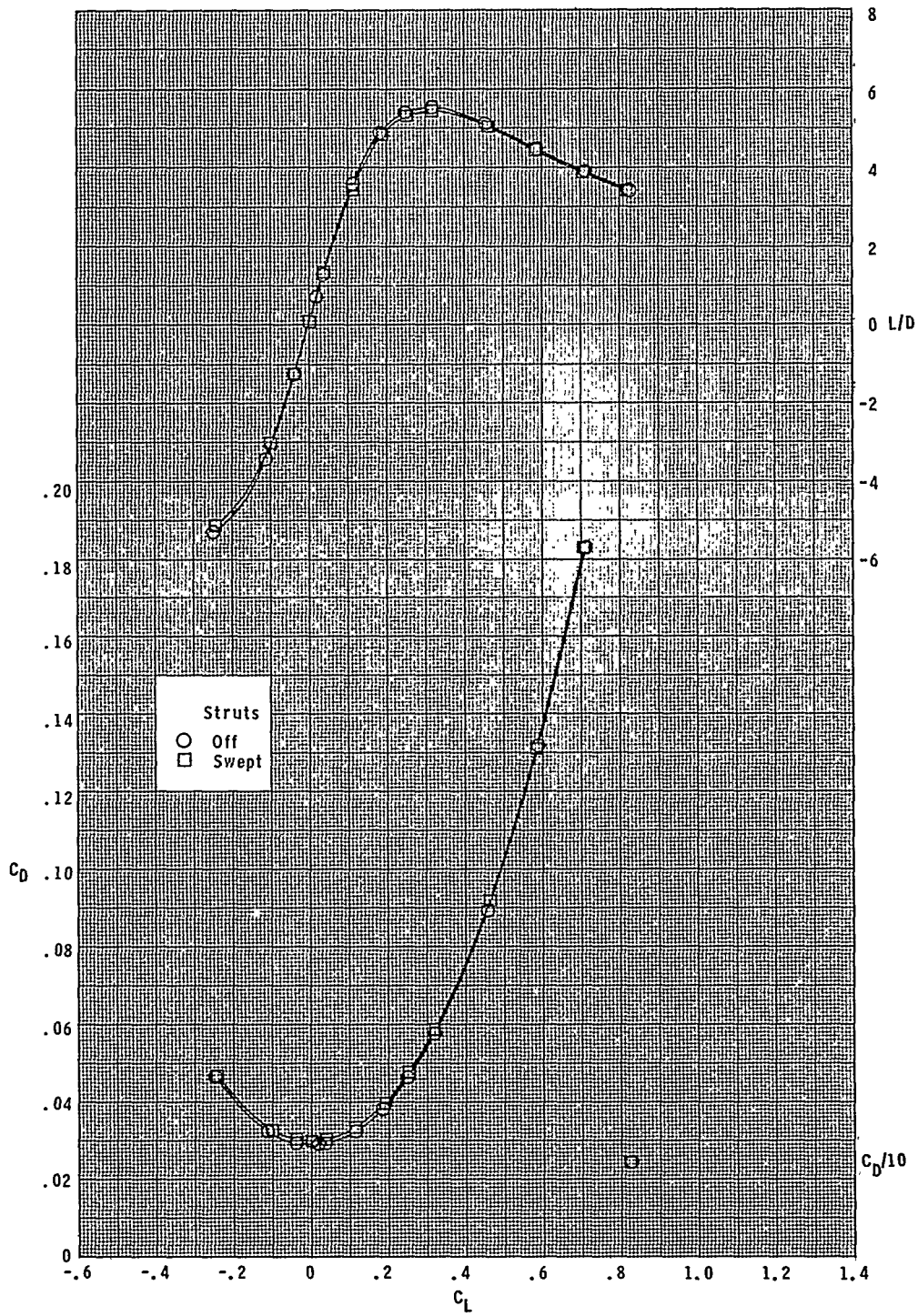Figure 6.- Continued.

(e) M = 0.98.

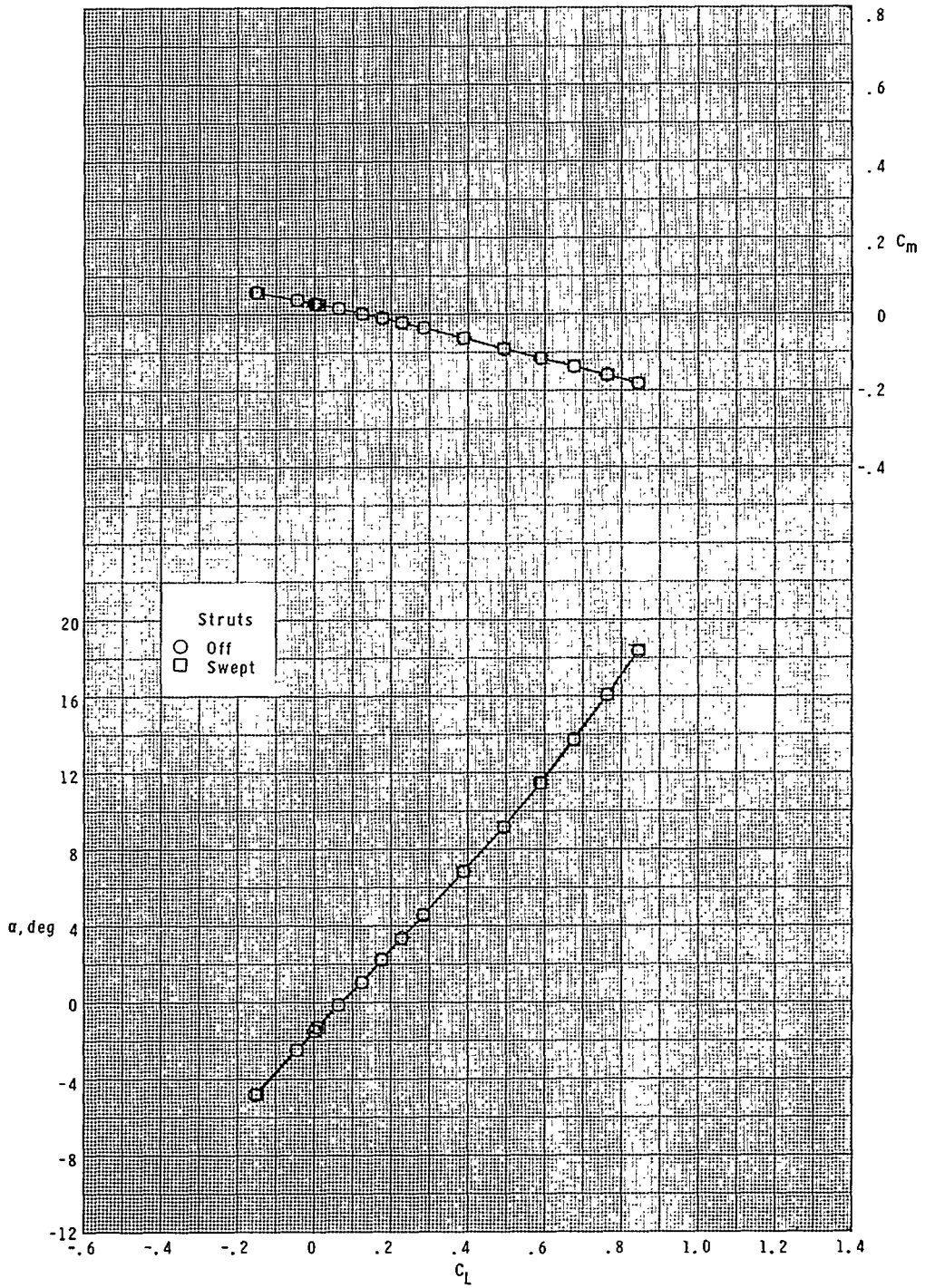Figure 6.- Continued.
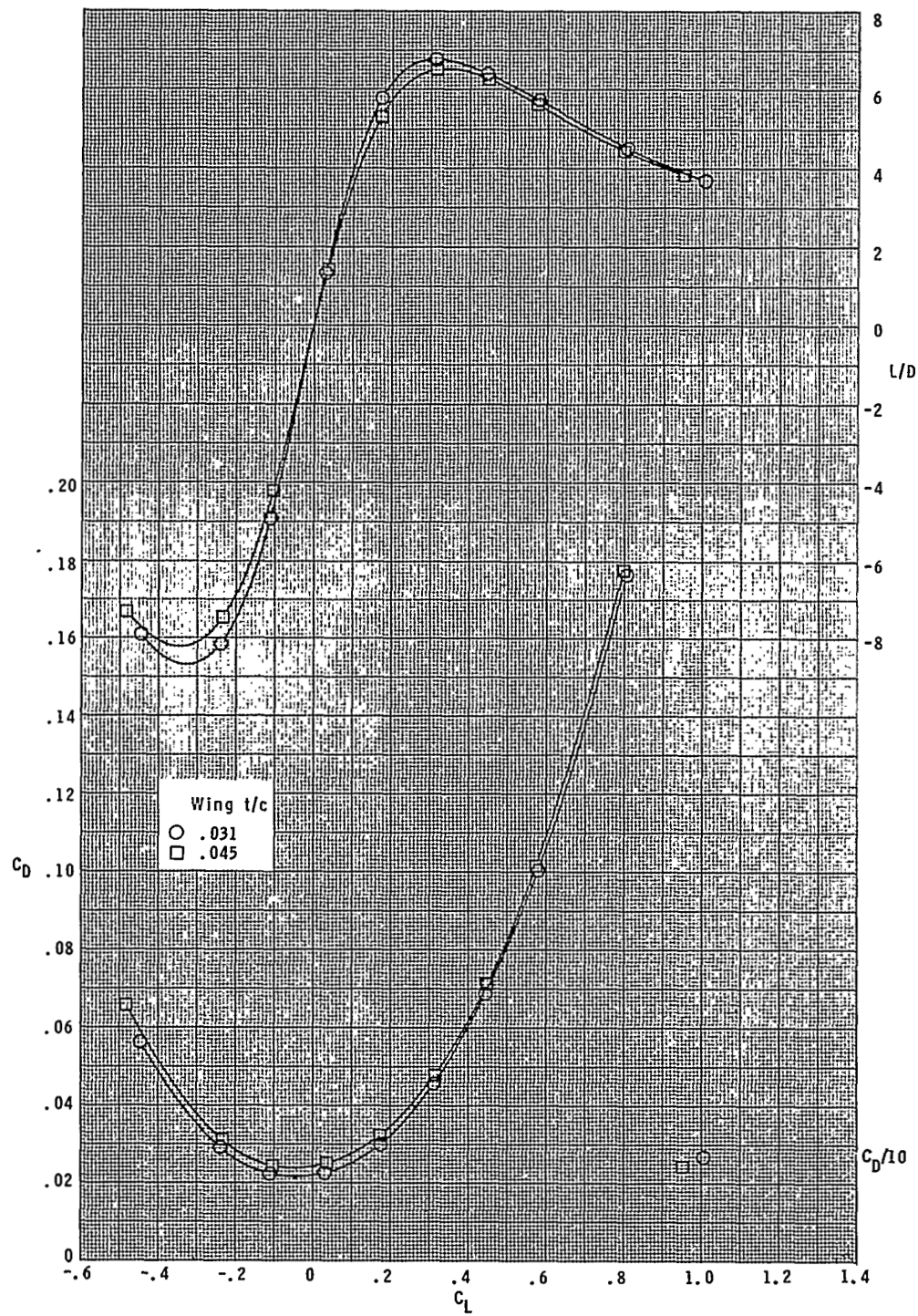
(e) Concluded.
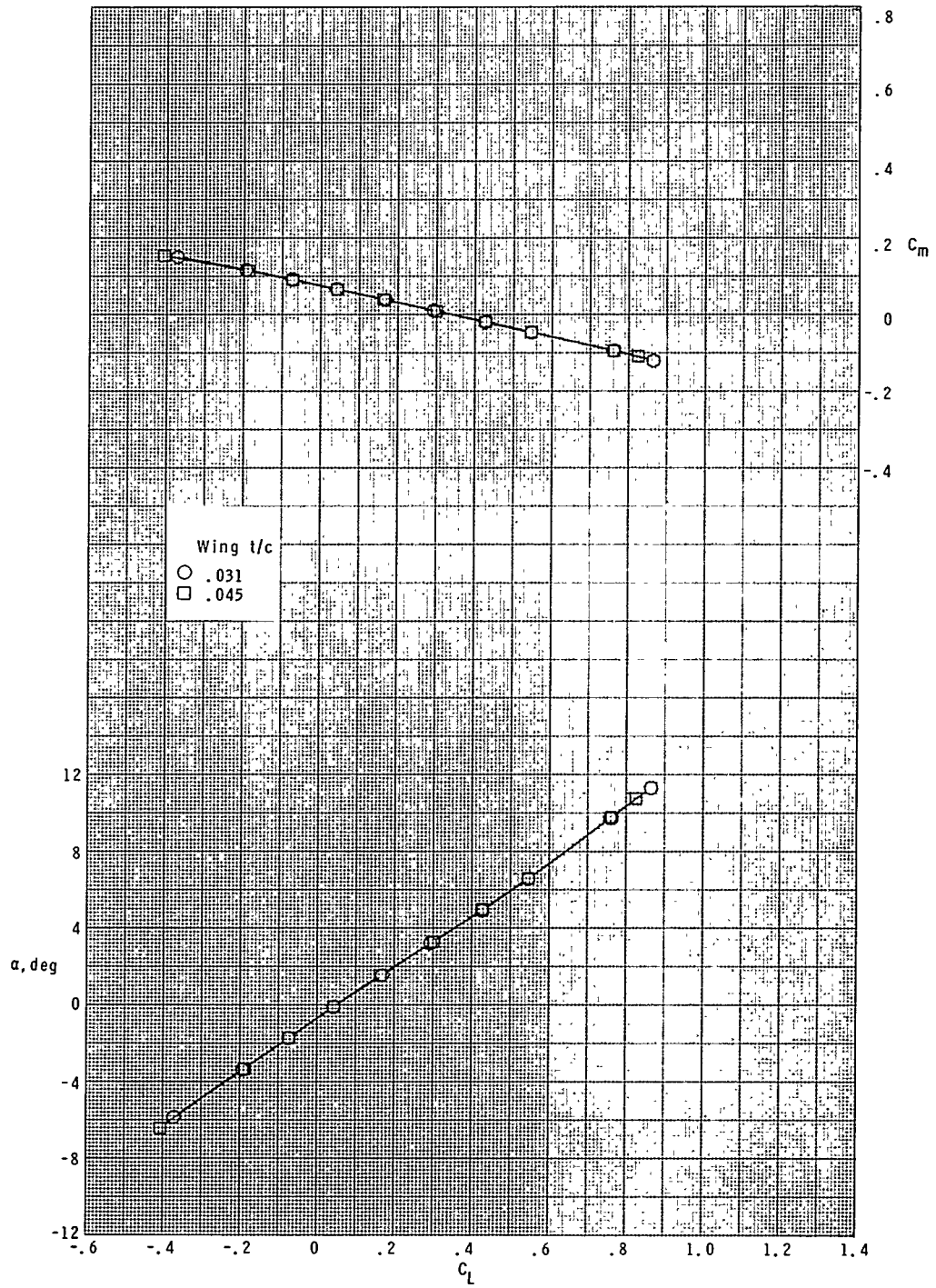
Figure 6.- Continued.

(f) M = 1.20.

Figure 6.- Continued.
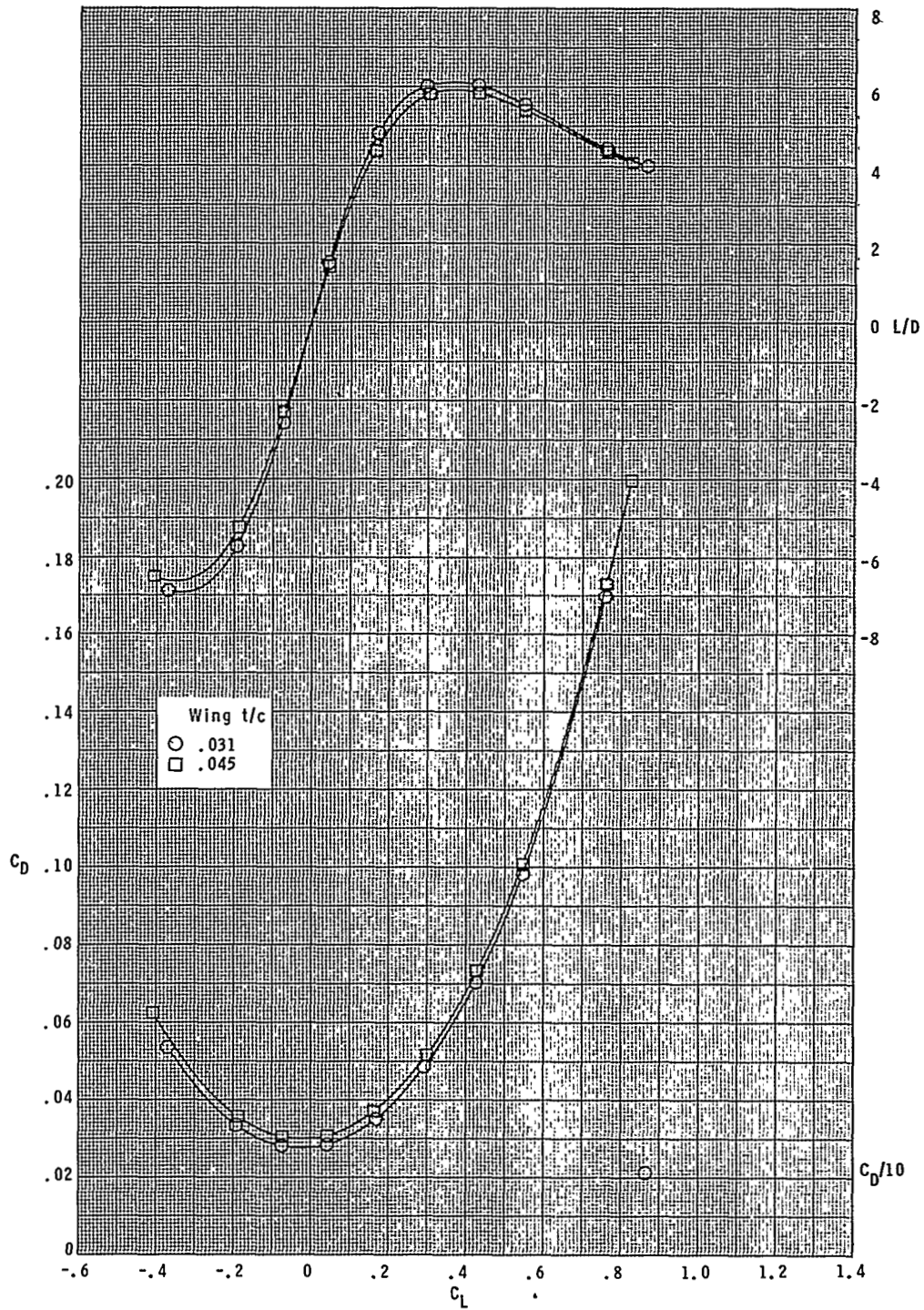
(f) Concluded.
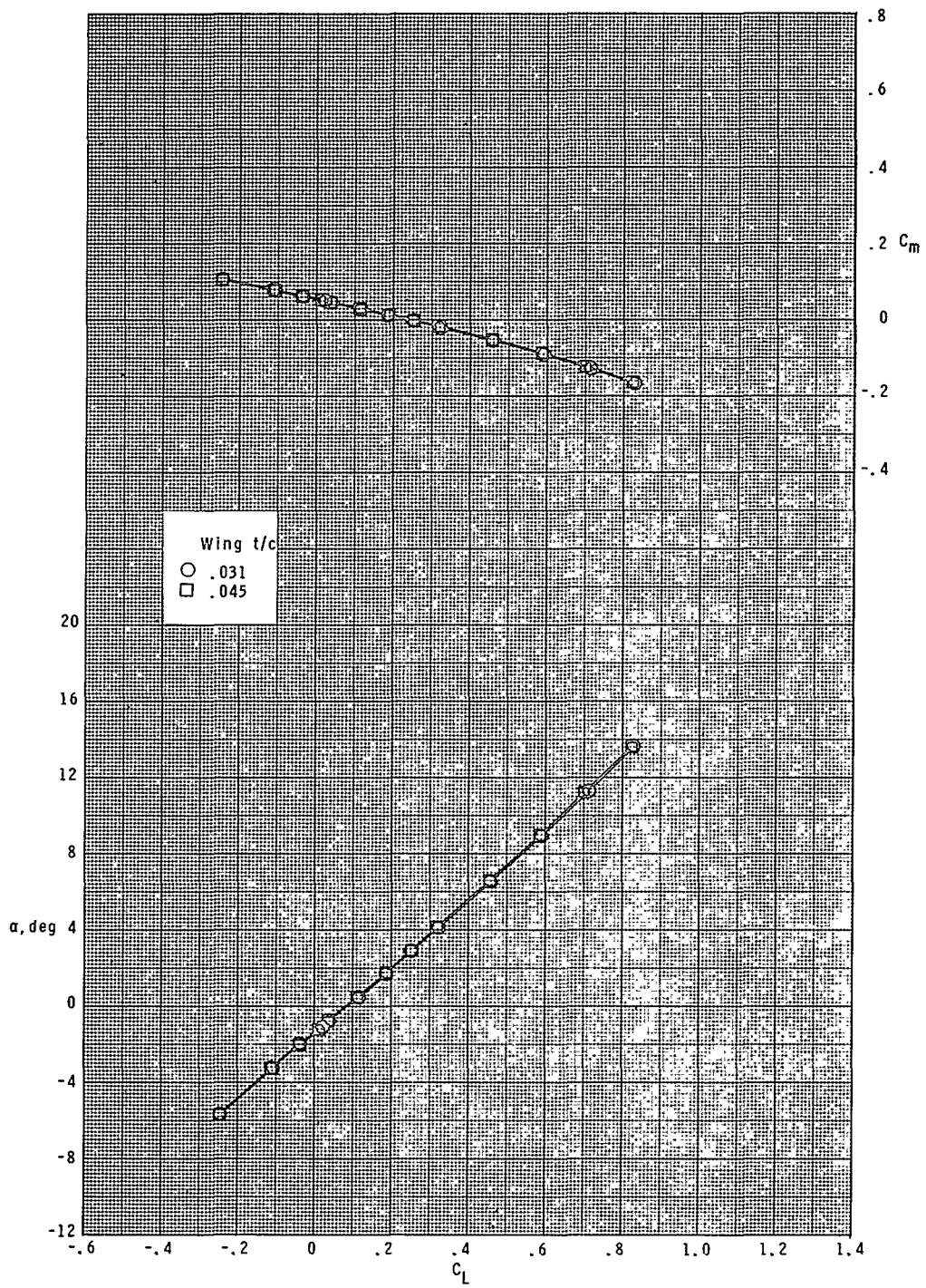
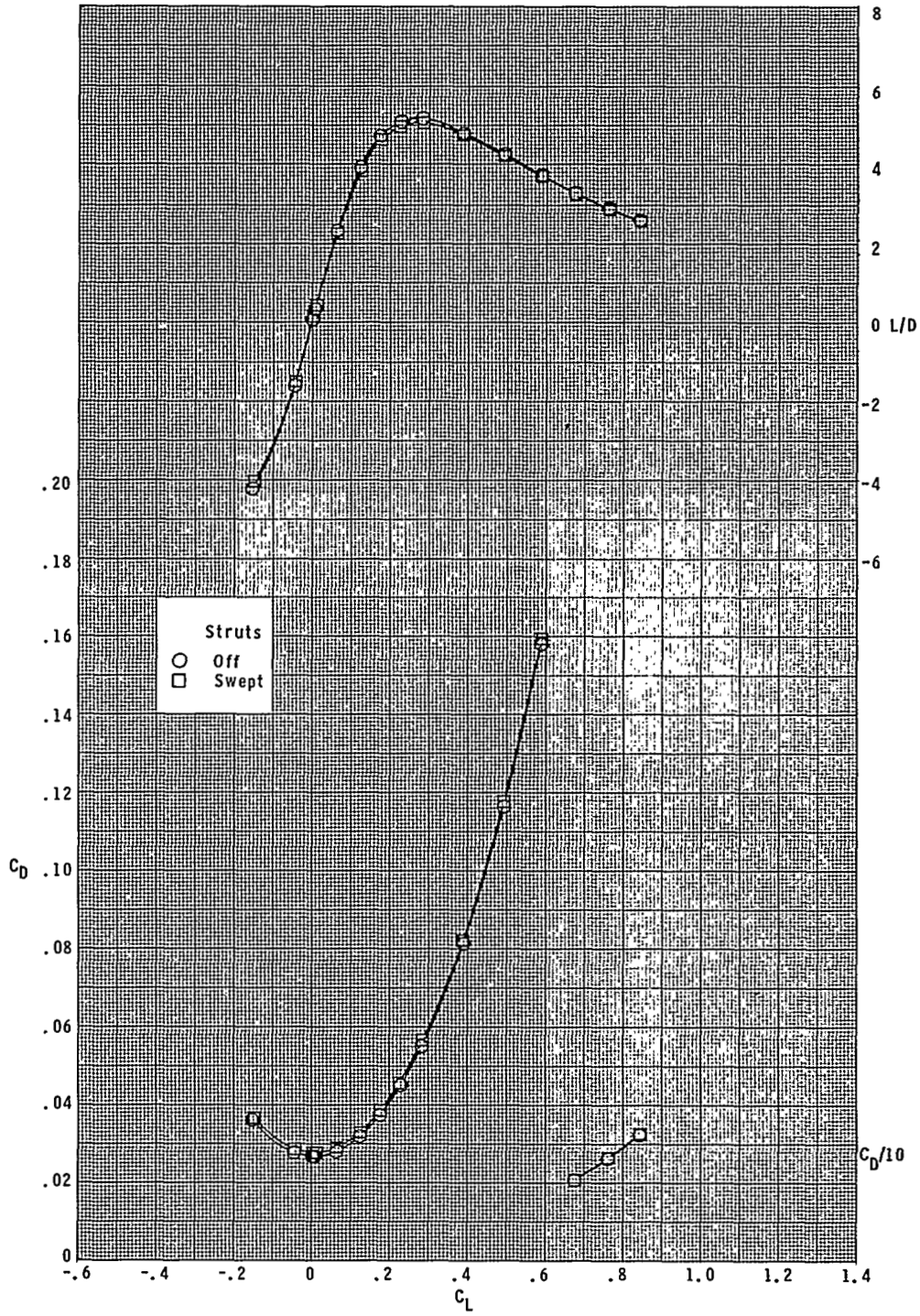Figure 6.- Continued.

(g)   M = 1.60.

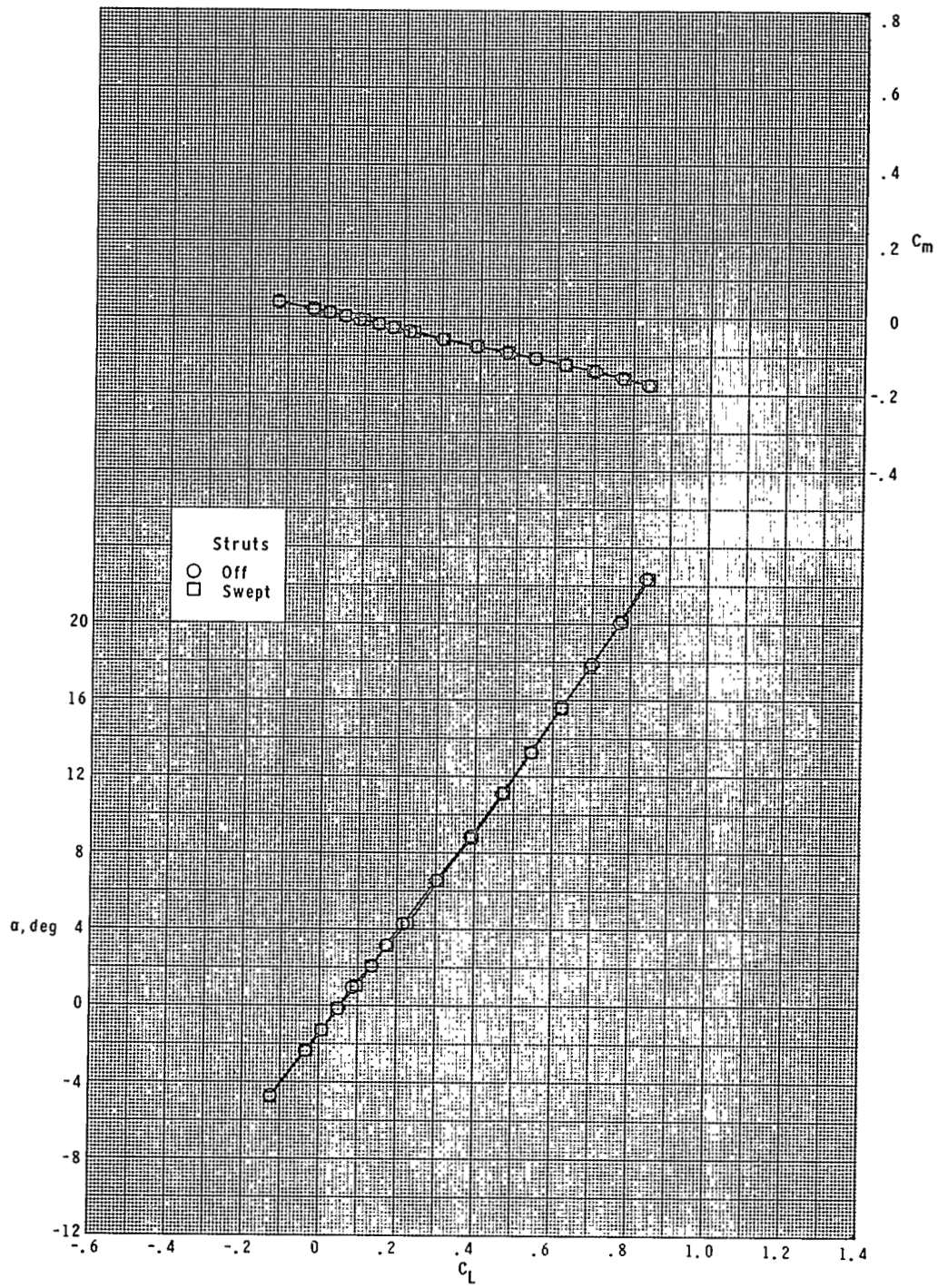Figure 6.- Continued.
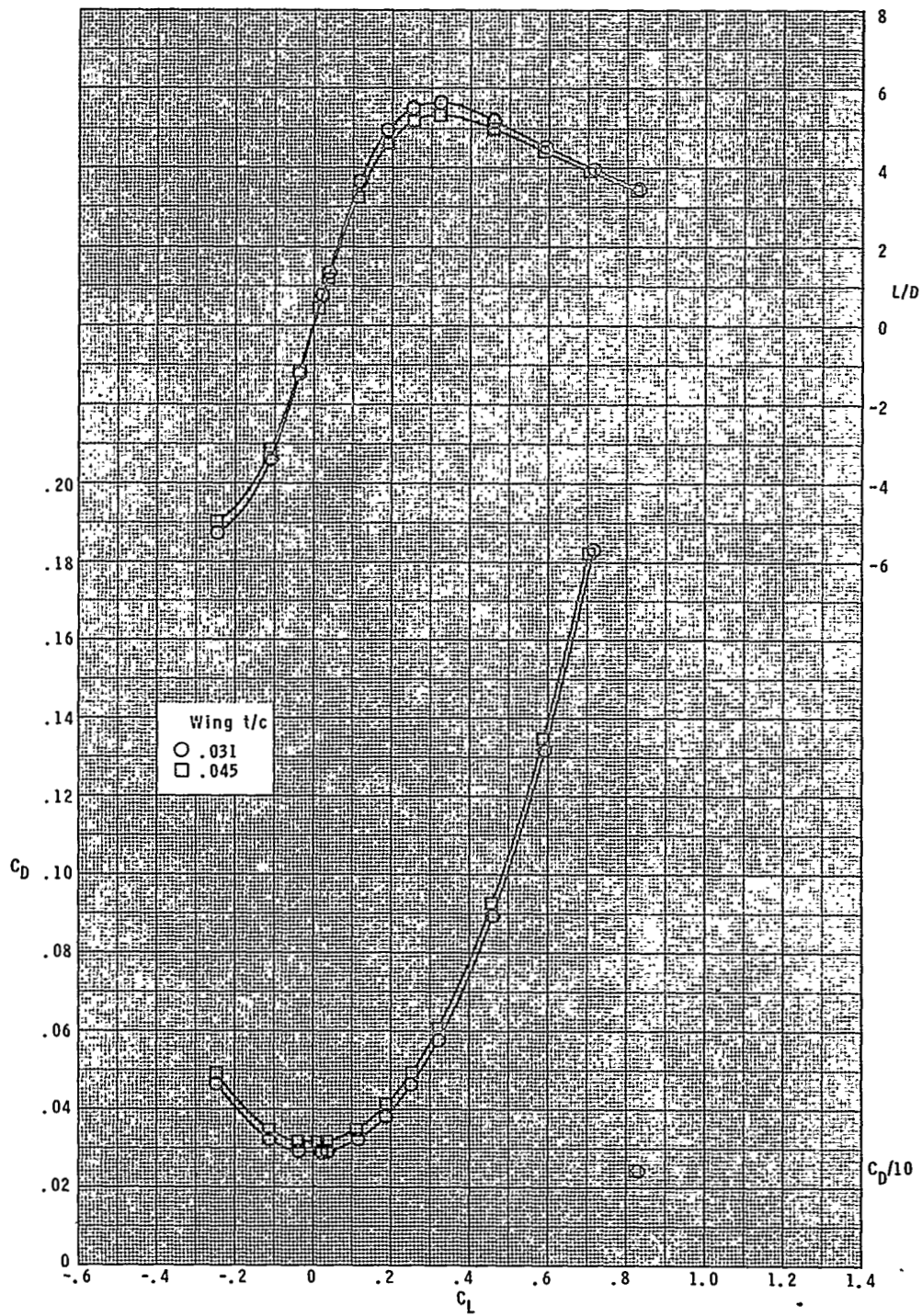
(g) Concluded.
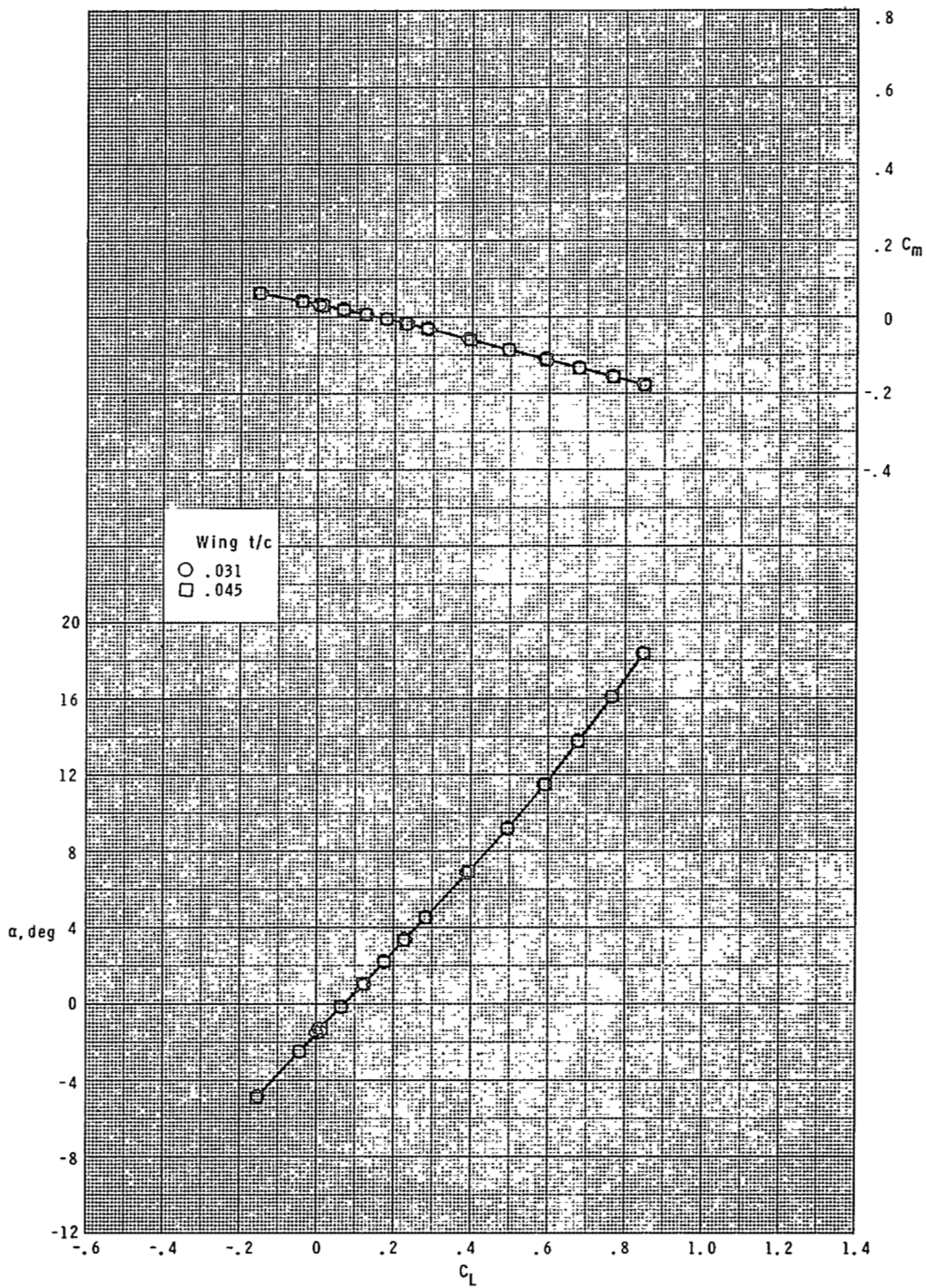
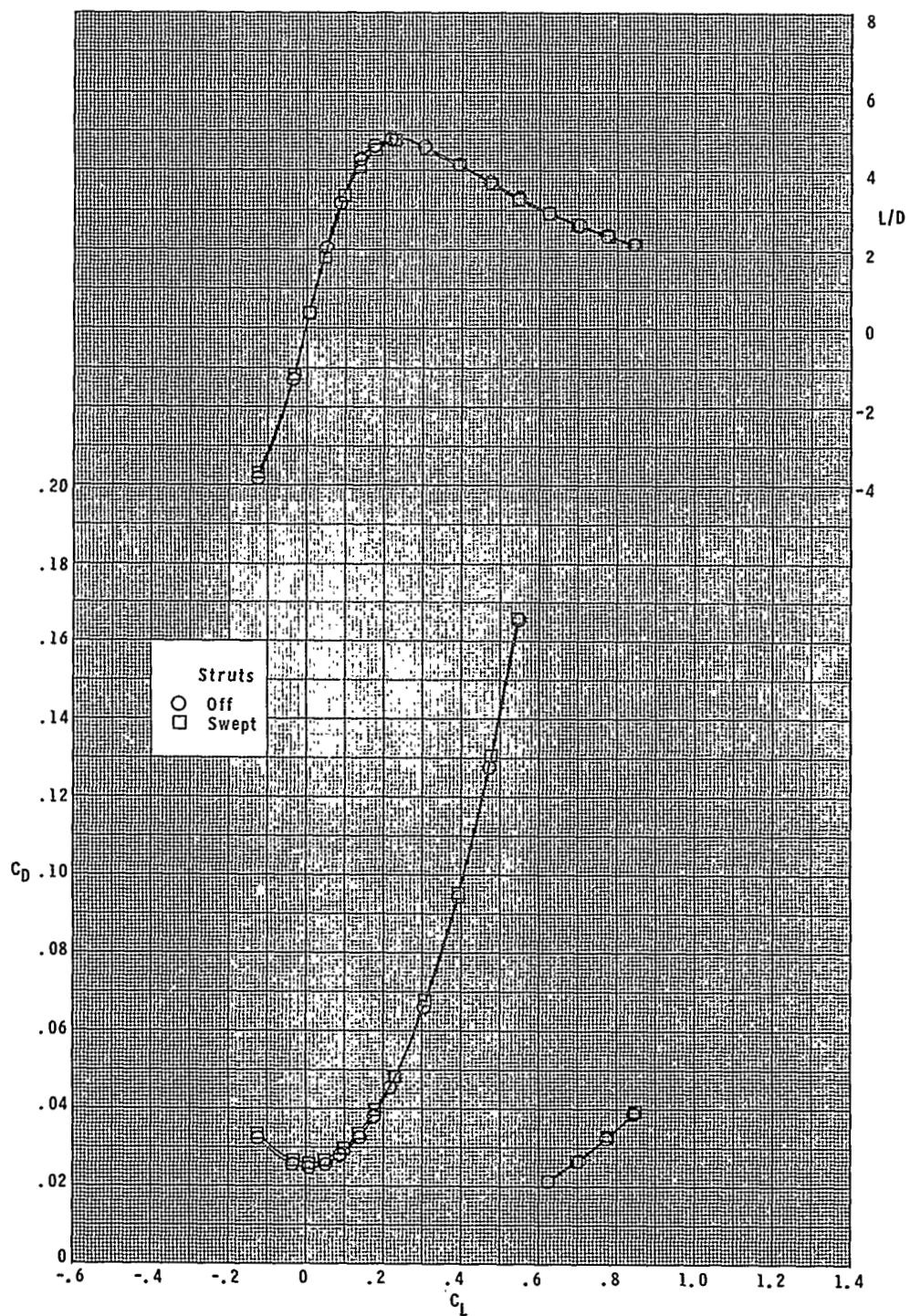Figure 6.- Continued.

(h)   M = 2.00.

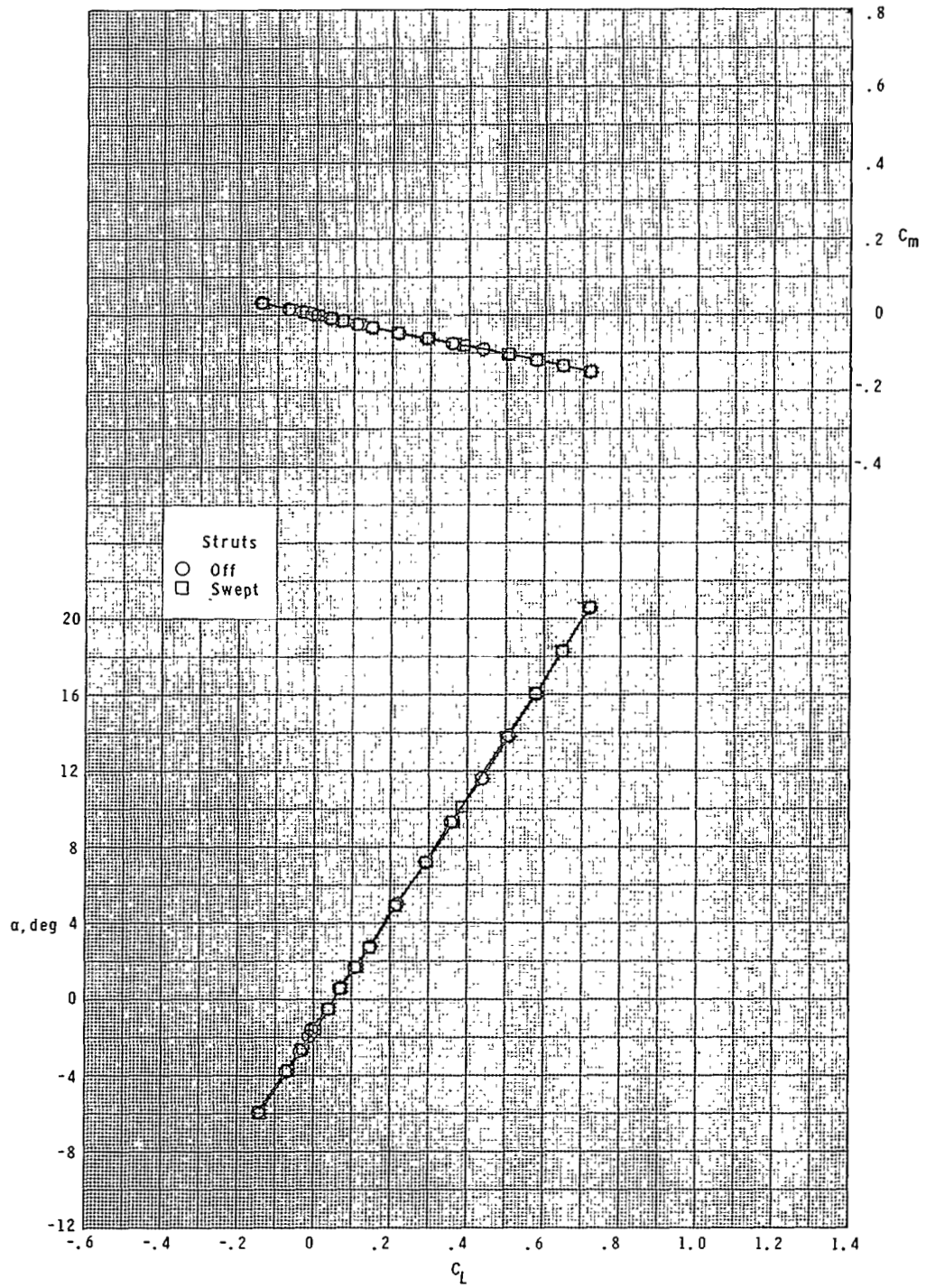Figure 6.- Continued.
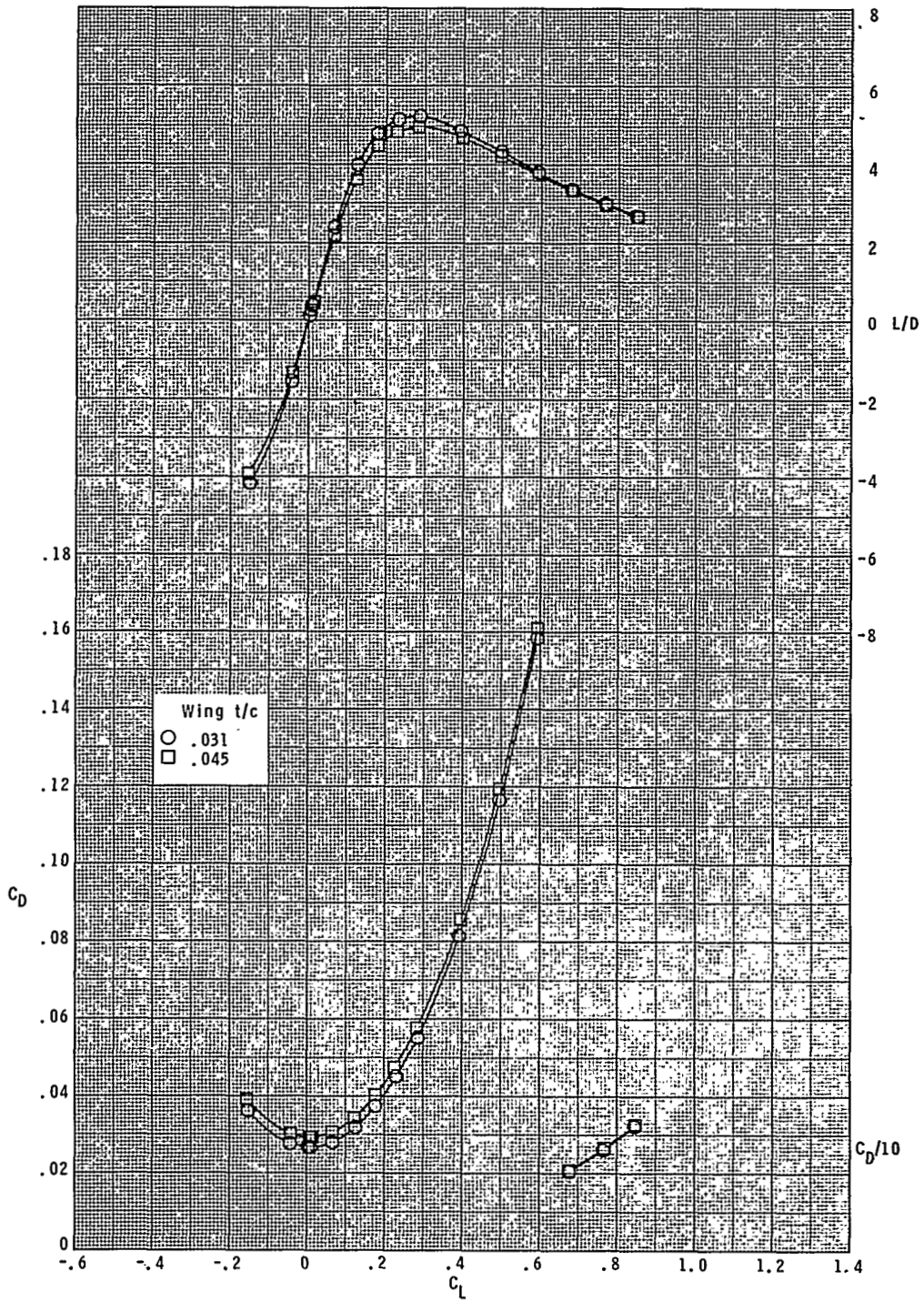
(h) Concluded.
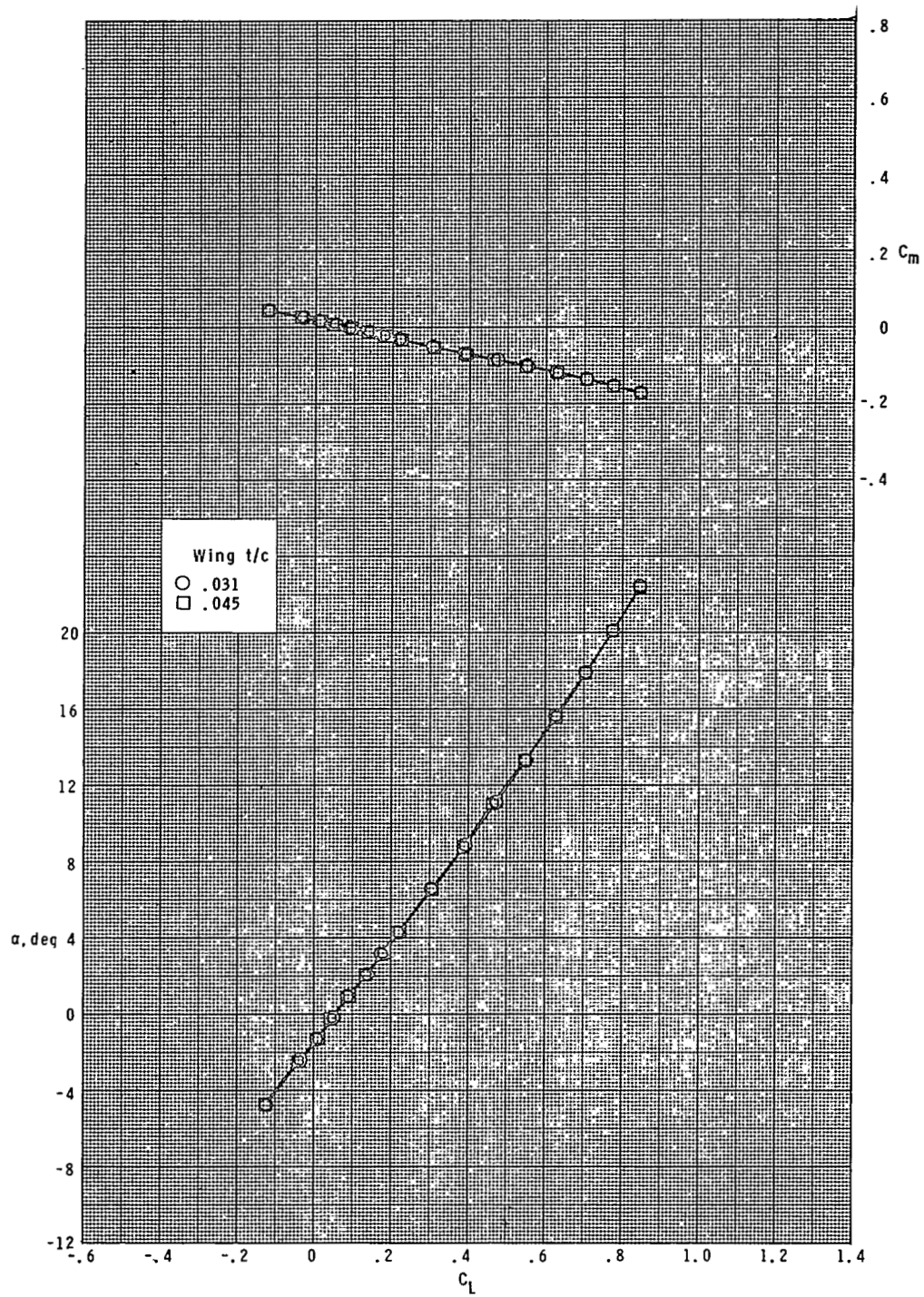
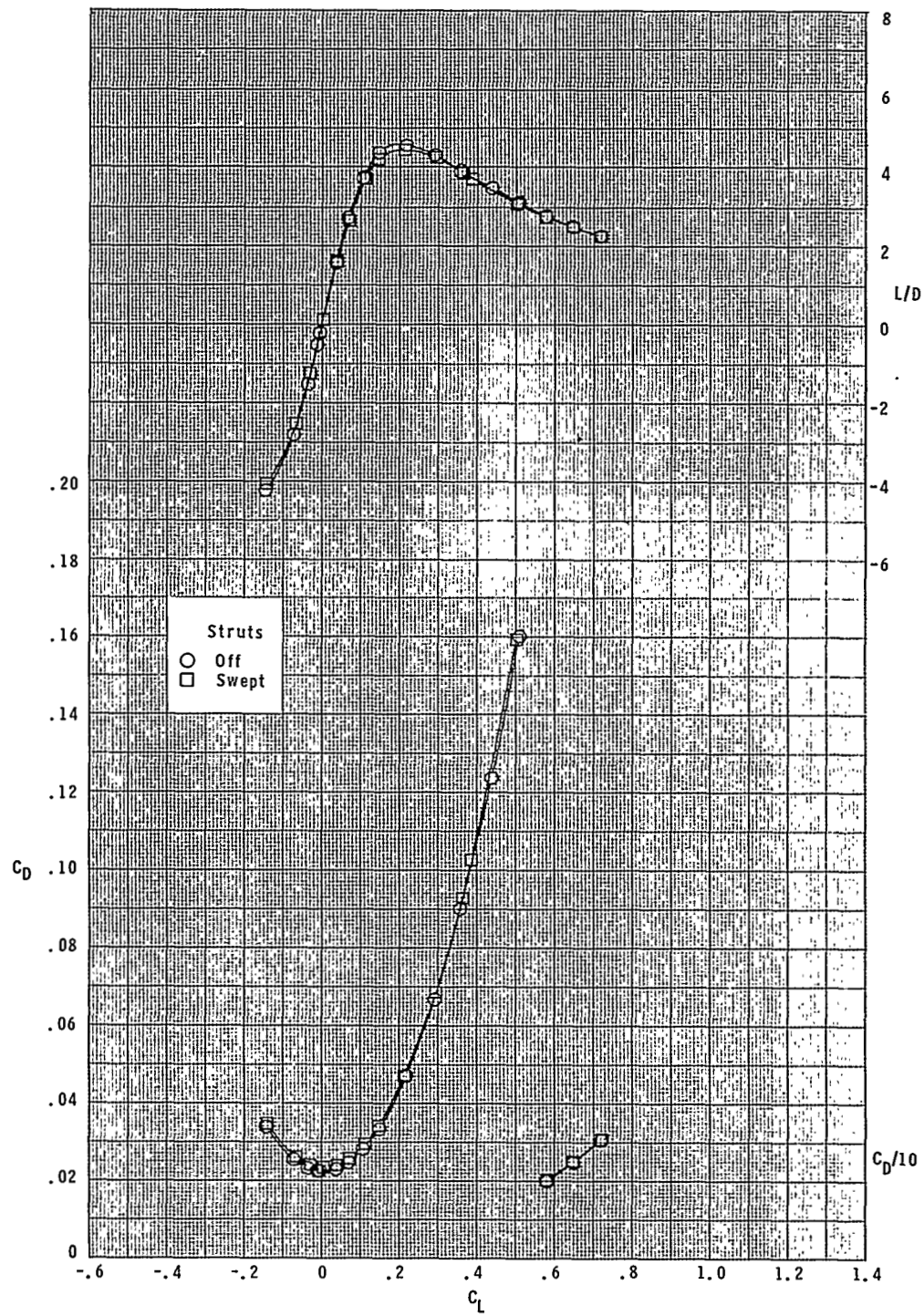Figure 6.- Continued.

(i) M = 2.50.

Figure 6.- Continued.
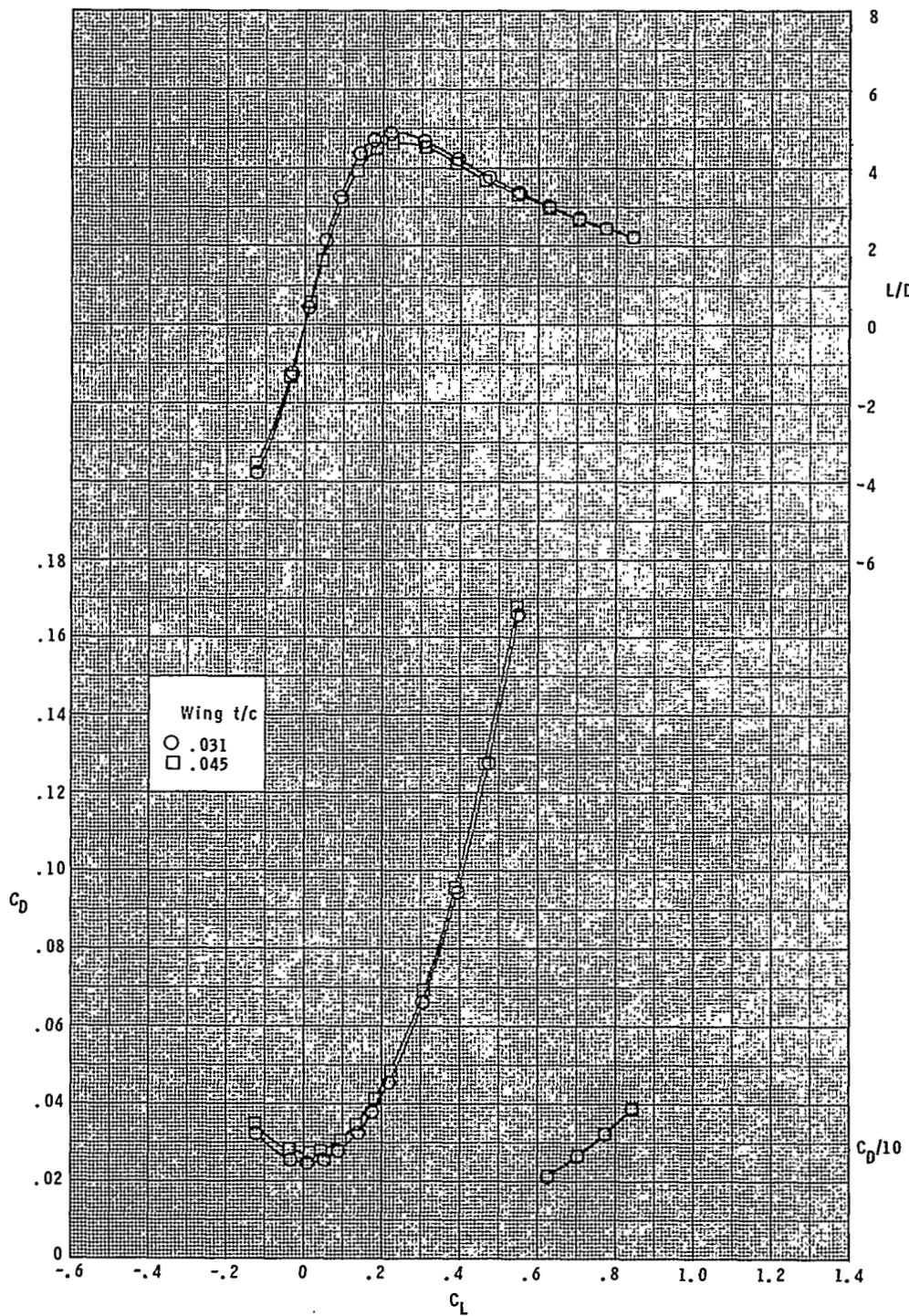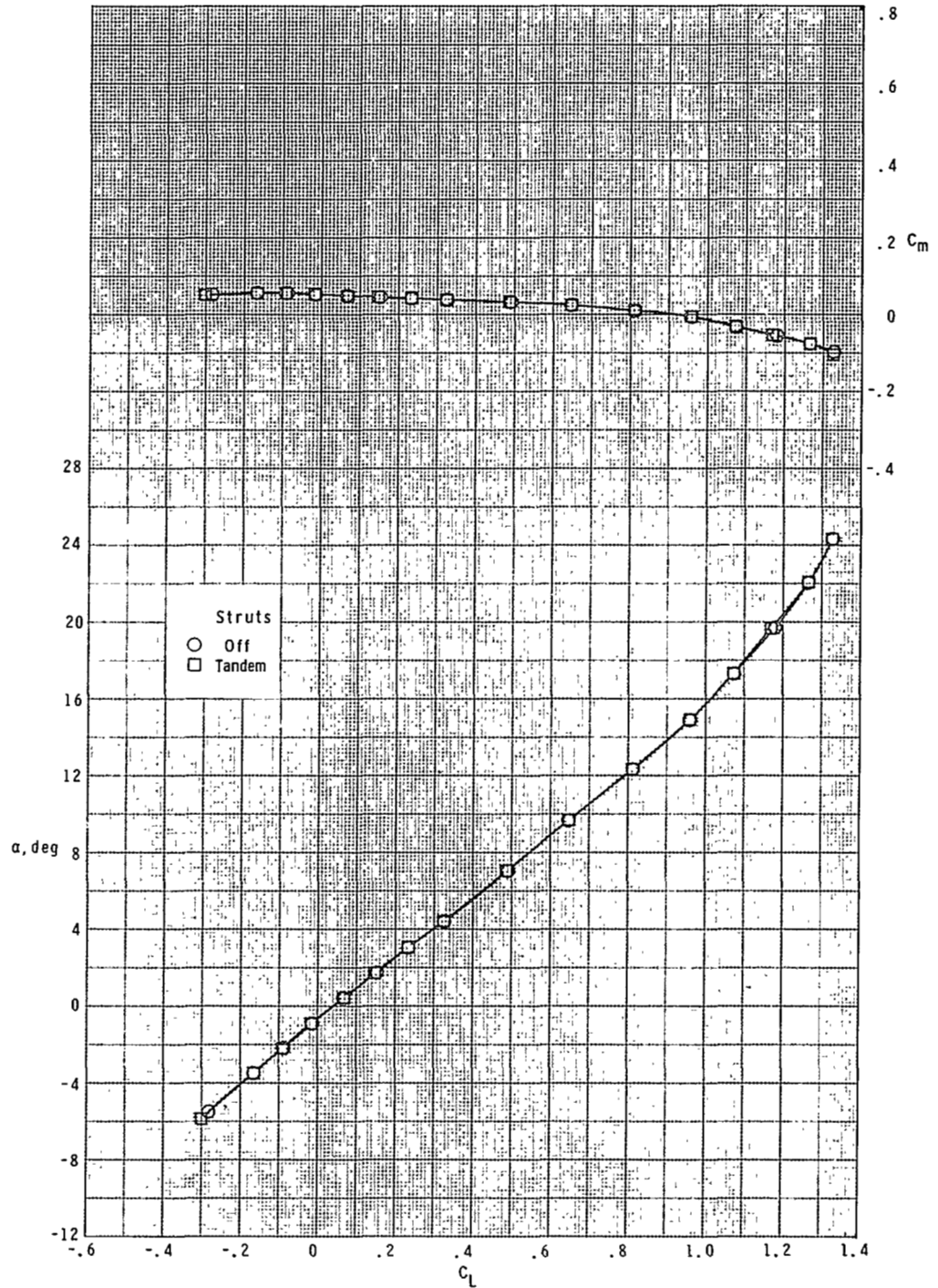
(i) Concluded.
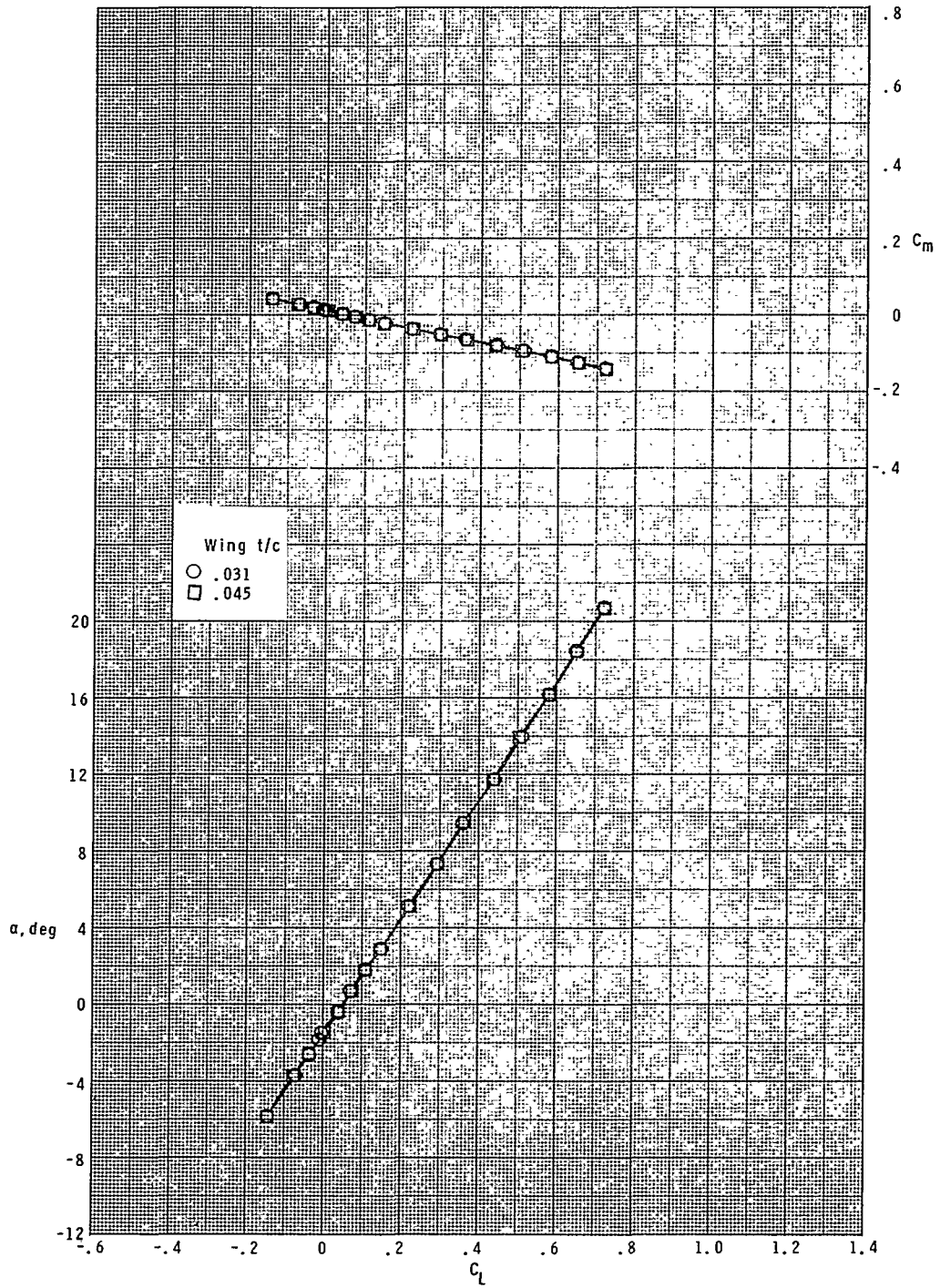
Figure 6.- Continued.

(j) M = 2.86.

Figure 6.- Continued.
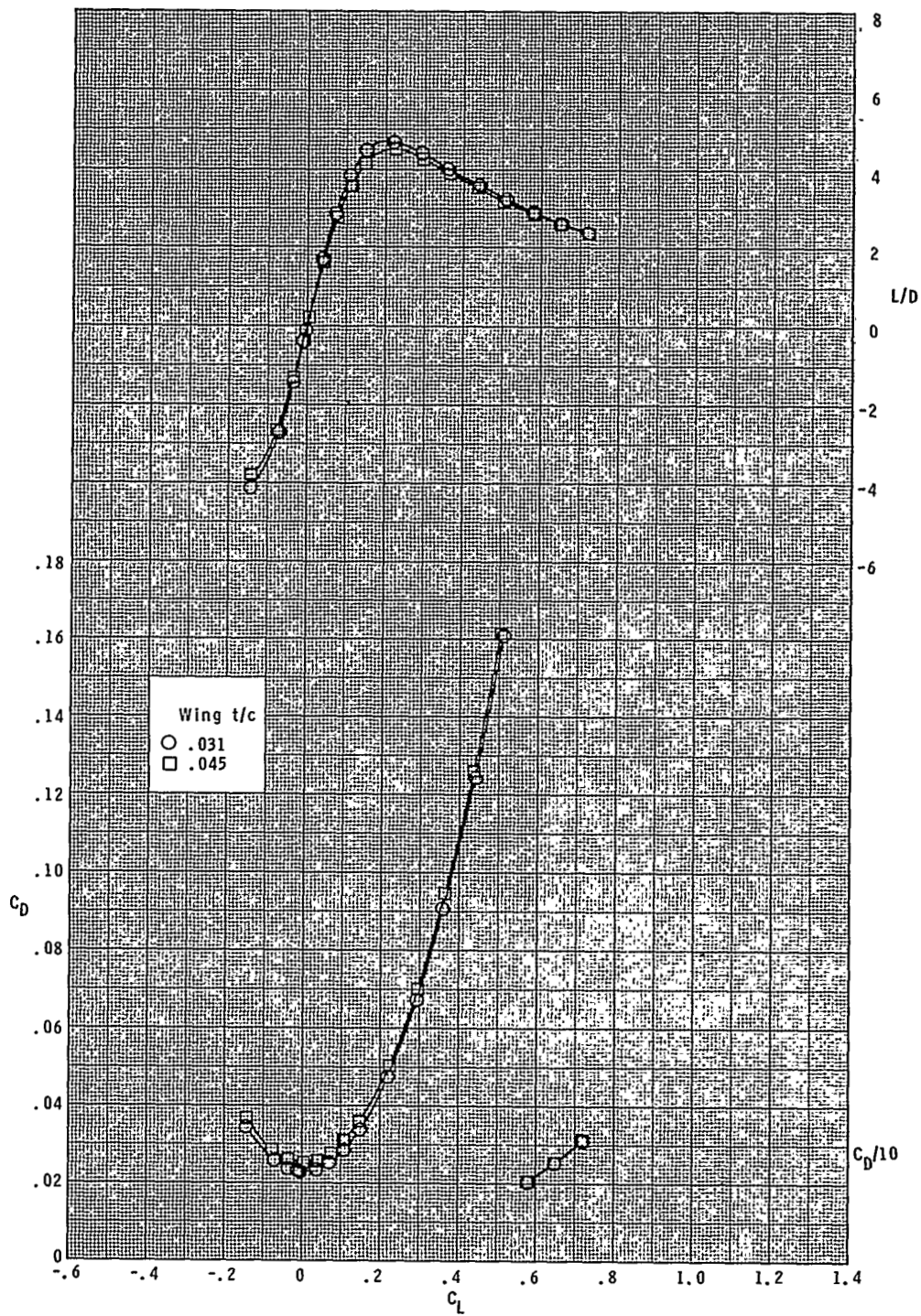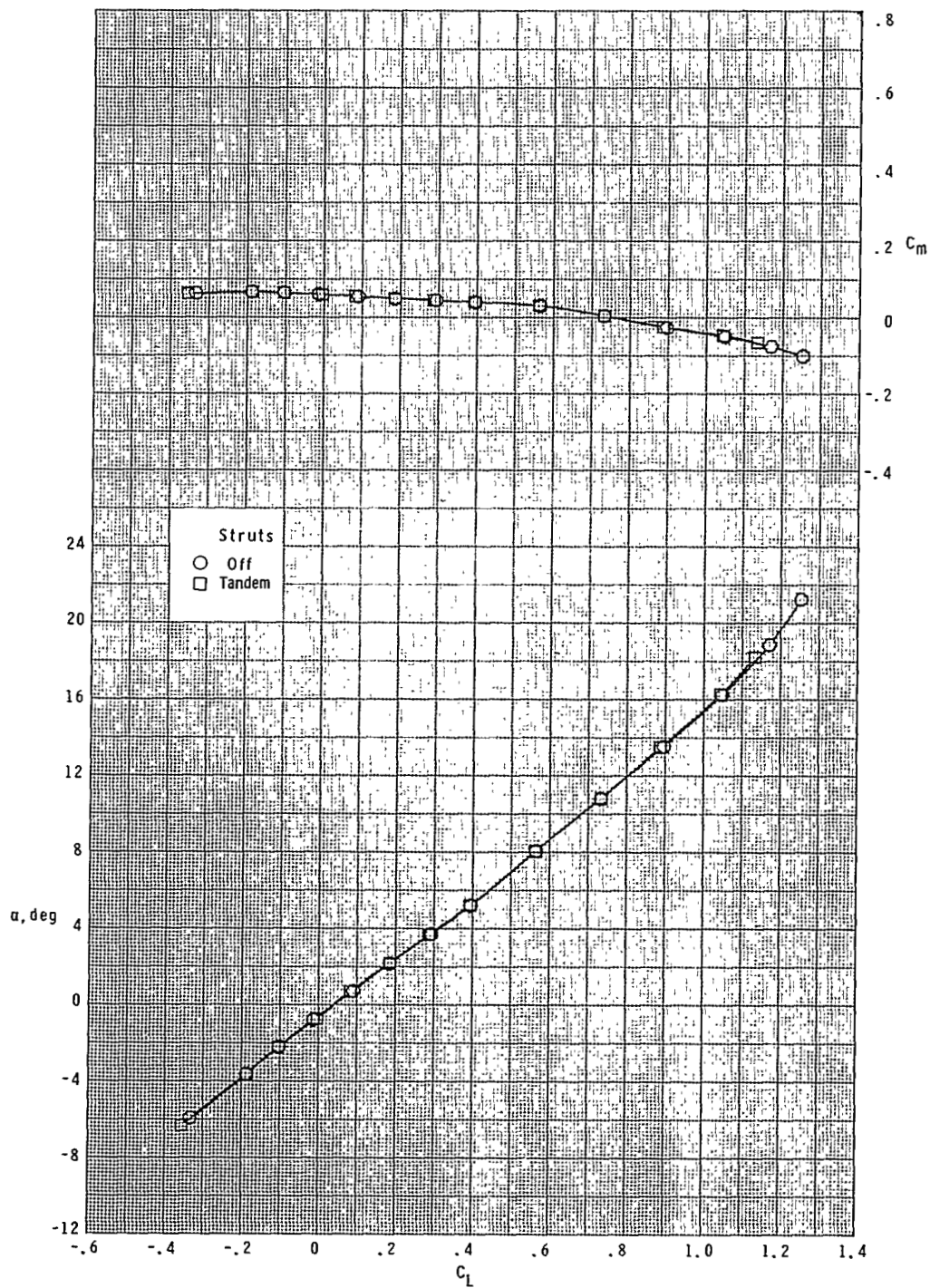
(j) Concluded.

Figure 6.- Concluded.
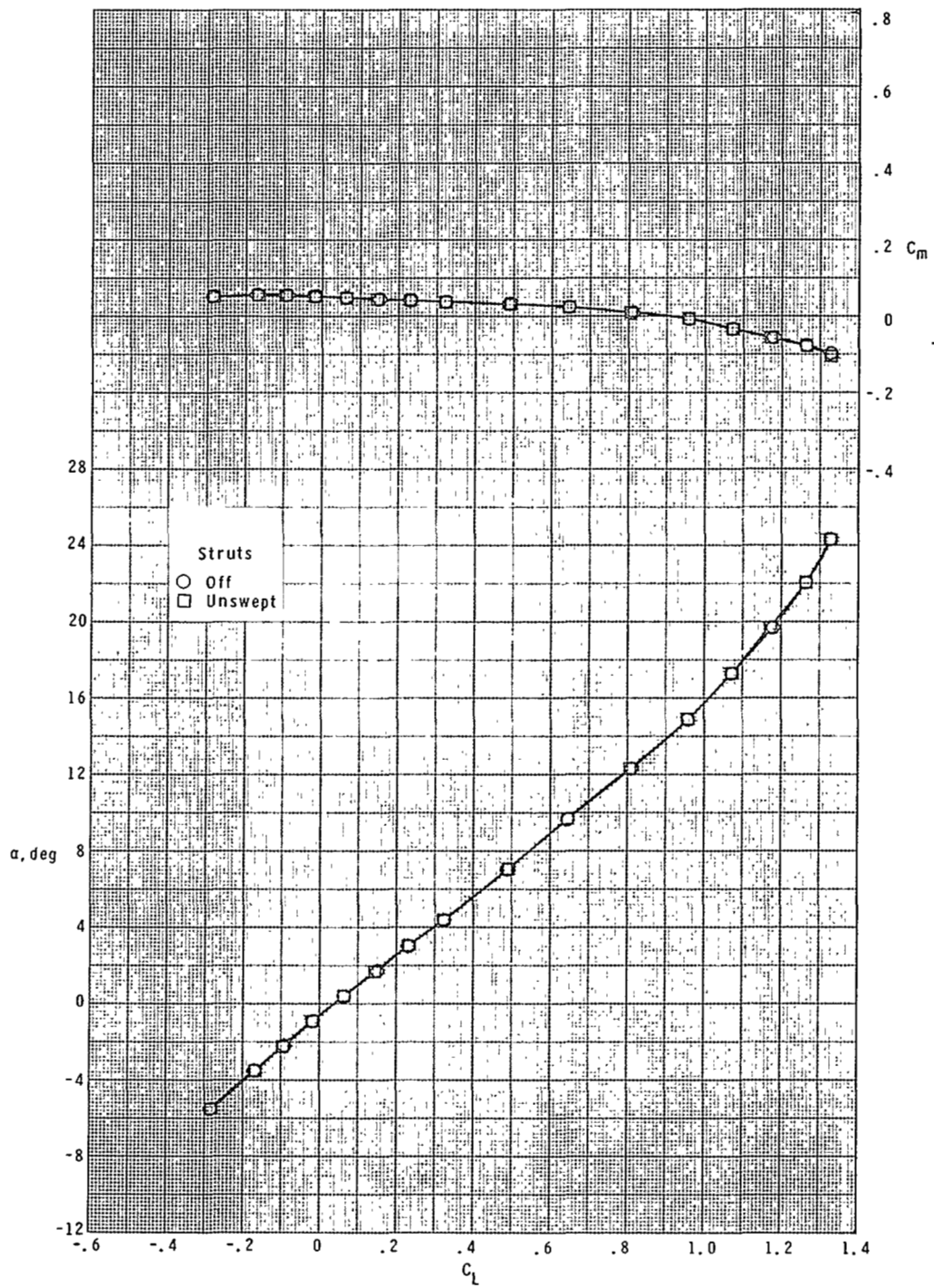
(a) M = 0.60.

Figure 7.- Effect of single unswept strut on longitudinal aerodynamic characteristics
for $\delta_h = 0^\circ$.
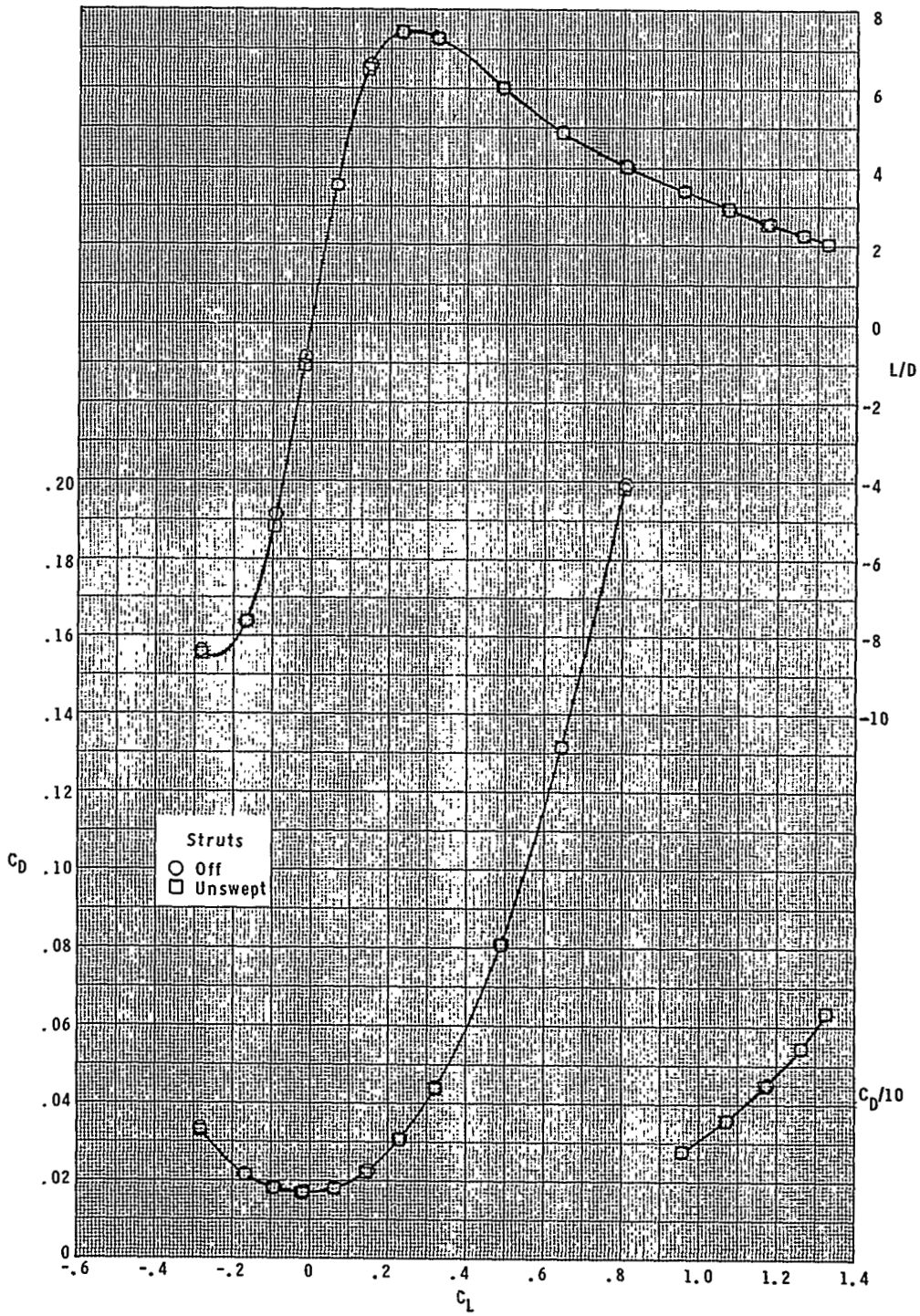
(a) Concluded.
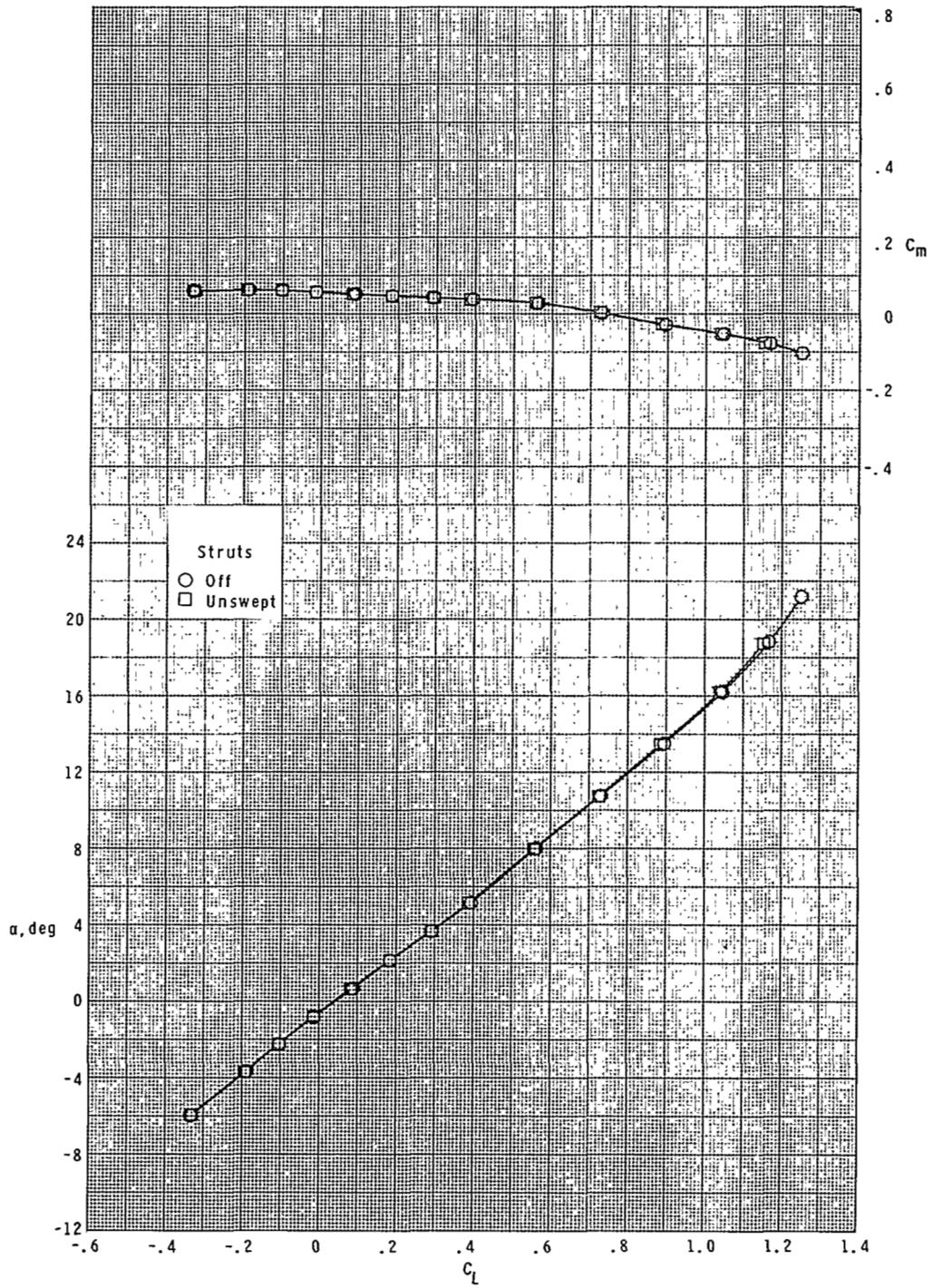
Figure 7.- Continued.

(b) M = 0.80.

Figure 7.- Continued.
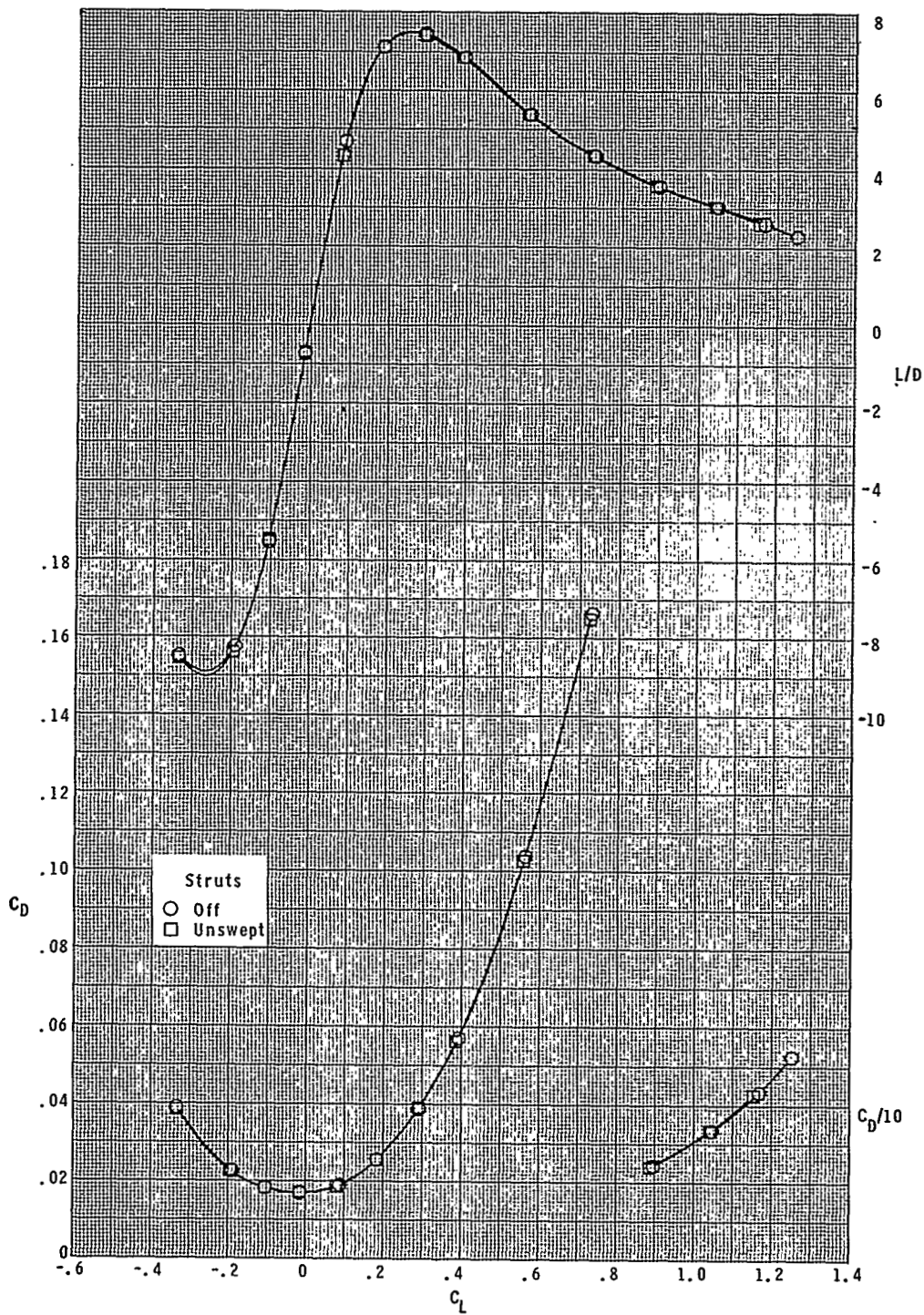
(b) Concluded.
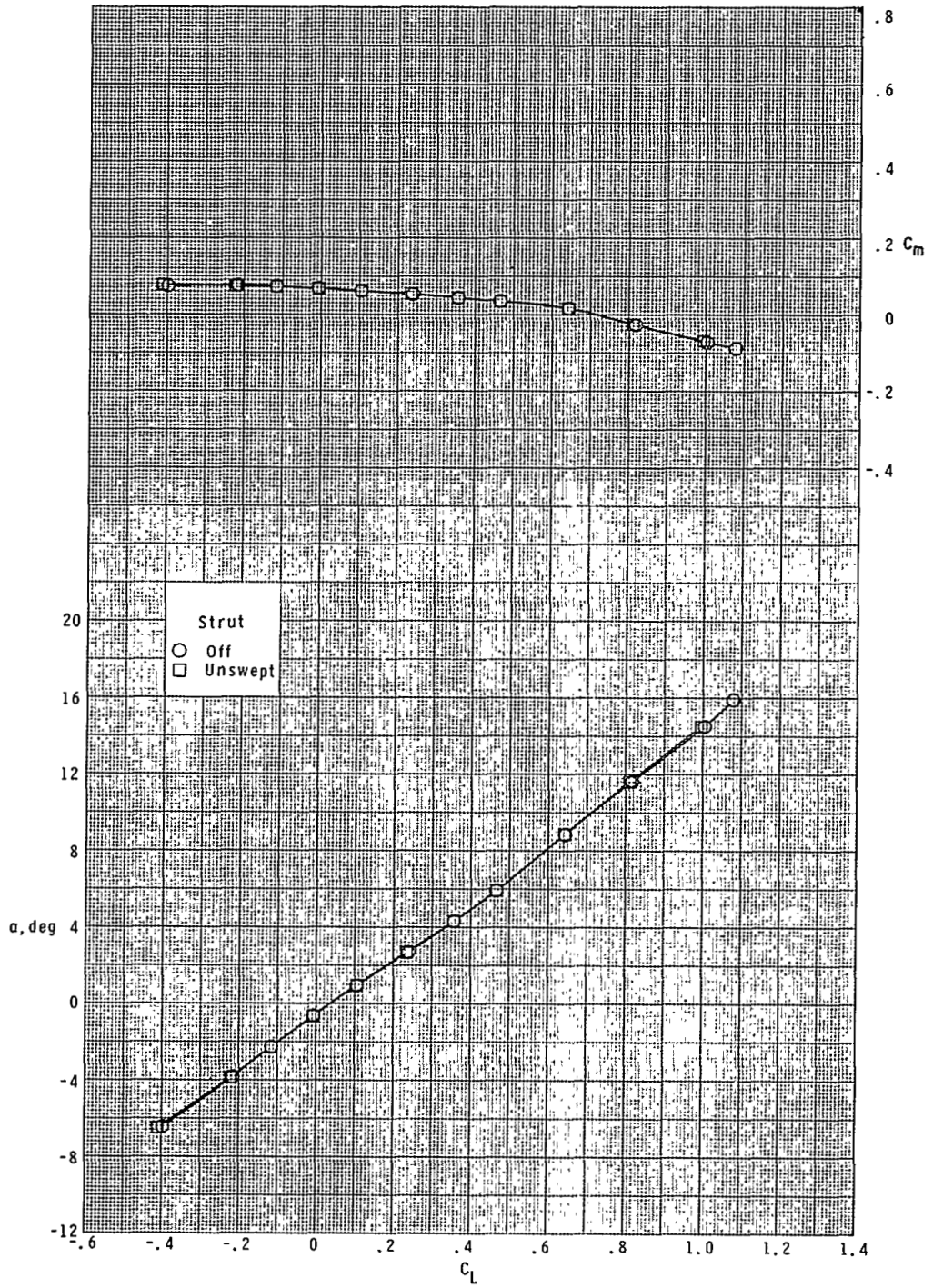
Figure 7.- Continued.

(c)   M = 0.90.

Figure 7.- Continued.
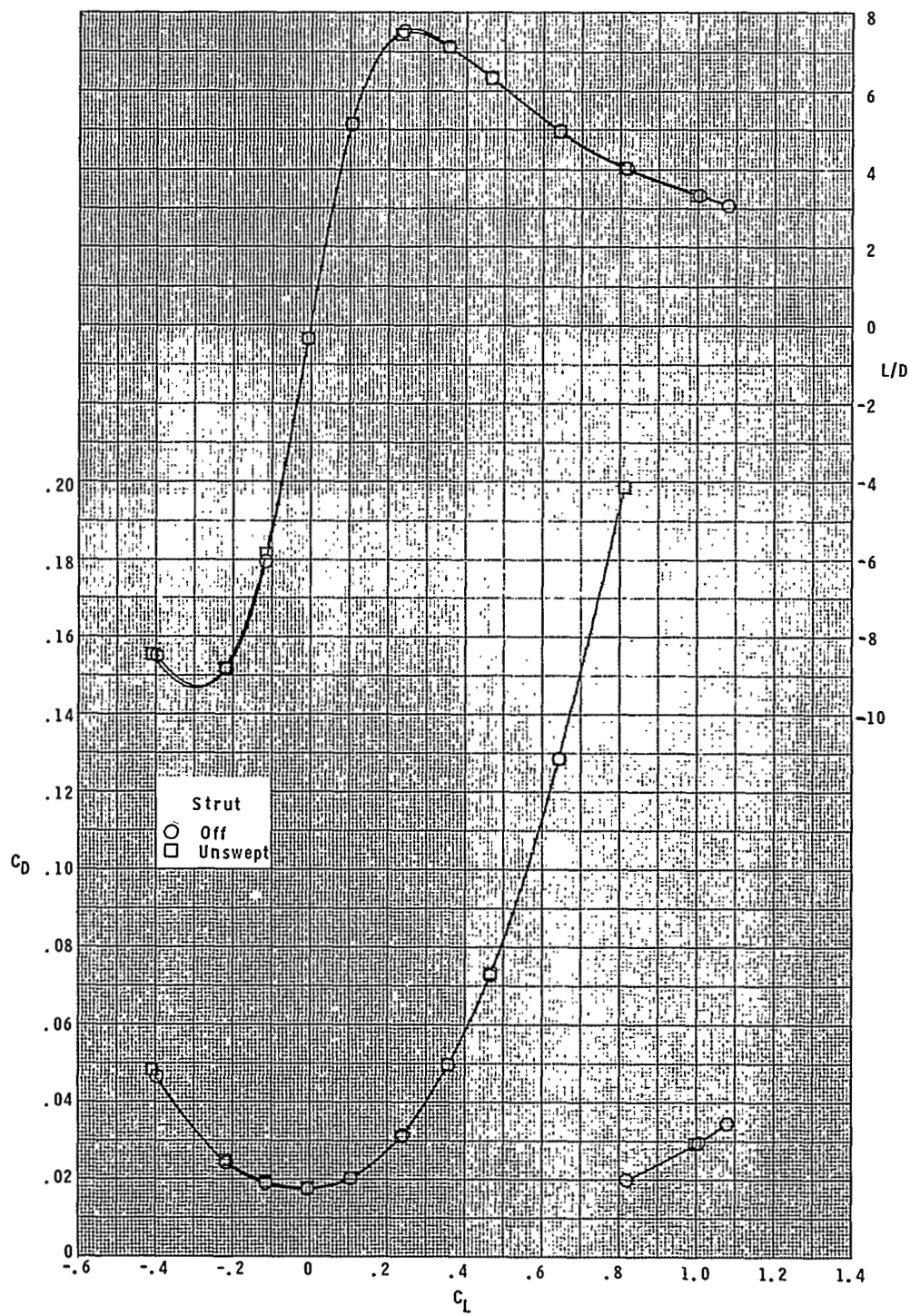
(c) Concluded.
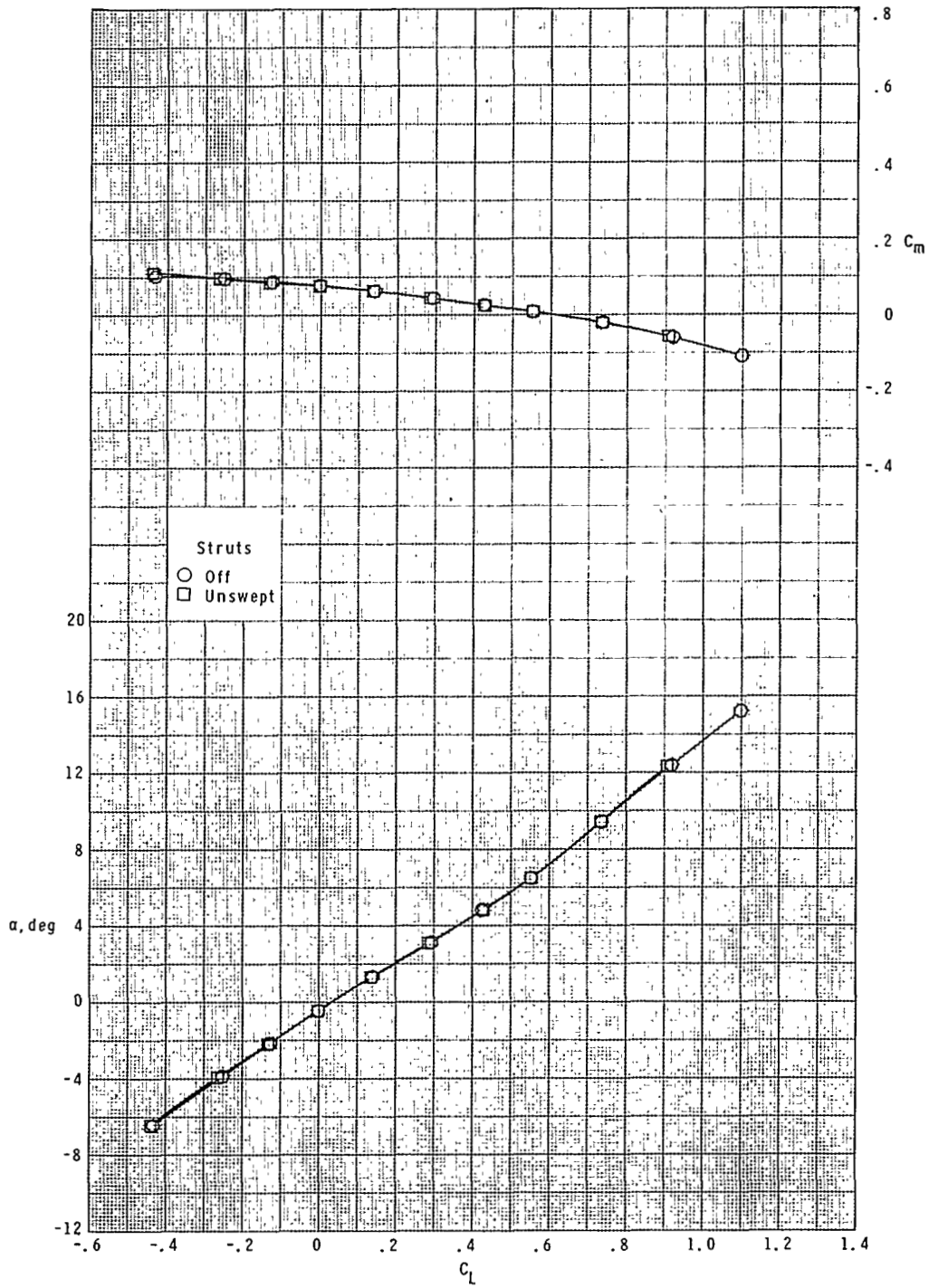
Figure 7.- Continued.

(d)   M = 0.95.

Figure 7.- Continued.
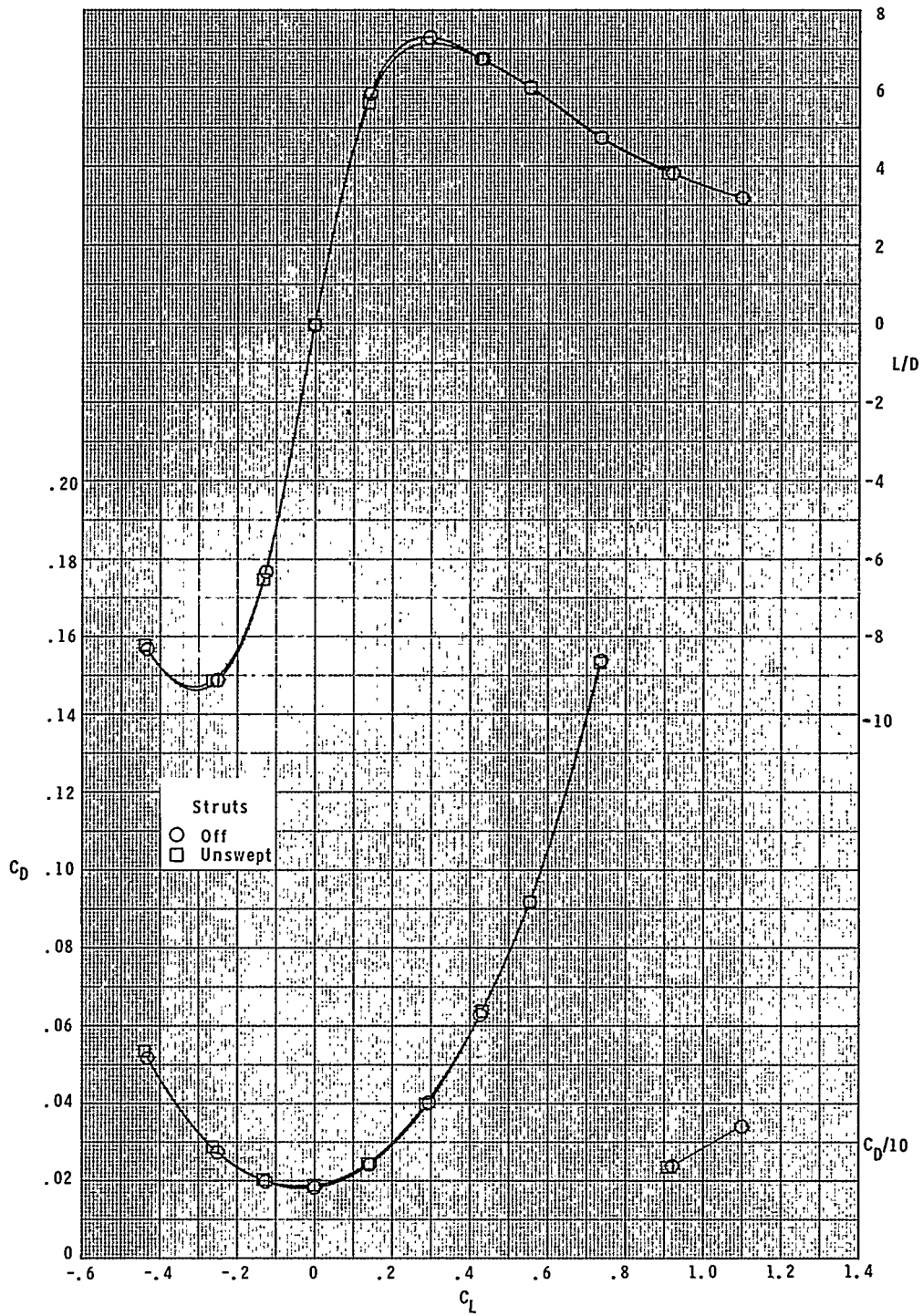
(d) Concluded.
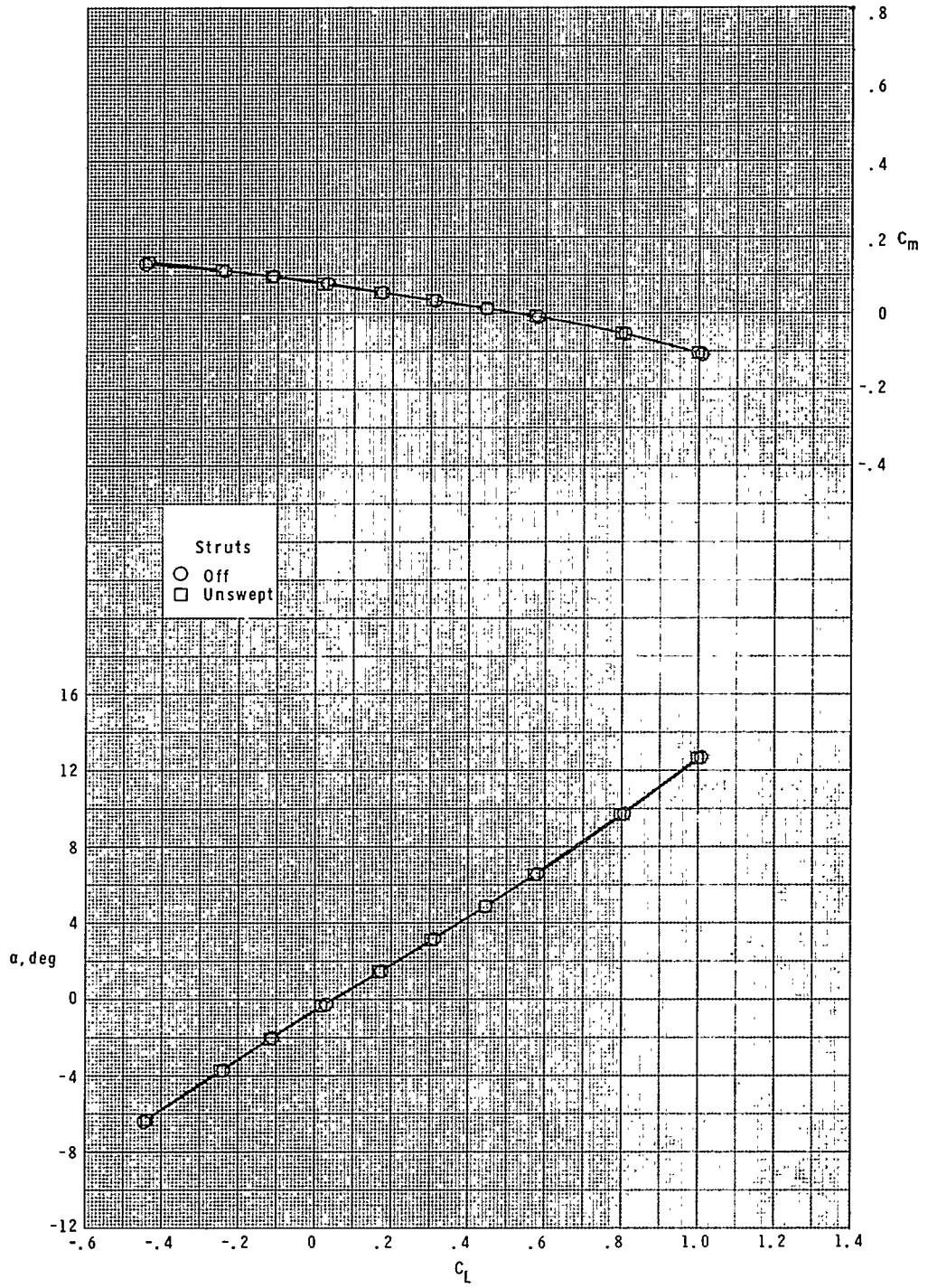
Figure 7.- Continued.

(e) M = 0.98.

Figure 7.- Continued.
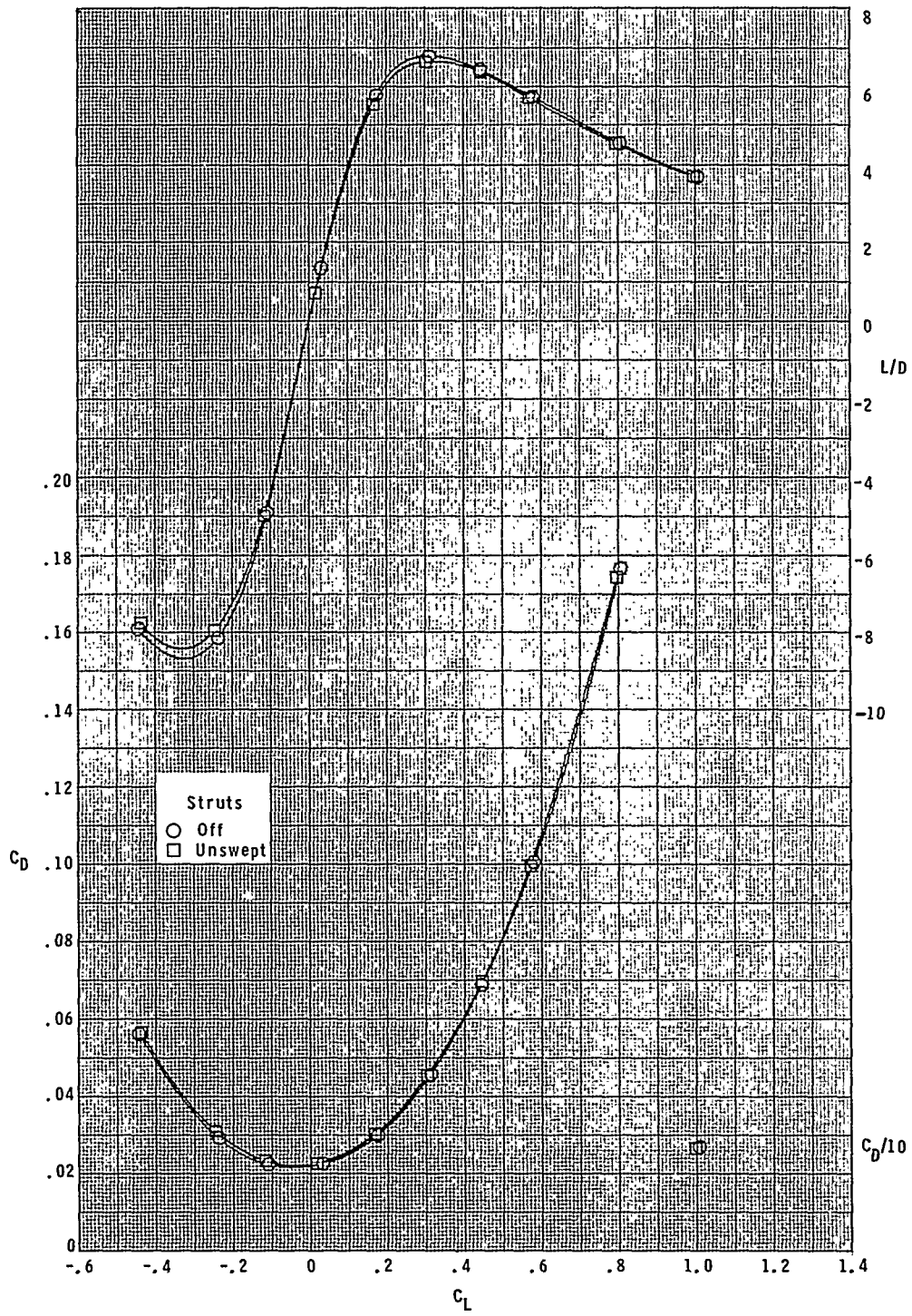
(e) Concluded.
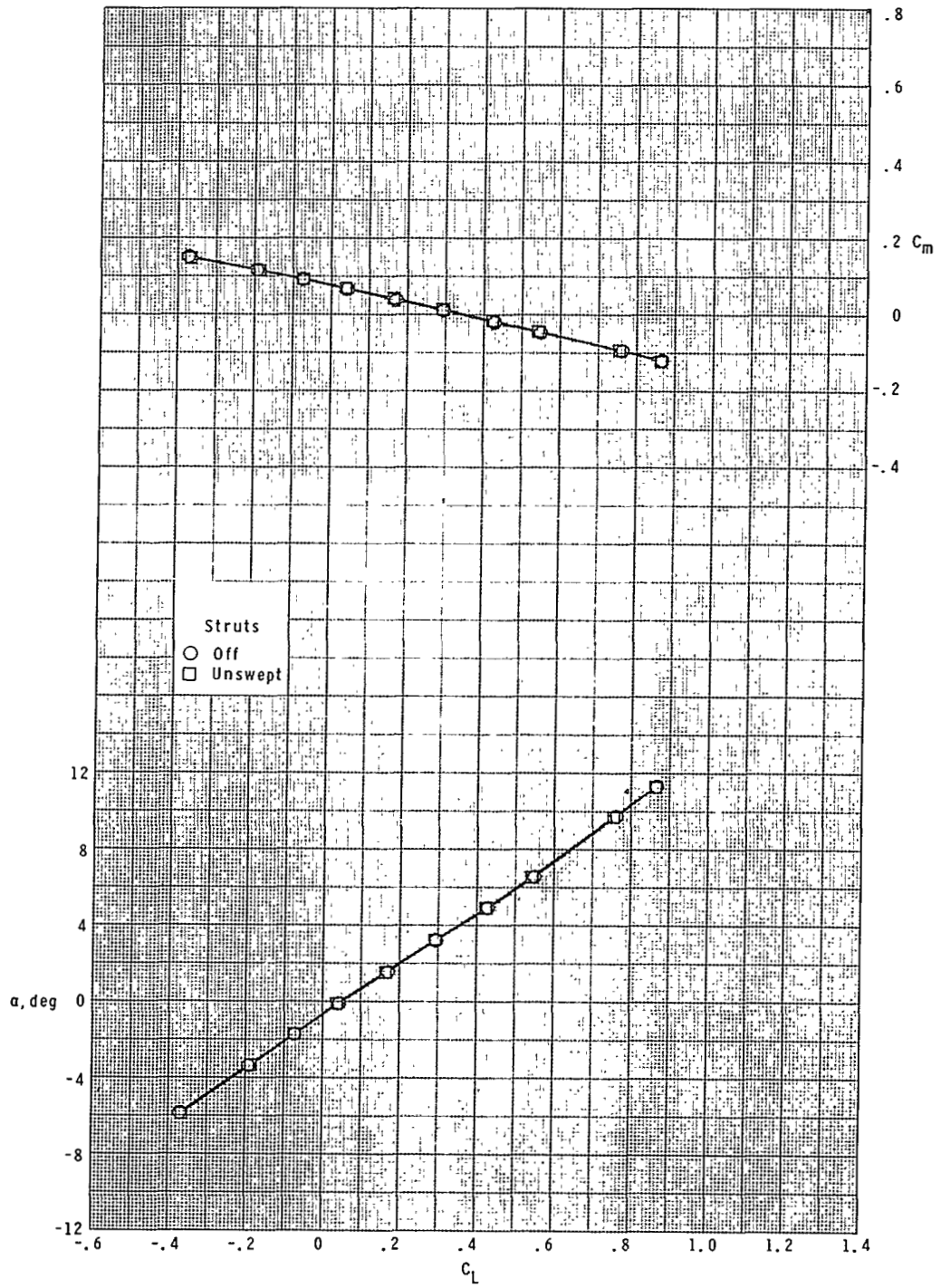
Figure 7.- Continued.

(f)   M = 1.20.

Figure 7.- Continued.
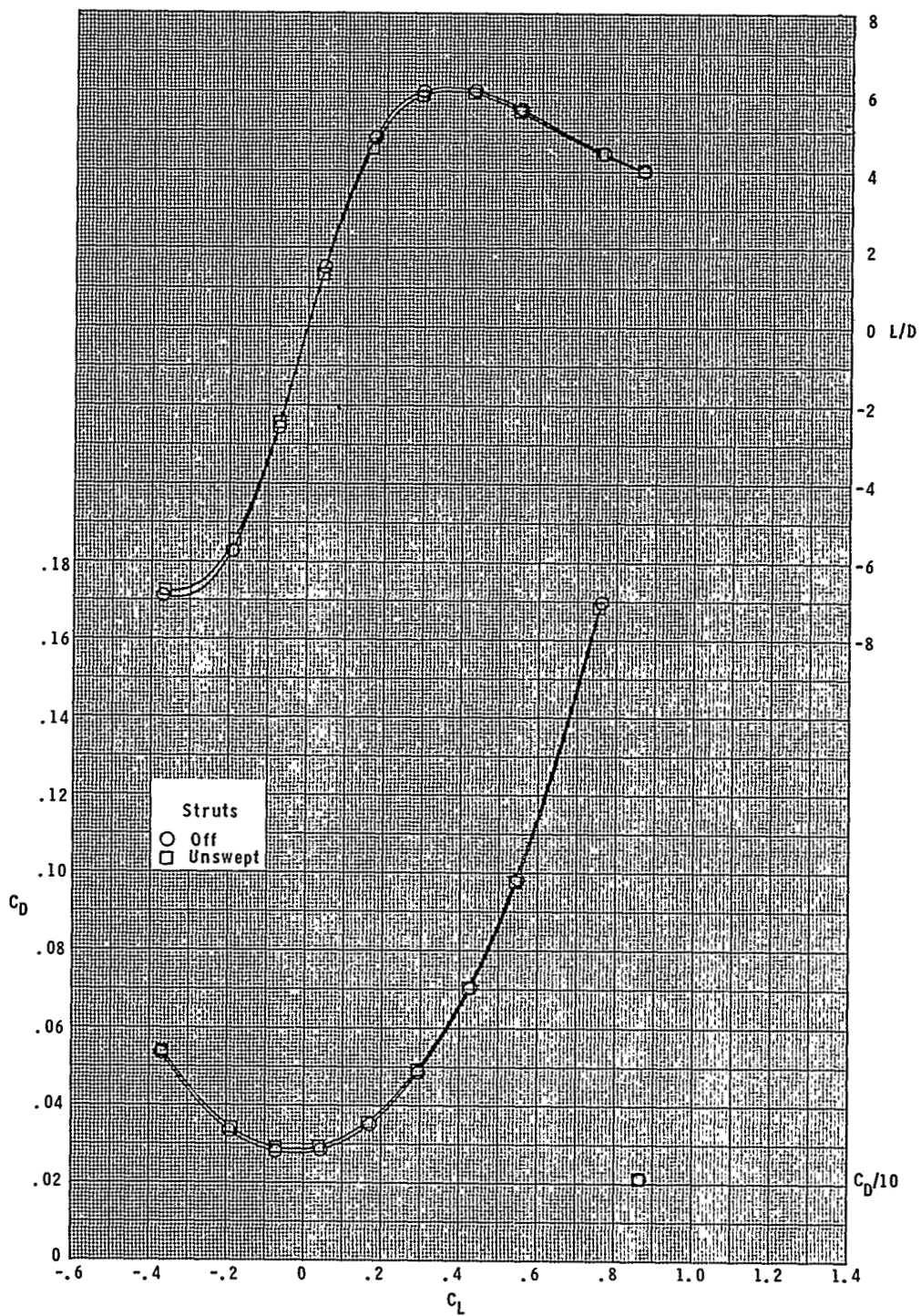
(f) Concluded.
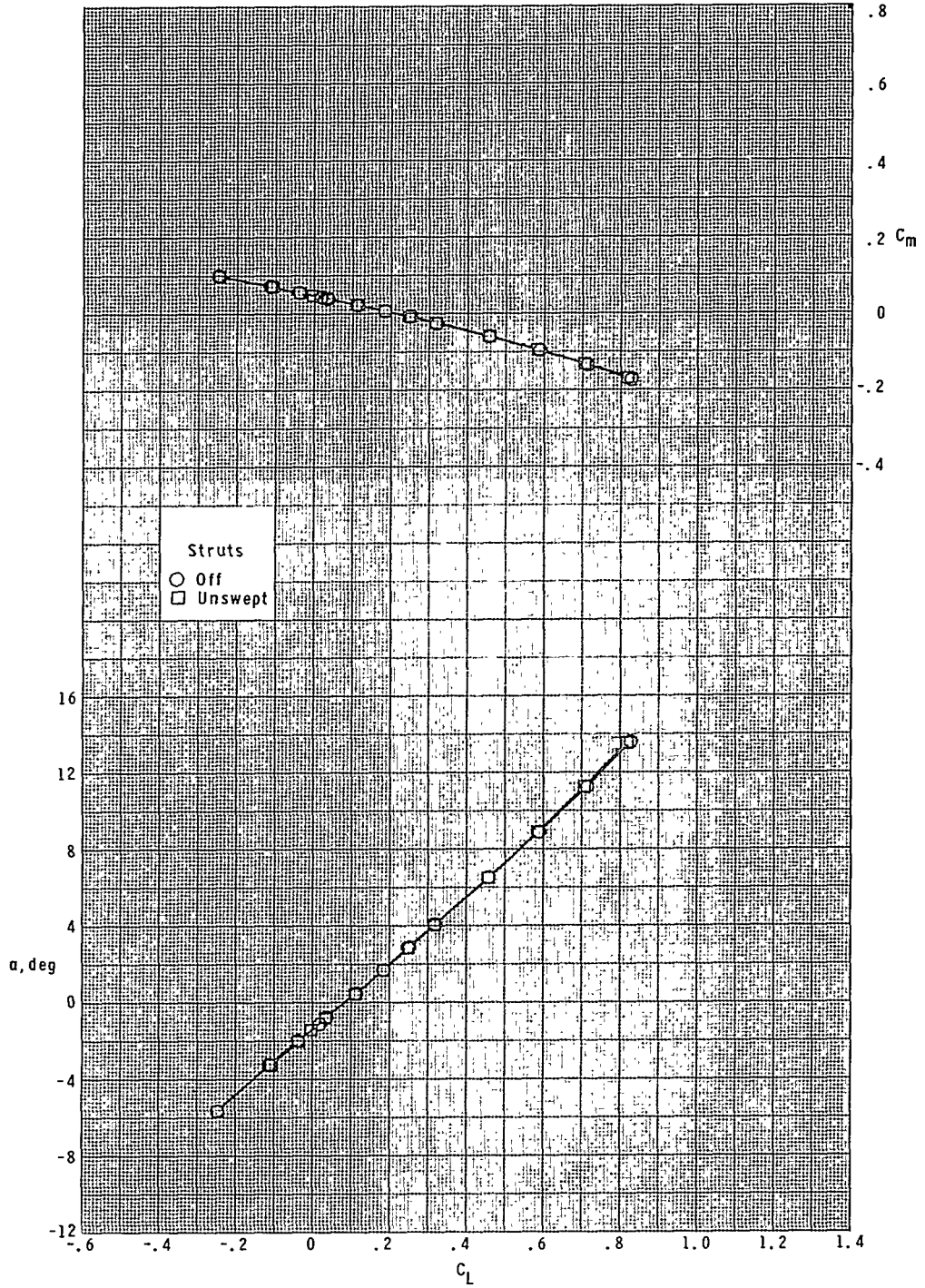
Figure 7.- Continued.

(g)   M = 1.60.

Figure 7.- Continued.
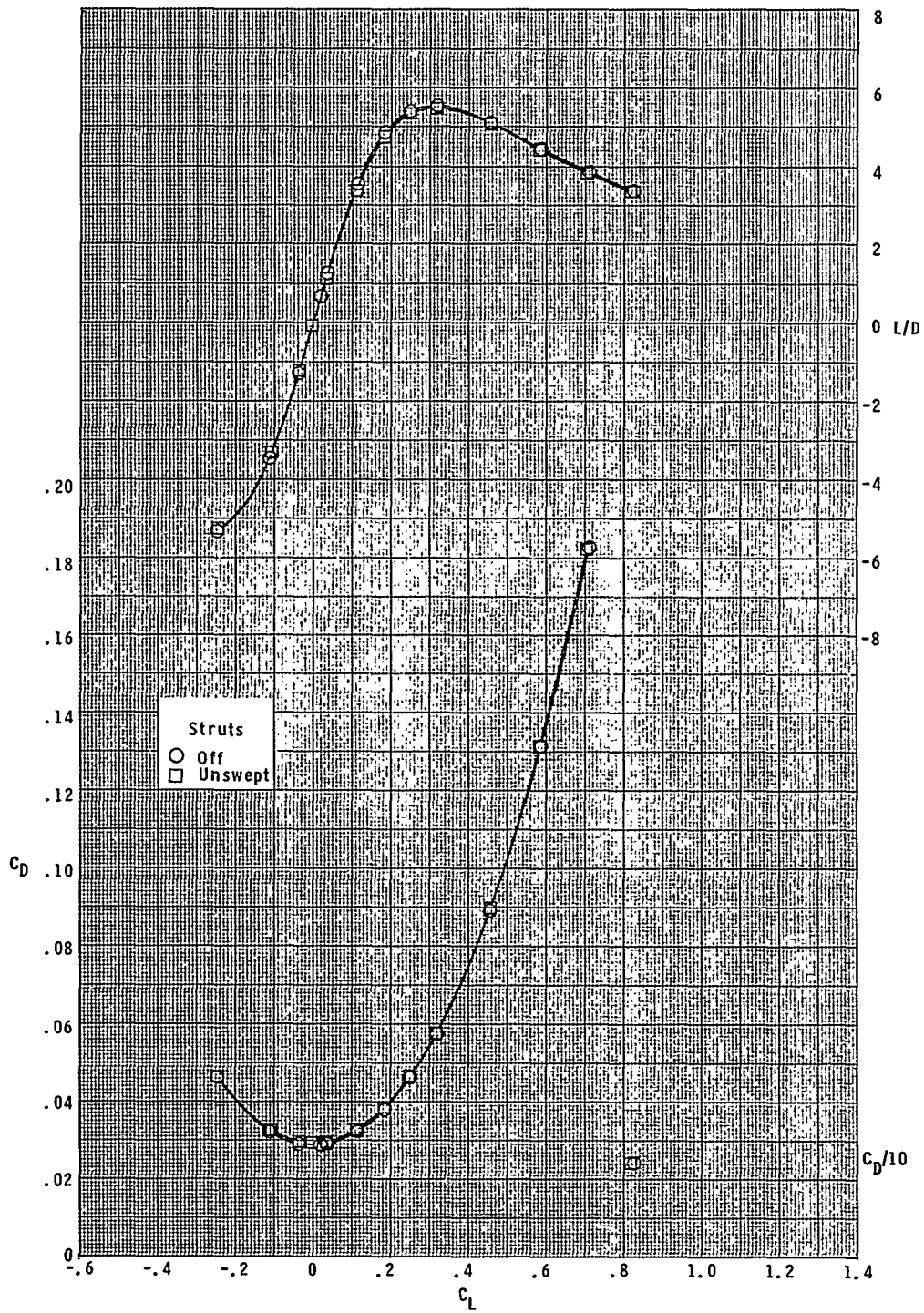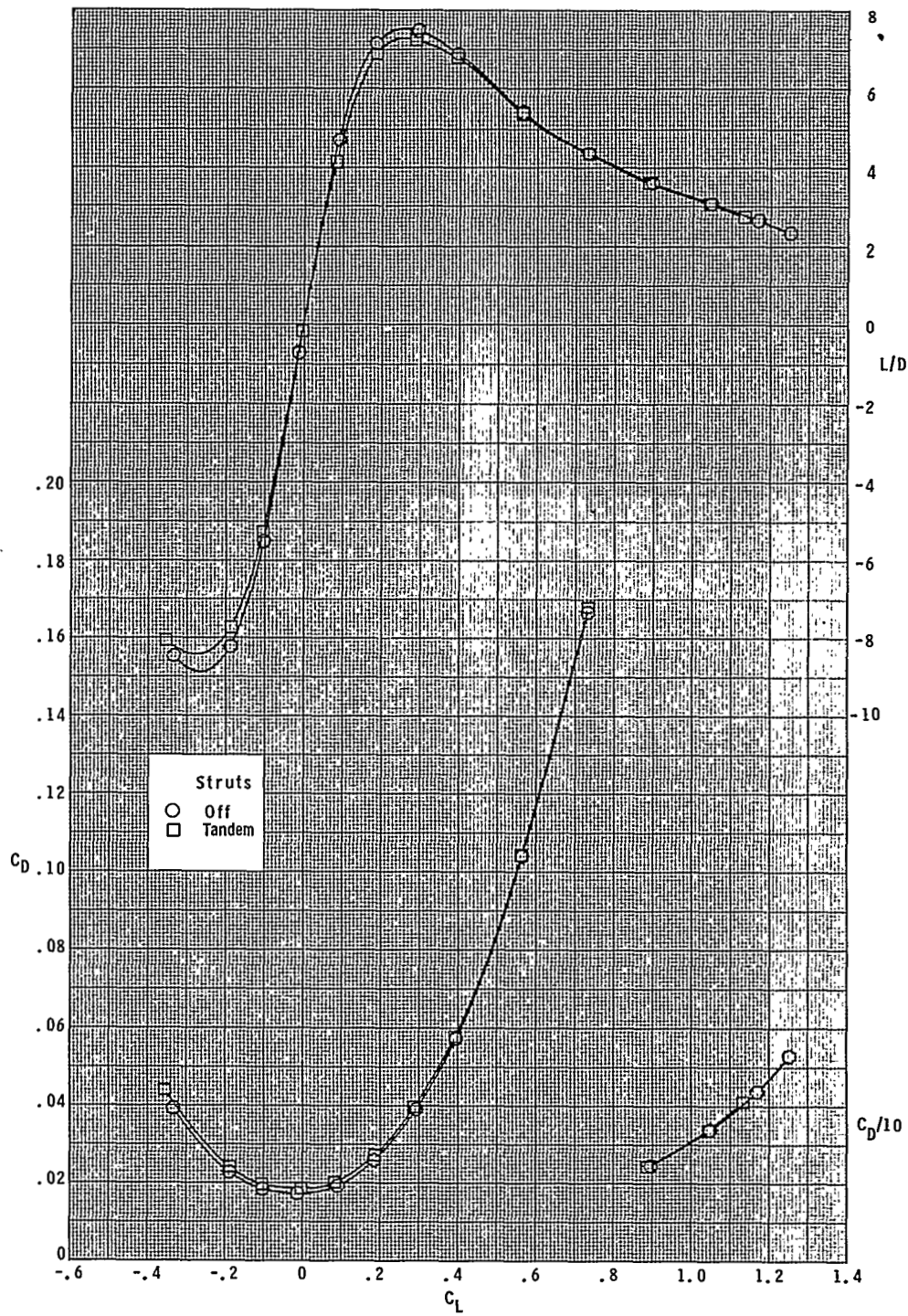
(g) Concluded.
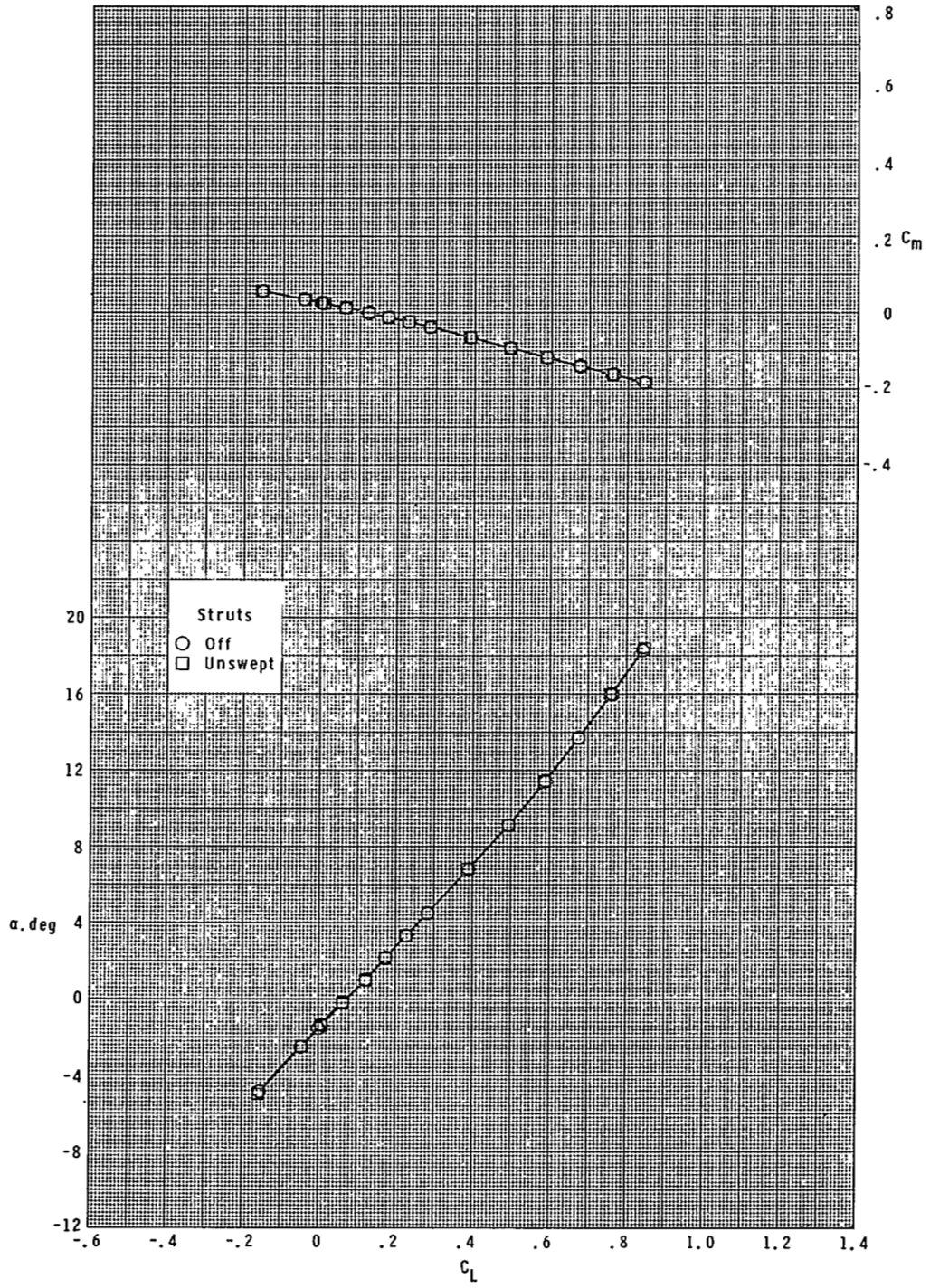
Figure 7.- Continued.

(h) M = 2.00.

Figure 7.- Continued.
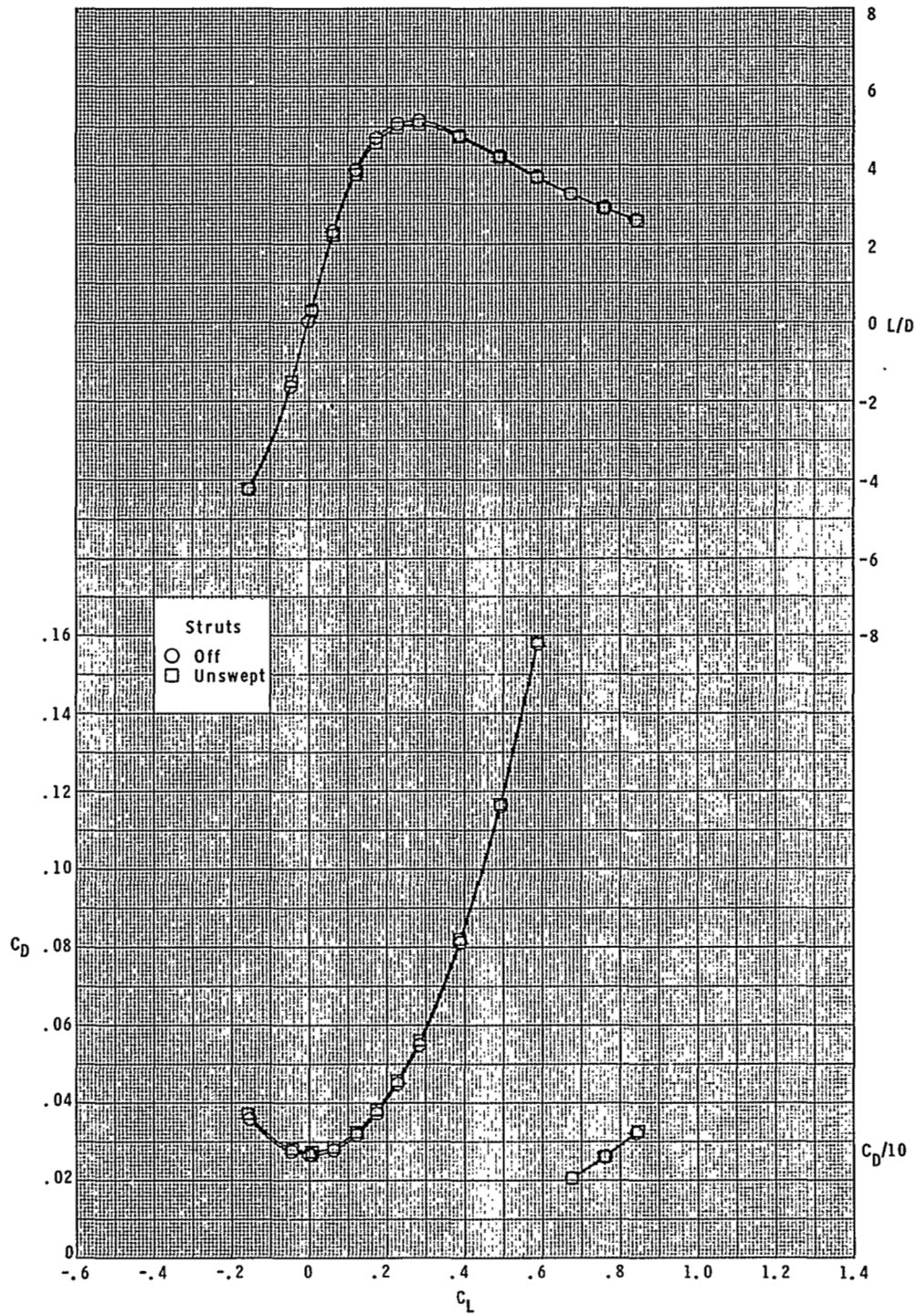
(h) Concluded.
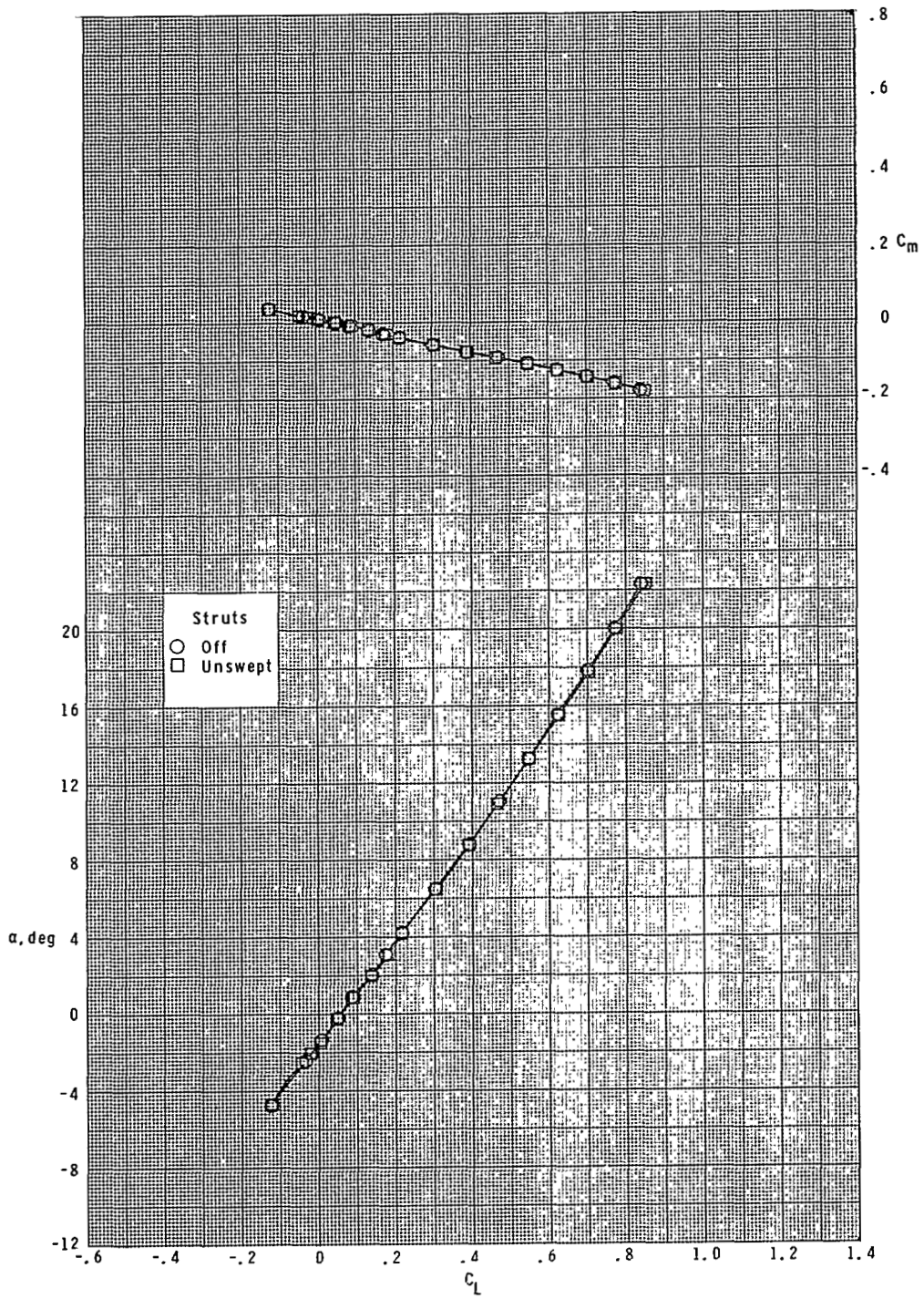
Figure 7.- Continued.

(i) M = 2.50.

Figure 7.- Continued.
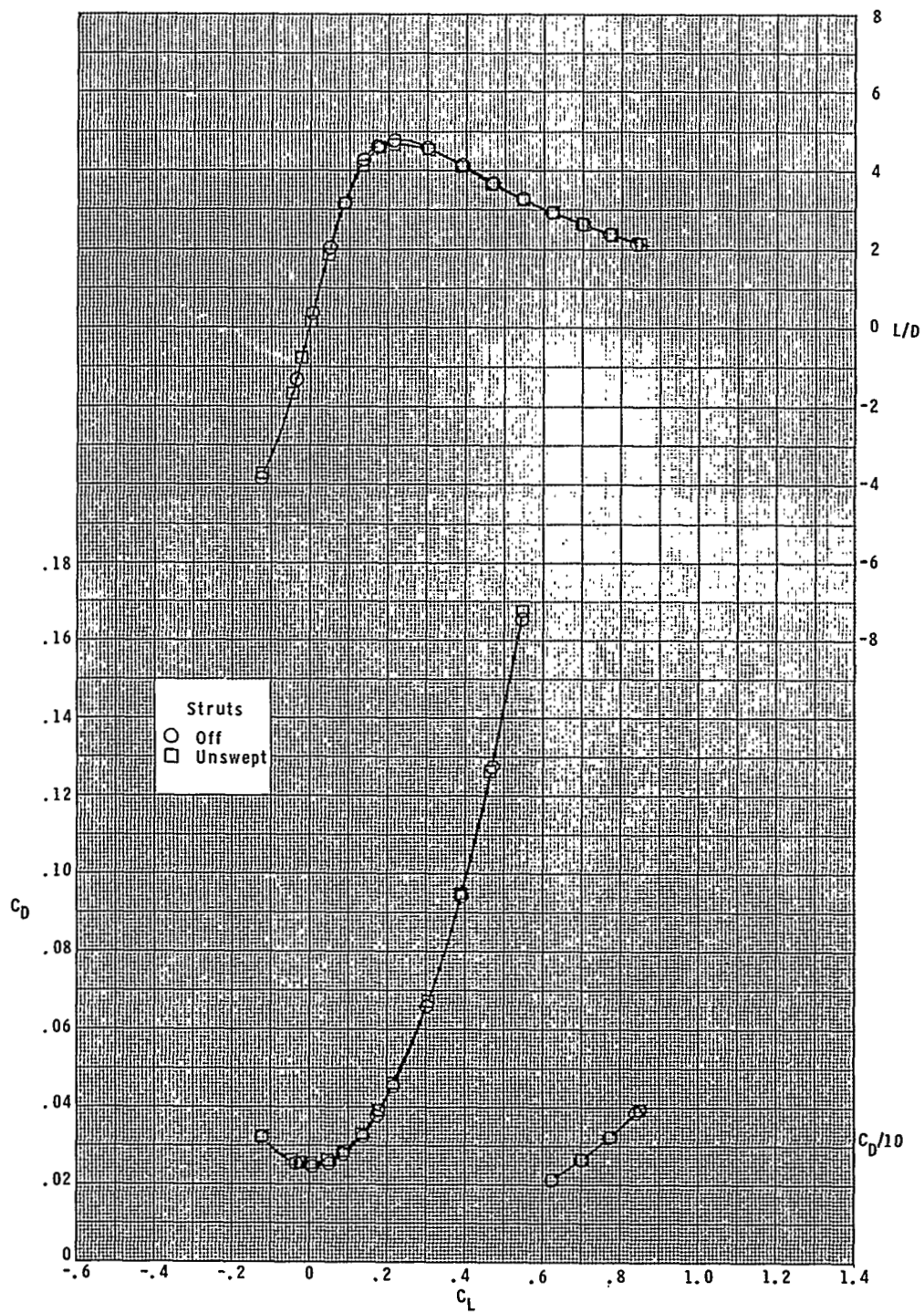
(i) Concluded.
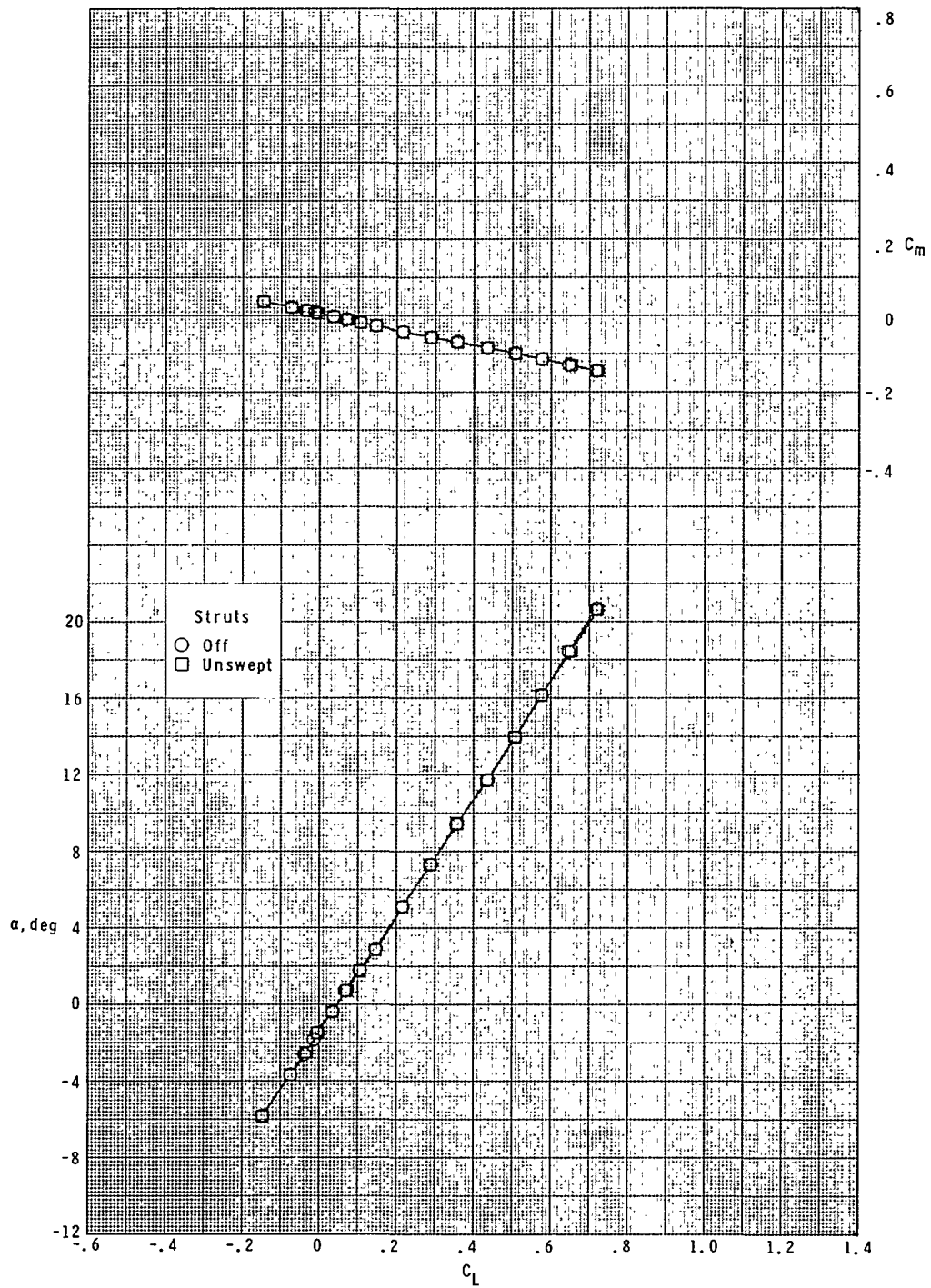
Figure 7.- Continued.

(j)   M = 2.86.

Figure 7.- Continued.
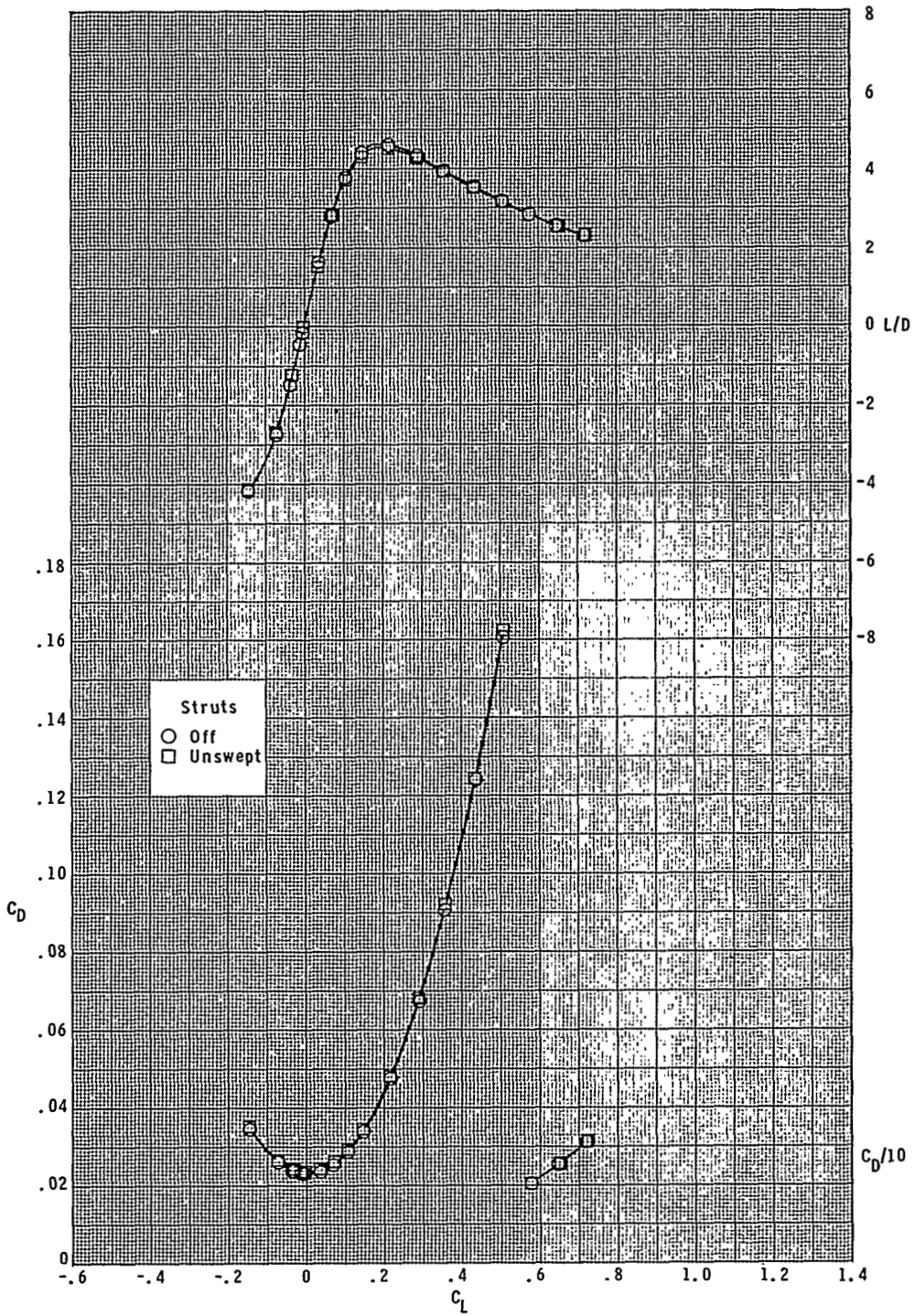
(j) Concluded.

Figure 7.- Concluded.
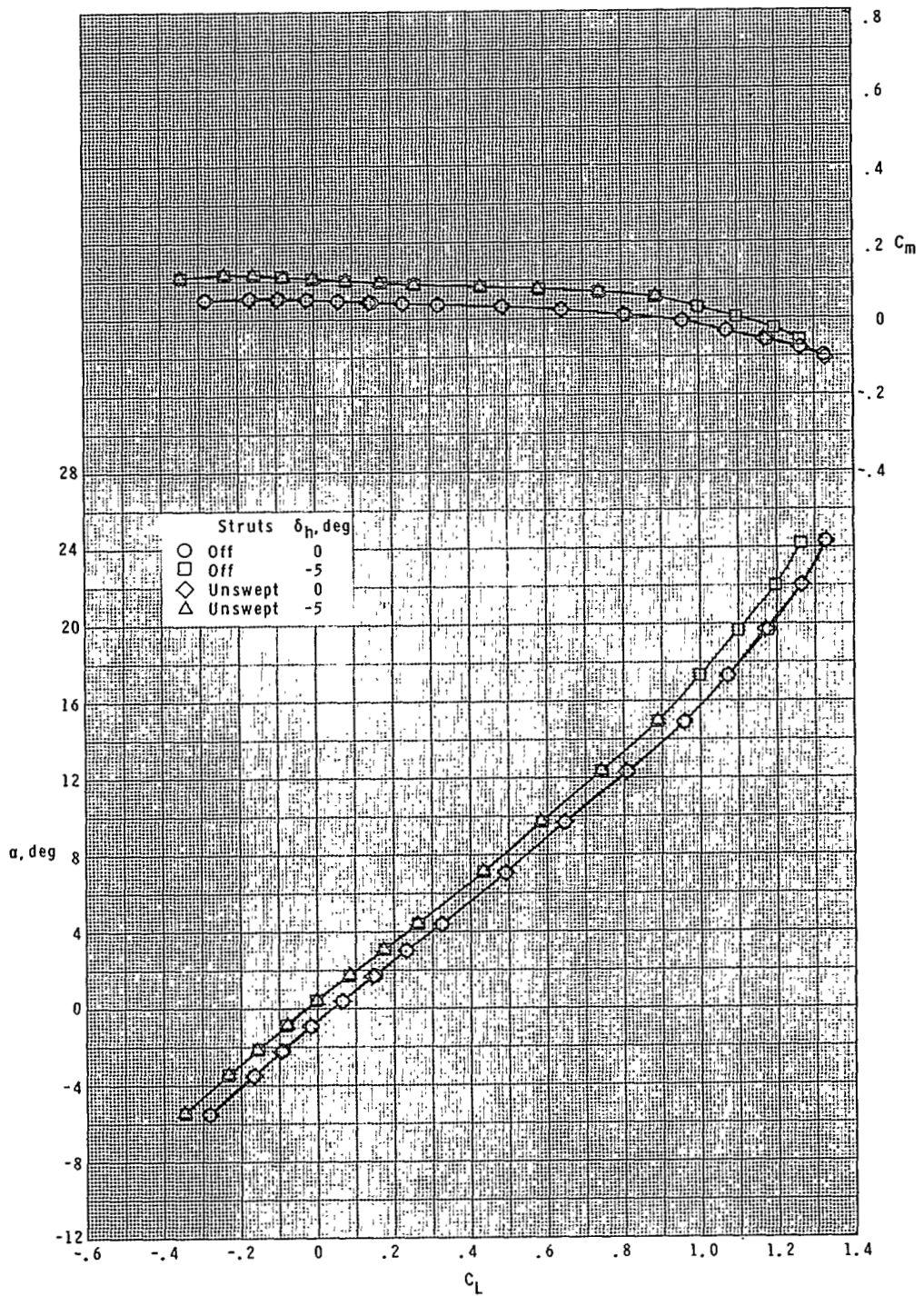
(a) M = 0.60.

Figure 8.- Effect of single unswept strut on longitudinal control characteristics for $\delta_h = 0^{\circ}$ and -5°.
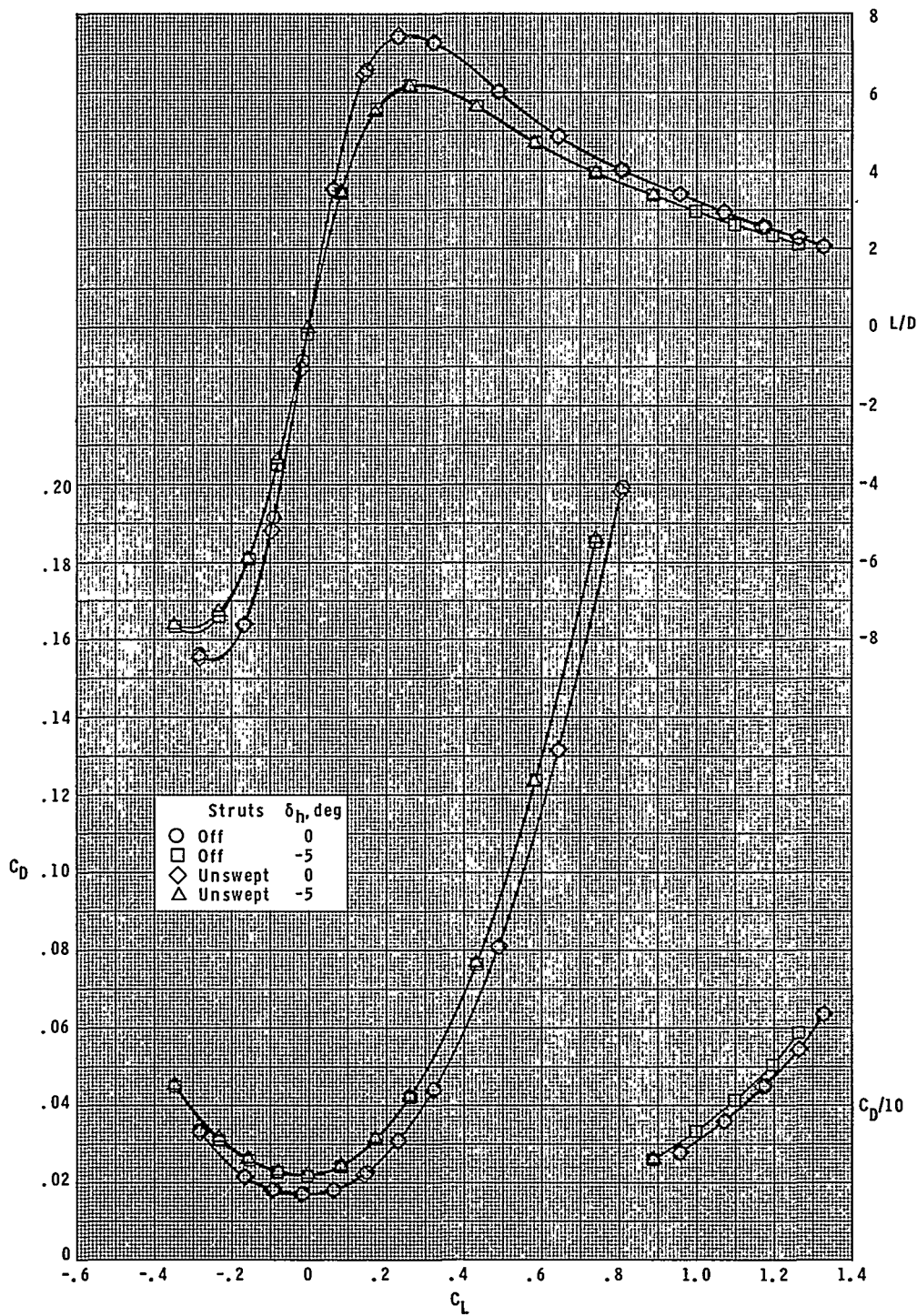
(a) Concluded.

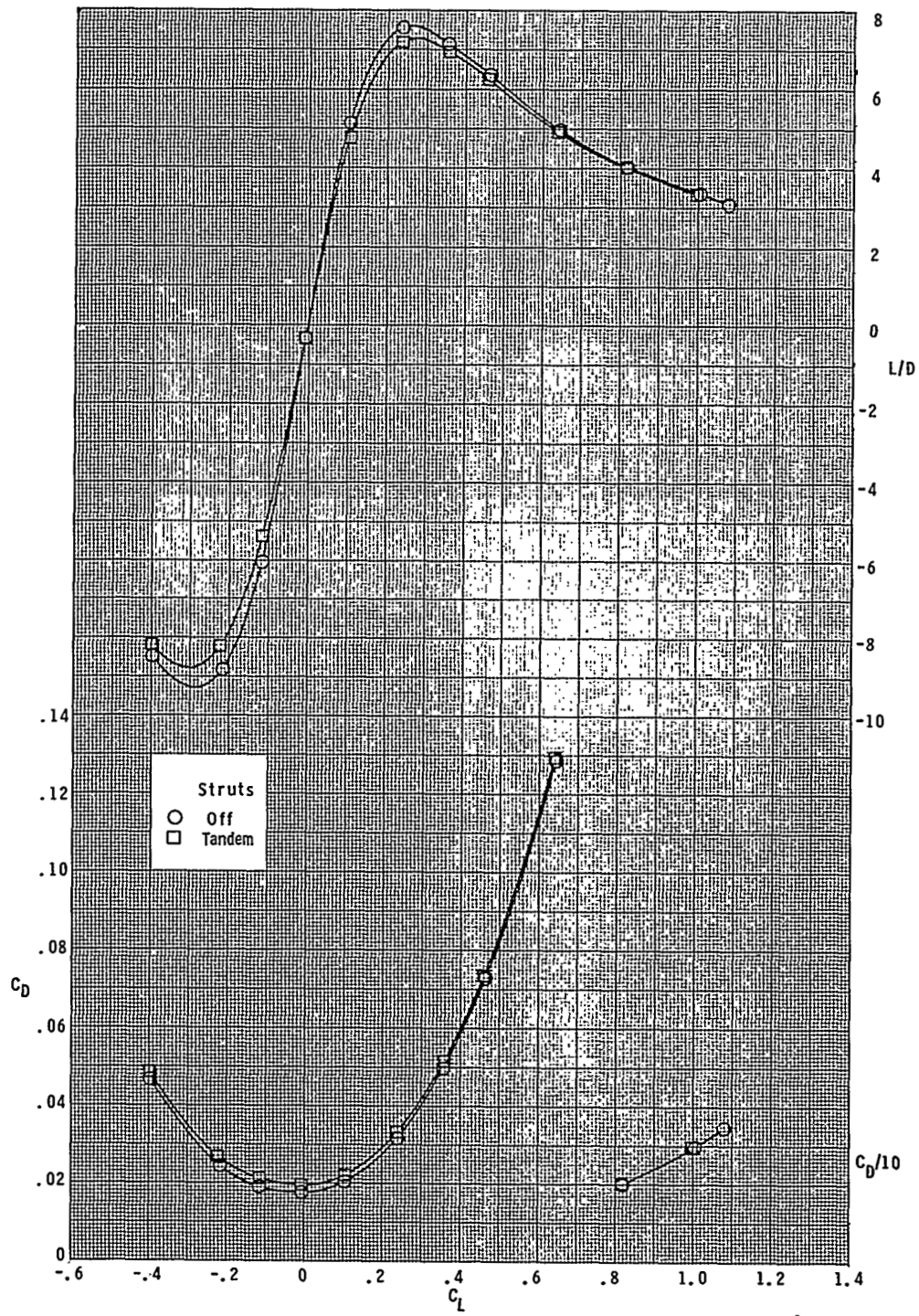Figure 8.- Continued.
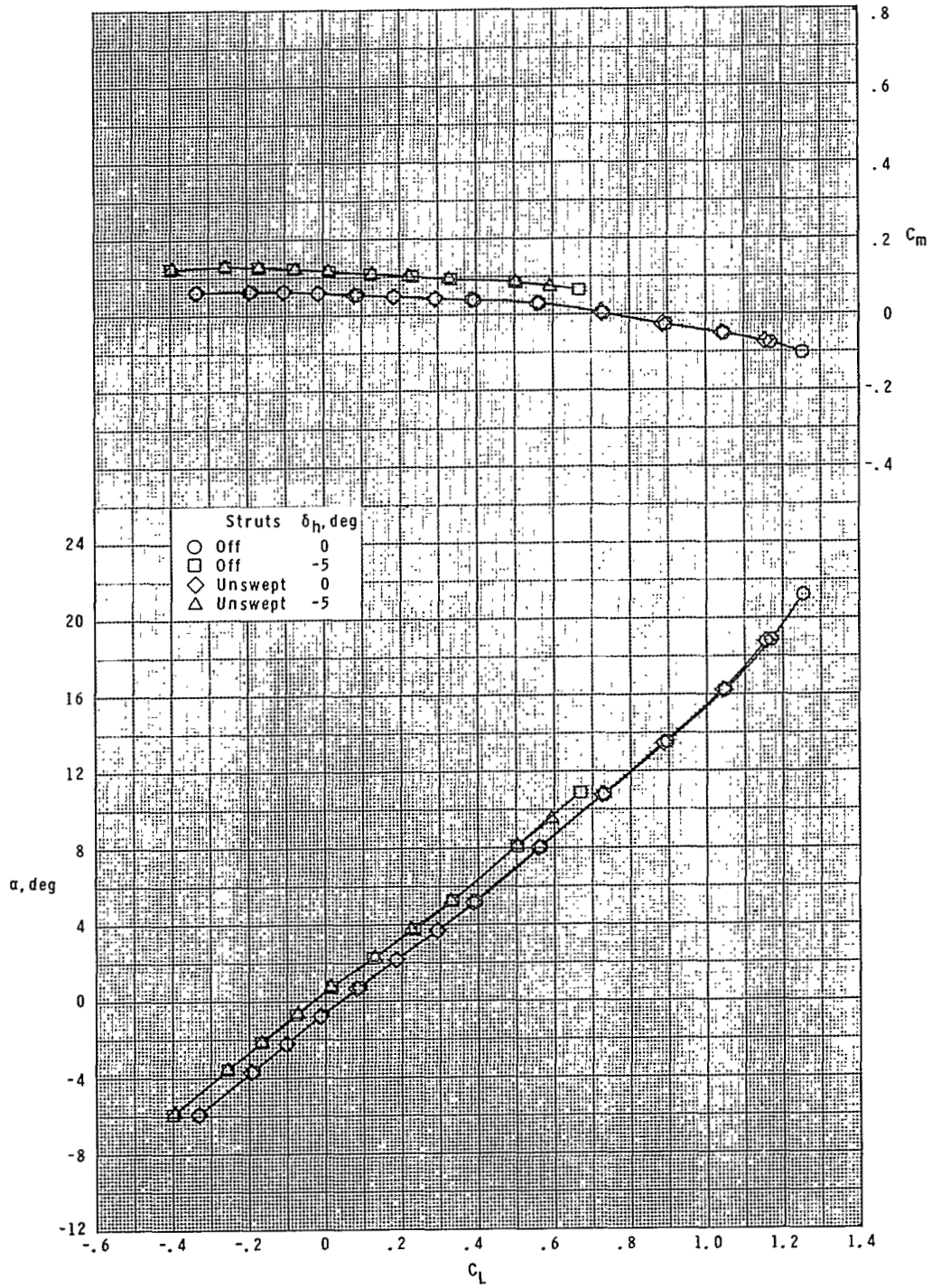
(b)   M = 0.80.

Figure 8.- Continued.
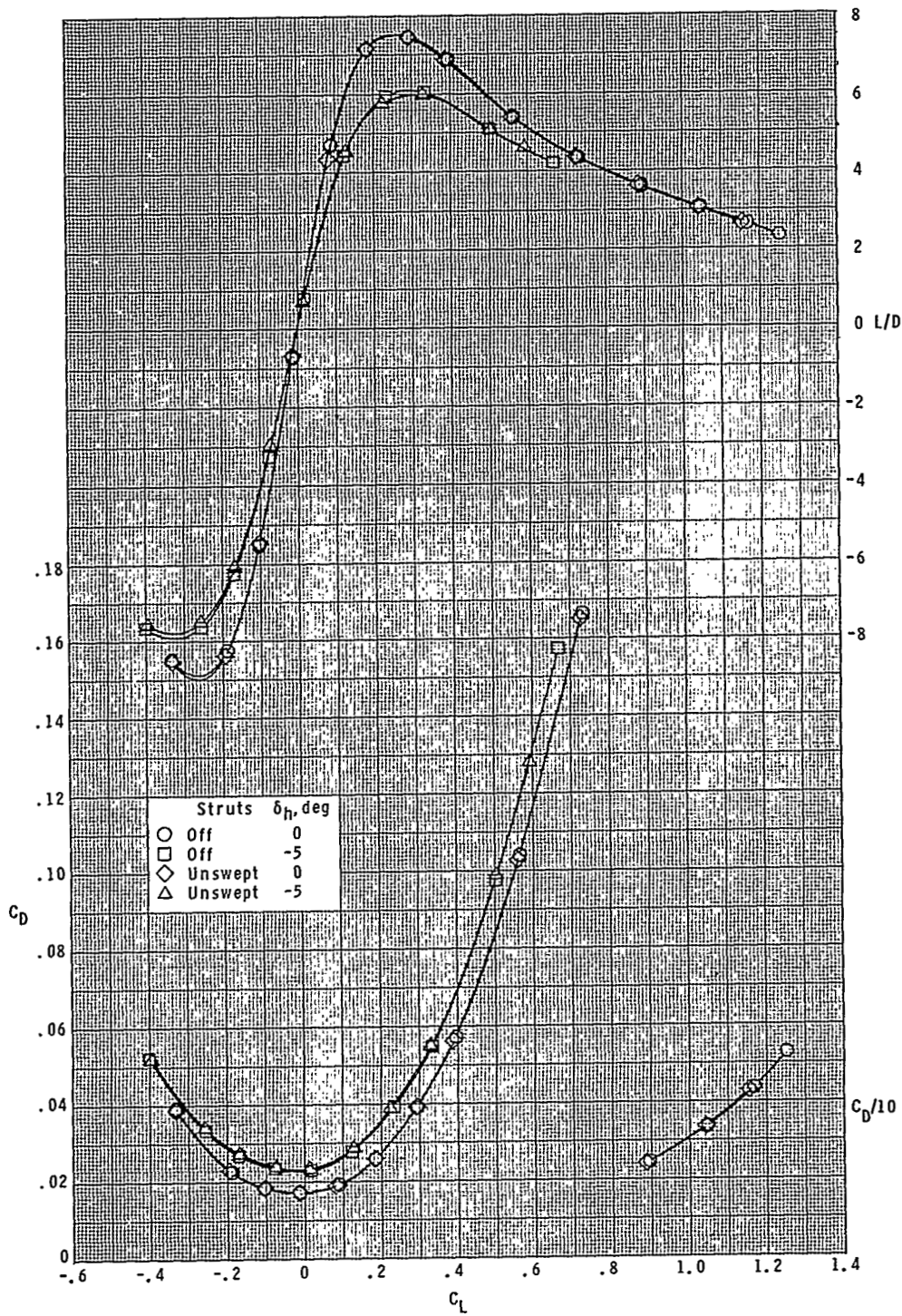
(b) Concluded.
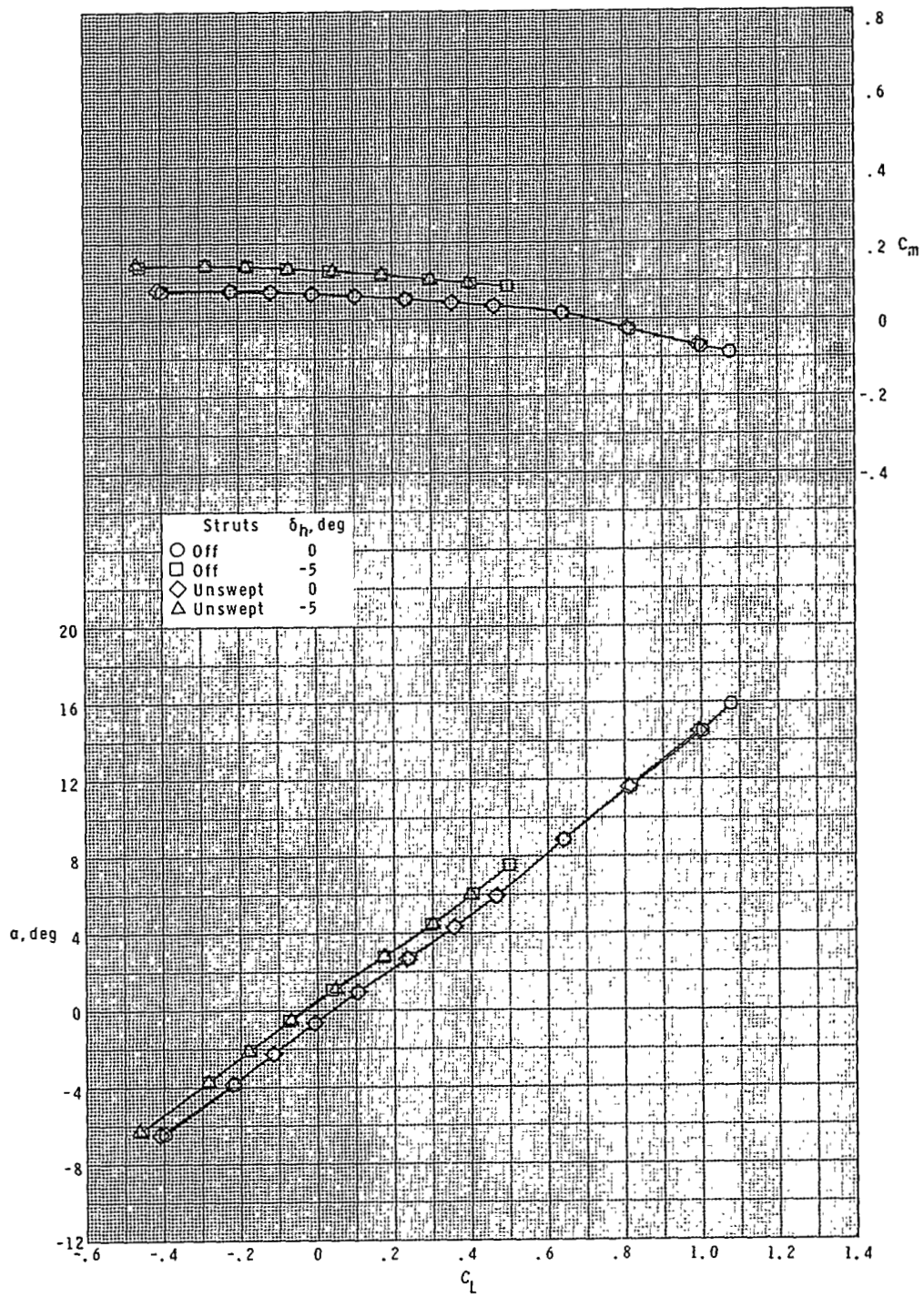
Figure 8.- Continued.

(c)   M = 0.90.

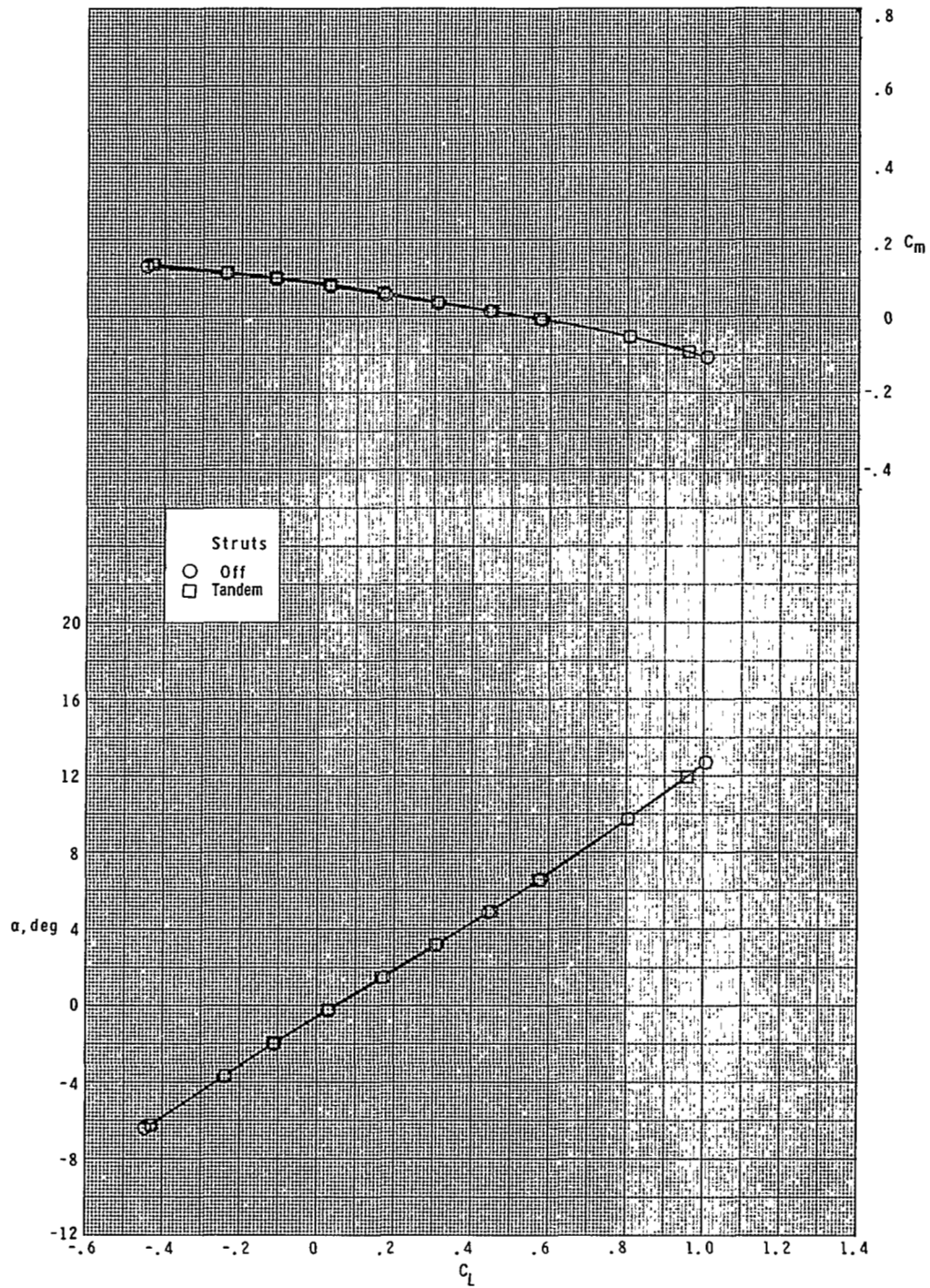Figure 8.- Continued.
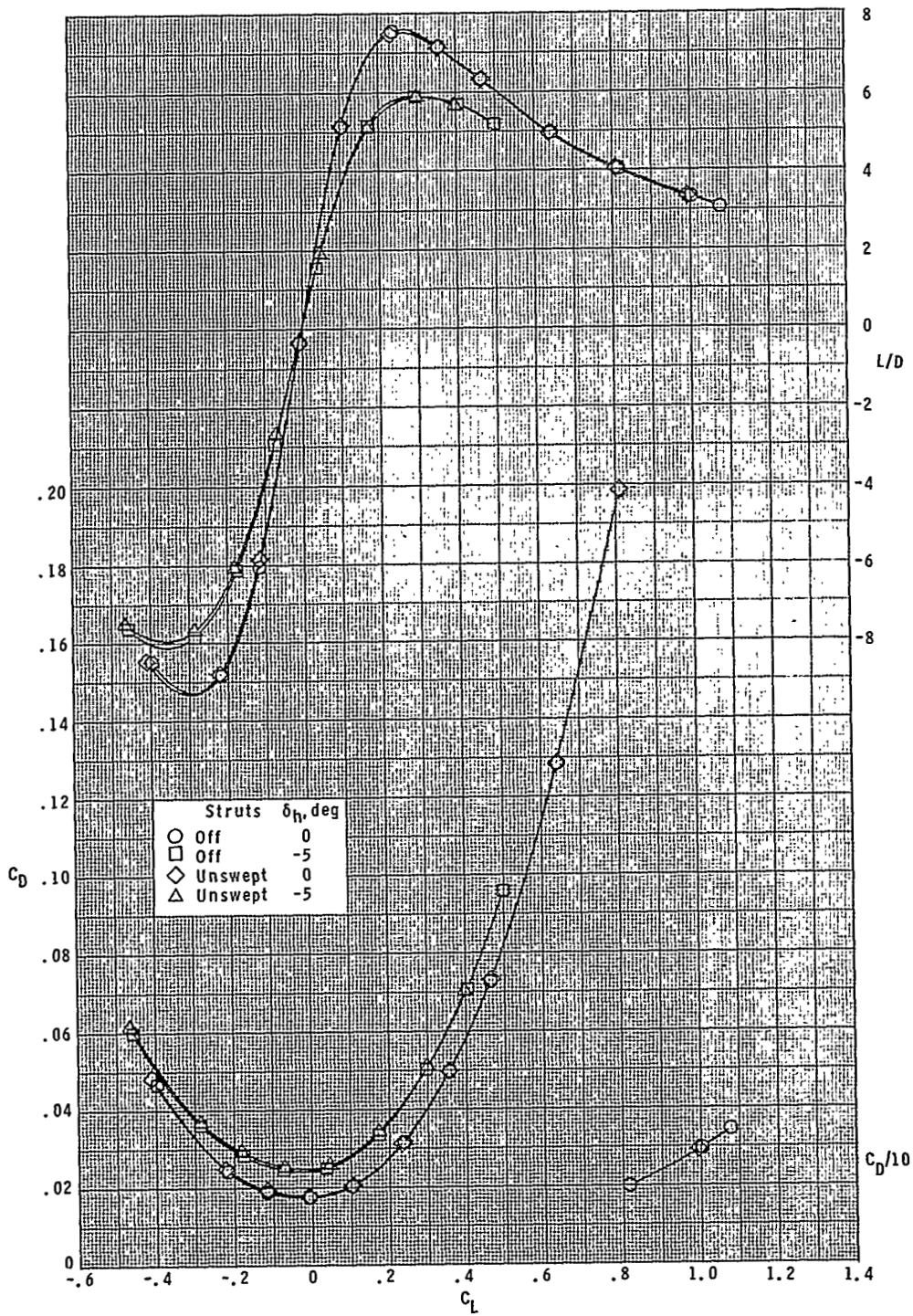
(c) Concluded.
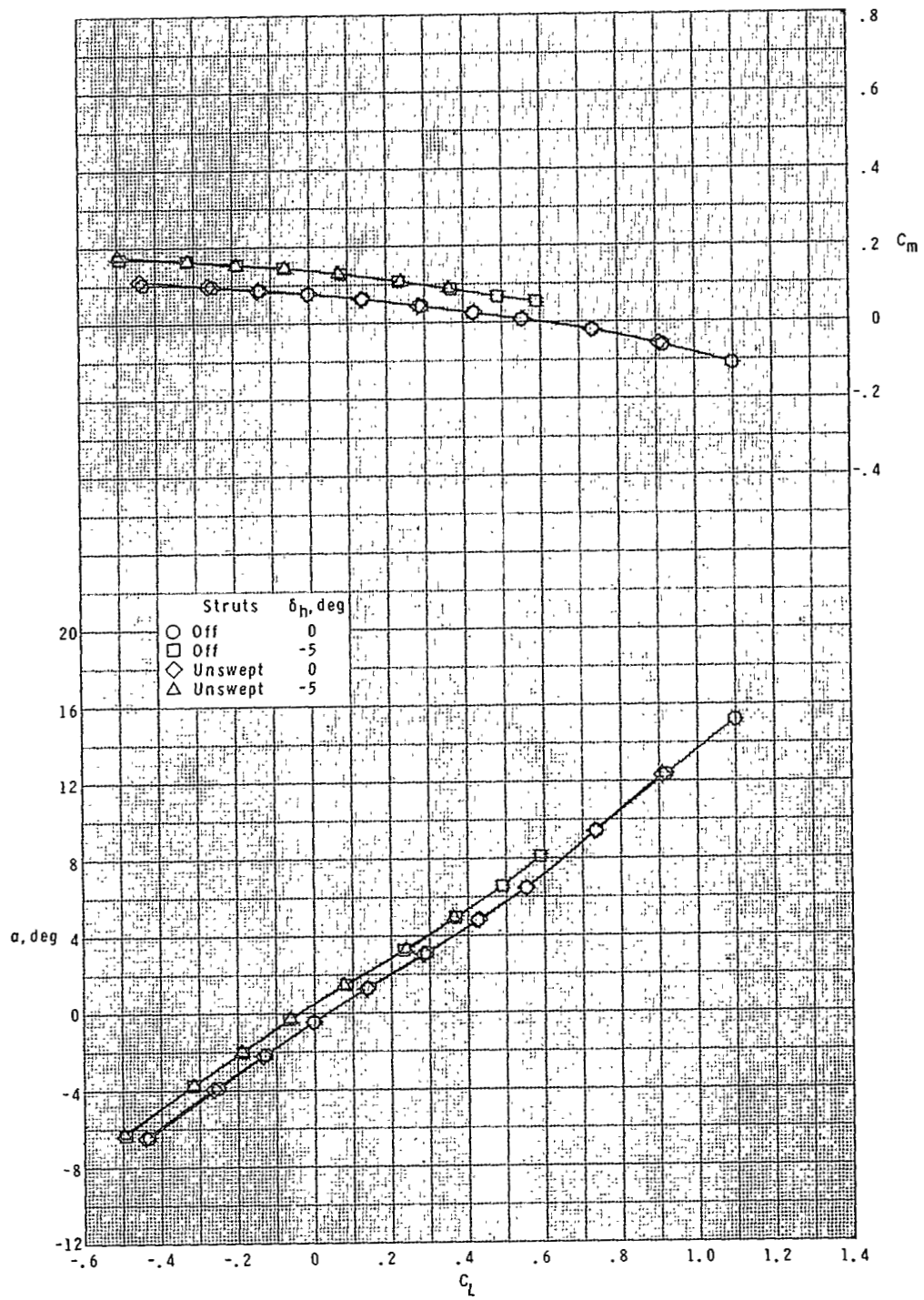
Figure 8.- Continued.

(d) M = 0.95.

Figure 8.- Continued.
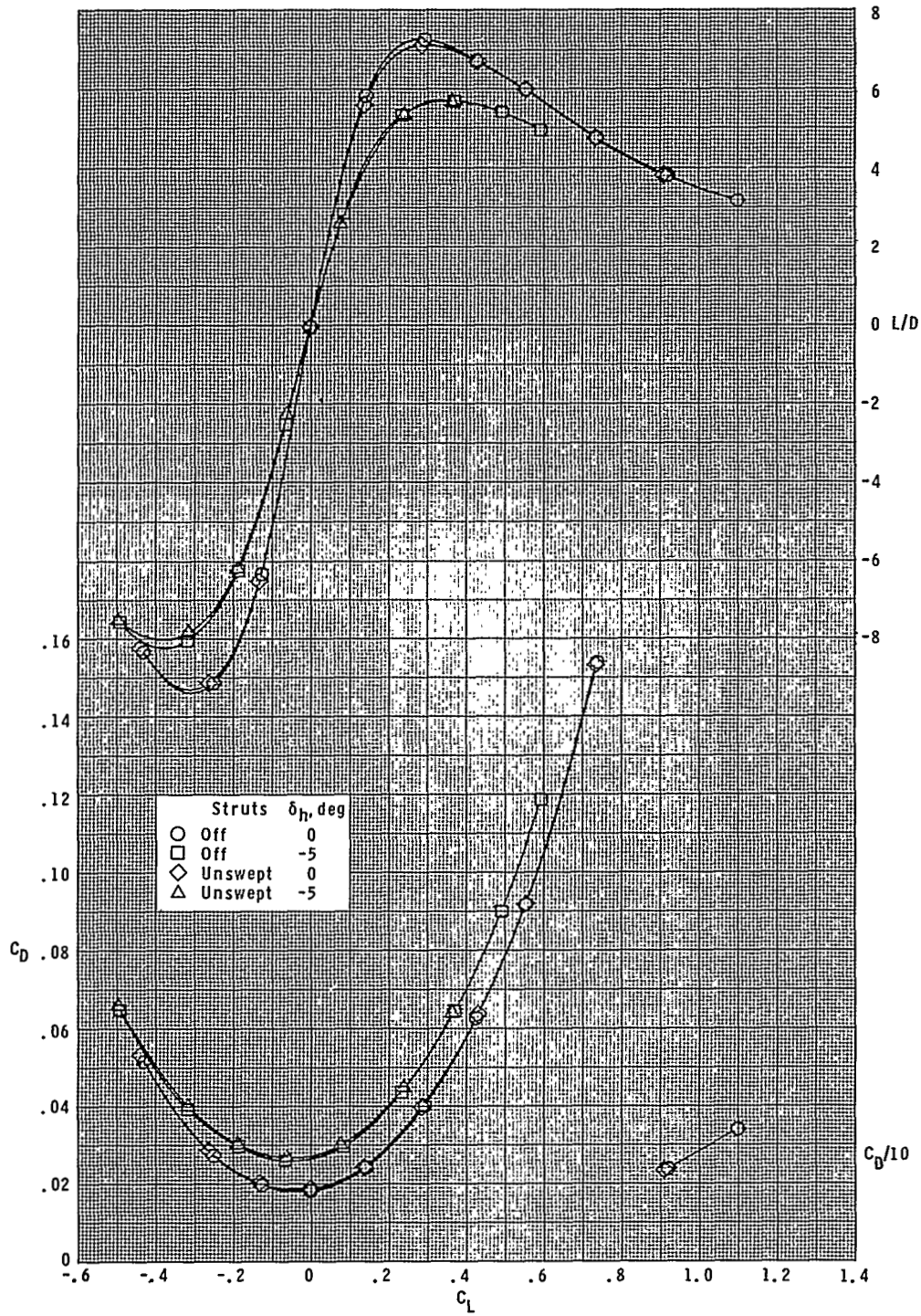
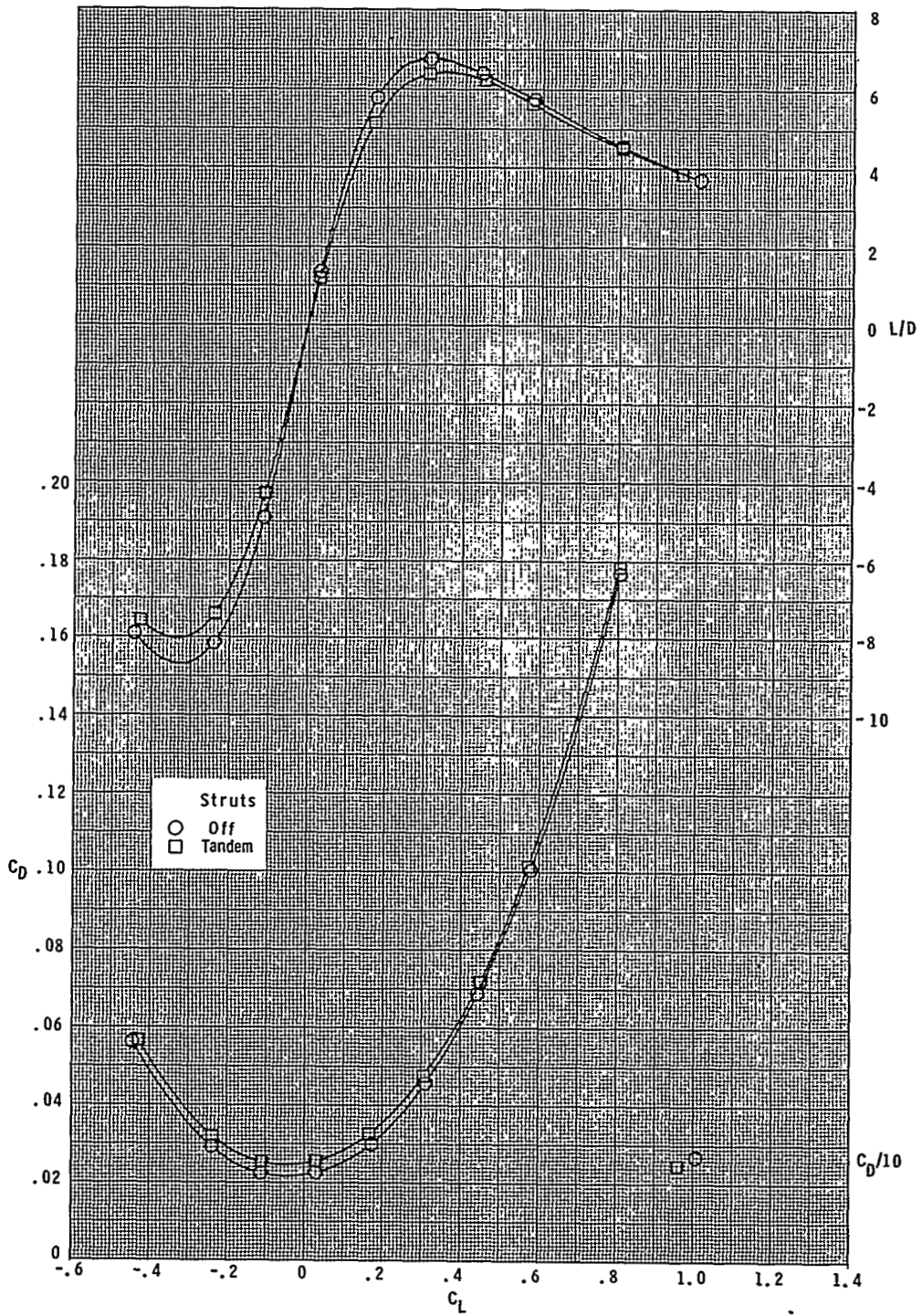(d) Concluded.
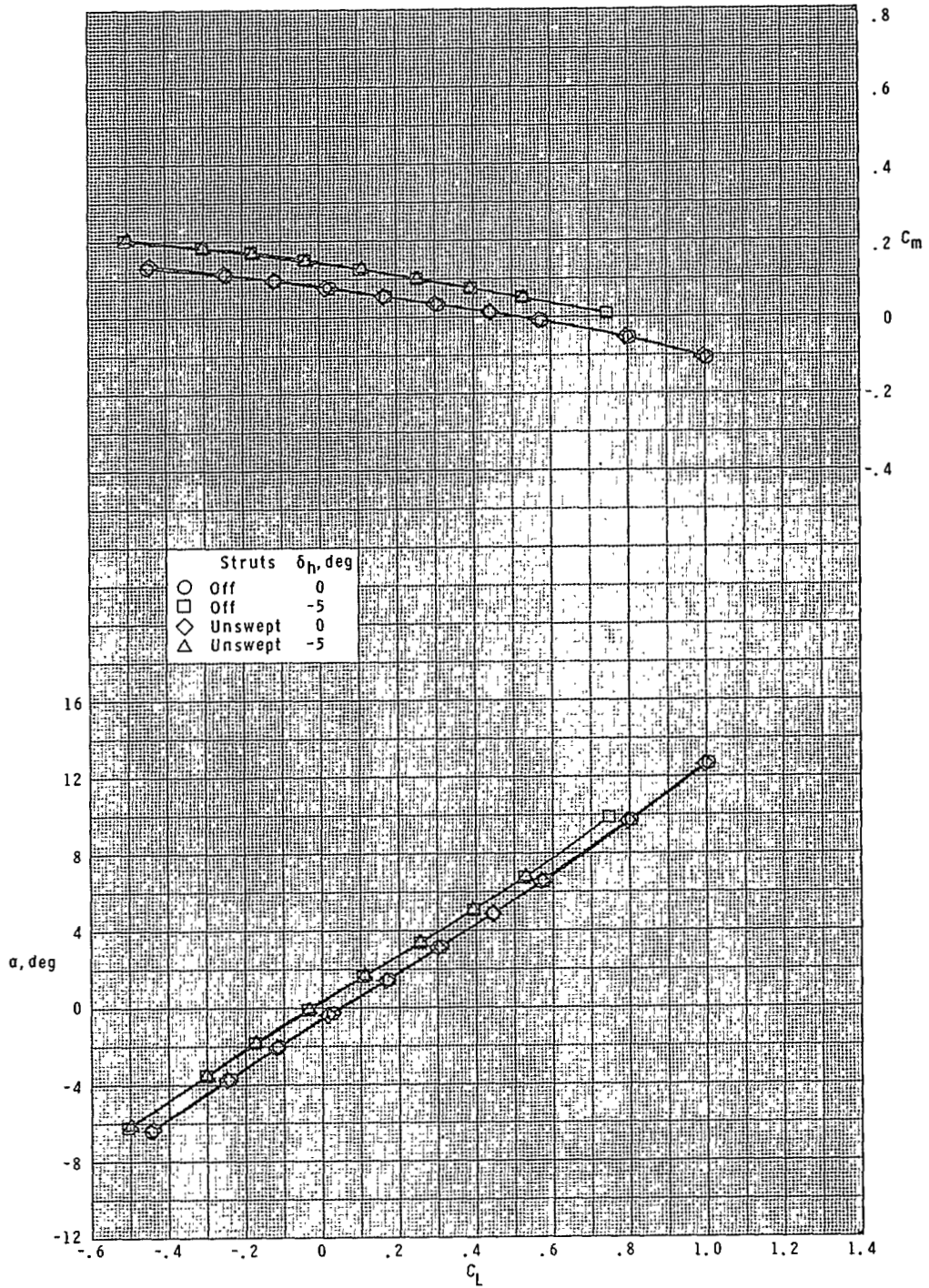
Figure 8.- Continued.

(e)   M = 0.98.

Figure 8.- Continued.
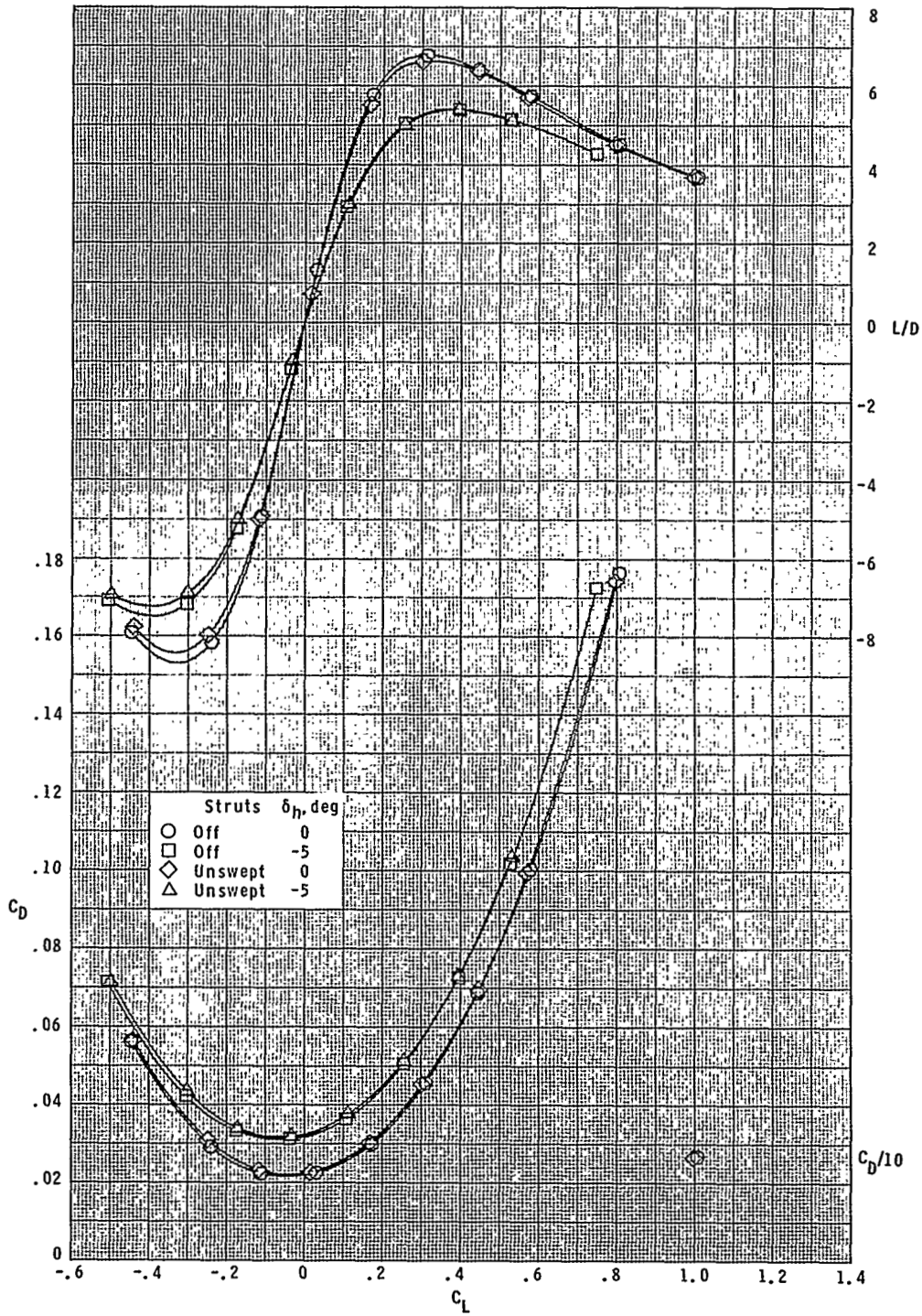
(e) Concluded.
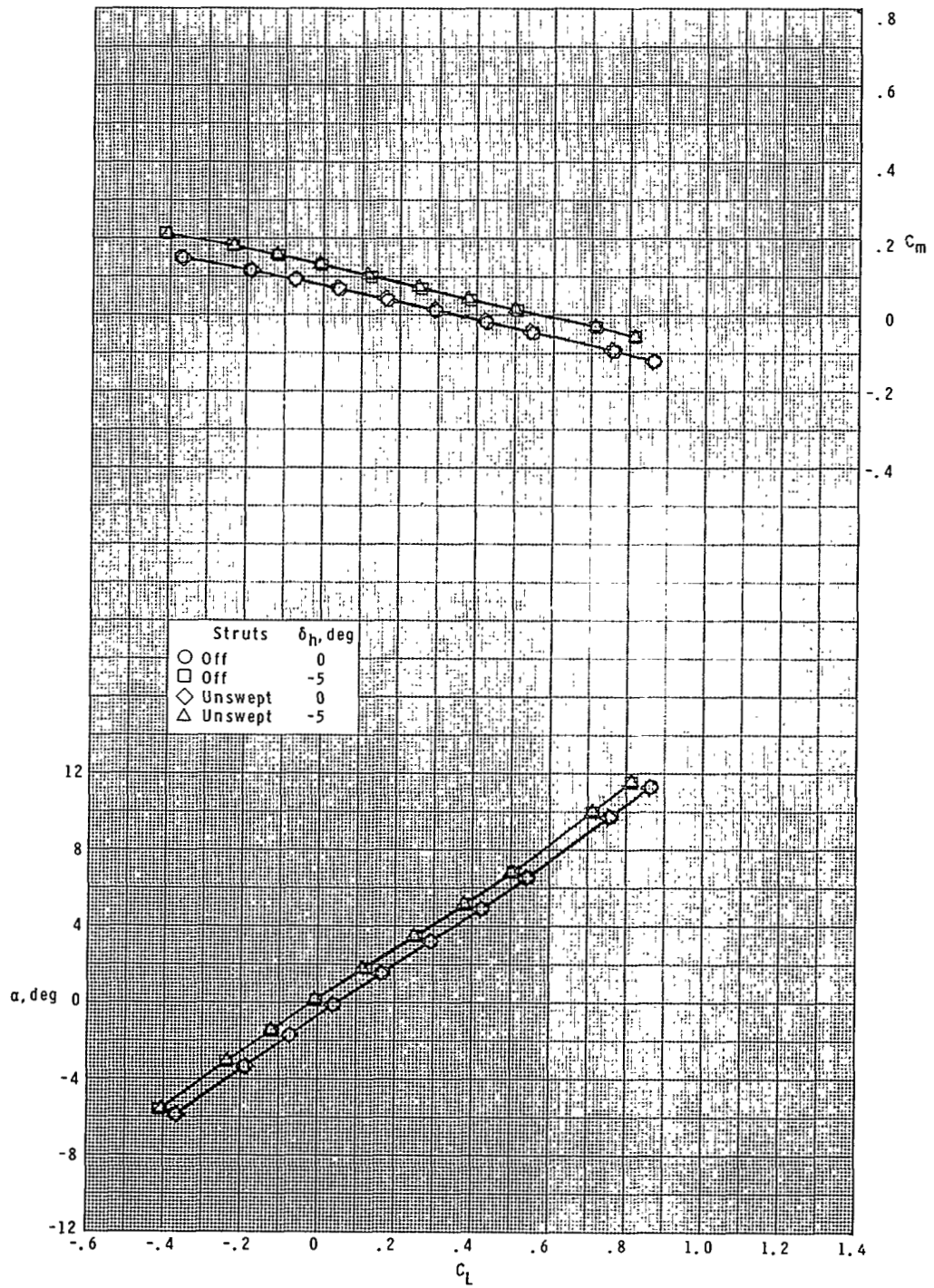
Figure 8.- Continued.

(f) M = 1.20.

Figure 8.- Continued.

(f) Concluded.

Figure 8.- Continued.

| Struts	δ_h, deg
○ Off	0
□ Off	-5
◇ Unswept	0
△ Unswept	-5
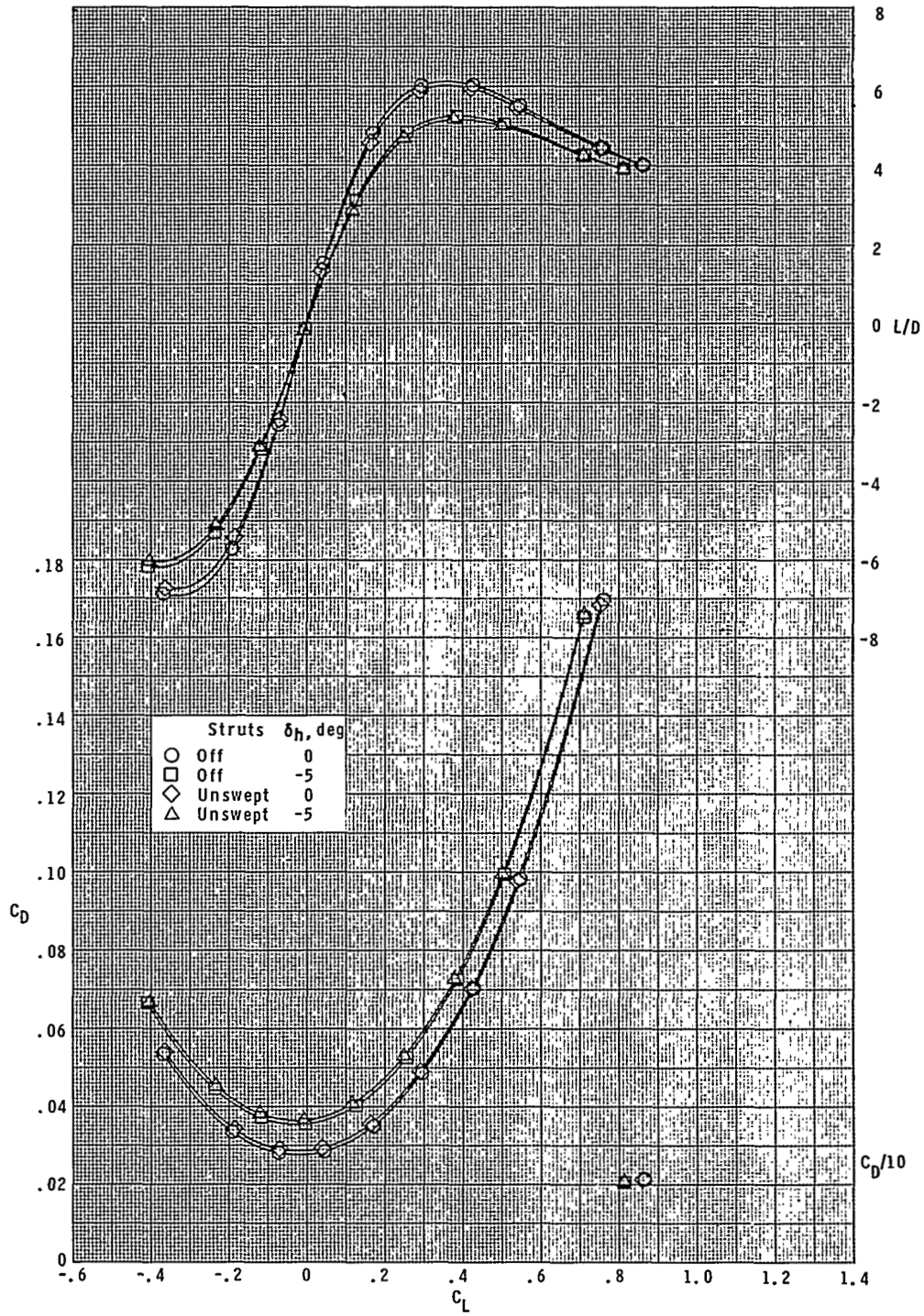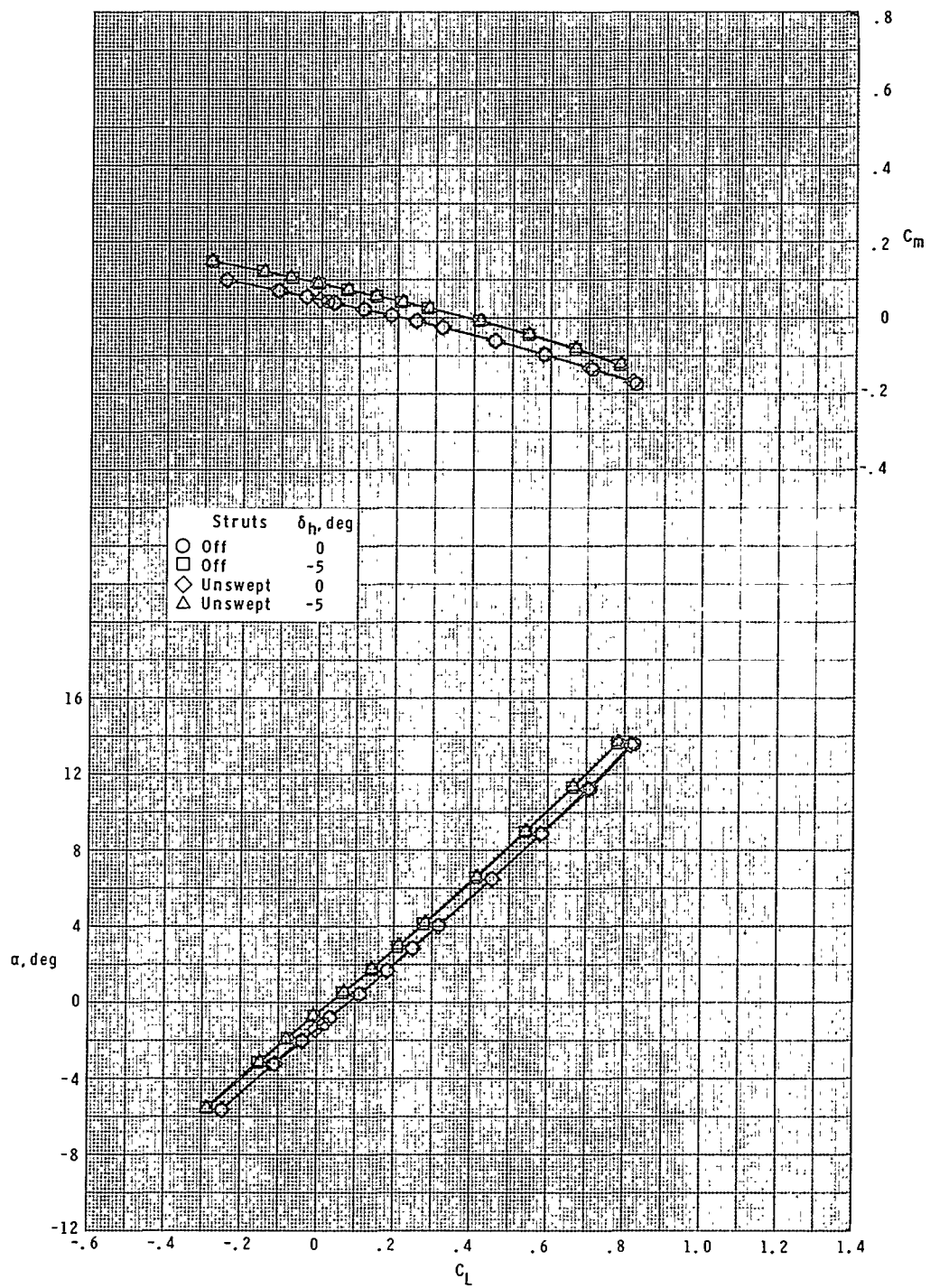
(g) M = 1.60.
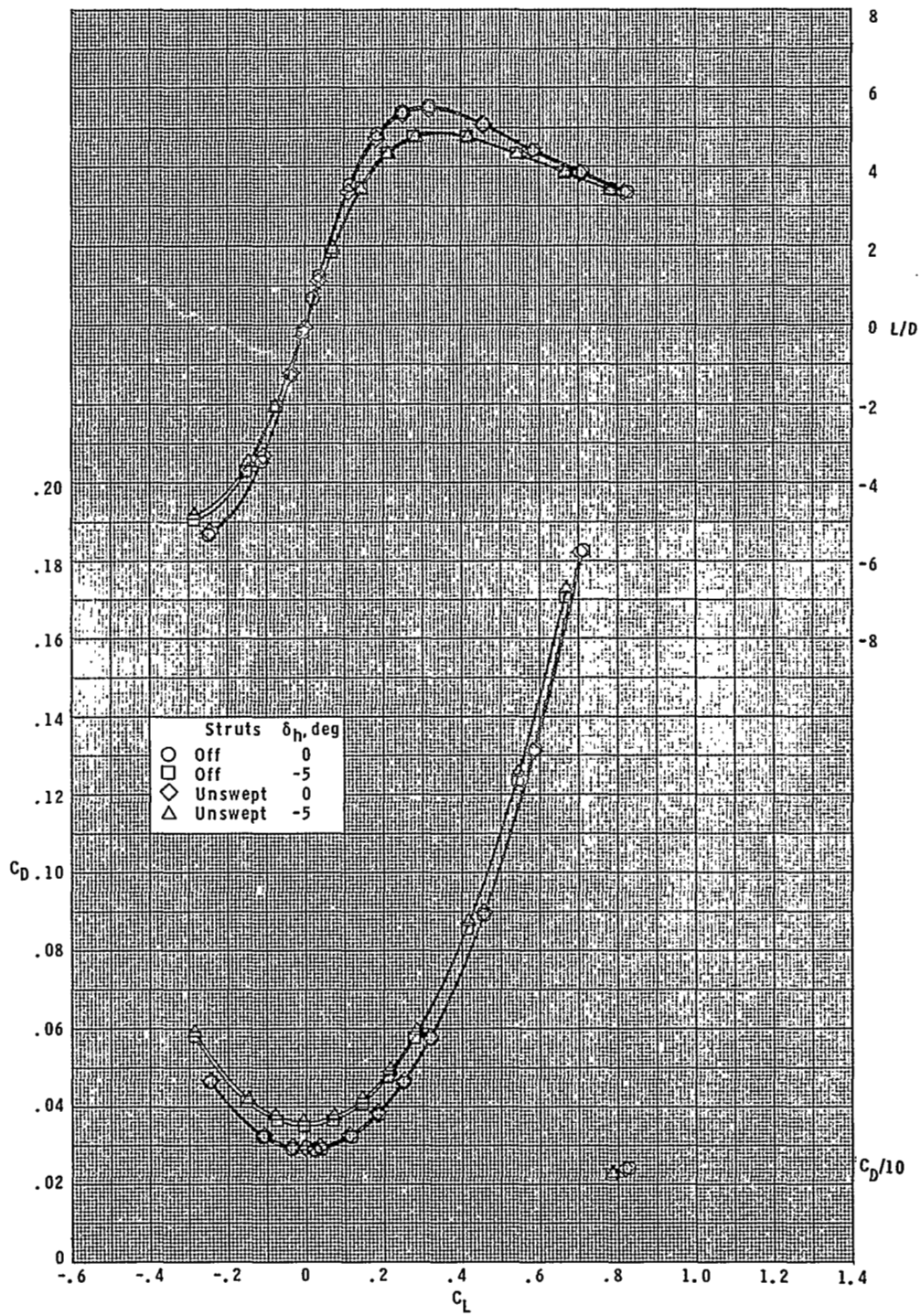
Figure 8.- Continued.

(g) Concluded.
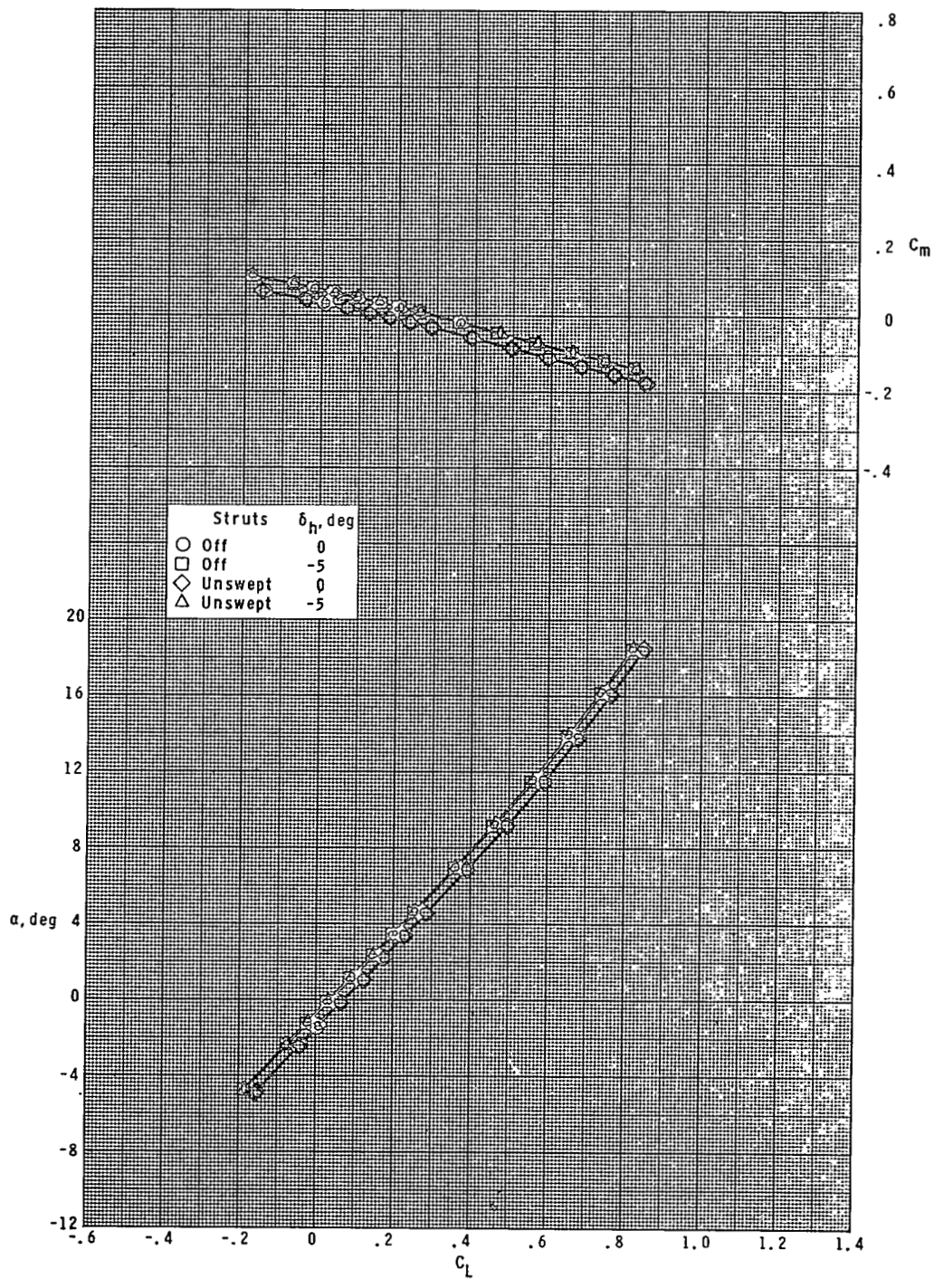
Figure 8.- Continued.

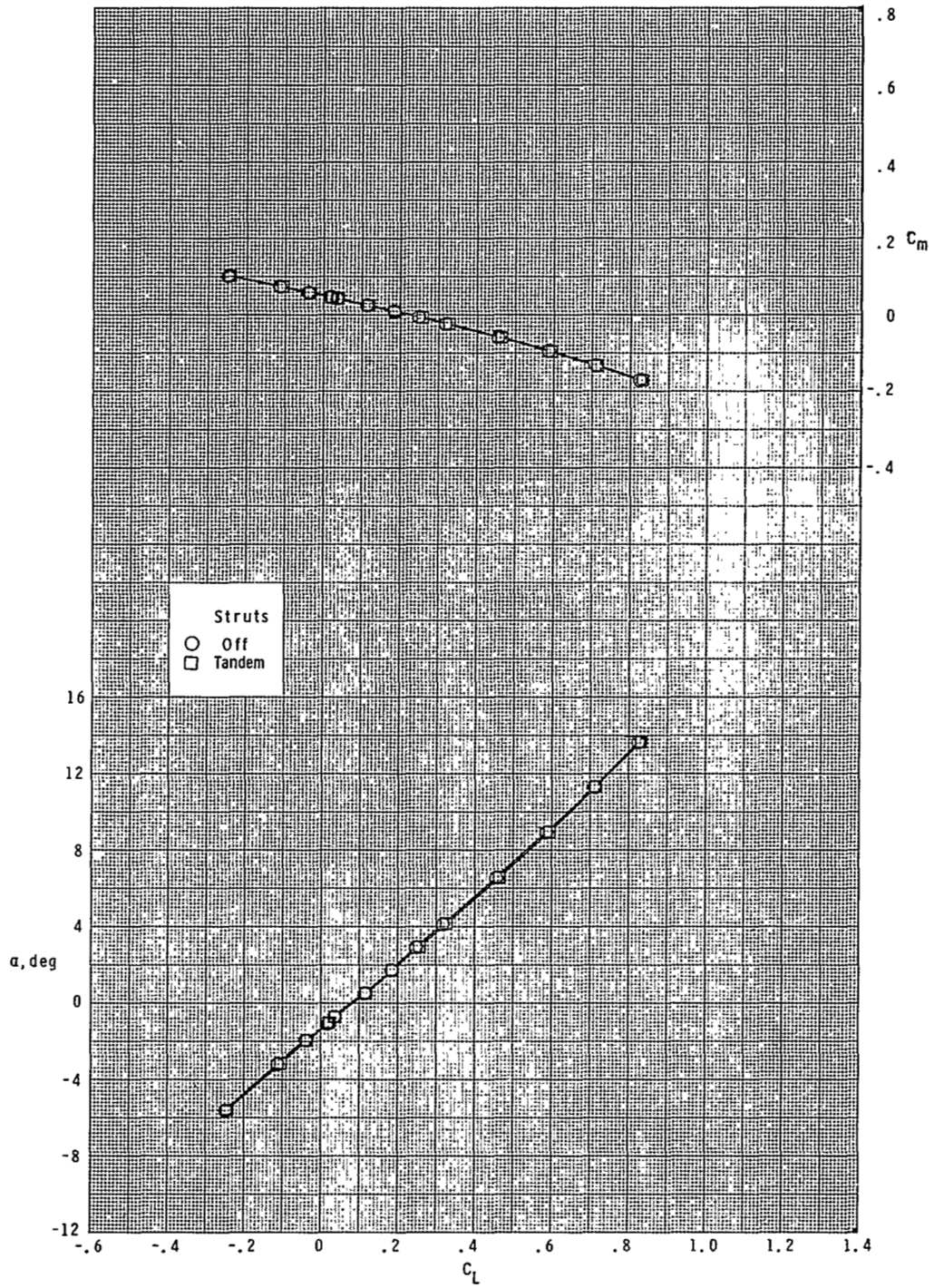(h)   M = 2.00.

Figure 8.- Continued.
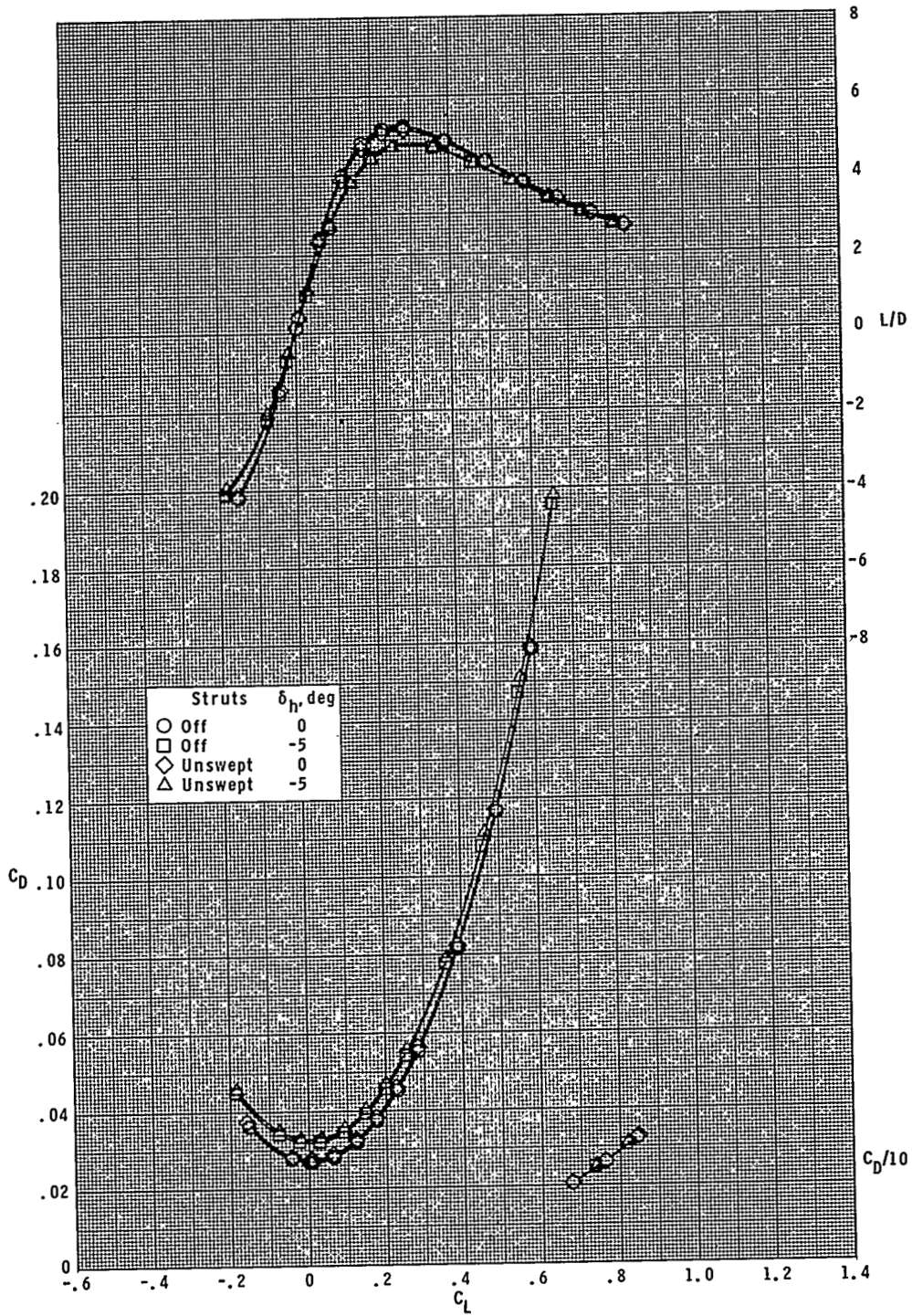
(h) Concluded.
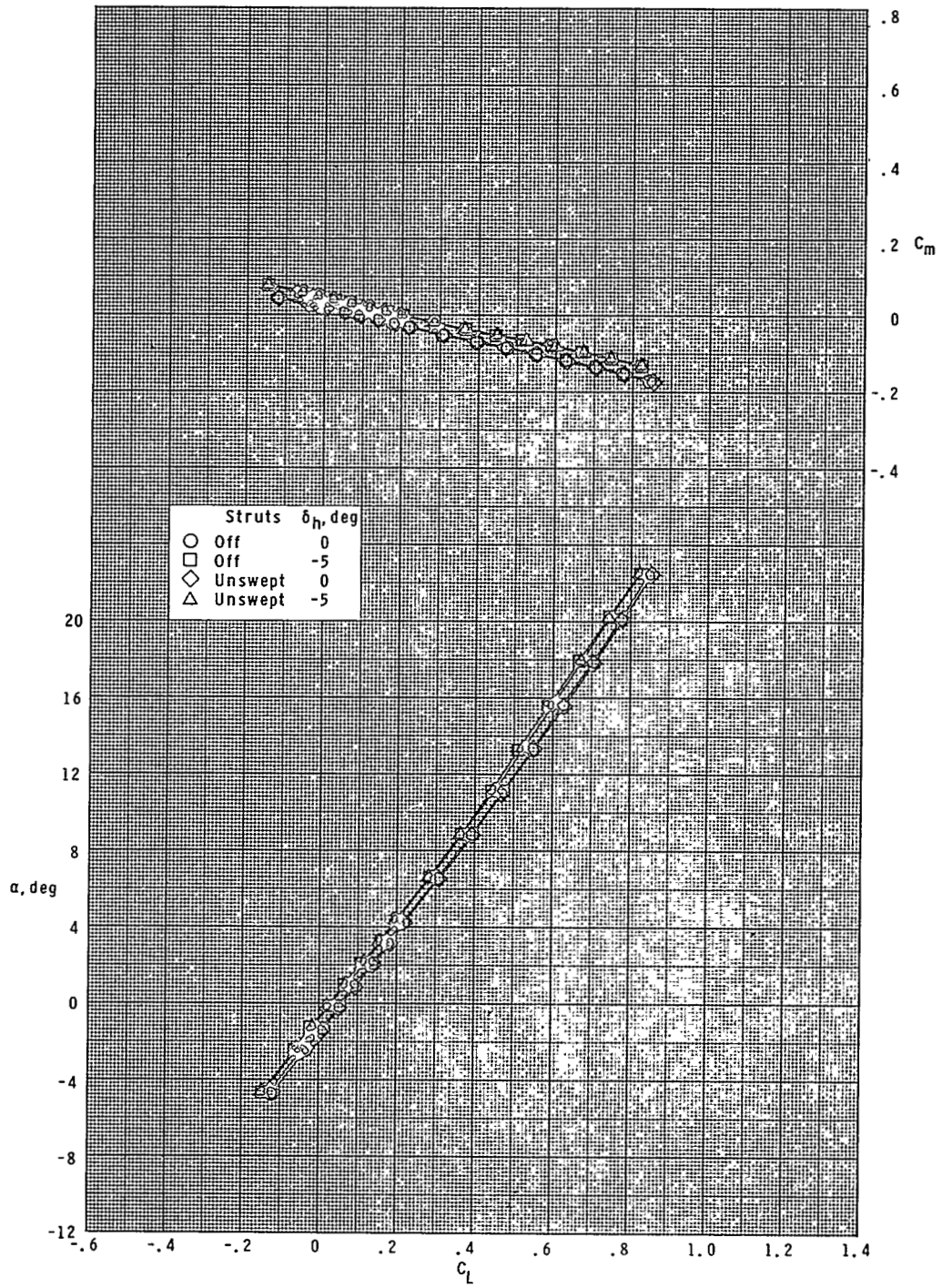
Figure 8.- Continued.

(i)   M = 2.50.

Figure 8.- Continued.
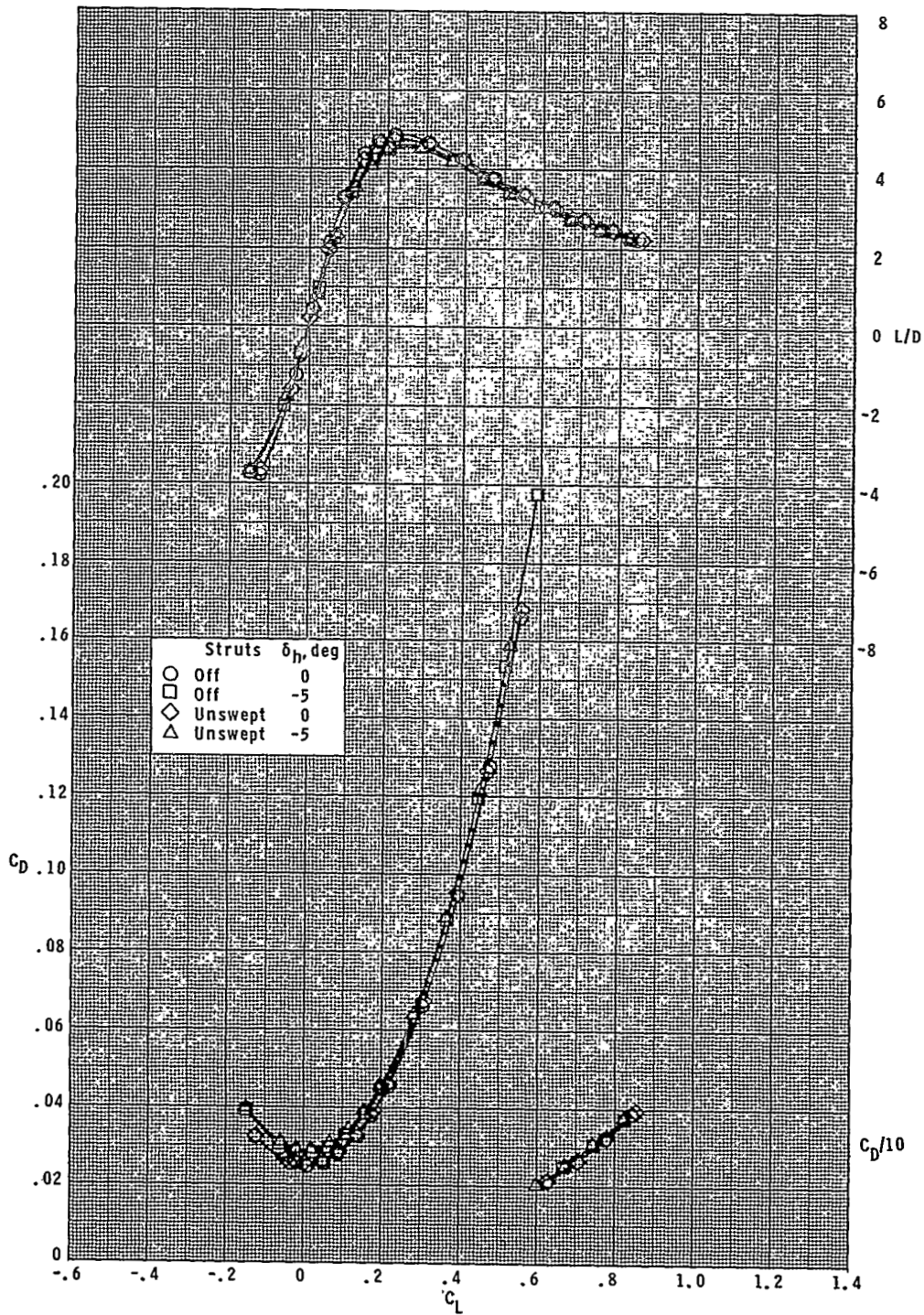
(i) Concluded.
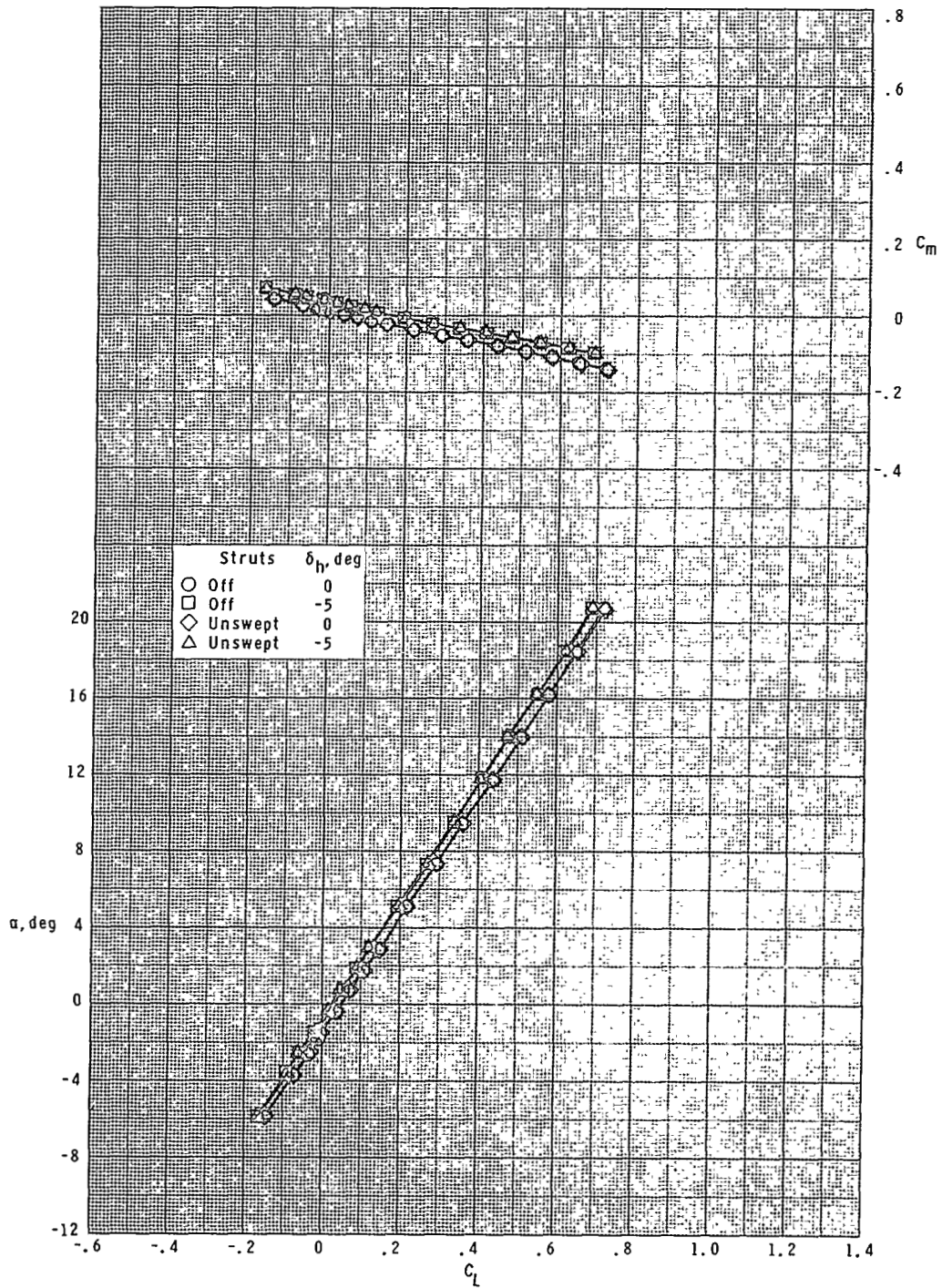
Figure 8.- Continued.

(j)   M = 2.86.

Figure 8.- Continued.
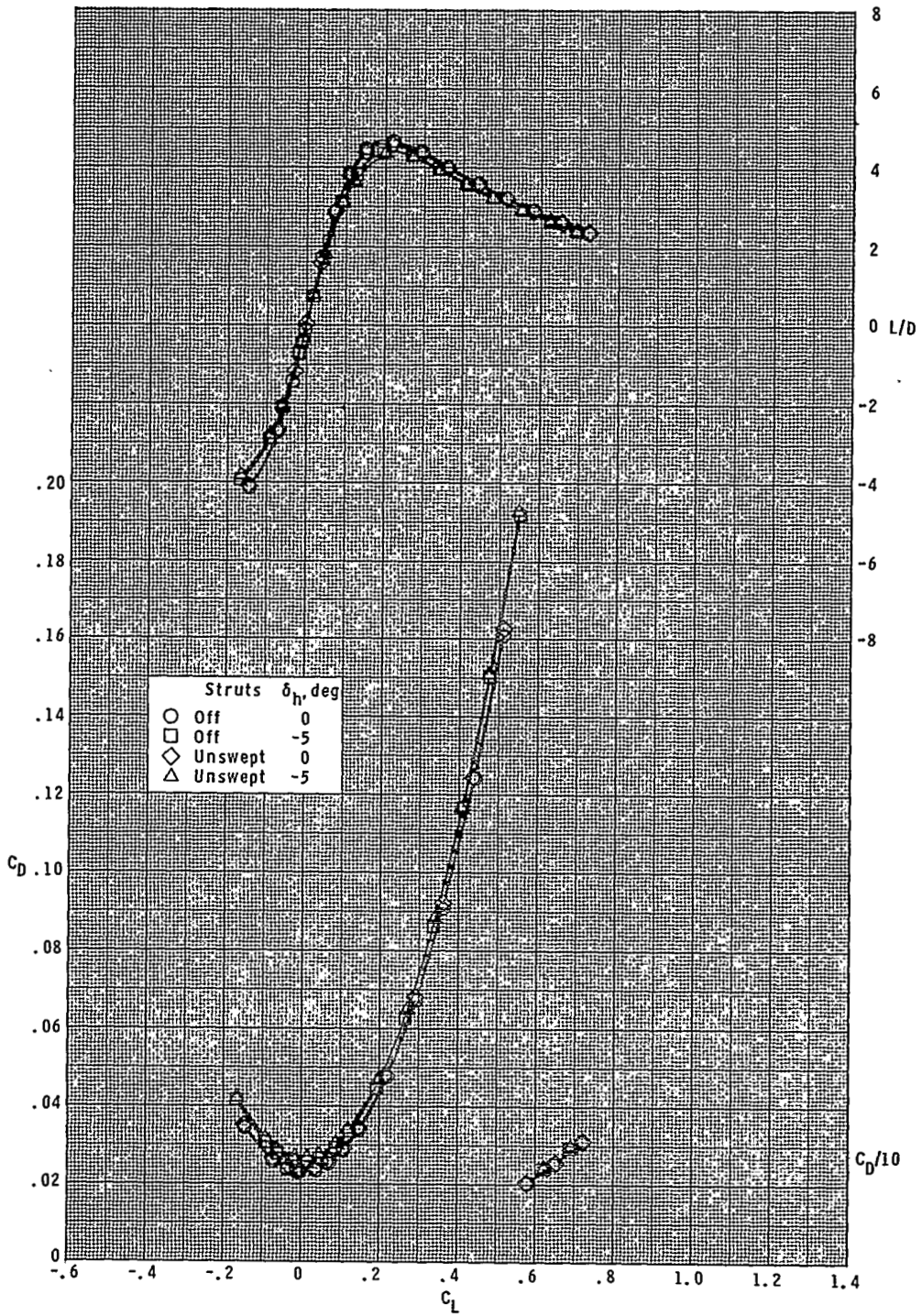
(j) Concluded.

Figure 8.- Concluded.
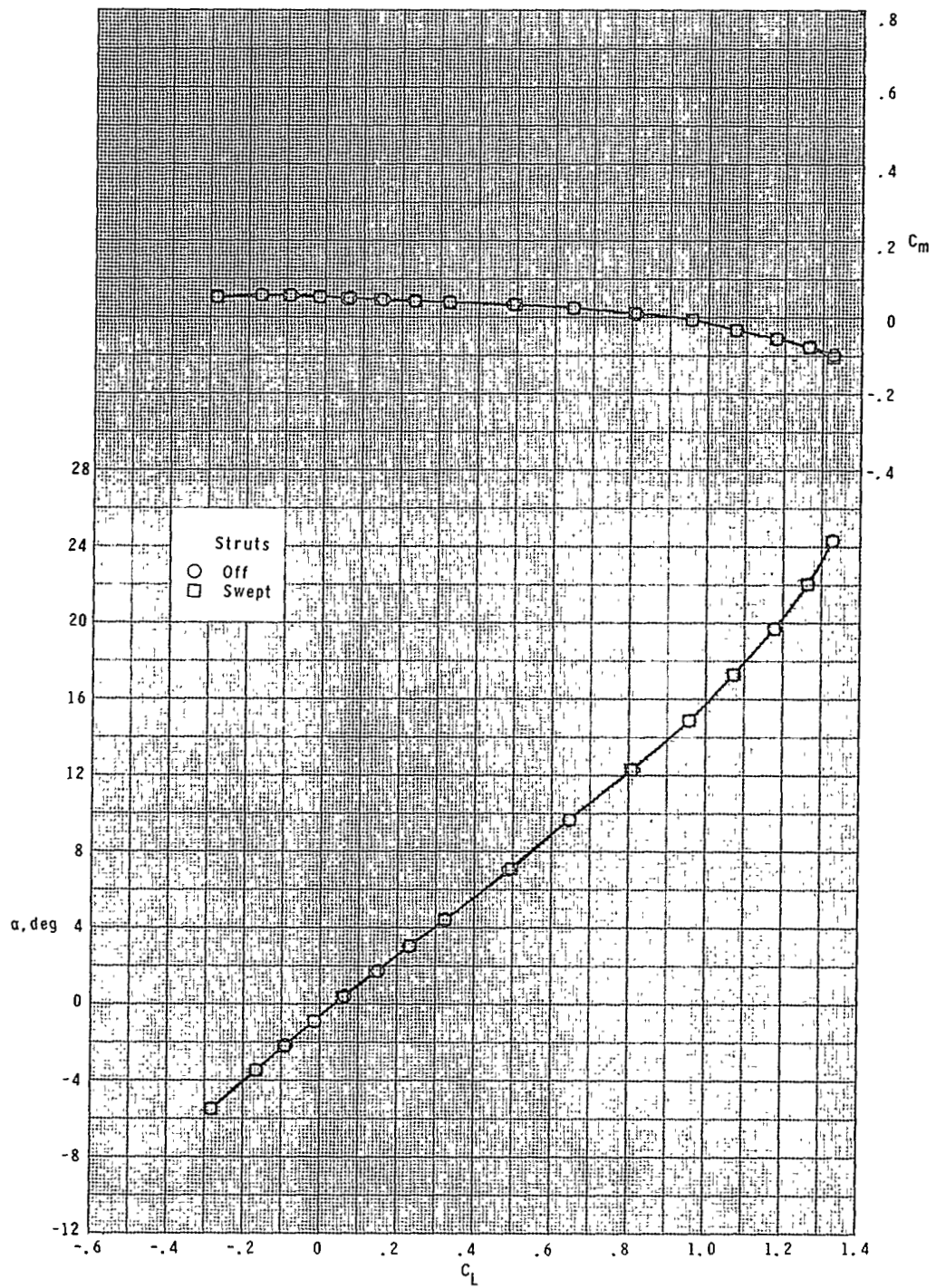
(a) M = 0.60.

Figure 9.- Effect of single swept strut on longitudinal aerodynamic characteristics
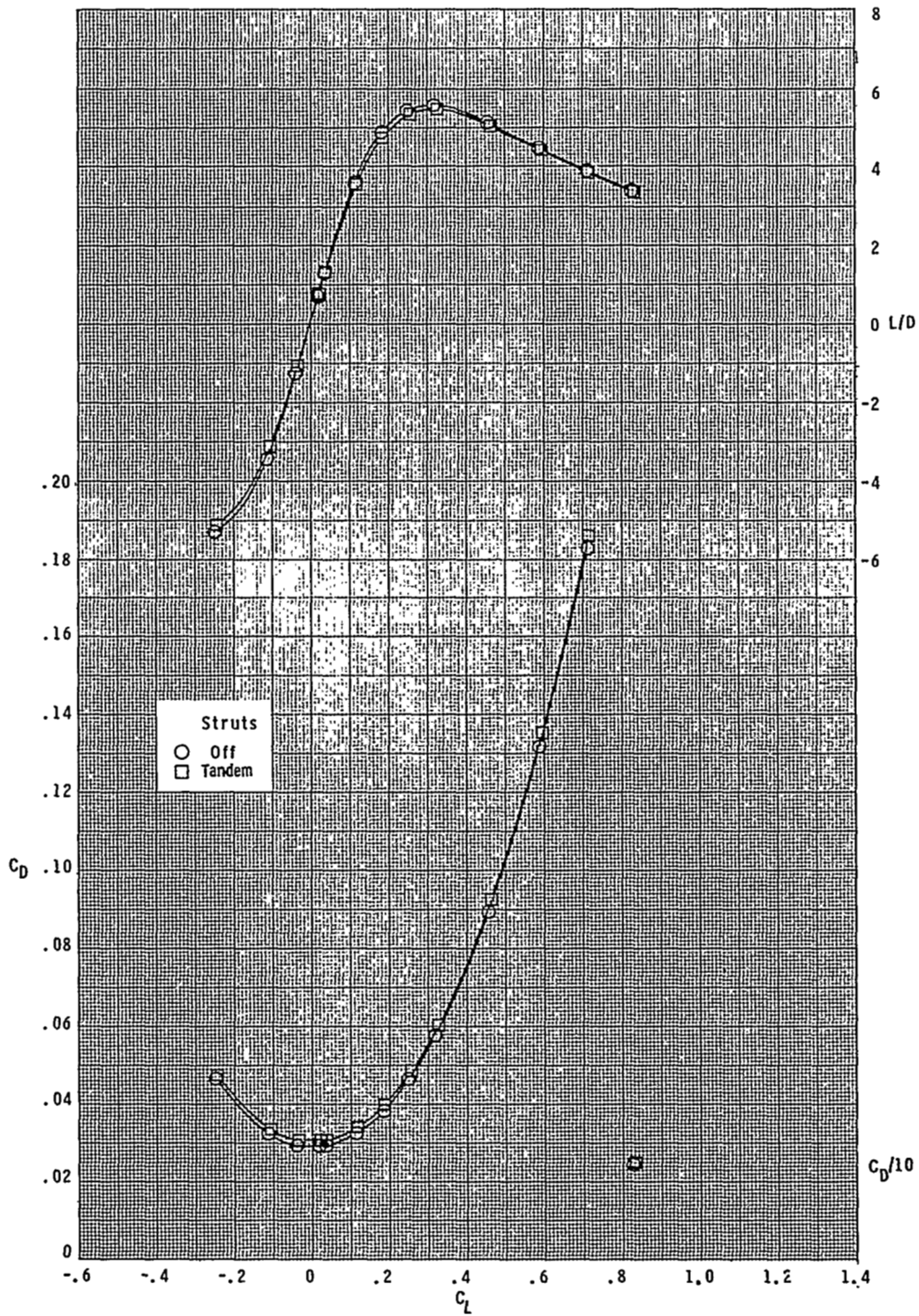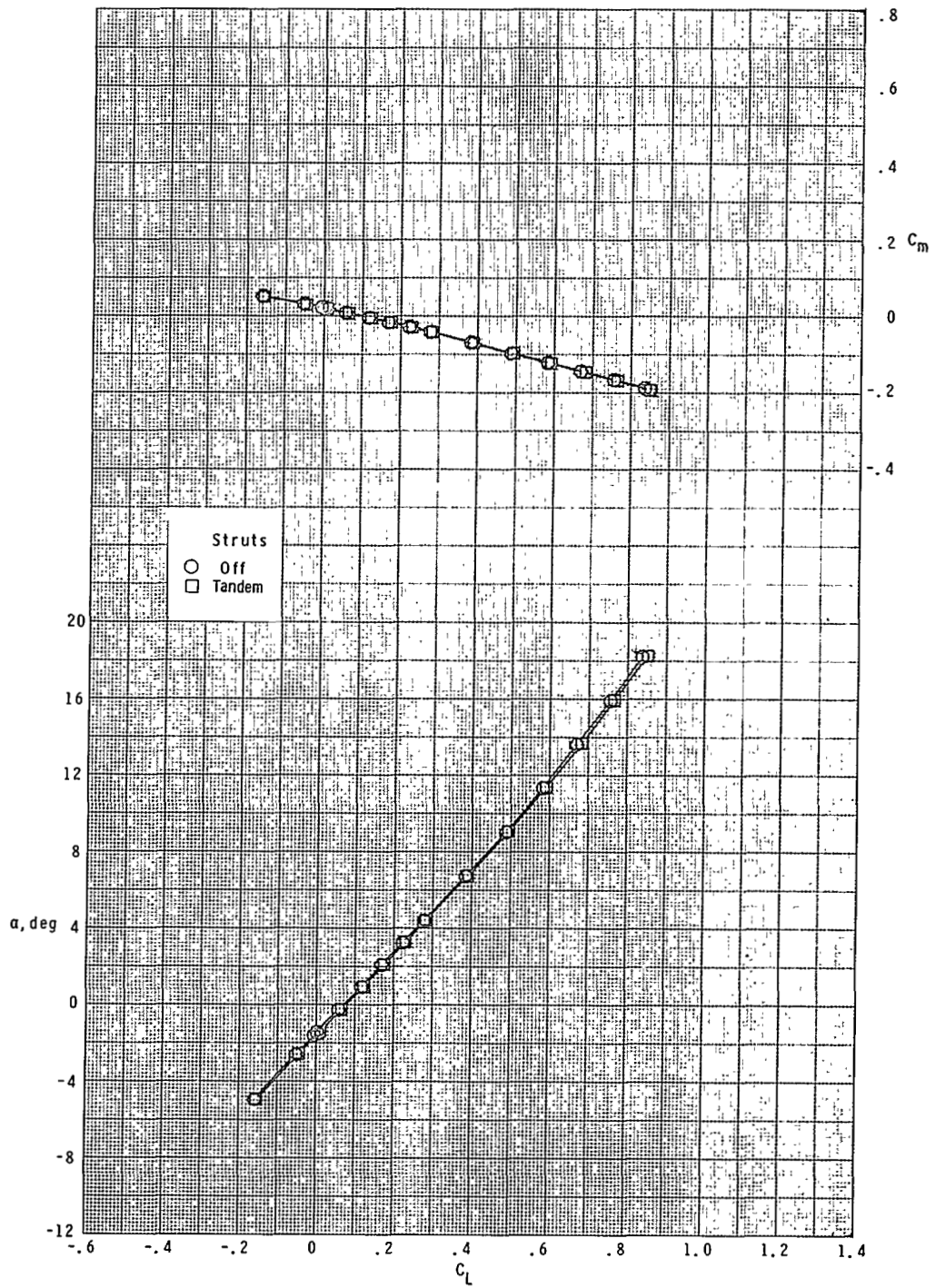for $\delta_h = 0^o$.

86
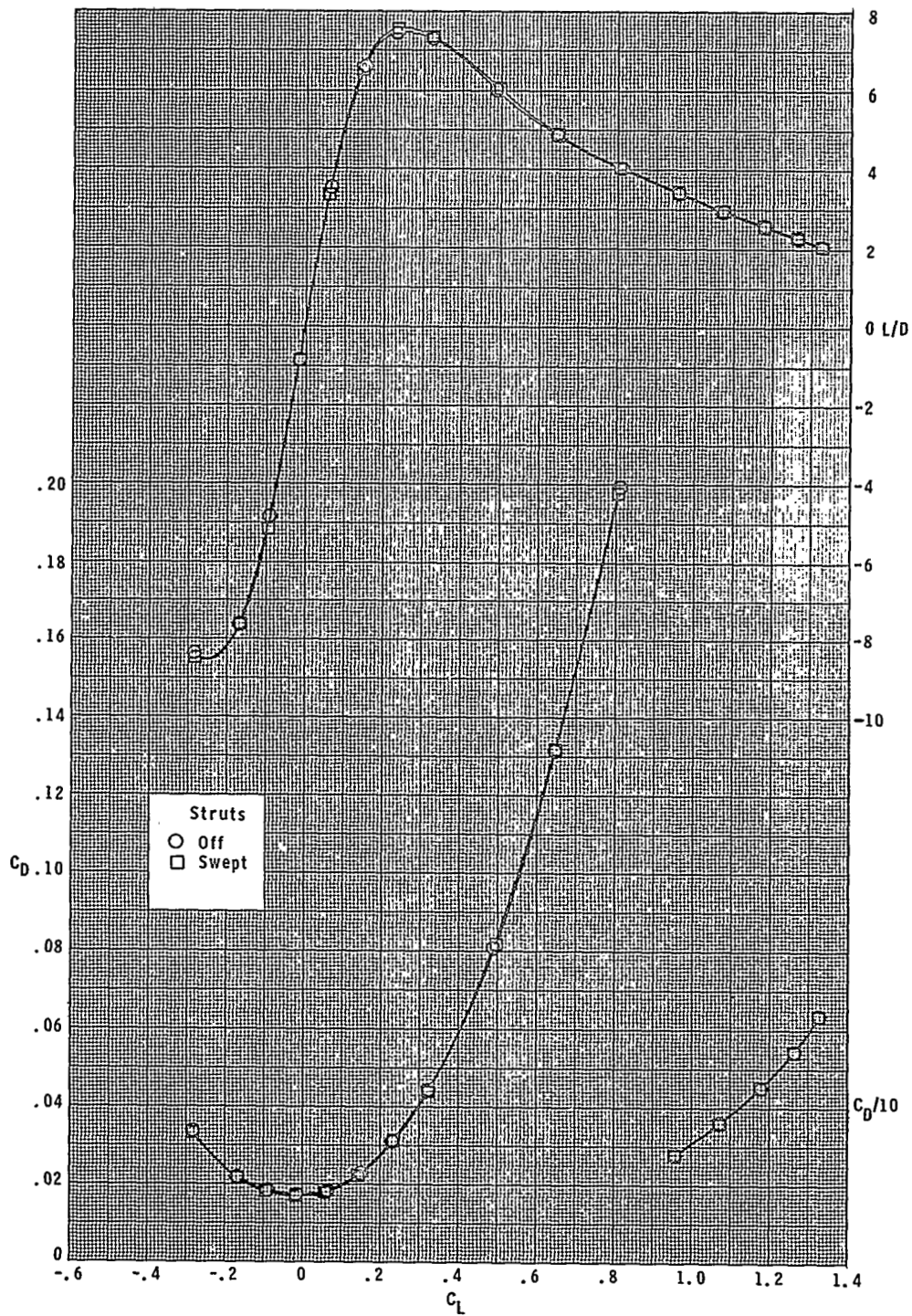
(a) Concluded.
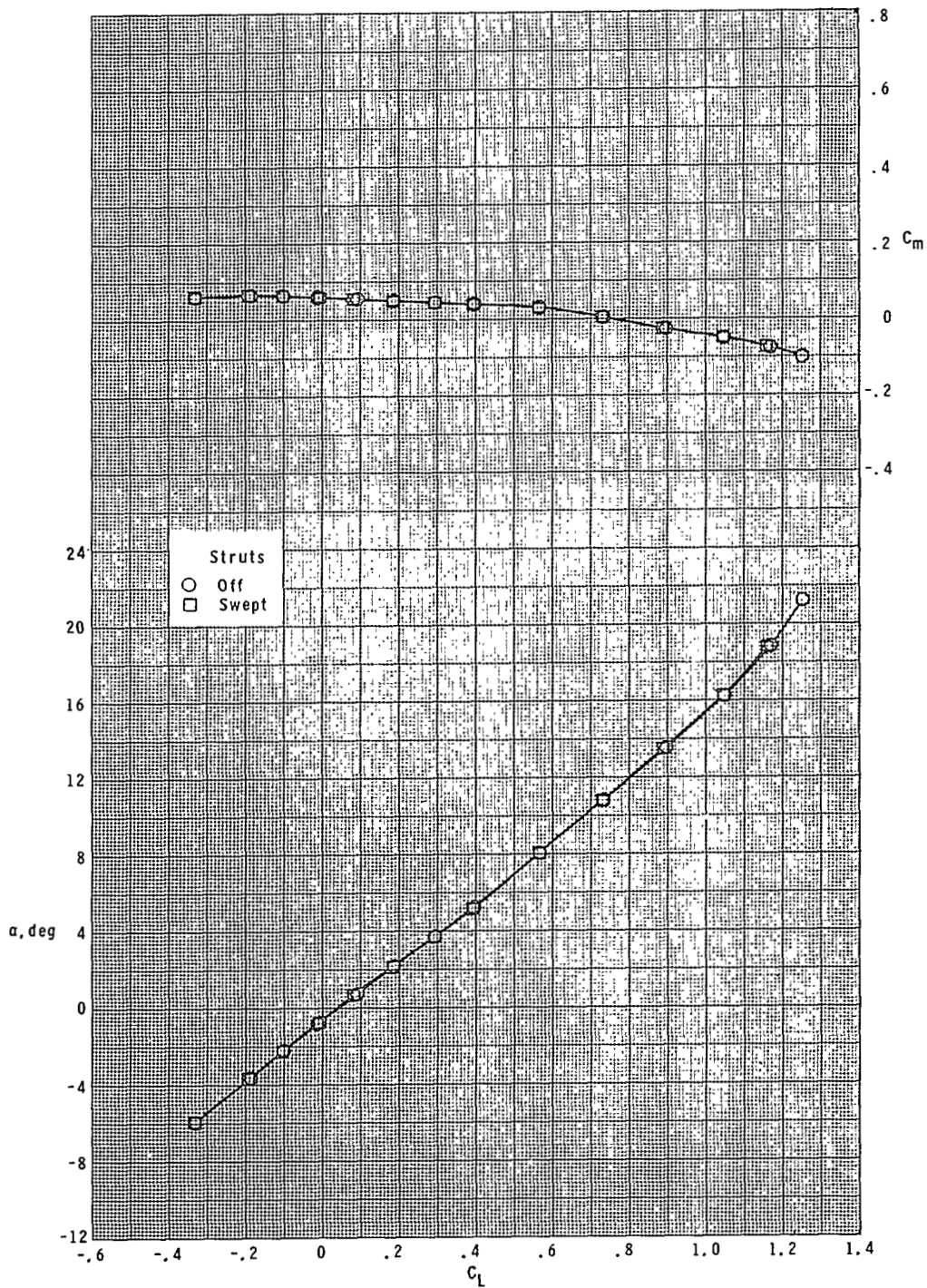
Figure 9.- Continued.

(b)   M = 0.80.

Figure 9.- Continued.
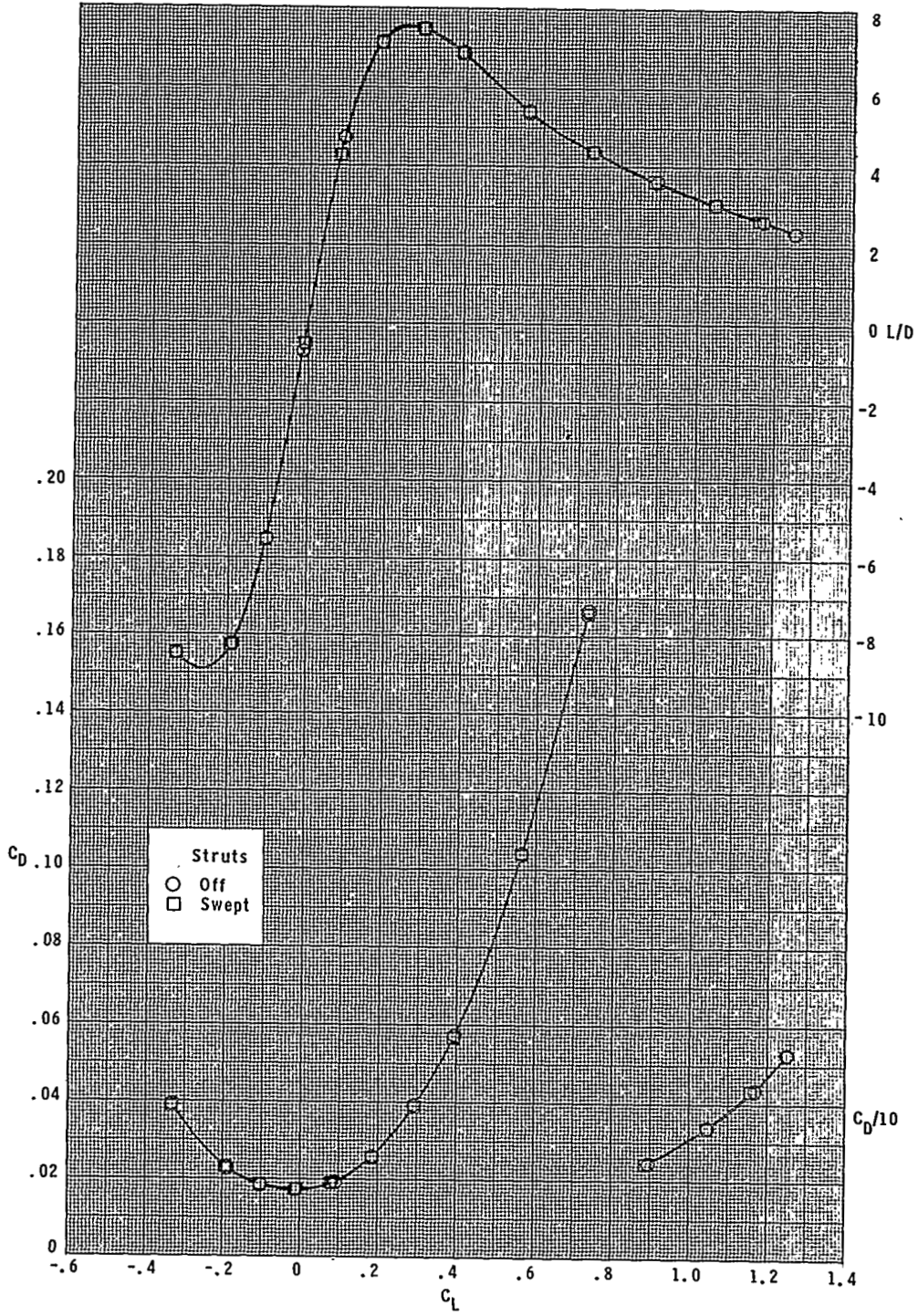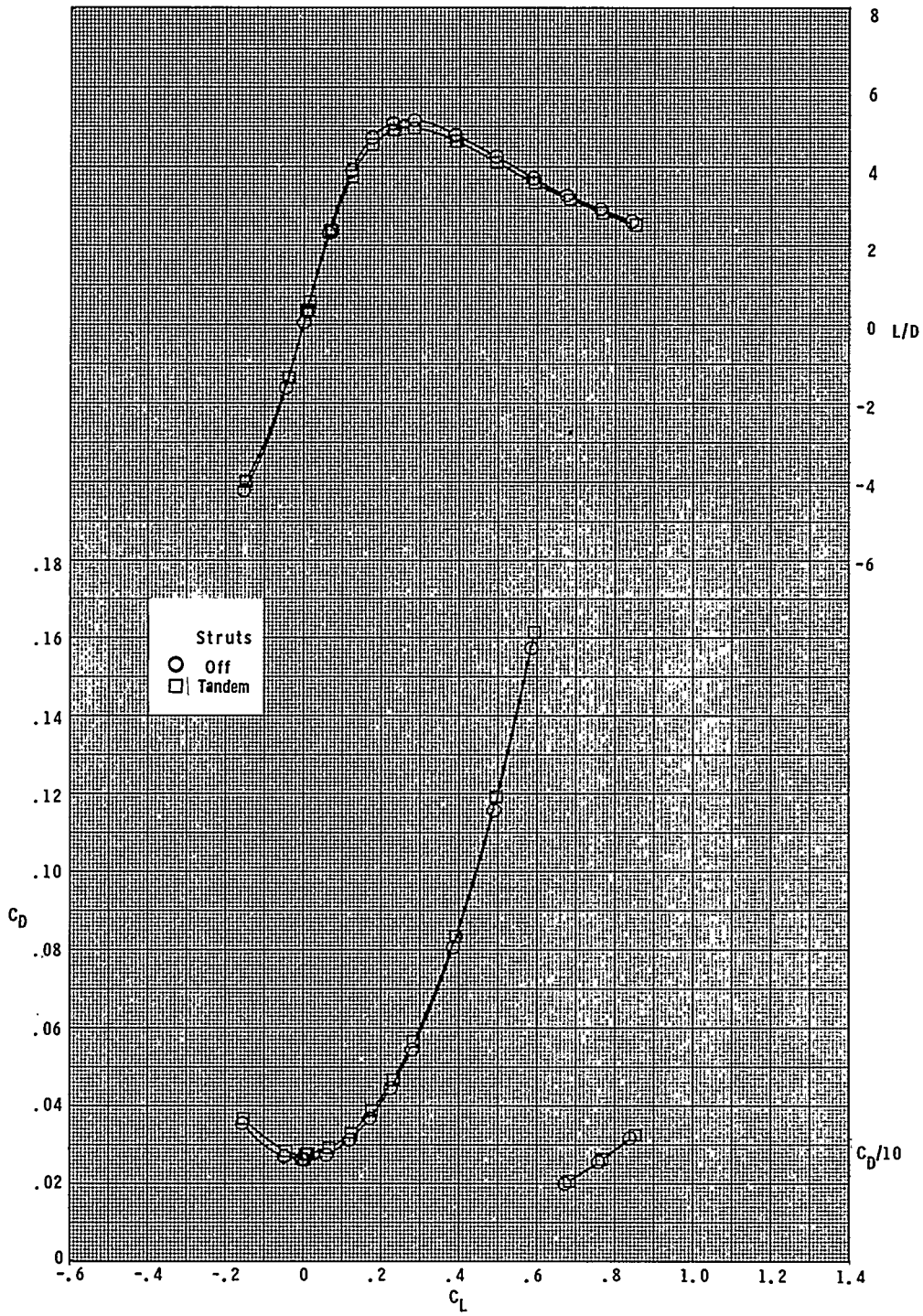
(b) Concluded.
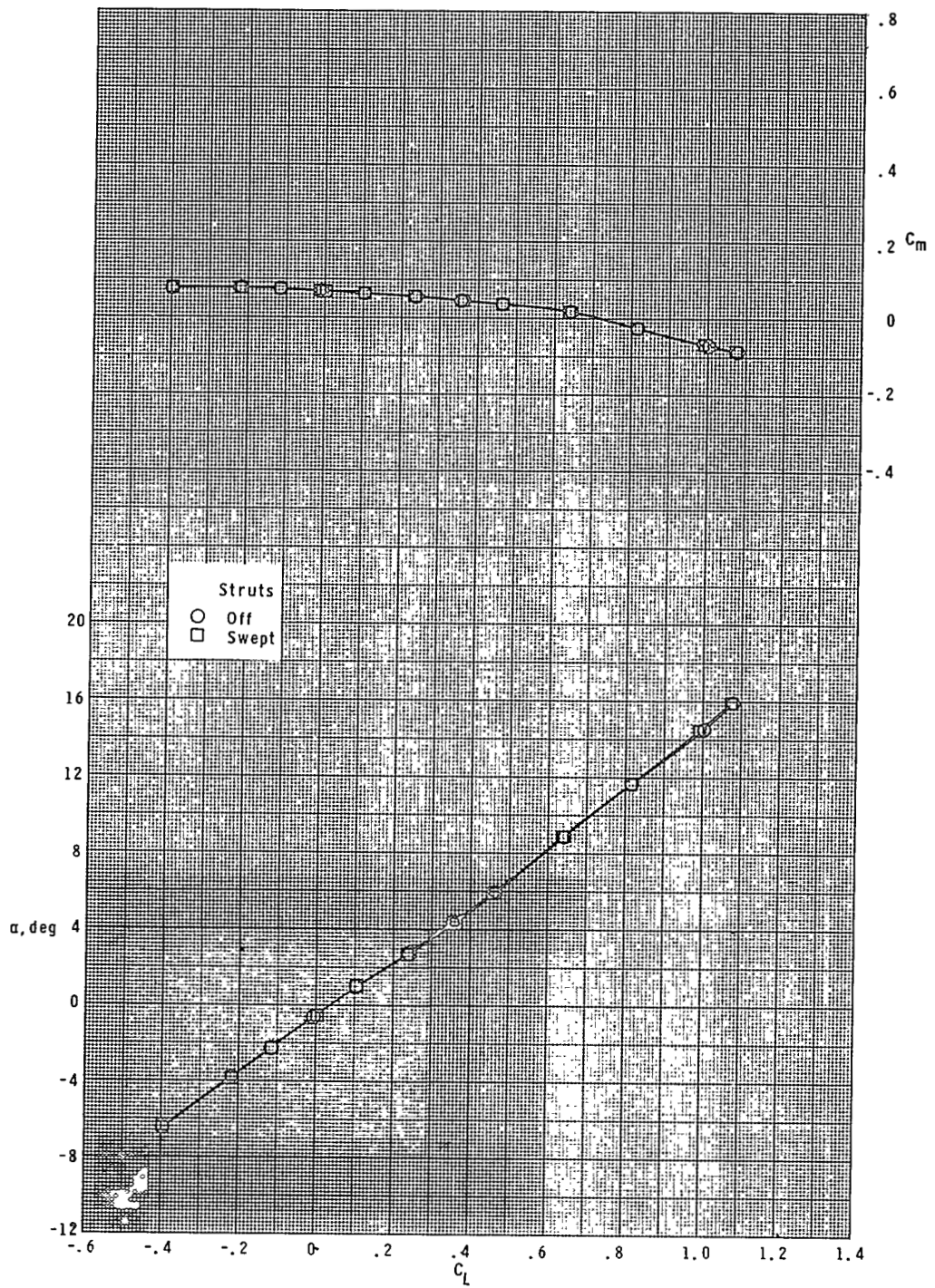
Figure 9.- Continued.

(c)   M = 0.90.

Figure 9.- Continued.
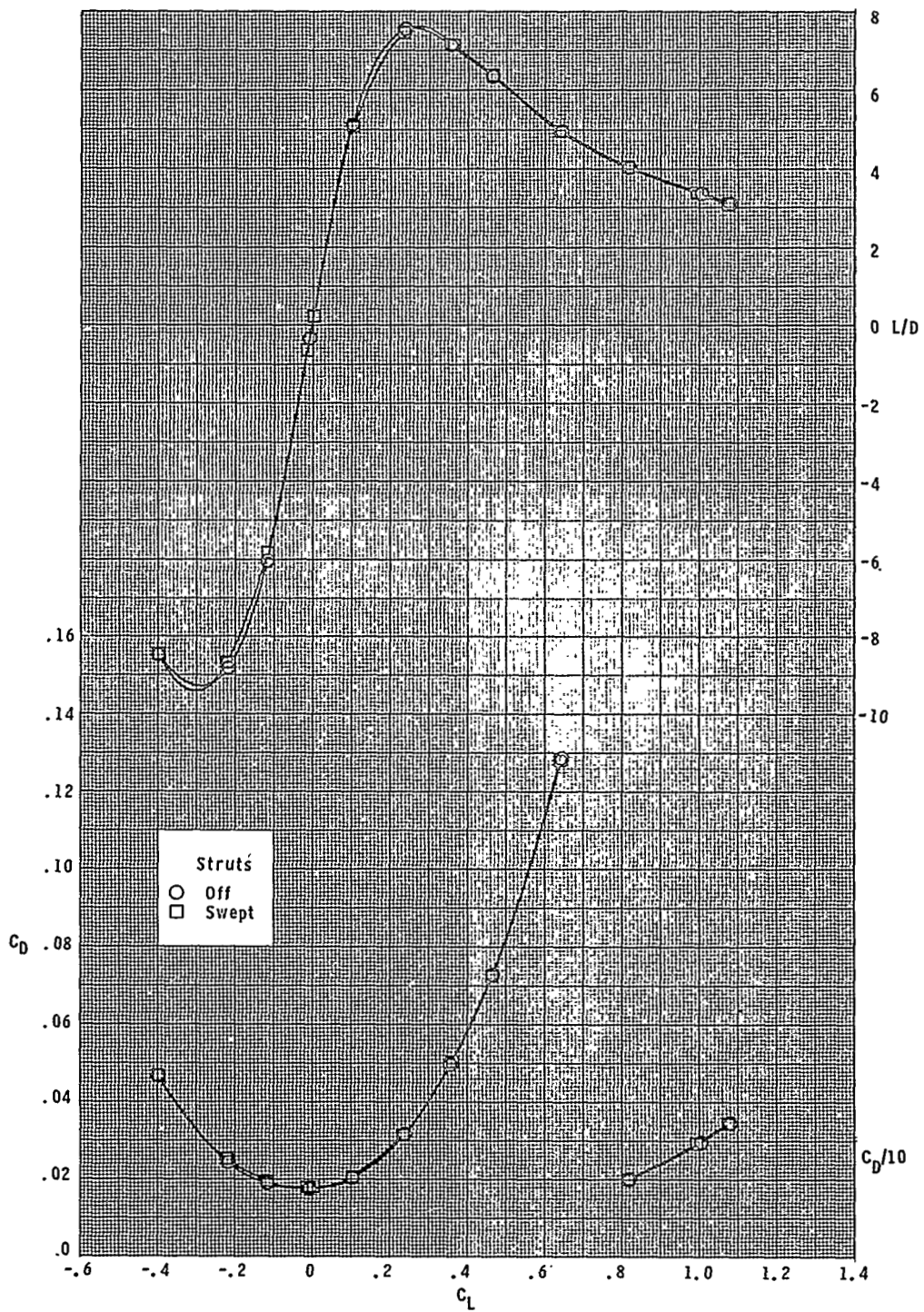
(c) Concluded.
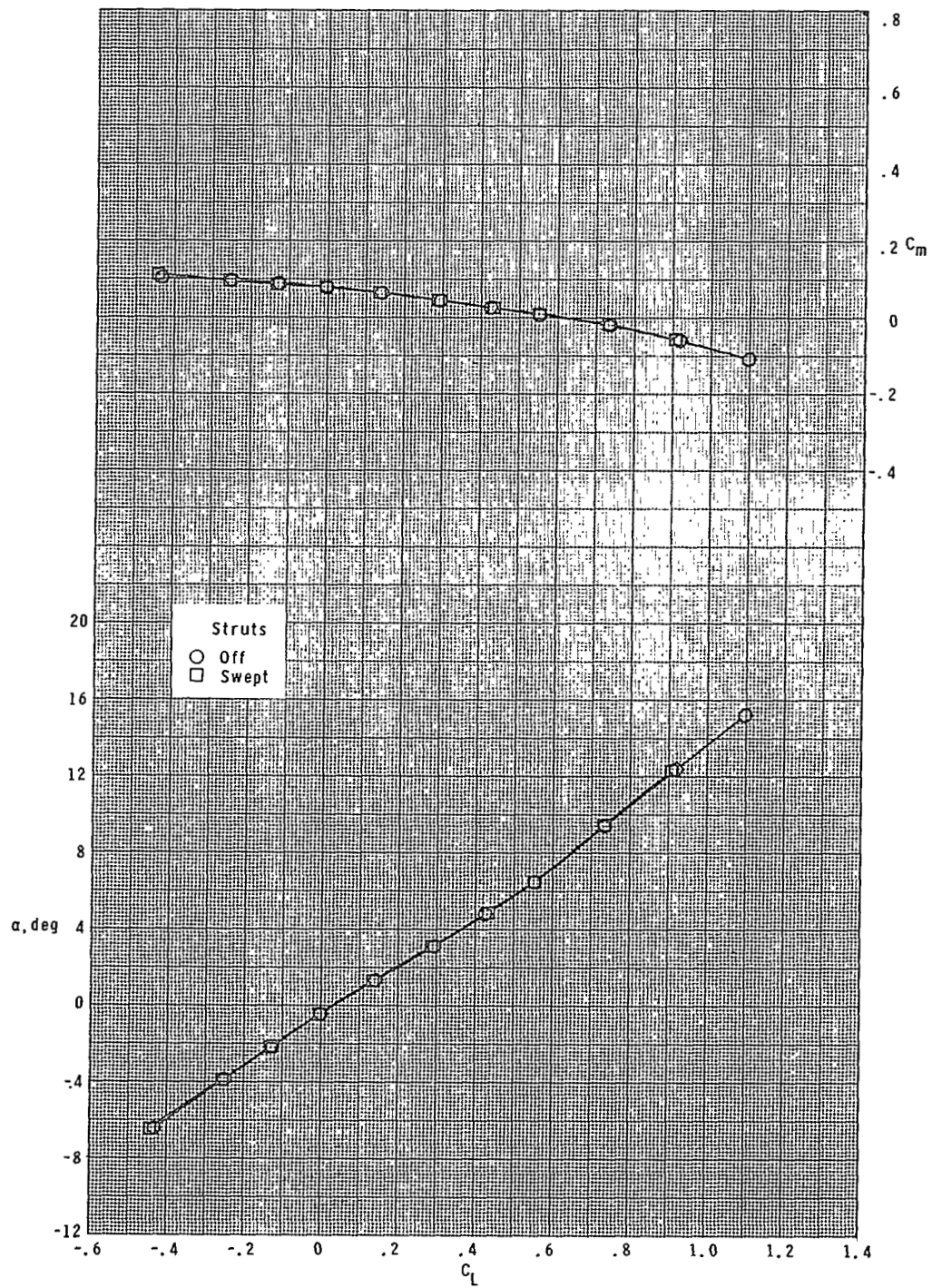
Figure 9.- Continued.

(d) M = 0.95.

Figure 9.- Continued.
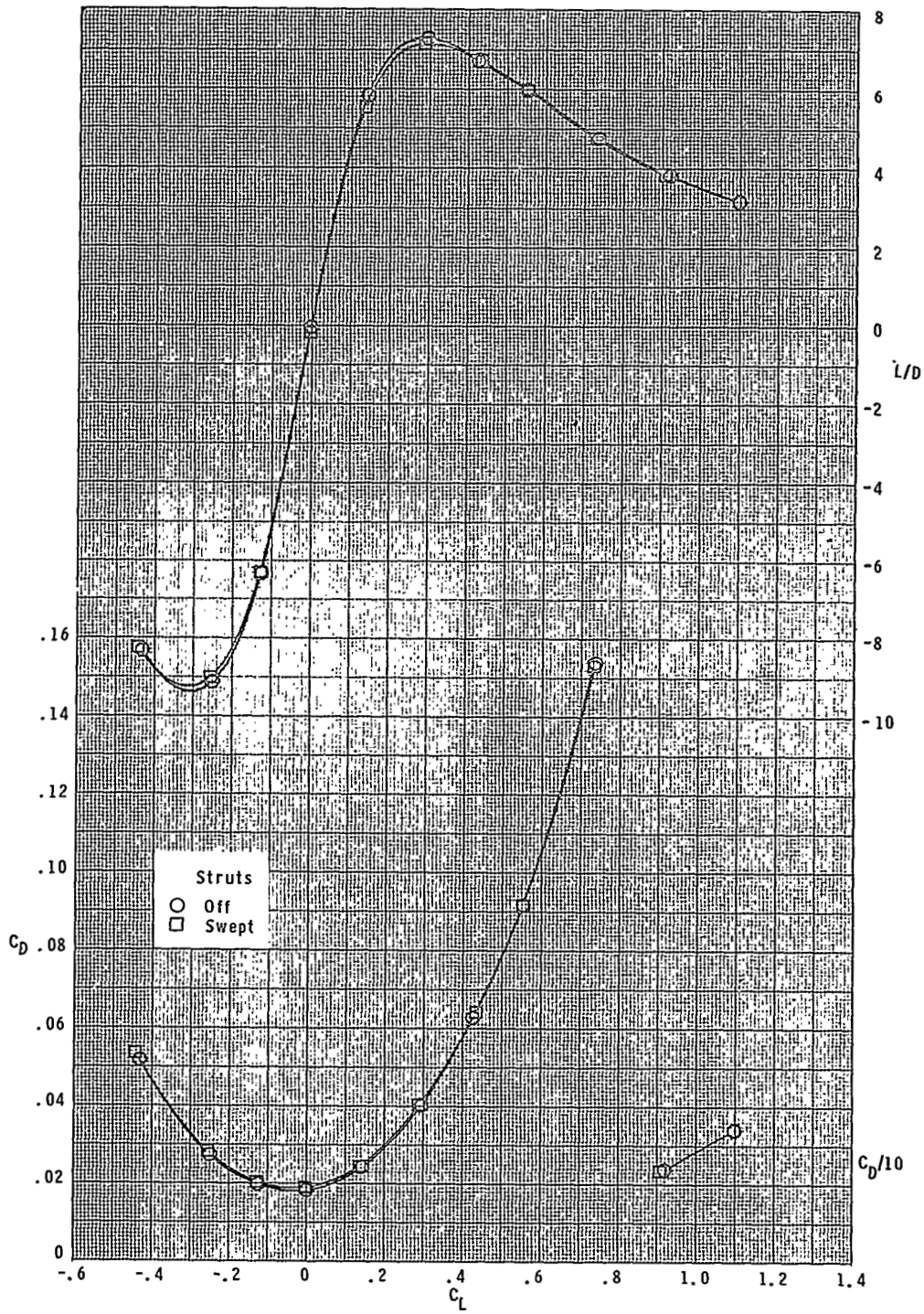
(d) Concluded.
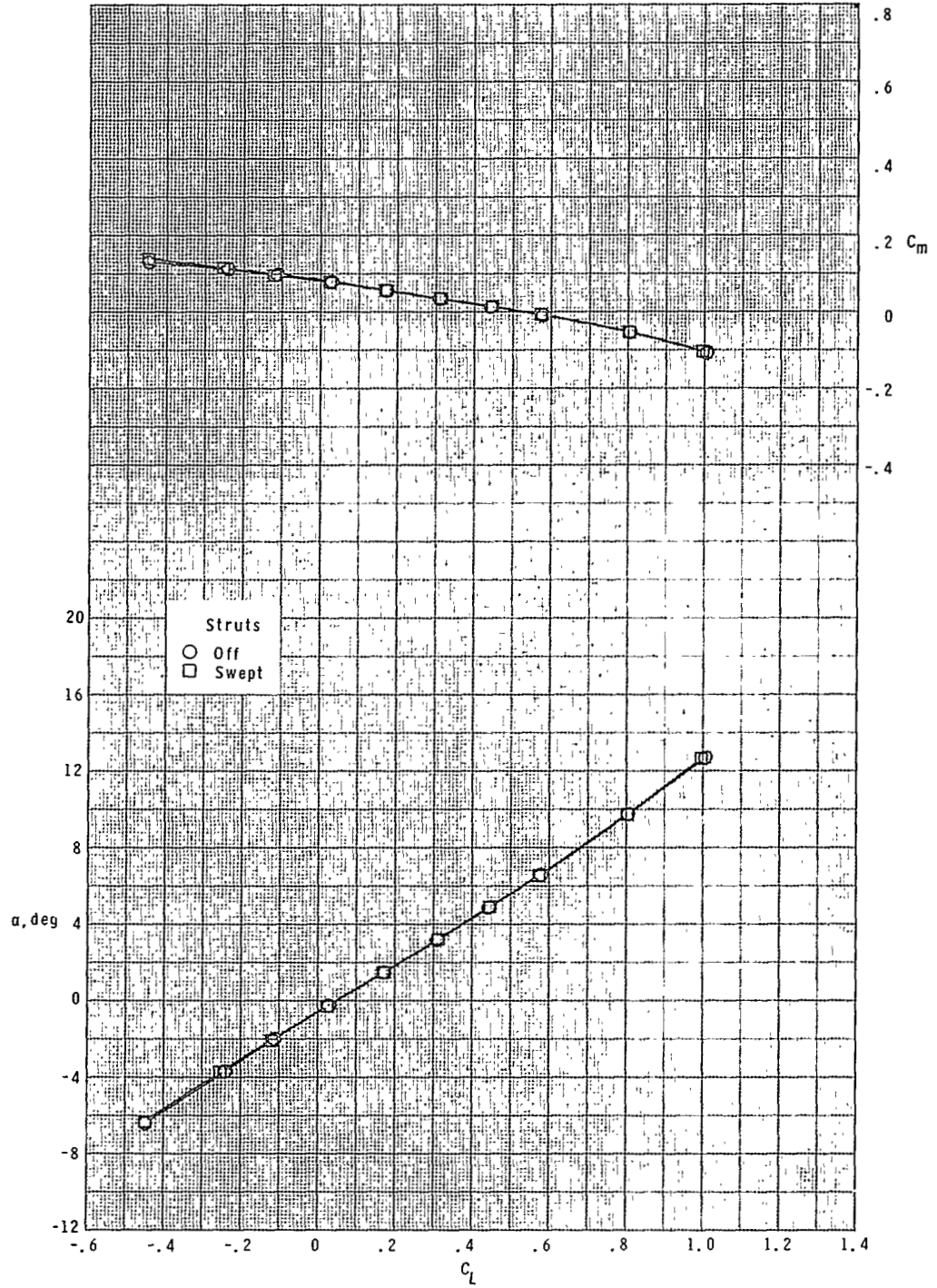
Figure 9.- Continued.

(e) M = 0.98.

Figure 9.- Continued.
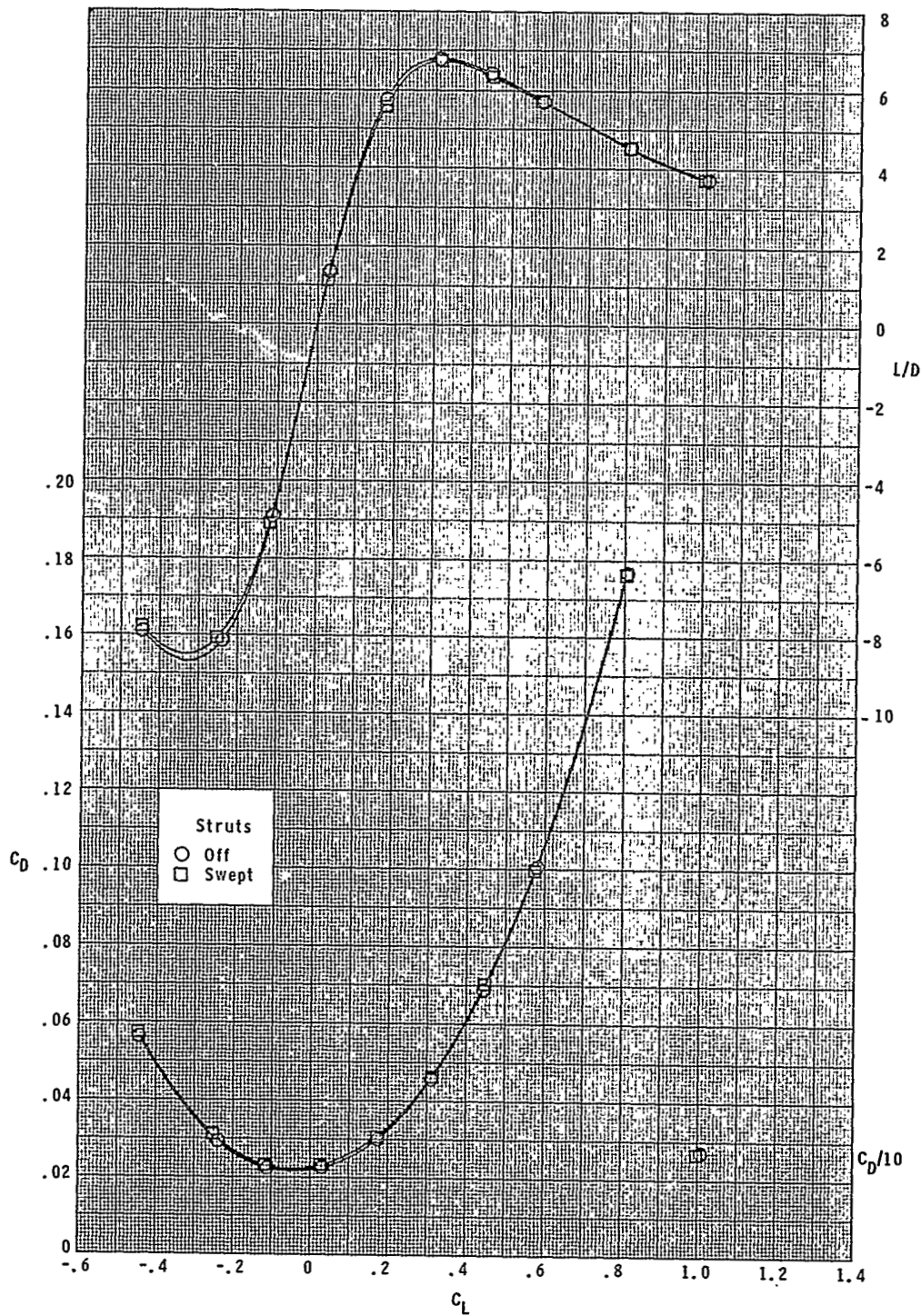
(e) Concluded.
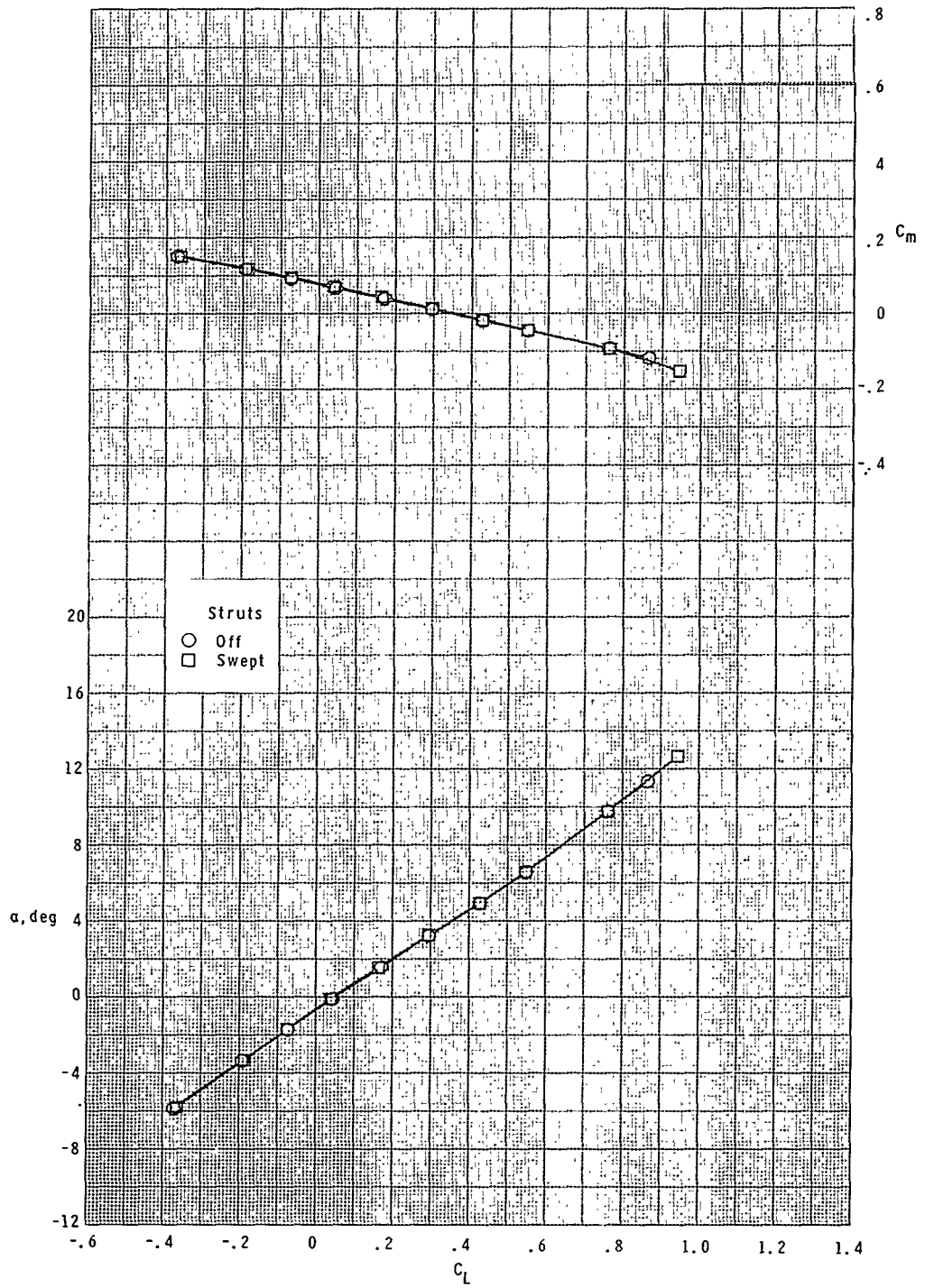
Figure 9.- Continued.

(f) M = 1.20.

Figure 9.- Continued.

(f) Concluded.

Figure 9.- Continued.

(g)   M = 1.60.

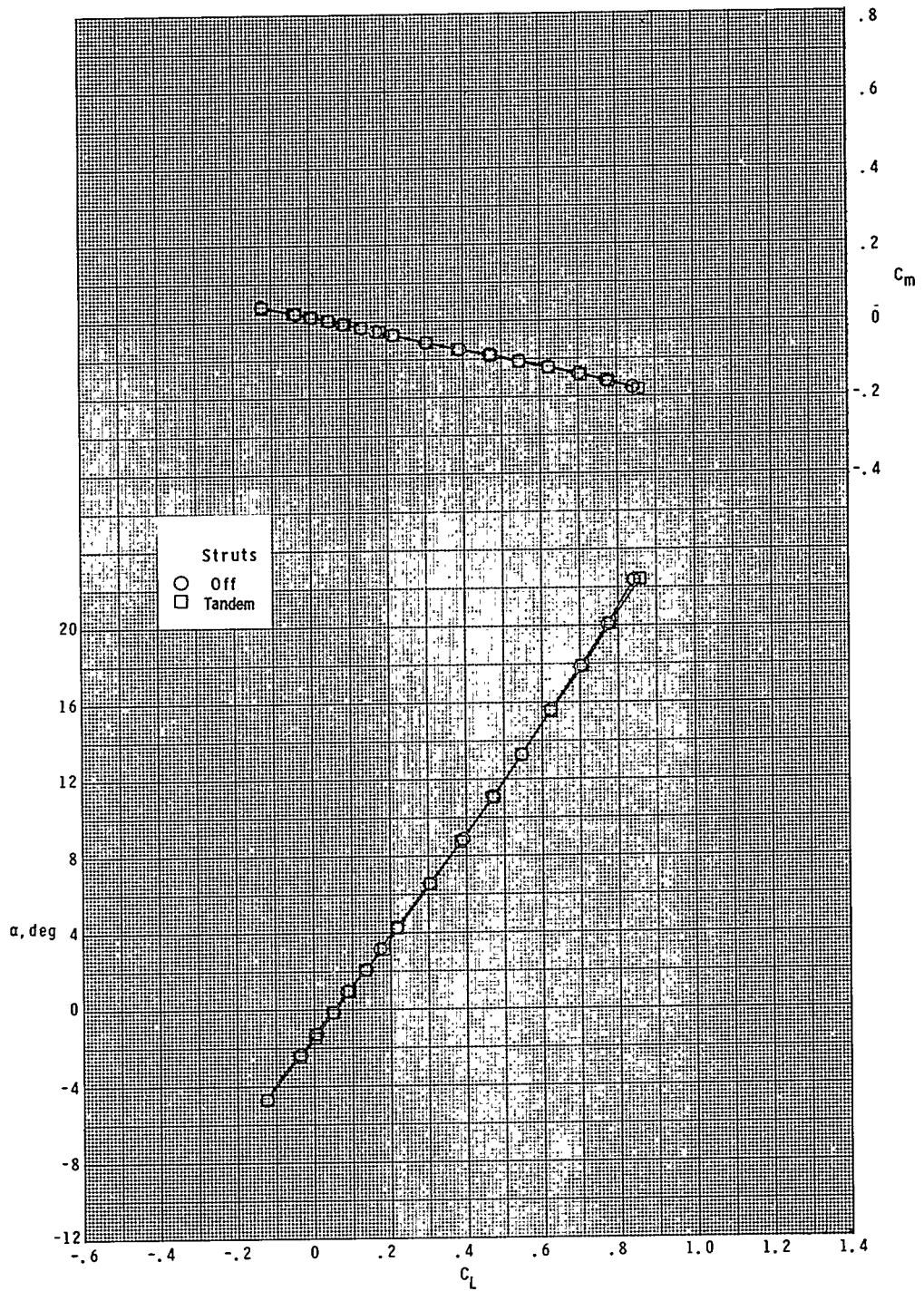Figure 9.- Continued.

(g) Concluded.

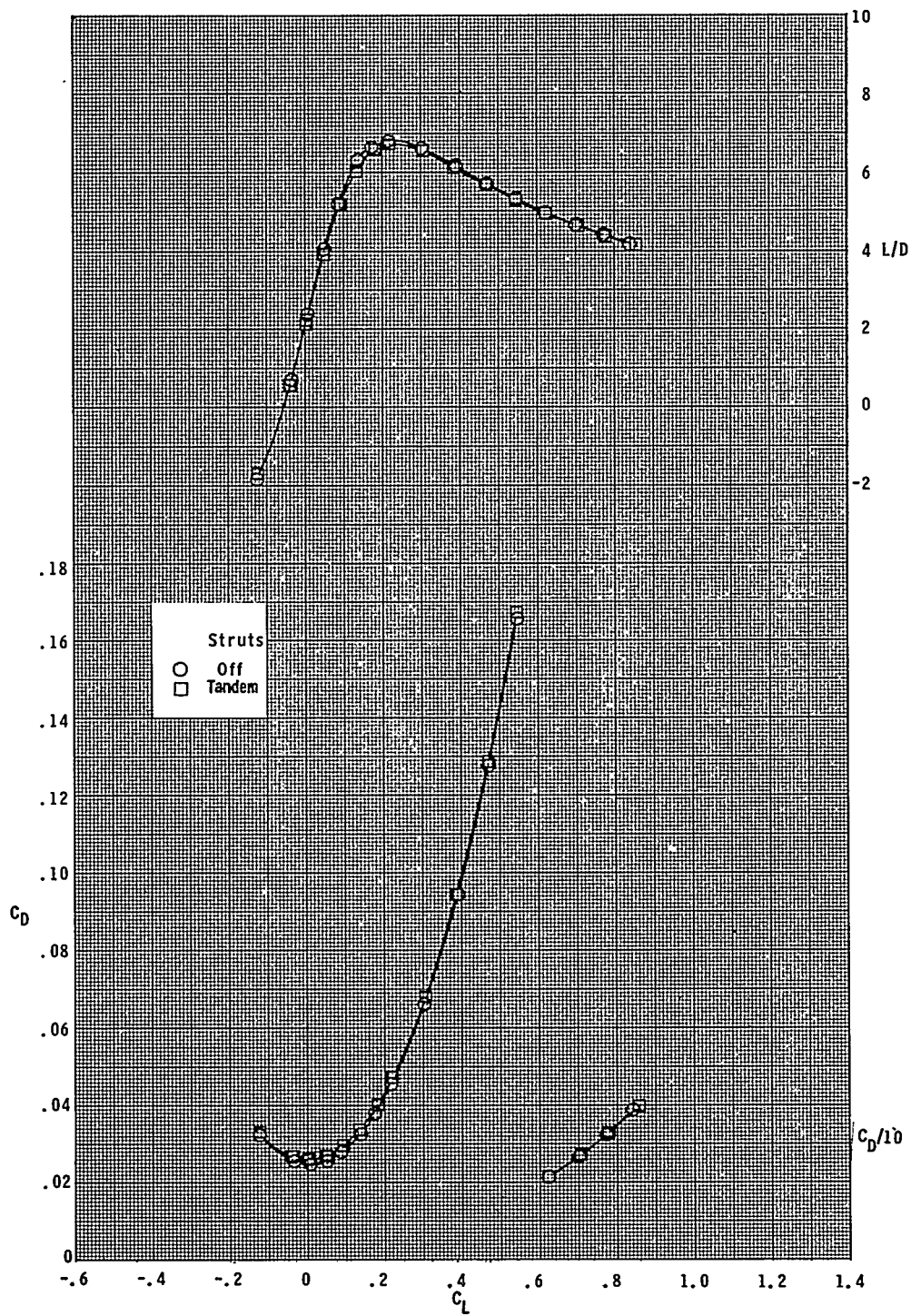Figure 9.- Continued.

(h)   M = 2.00.

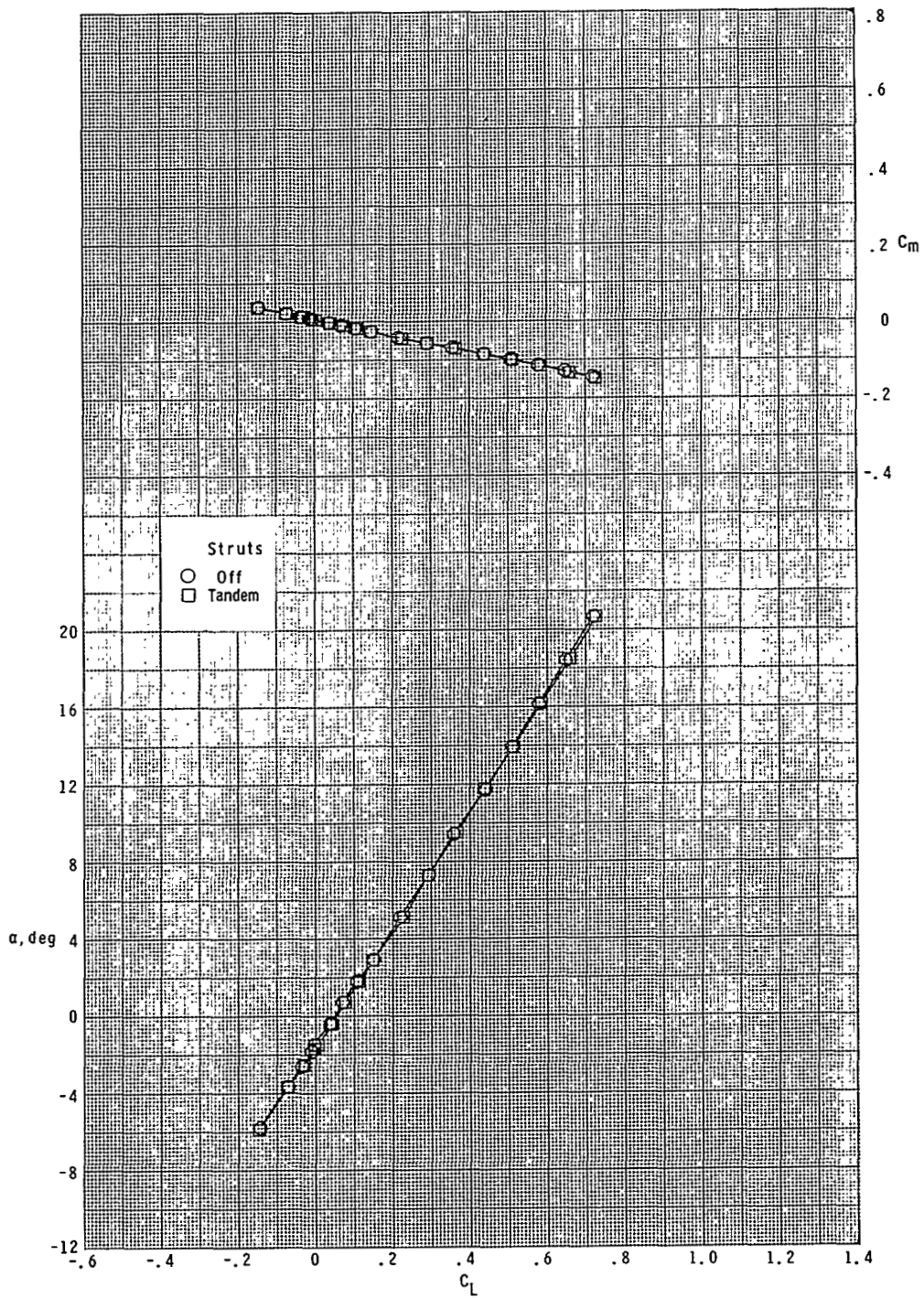Figure 9.- Continued.

(h) Concluded.

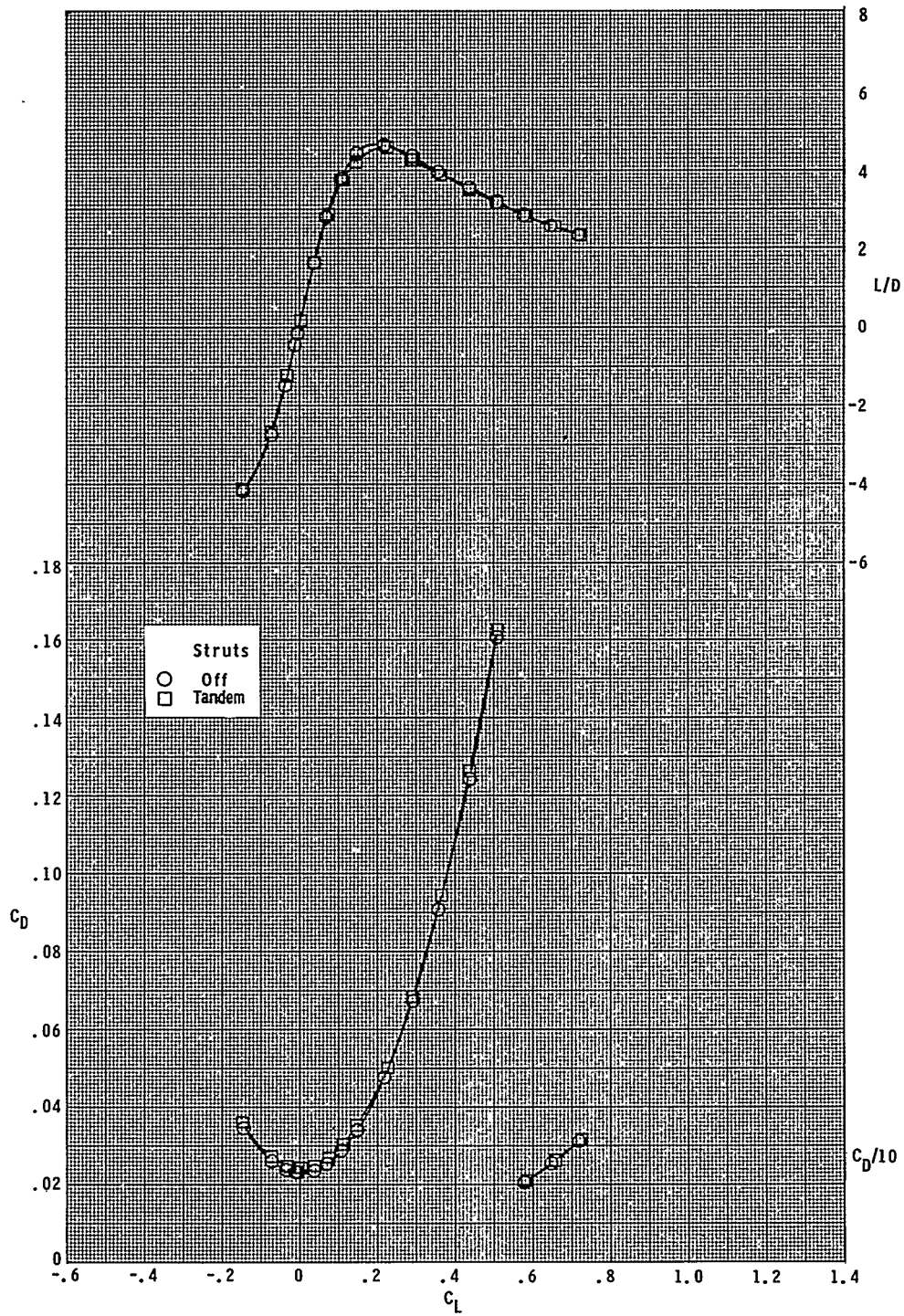Figure 9.- Continued.

(i)   M = 2.50.

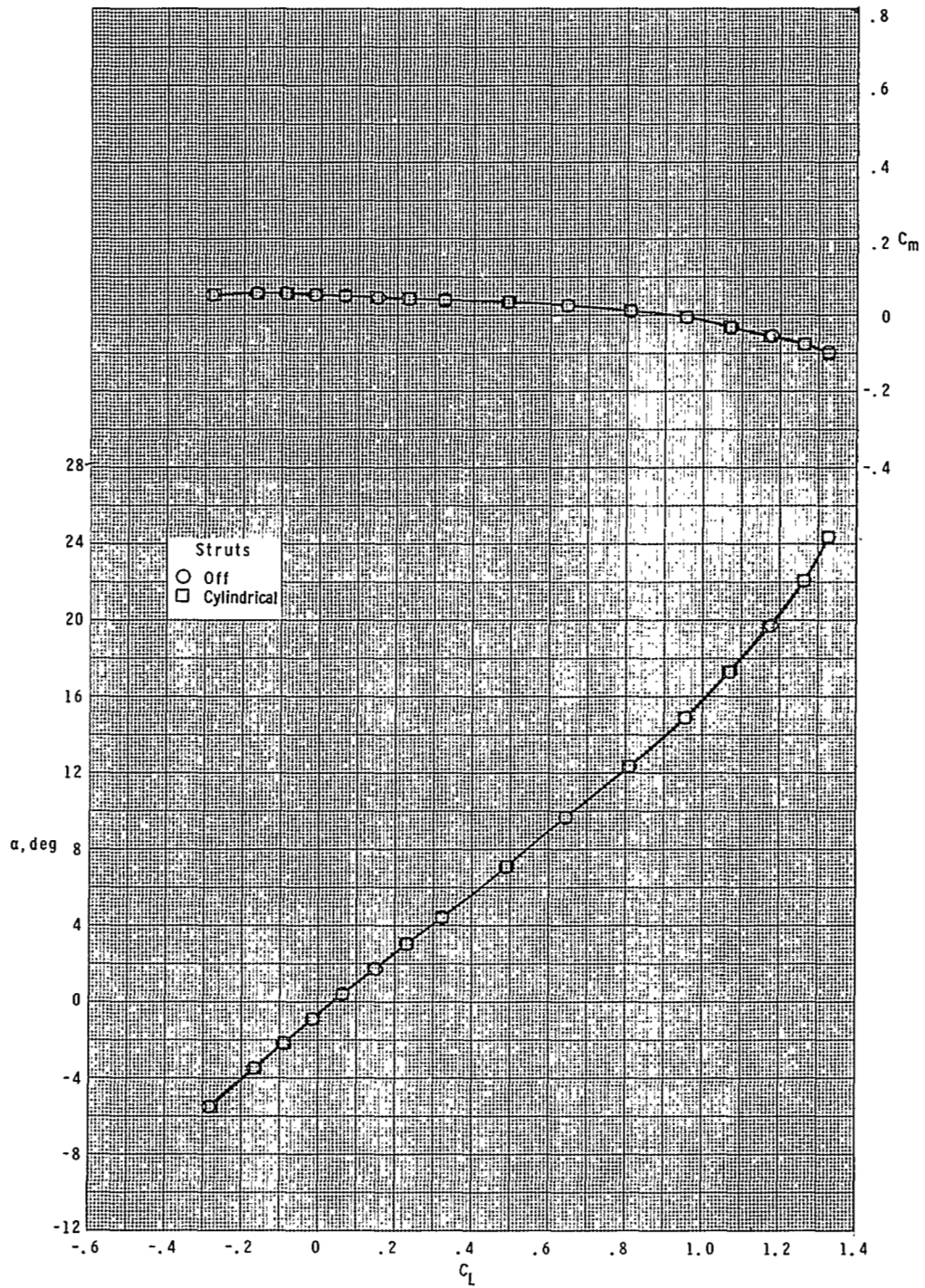Figure 9.- Continued.

(i) Concluded.

Figure 9.- Continued.

(j)   M = 2.86.

Figure 9.- Continued.
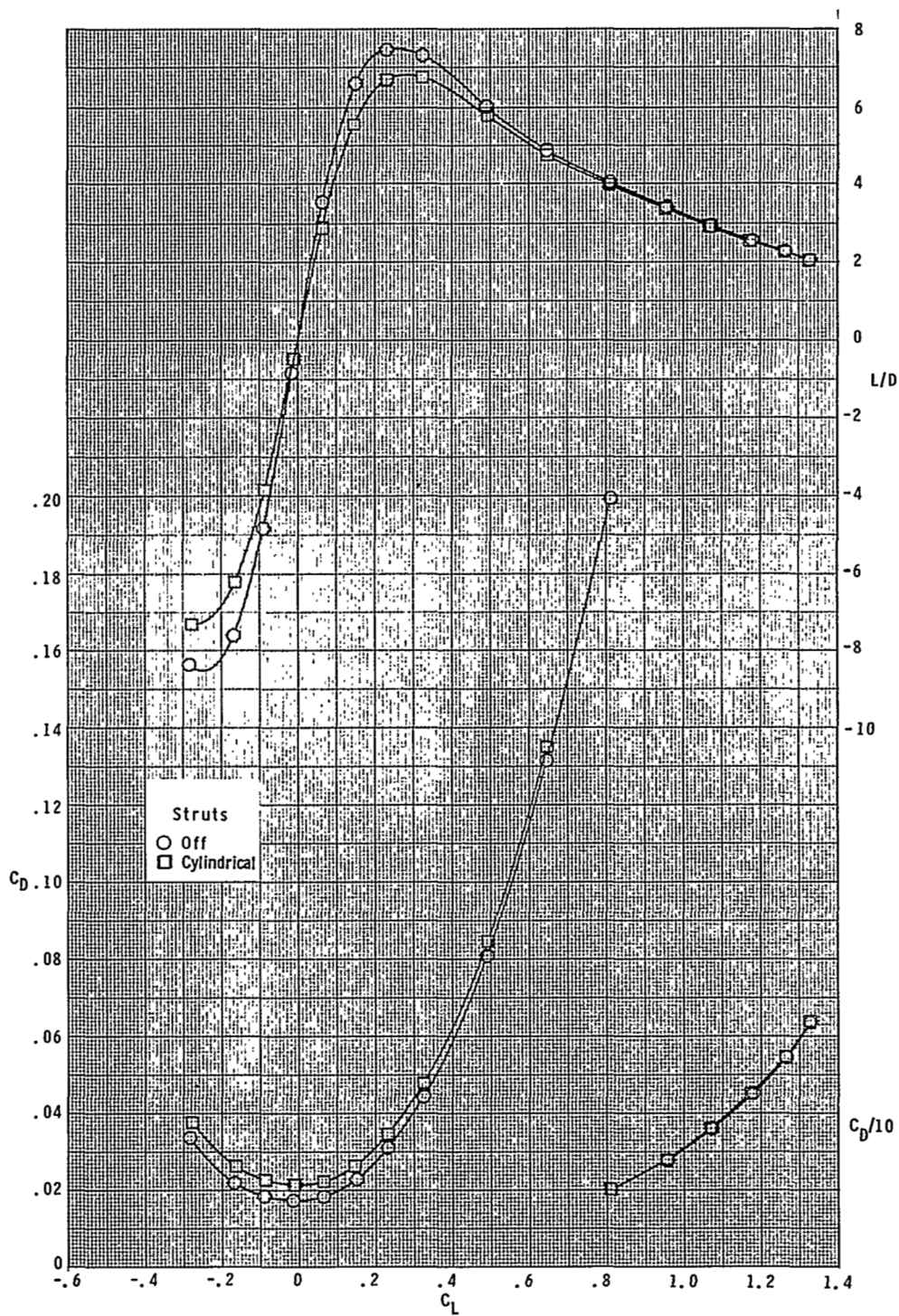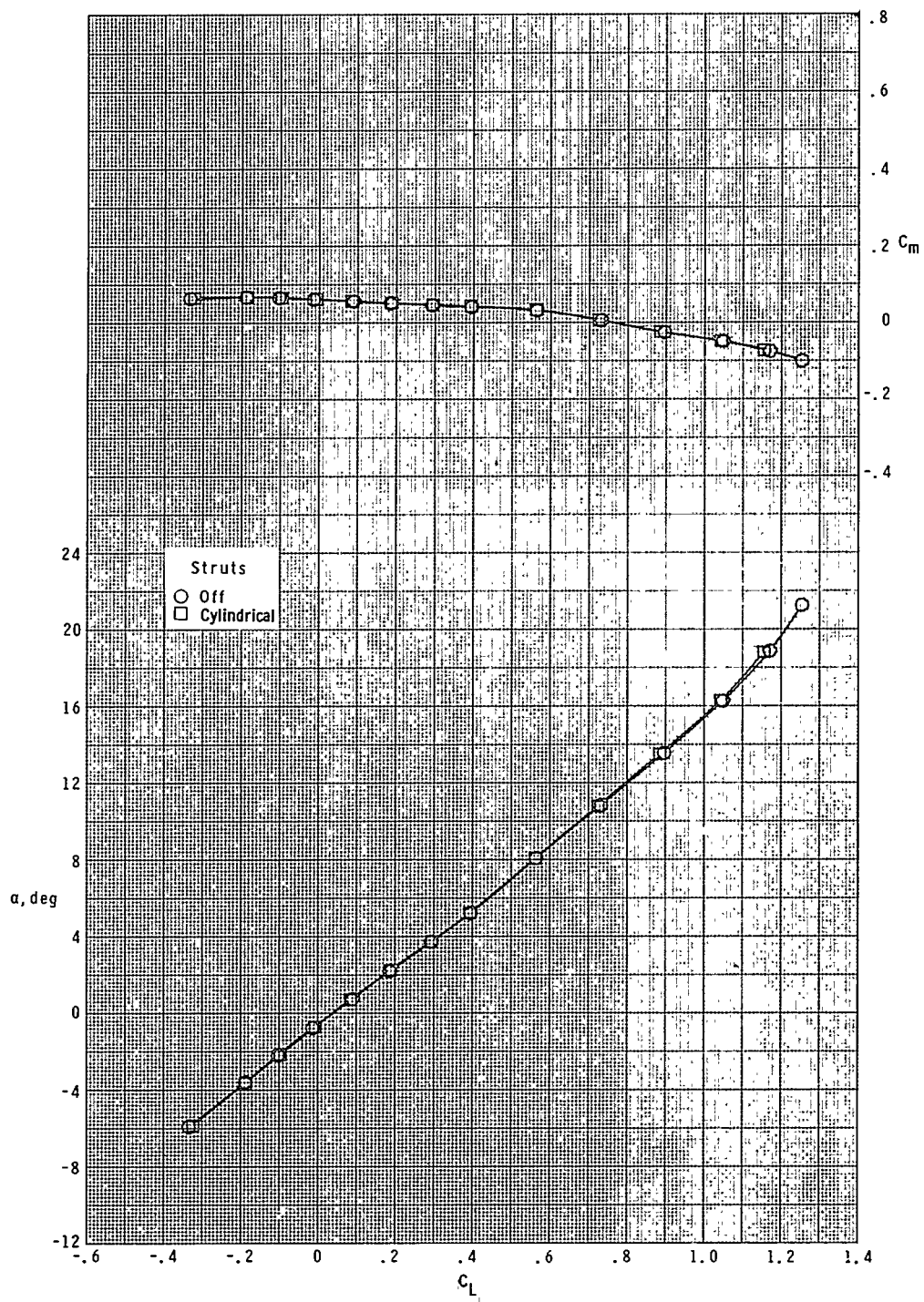
(j) Concluded.

Figure 9.- Concluded.

(a) M = 0.60.

Figure 10.- Effect of tandem struts on longitudinal aerodynamic characteristics
for $\delta_h = 0^\circ$.
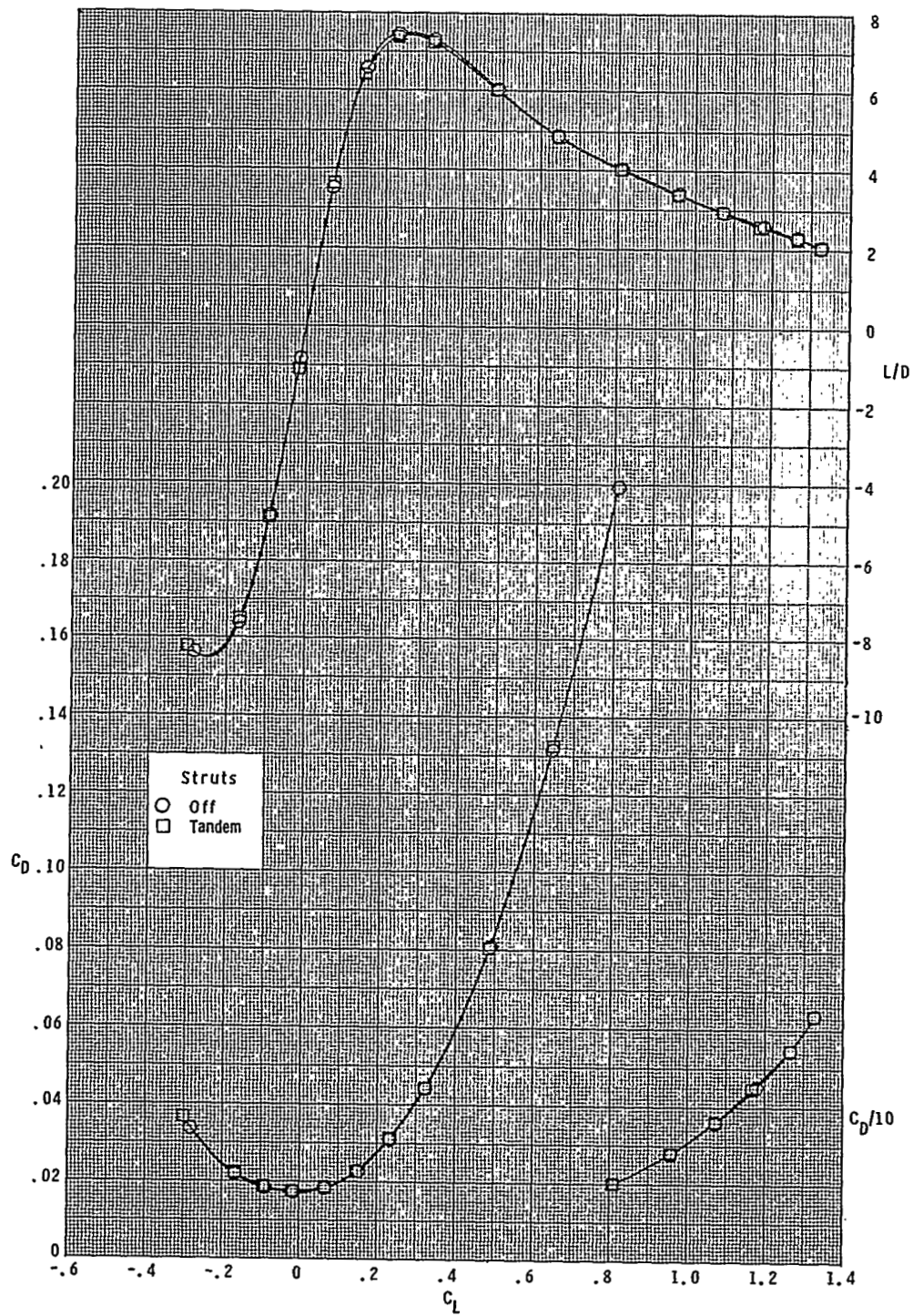
(a) Concluded.

Figure 10.- Continued.

(b)   M = 0.80.

Figure 10.- Continued.

(b) Concluded.

Figure 10.- Continued.
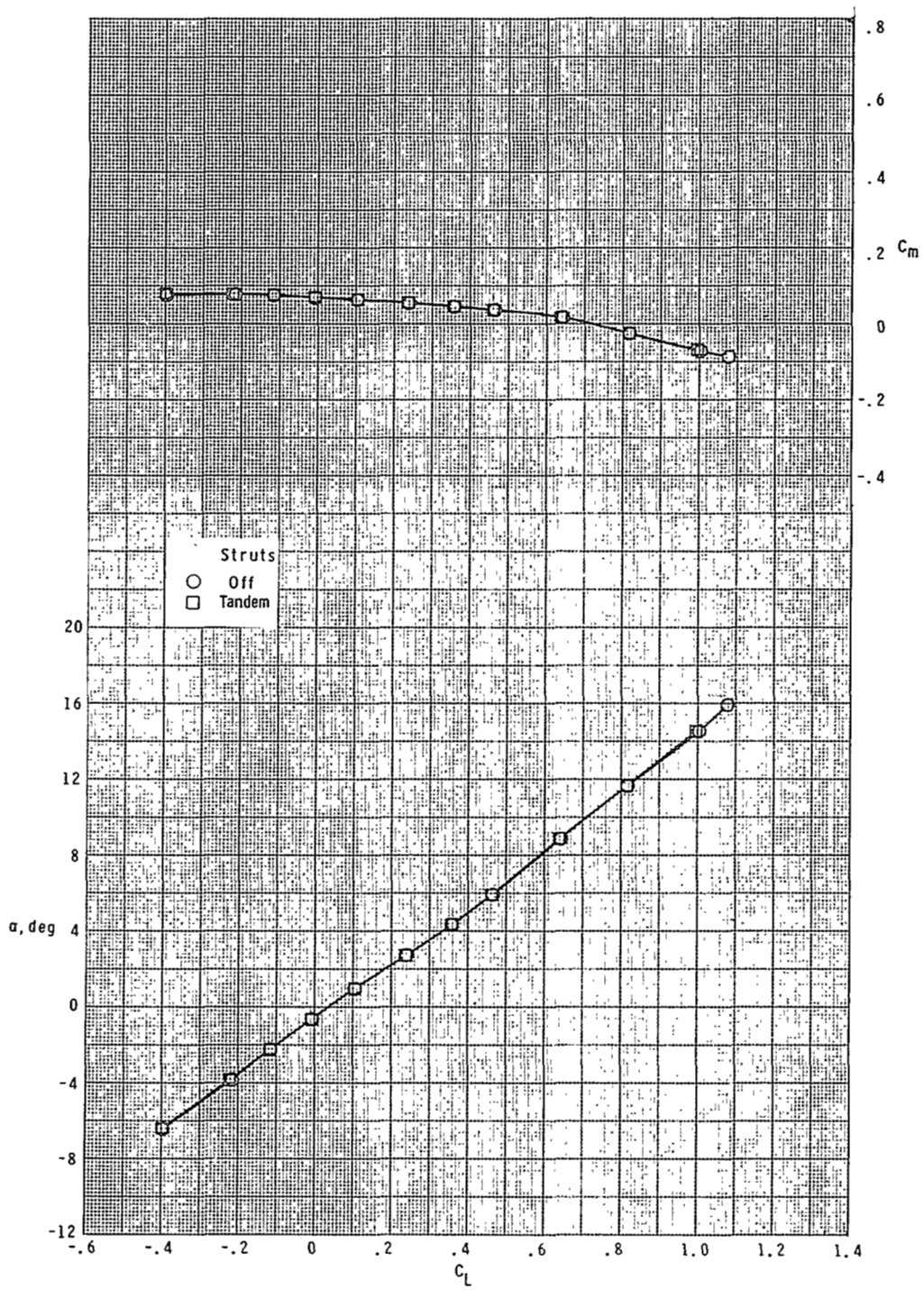
(c)   M = 0.90.

Figure 10.- Continued.

(c) Concluded.

Figure 10.- Continued.
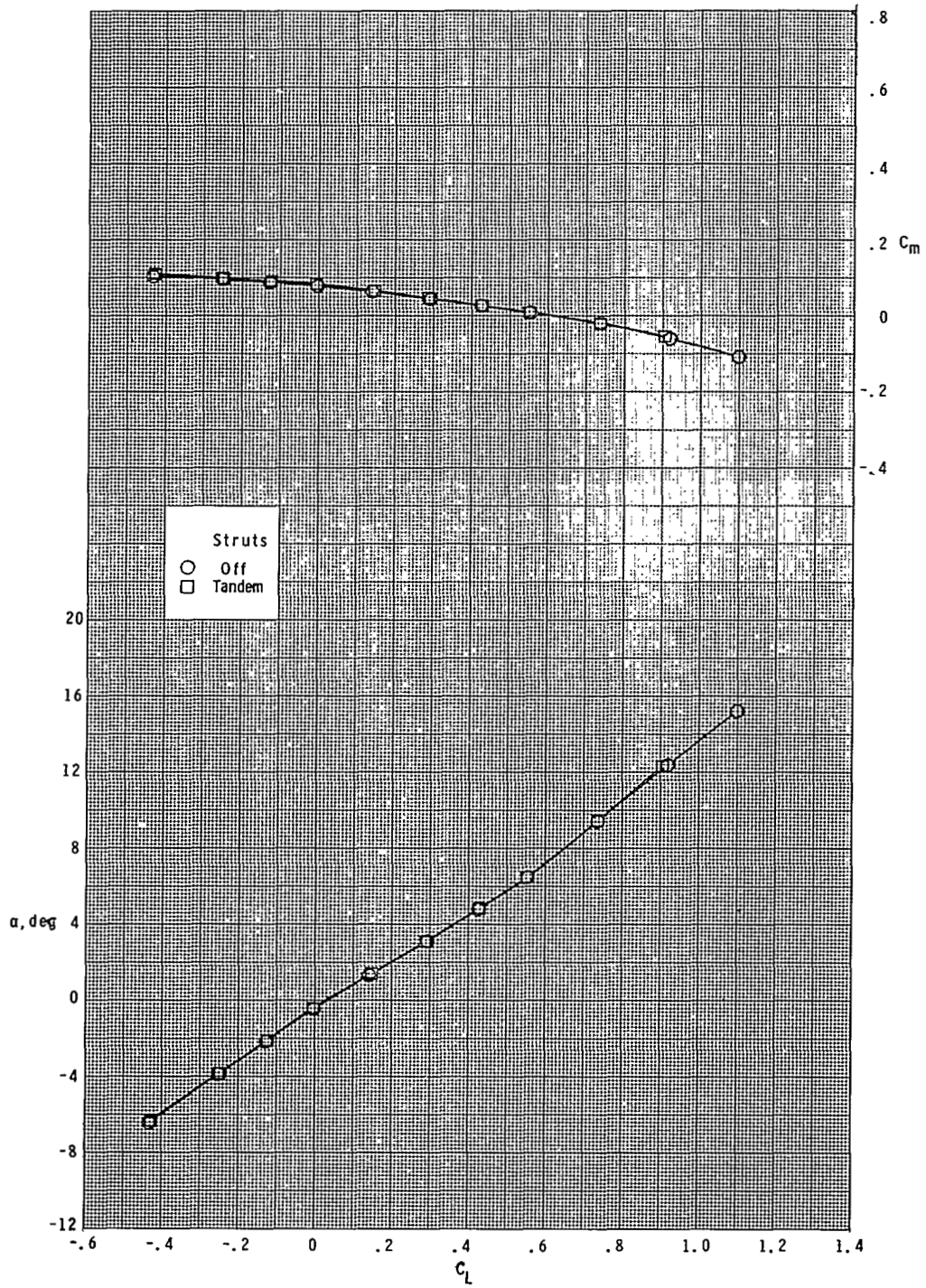
(d) M = 0.95.

Figure 10.- Continued.
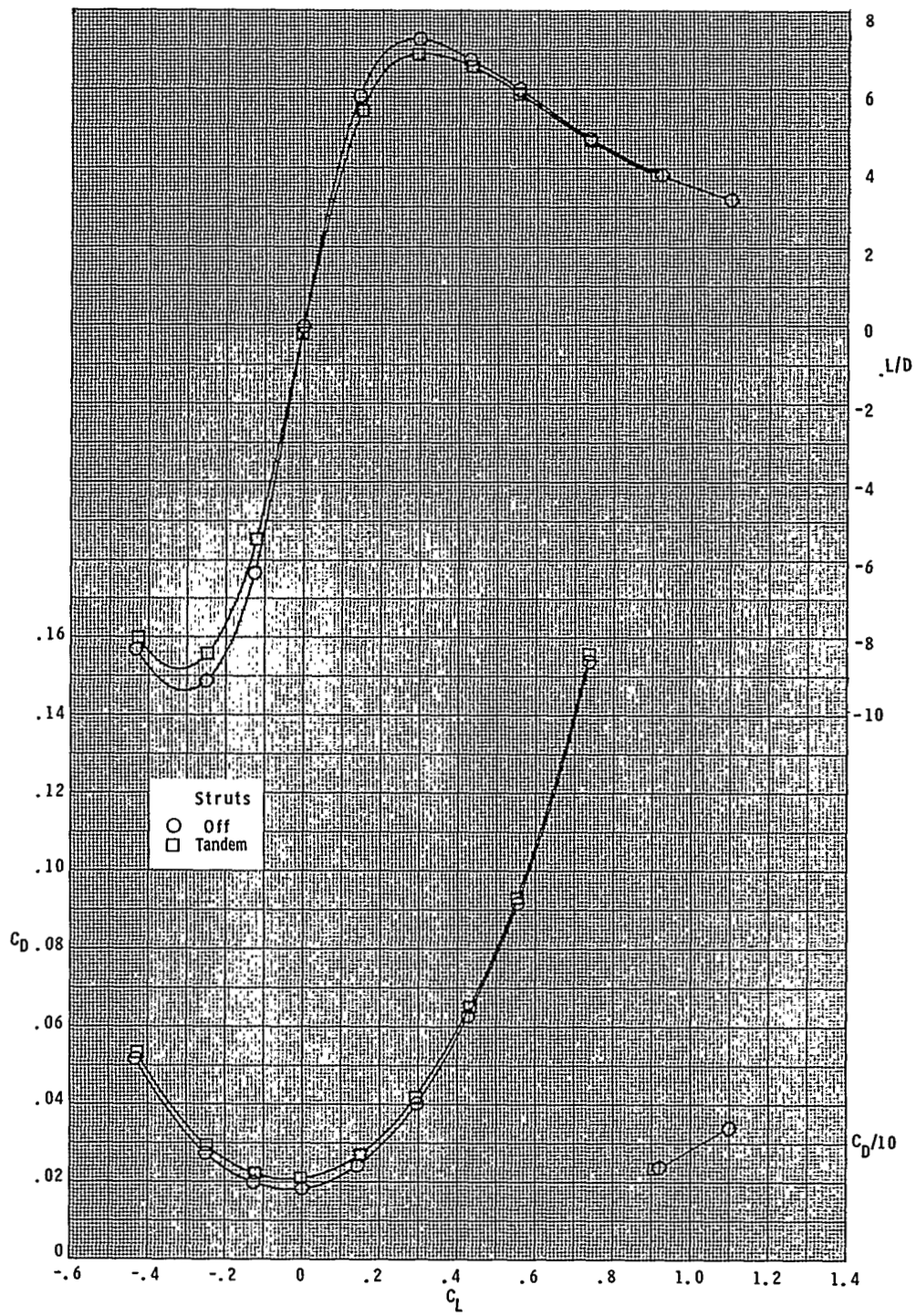
(d) Concluded.

Figure 10.- Continued.

(e)   M = 0.98.

Figure 10.- Continued.

(e) Concluded.

Figure 10.- Continued.
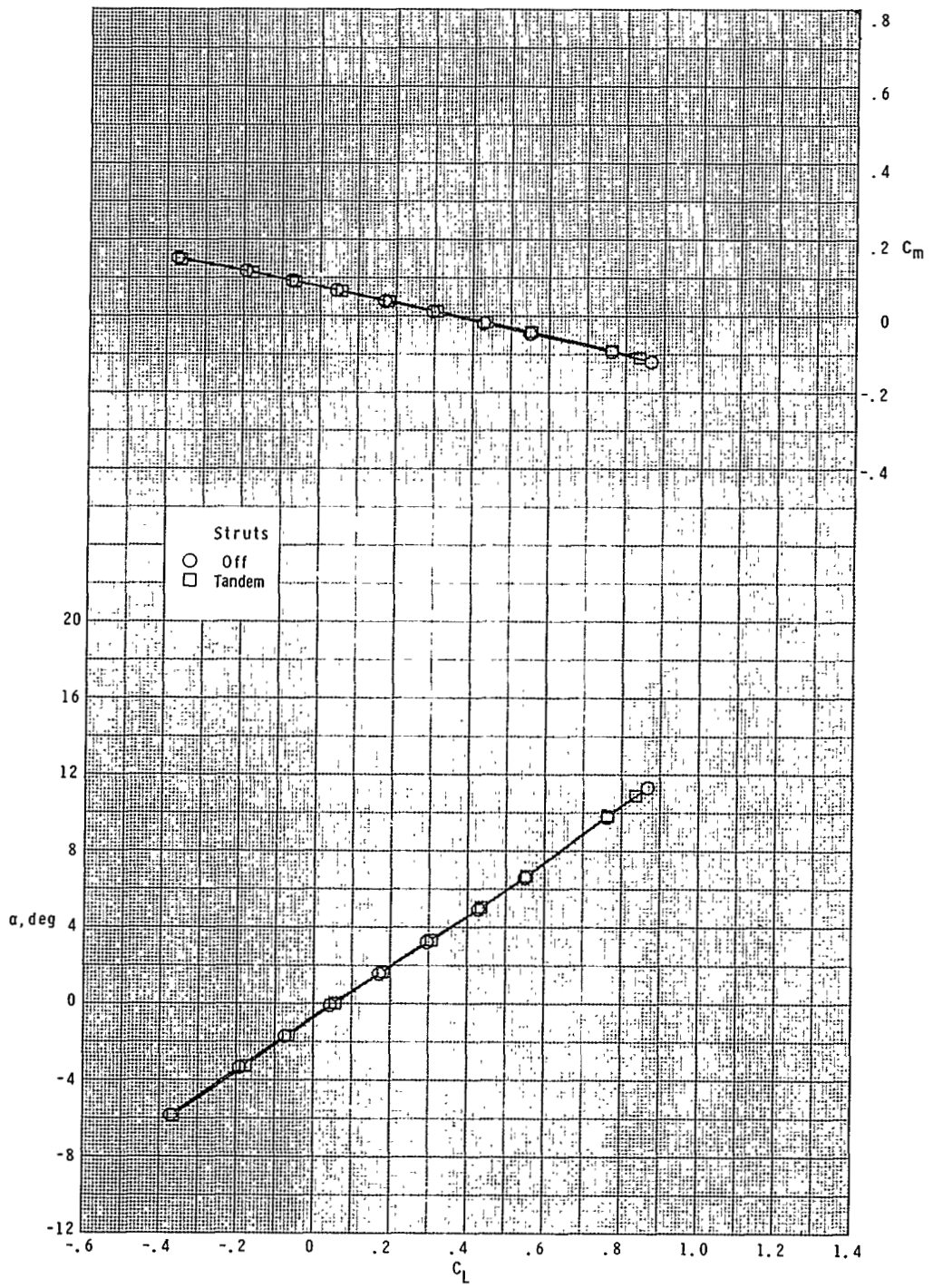
(f)   M = 1.20.

Figure 10.- Continued.
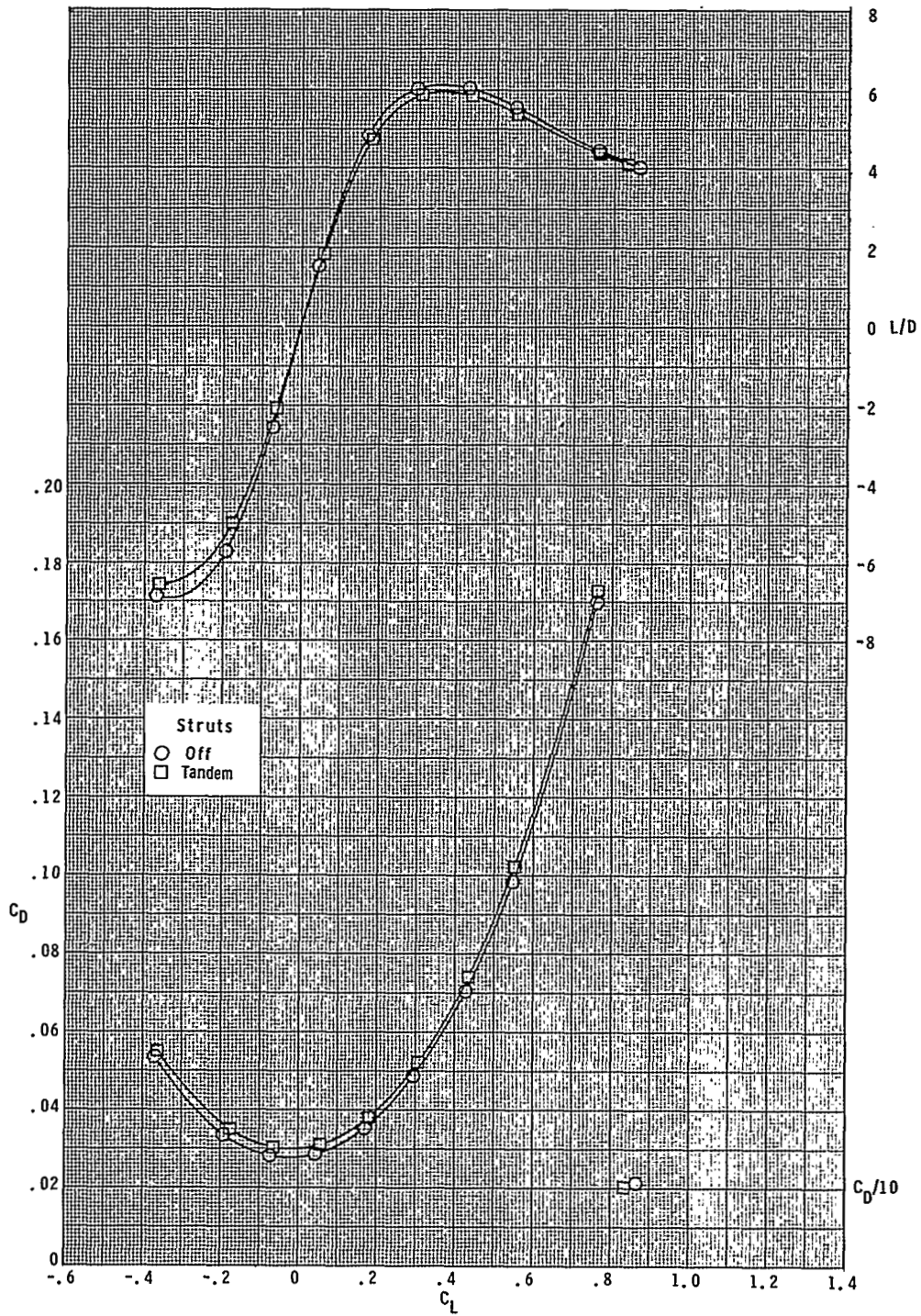
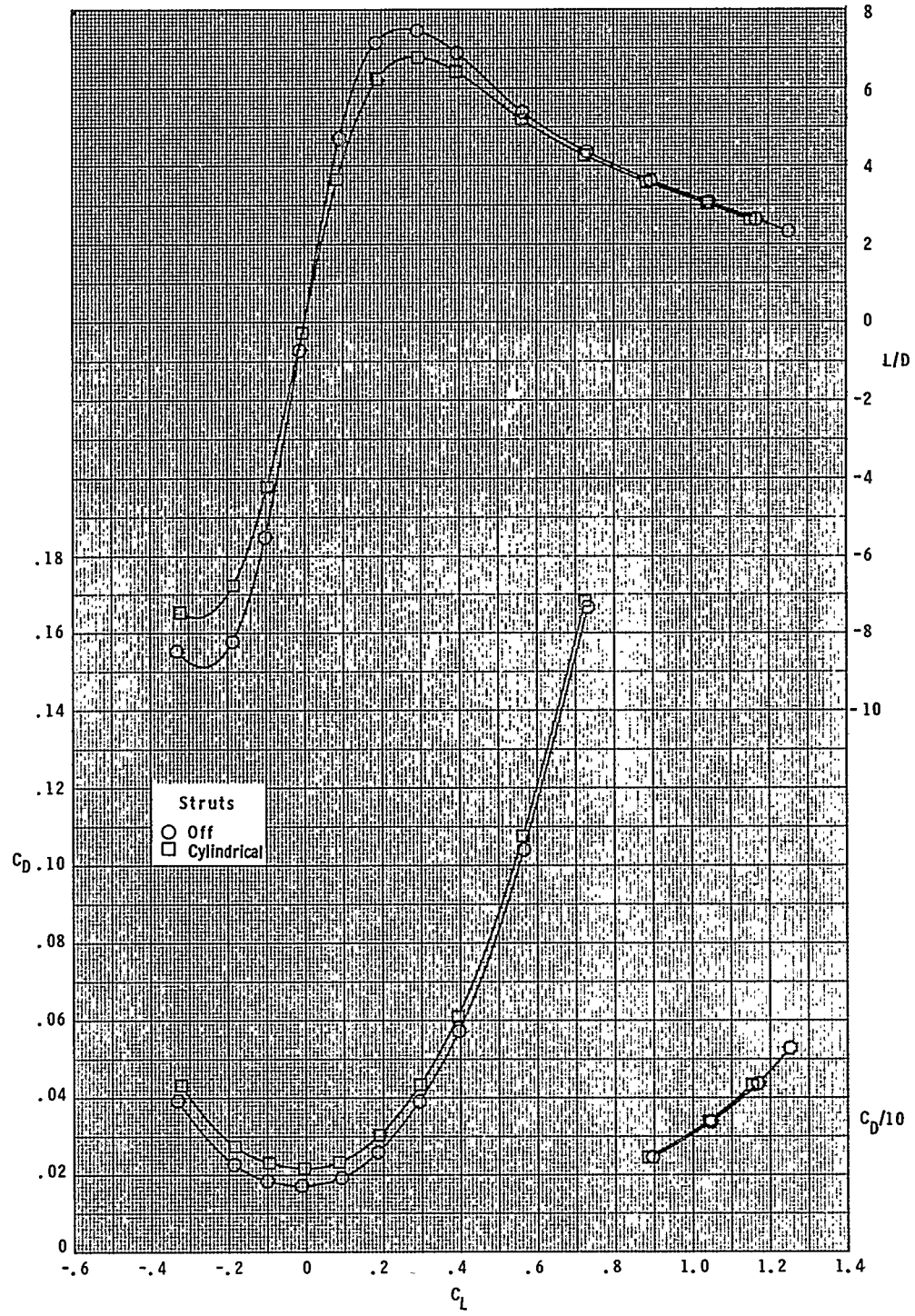(f) Concluded.

Figure 10.- Continued.

(g) M = 1.60.

Figure 10.- Continued.

(g) Concluded.

Figure 10.- Continued.

(h) M = 2.00.

Figure 10.- Continued.

(h) Concluded.

Figure 10.- Continued.

(i)   M = 2.50.

Figure 10.- Continued.

(i) Concluded.

Figure 10.- Continued.

(j)   M = 2.86.

Figure 10.- Continued.

(j) Concluded.

Figure 10.- Concluded.

(a) M = 0.60.

Figure 11.- Effect of cylindrical strut on longitudinal aerodynamic characteristics for $\delta_h = 0^\circ$.
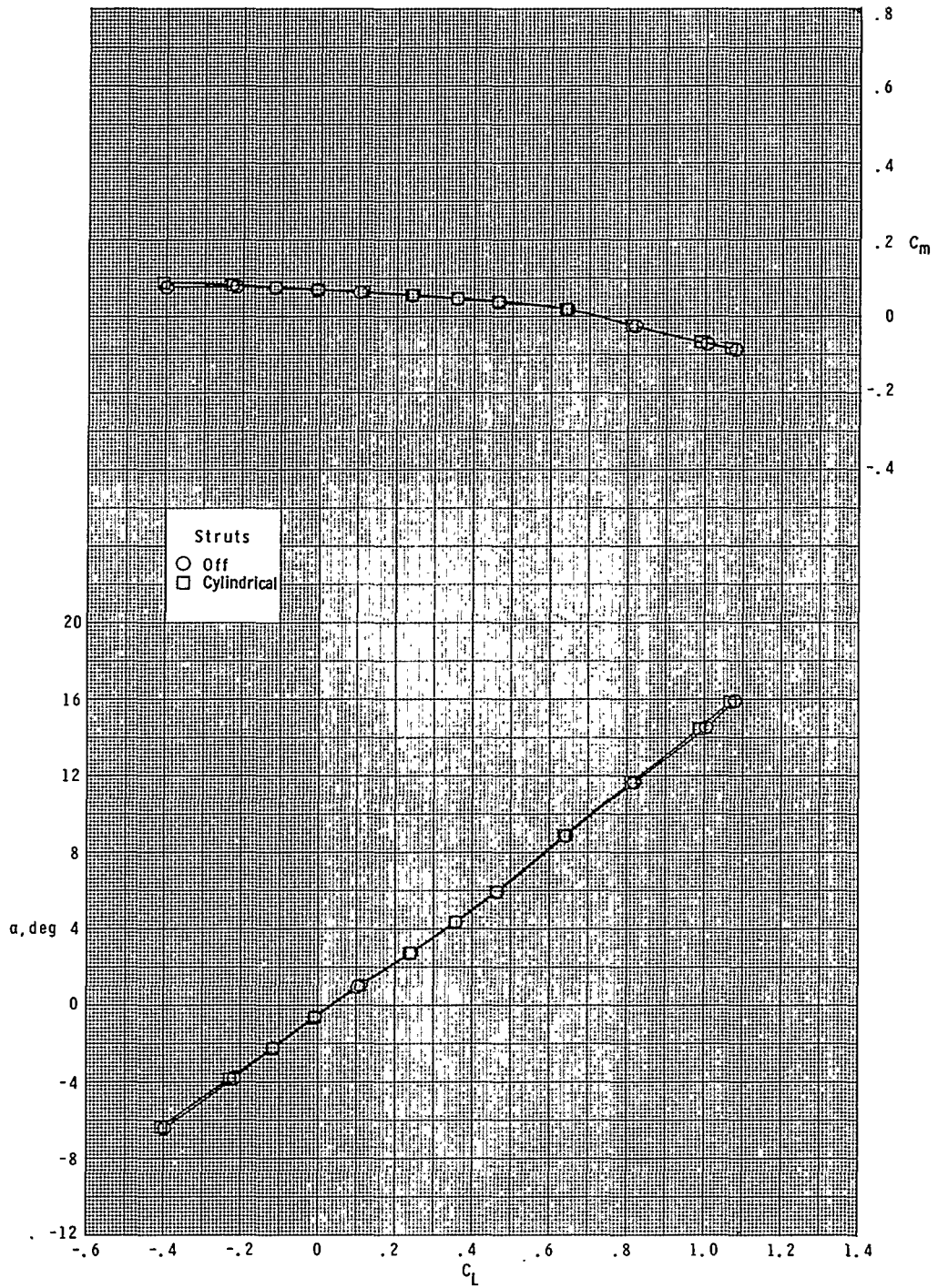
(a) Concluded.

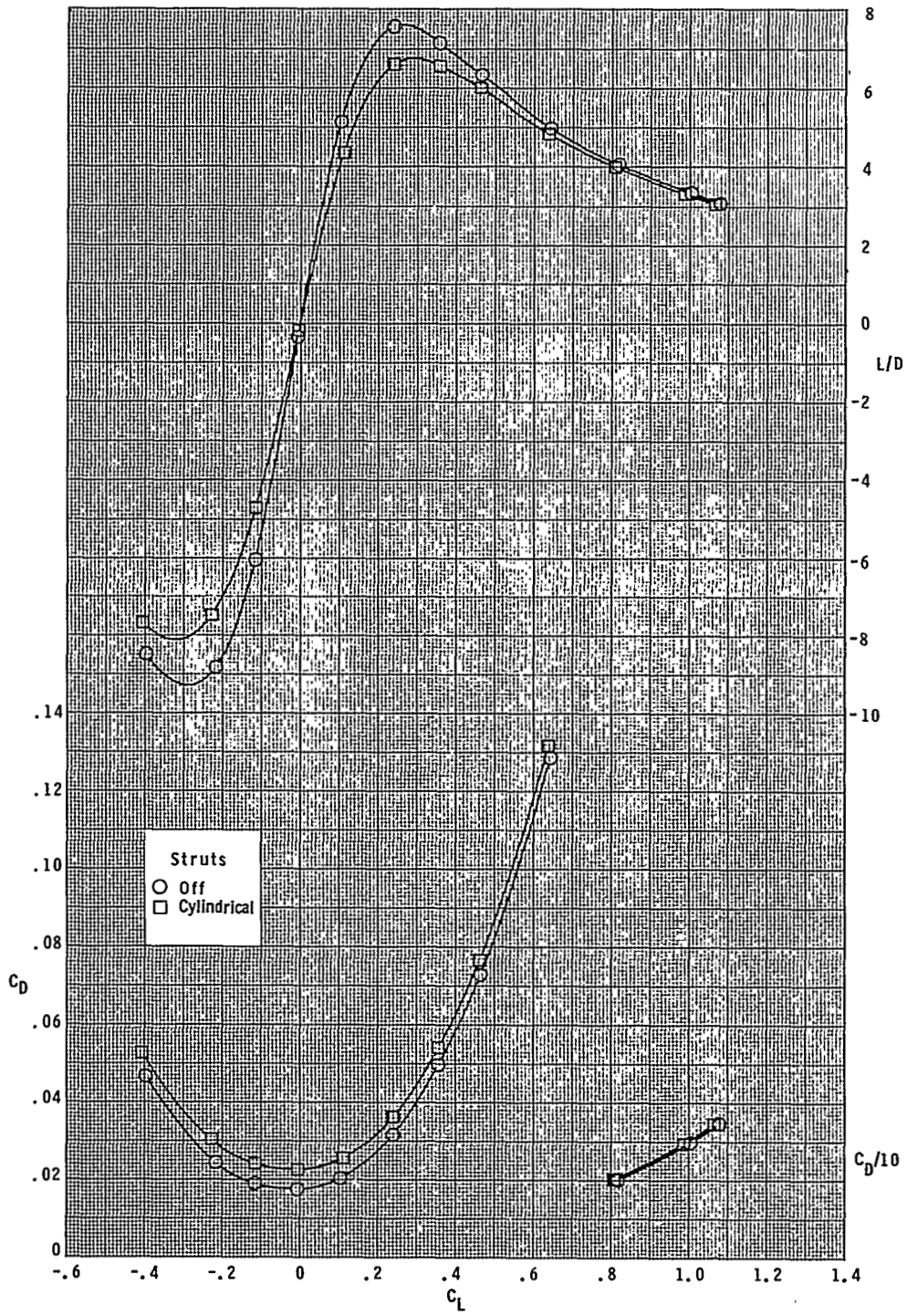Figure 11.- Continued.

(b)   M = 0.80.

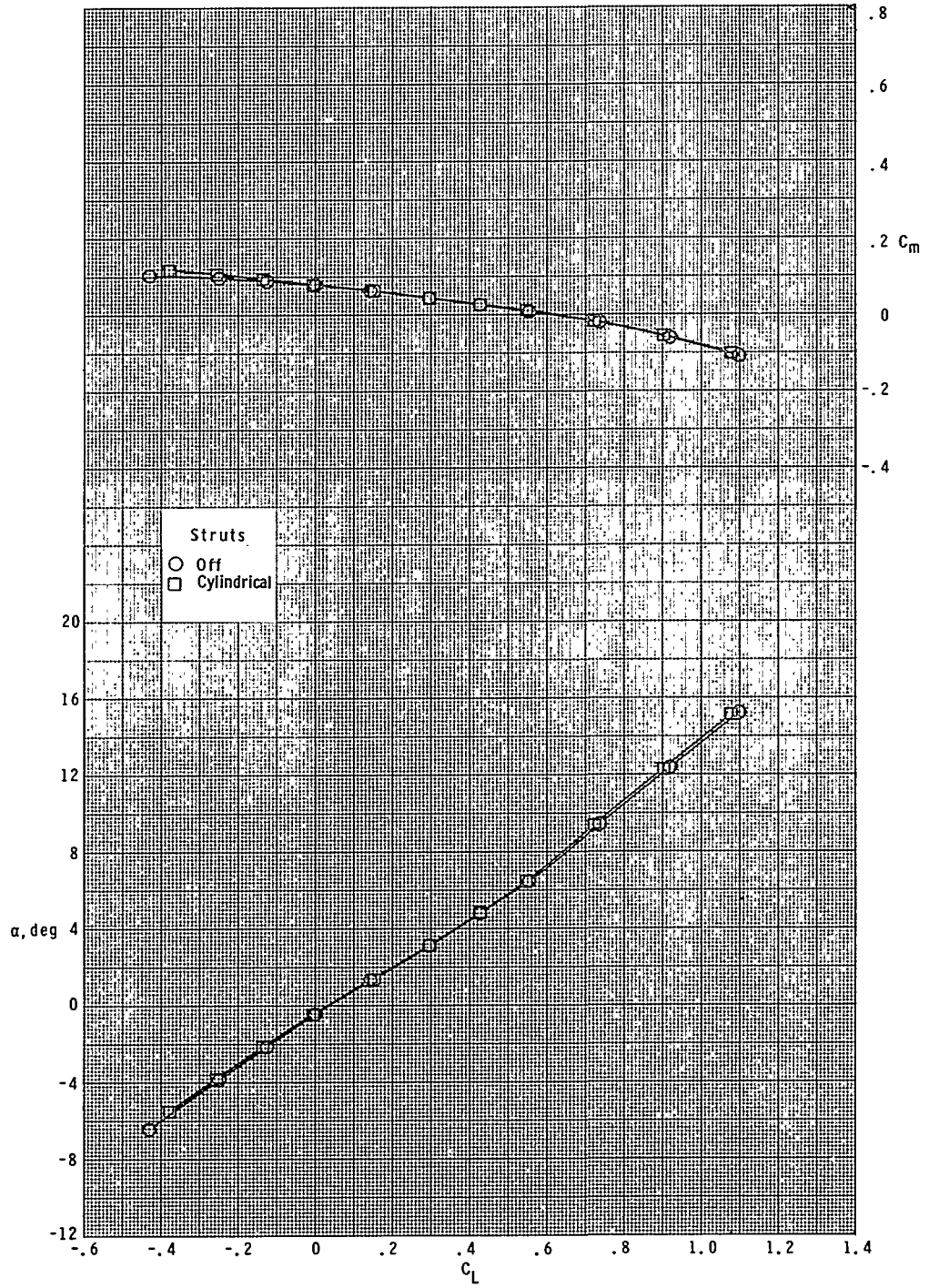Figure 11.- Continued.

(b) Concluded.

Figure 11.- Continued.

(c)   M = 0.90.

Figure 11.- Continued.

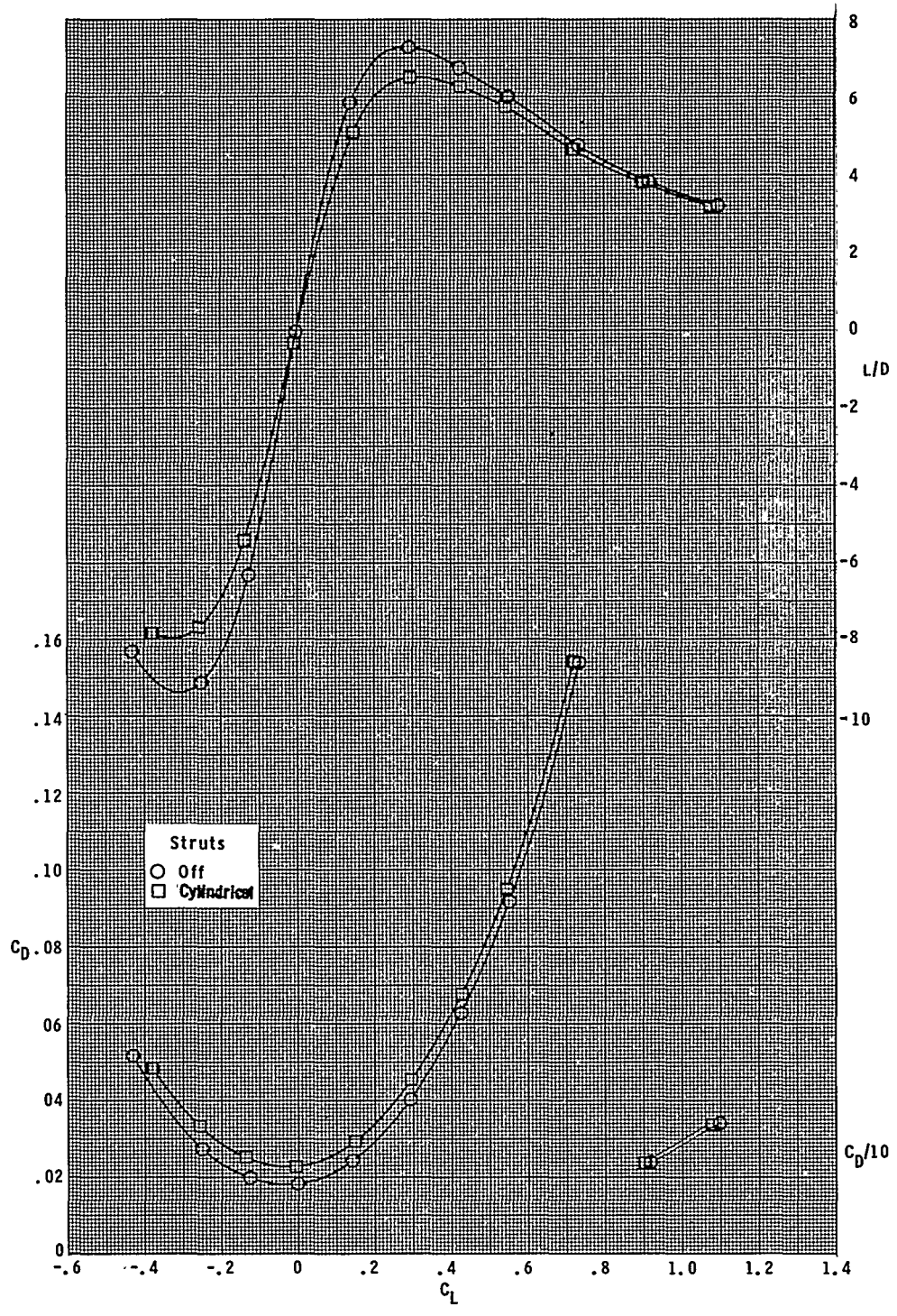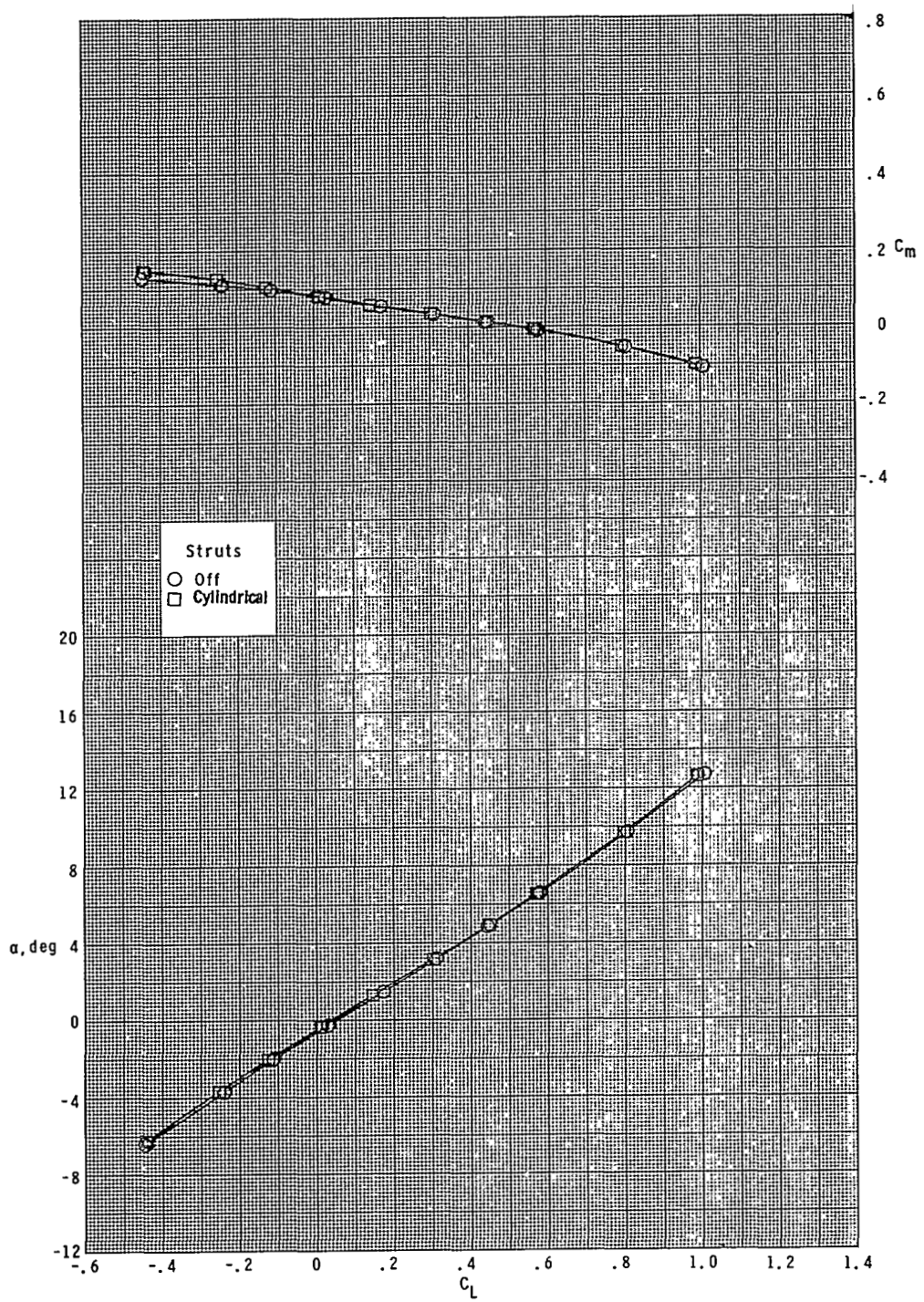(c) Concluded.

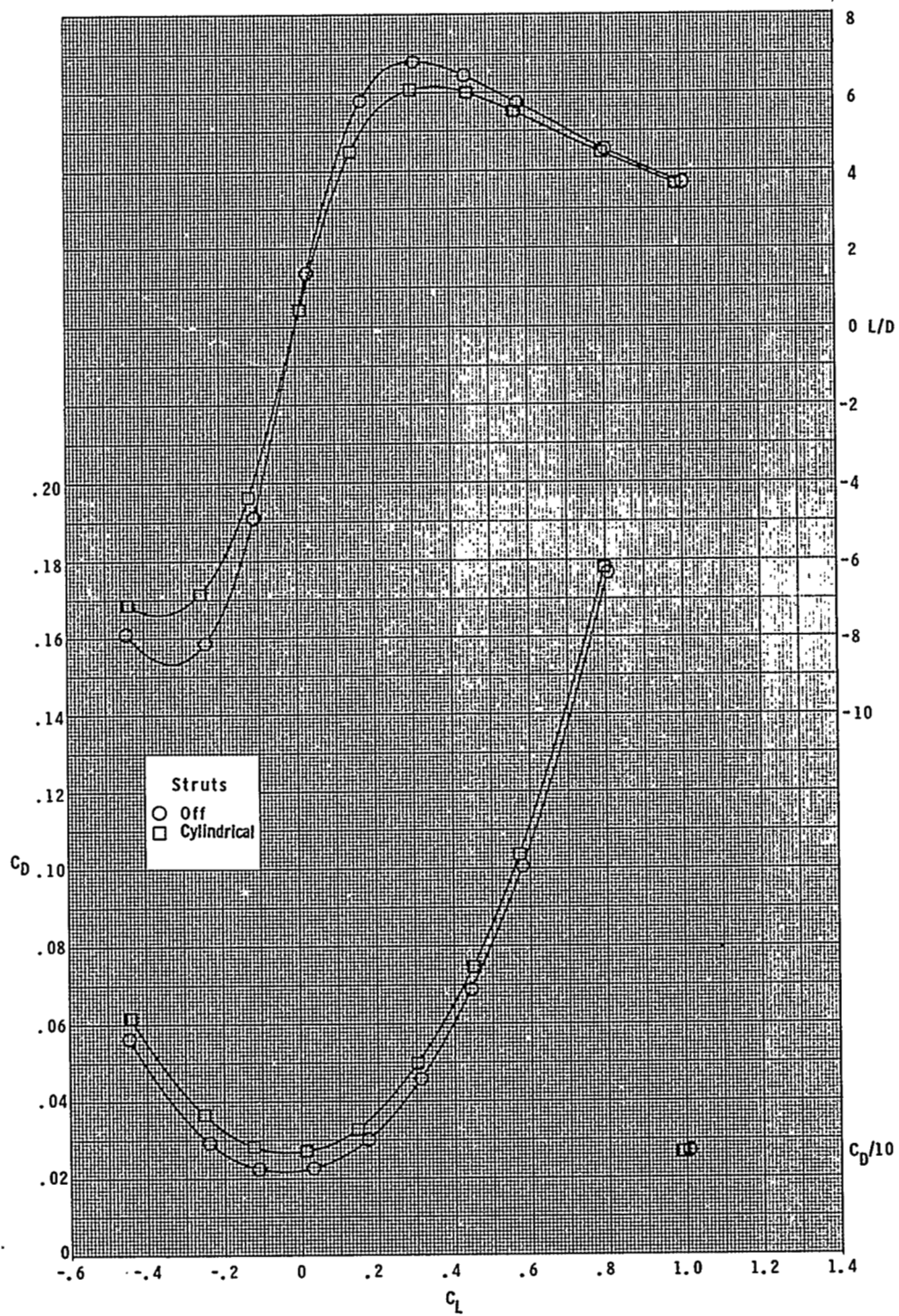Figure 11.- Continued.

(d)   M = 0.95.

Figure 11.- Continued.

(d) Concluded.

Figure 11.- Continued.

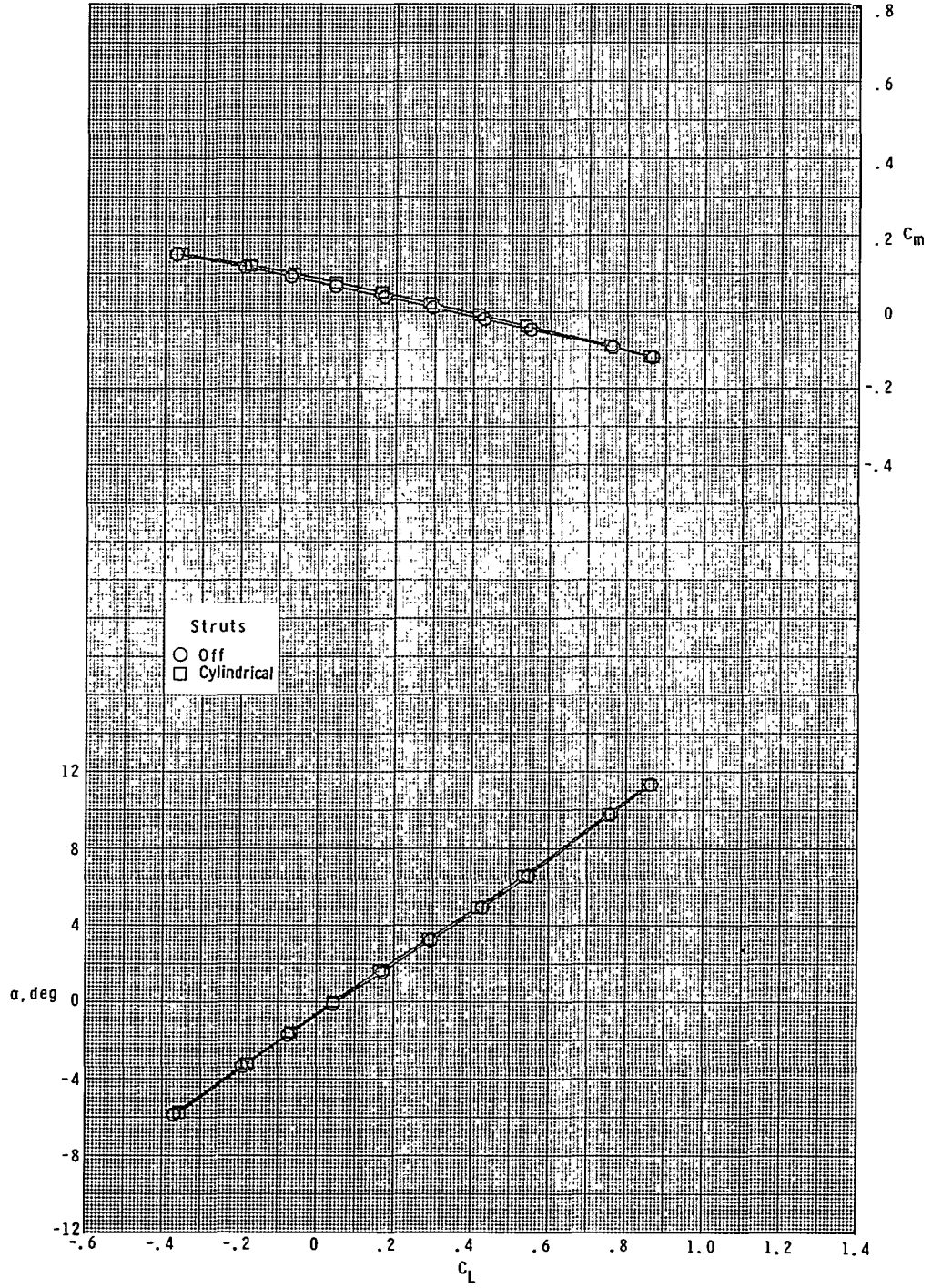(e) M = 0.98.

Figure 11.- Continued.

(e) Concluded.

Figure 11.- Continued.

(f) M = 1.20.

Figure 11.- Continued.

(f) Concluded.

Figure 11.- Continued.

(g)   M = 1.60.

Figure 11.- Continued.

(g) Concluded.

Figure 11.- Continued.

(h)   M = 2.00.

Figure 11.- Continued.

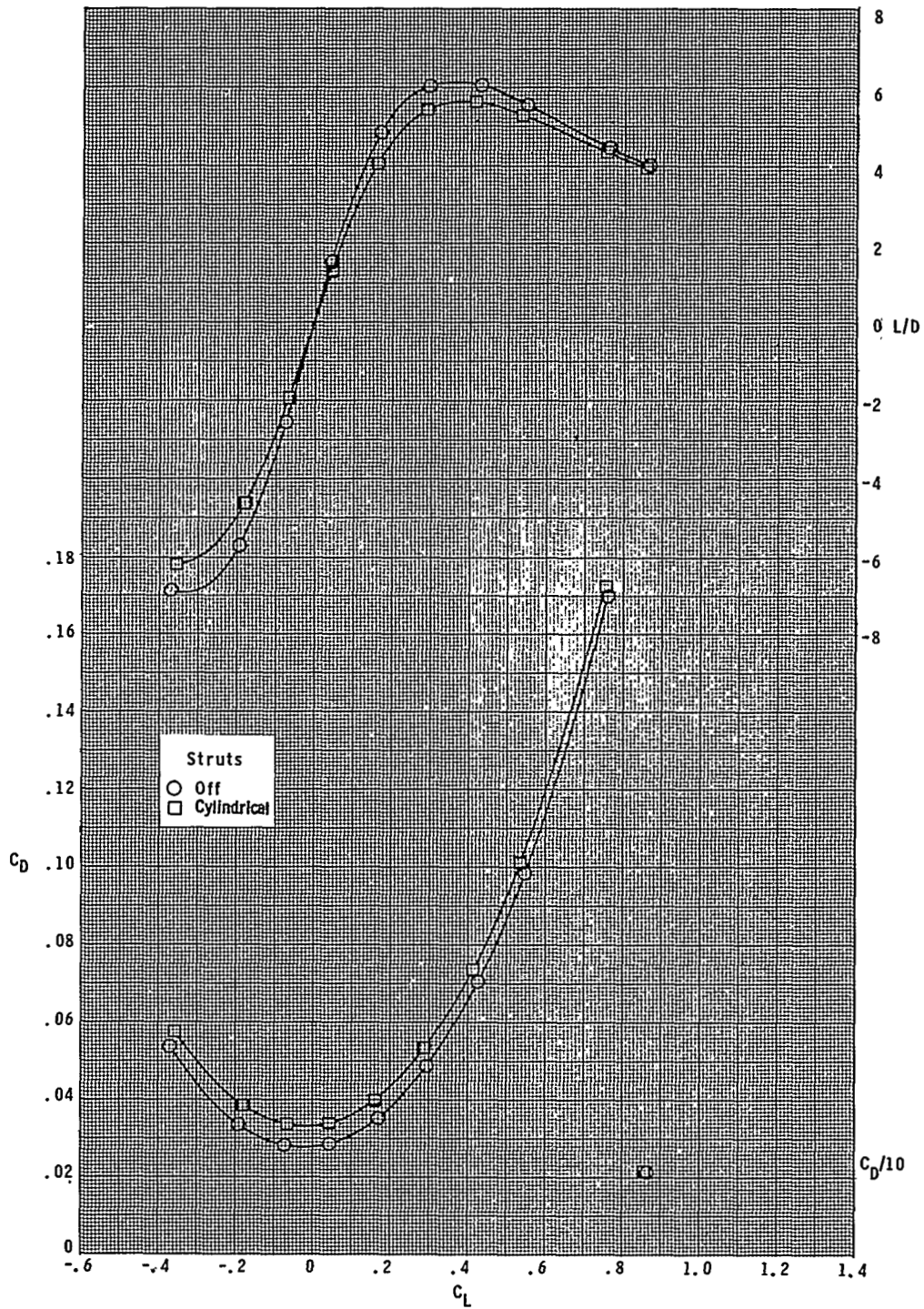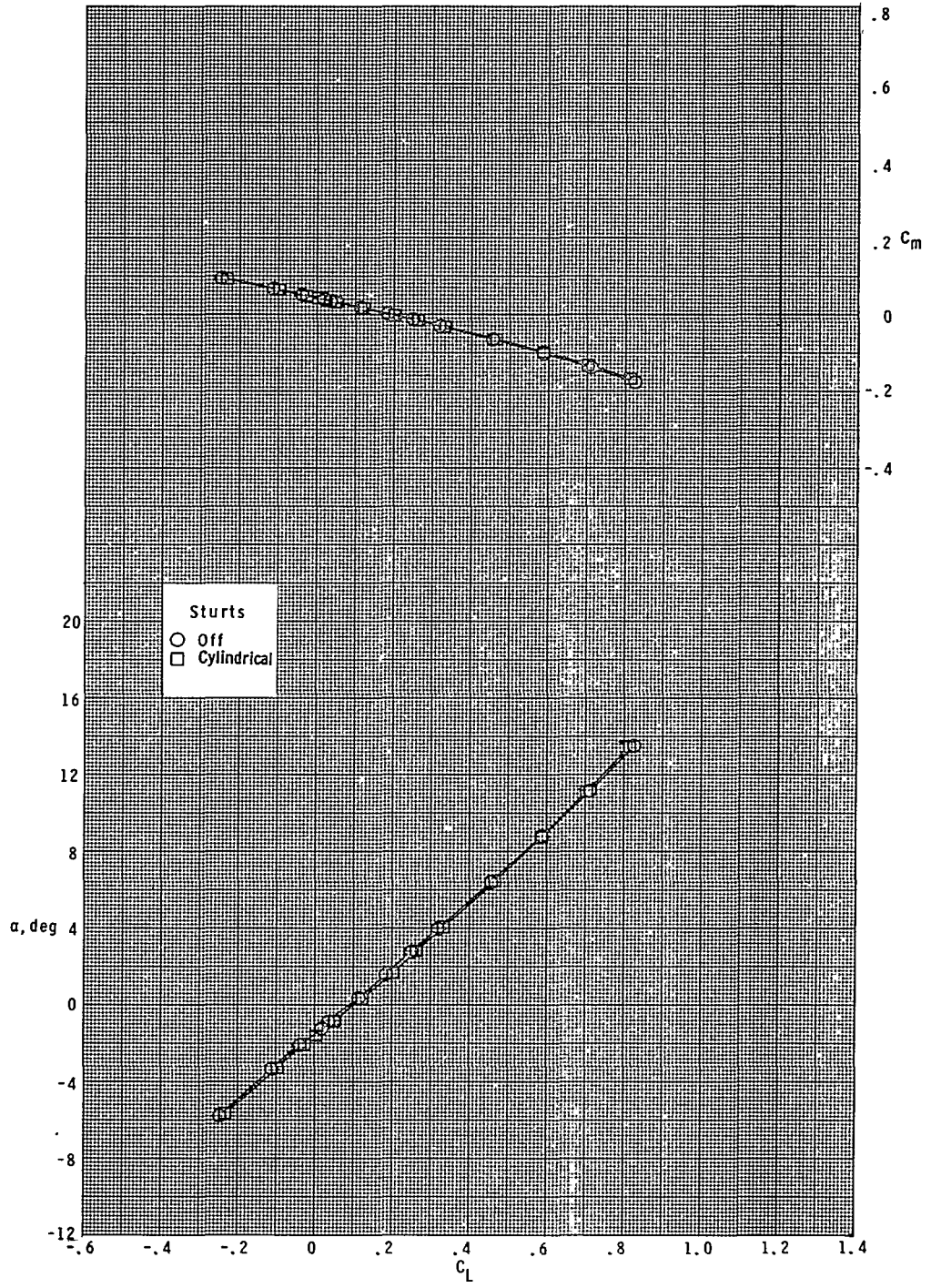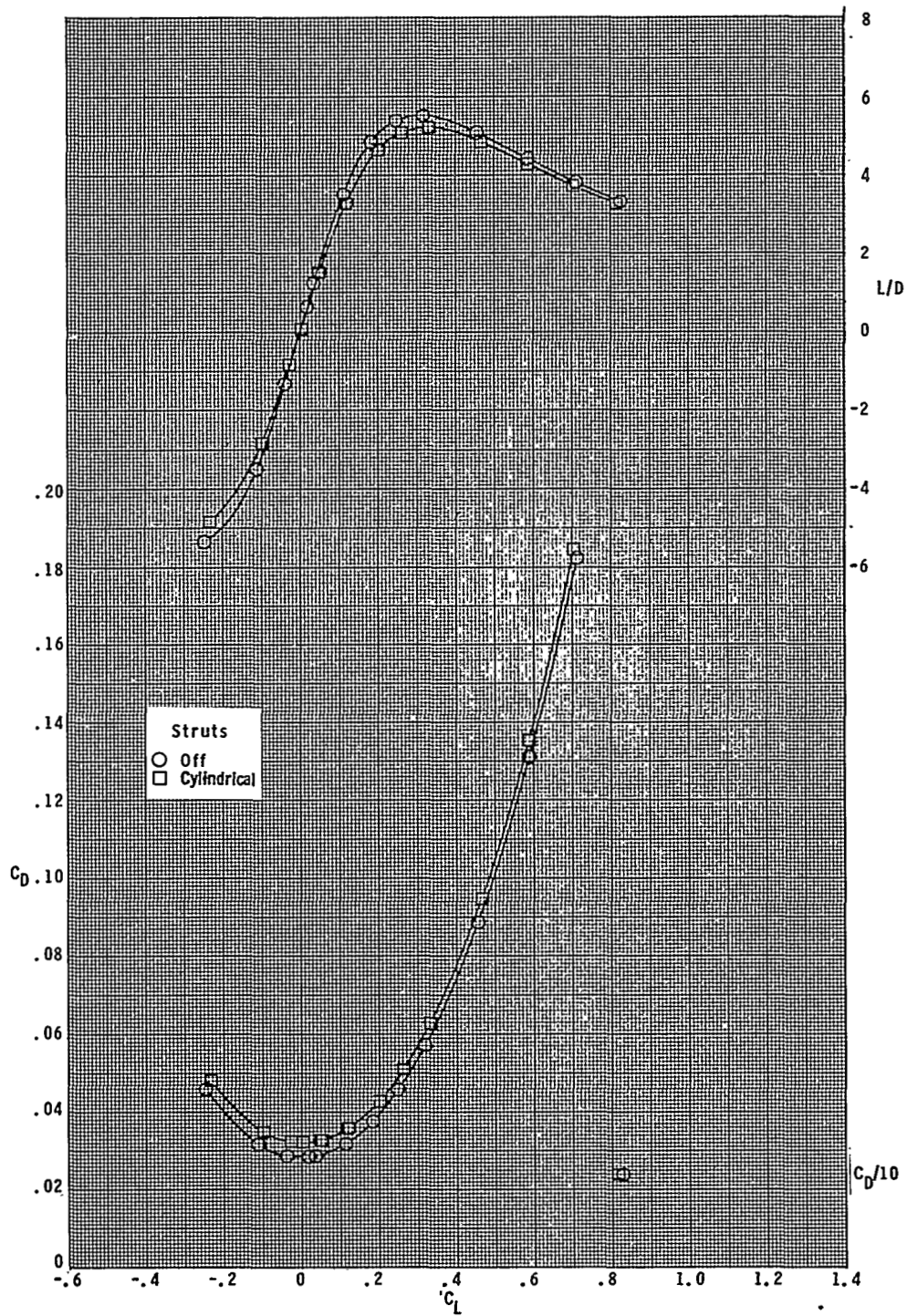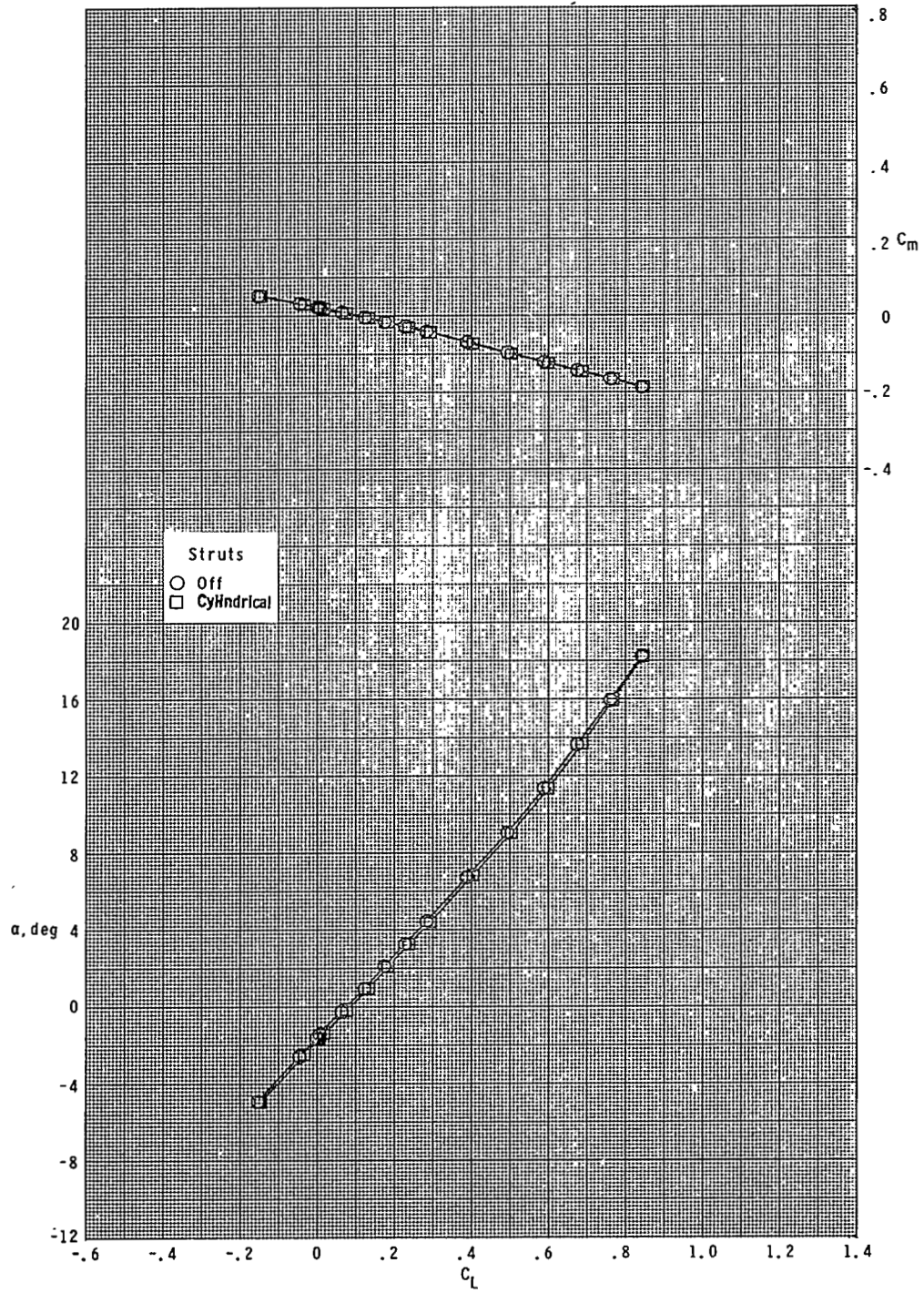(h) Concluded.

Figure 11.- Continued.
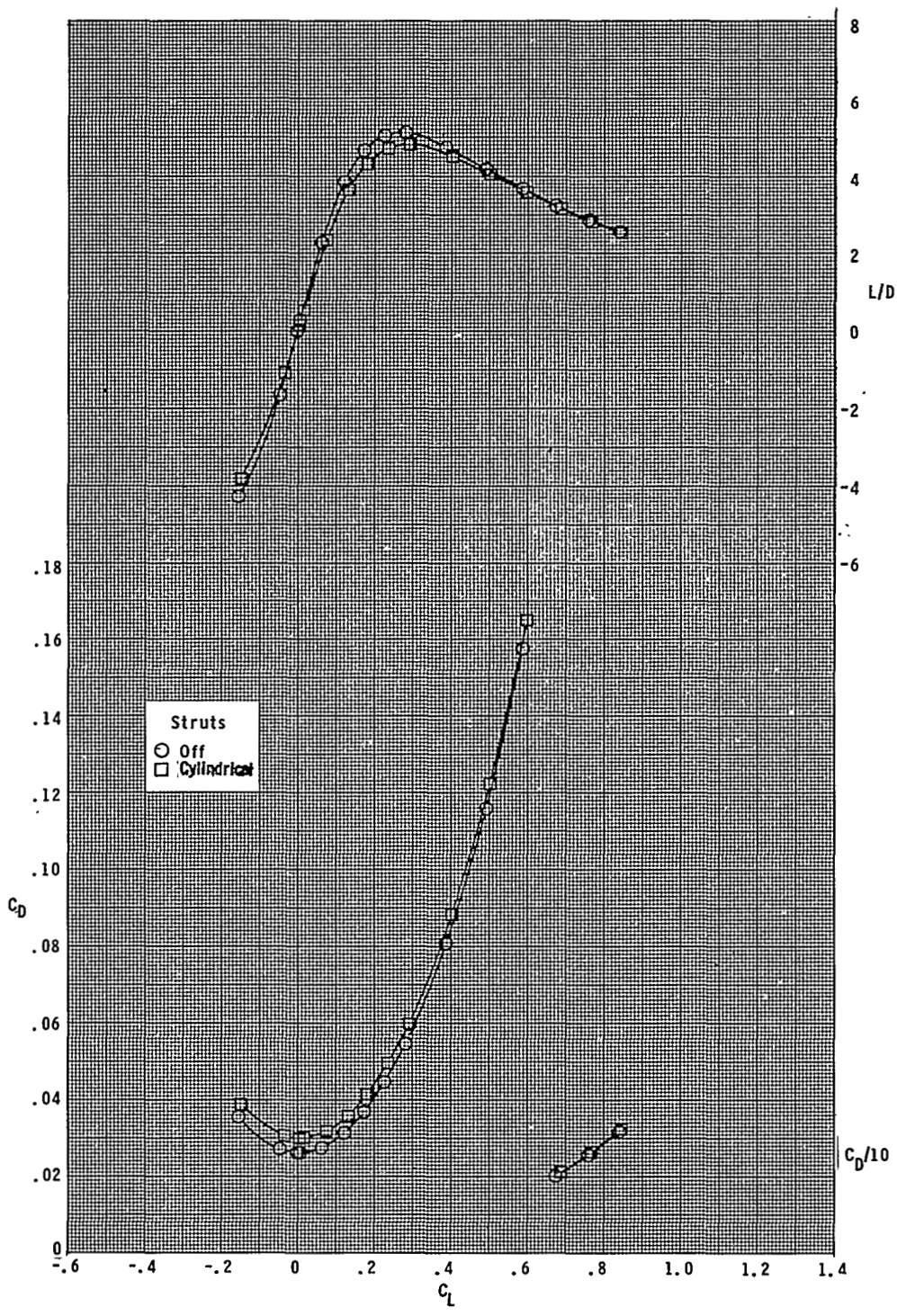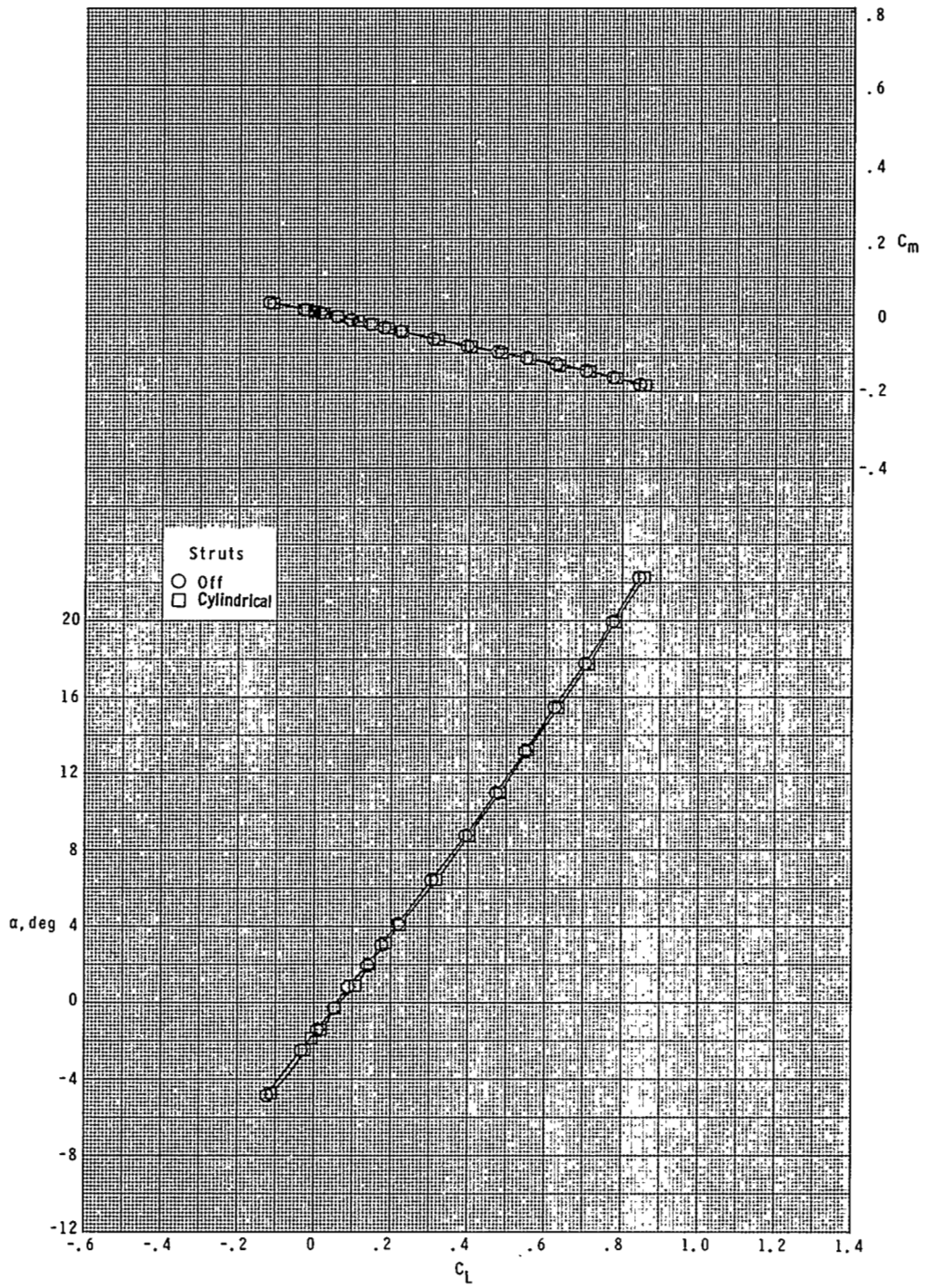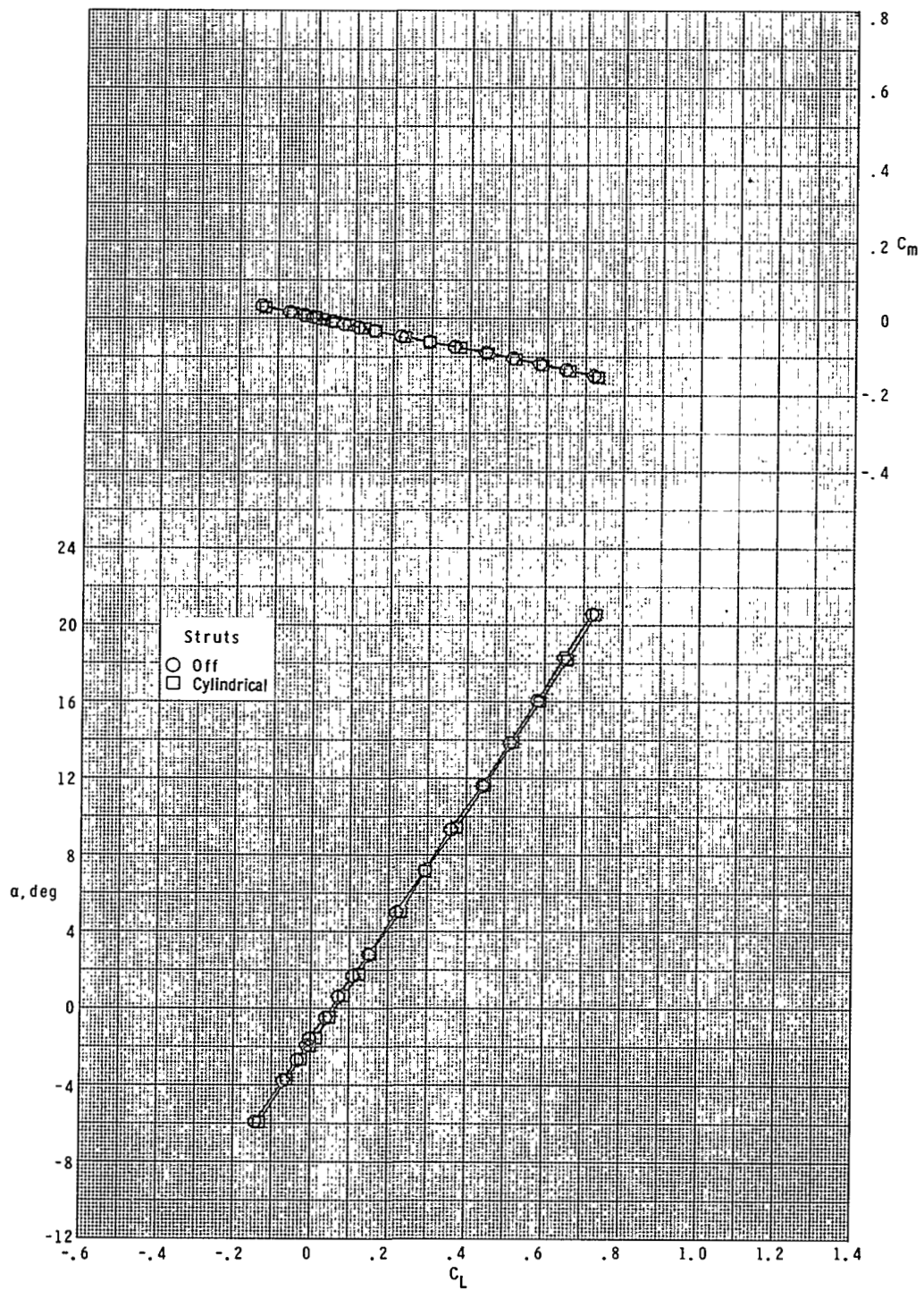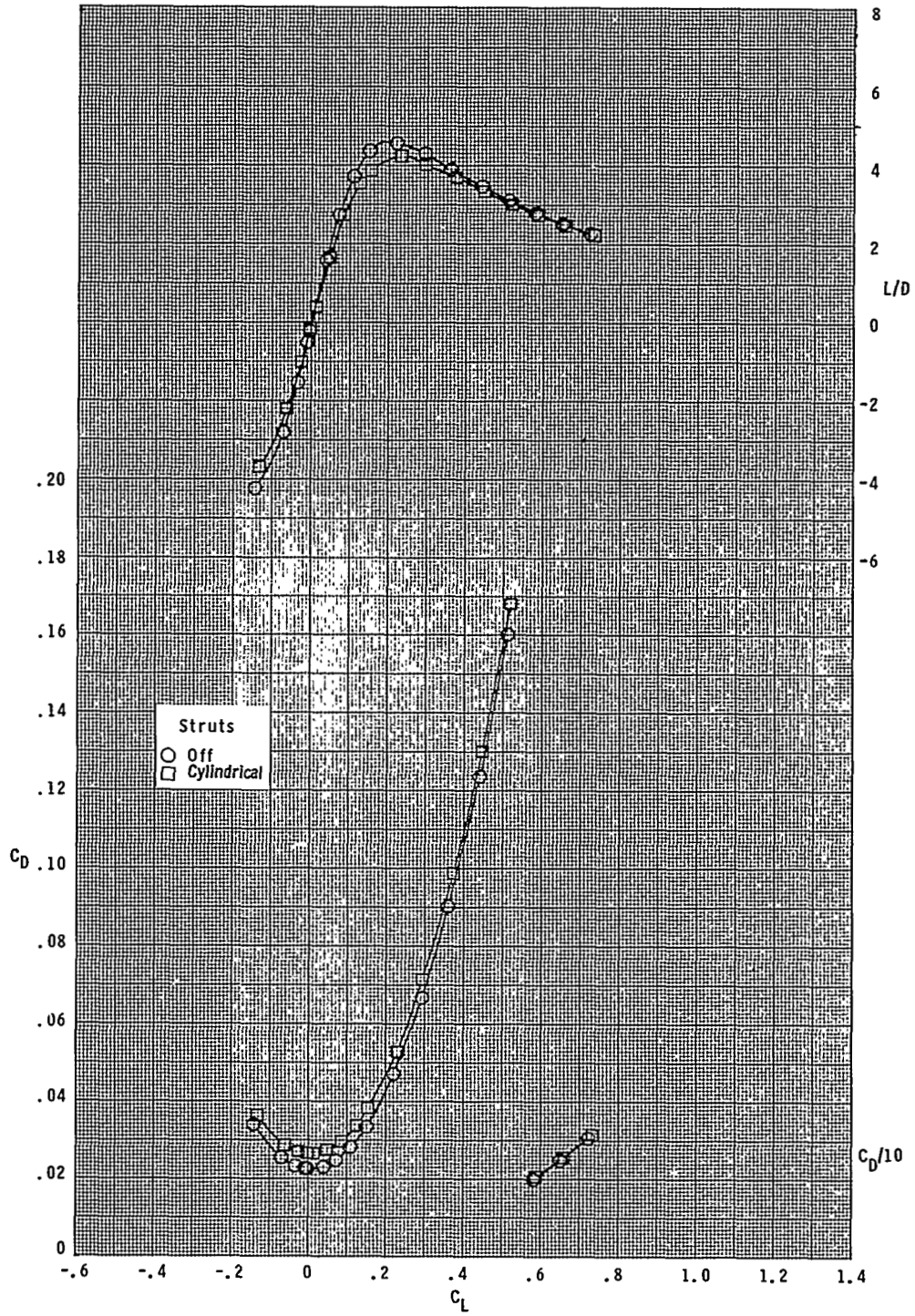
(i) M = 2.50.

Figure 11.- Continued.
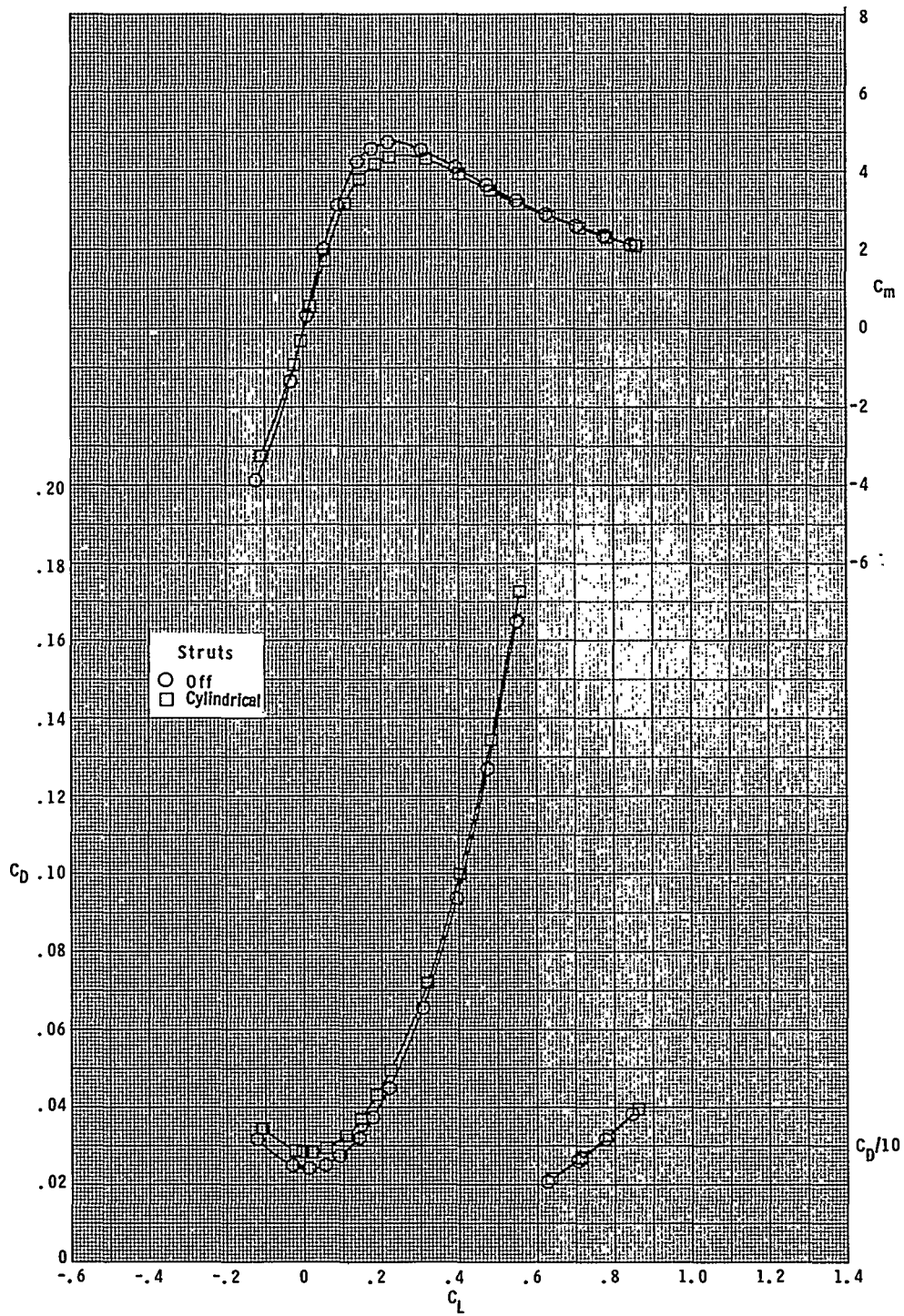
(i) Concluded.

Figure 11.- Continued.

(j)   M = 2.86.

Figure 11.- Continued.
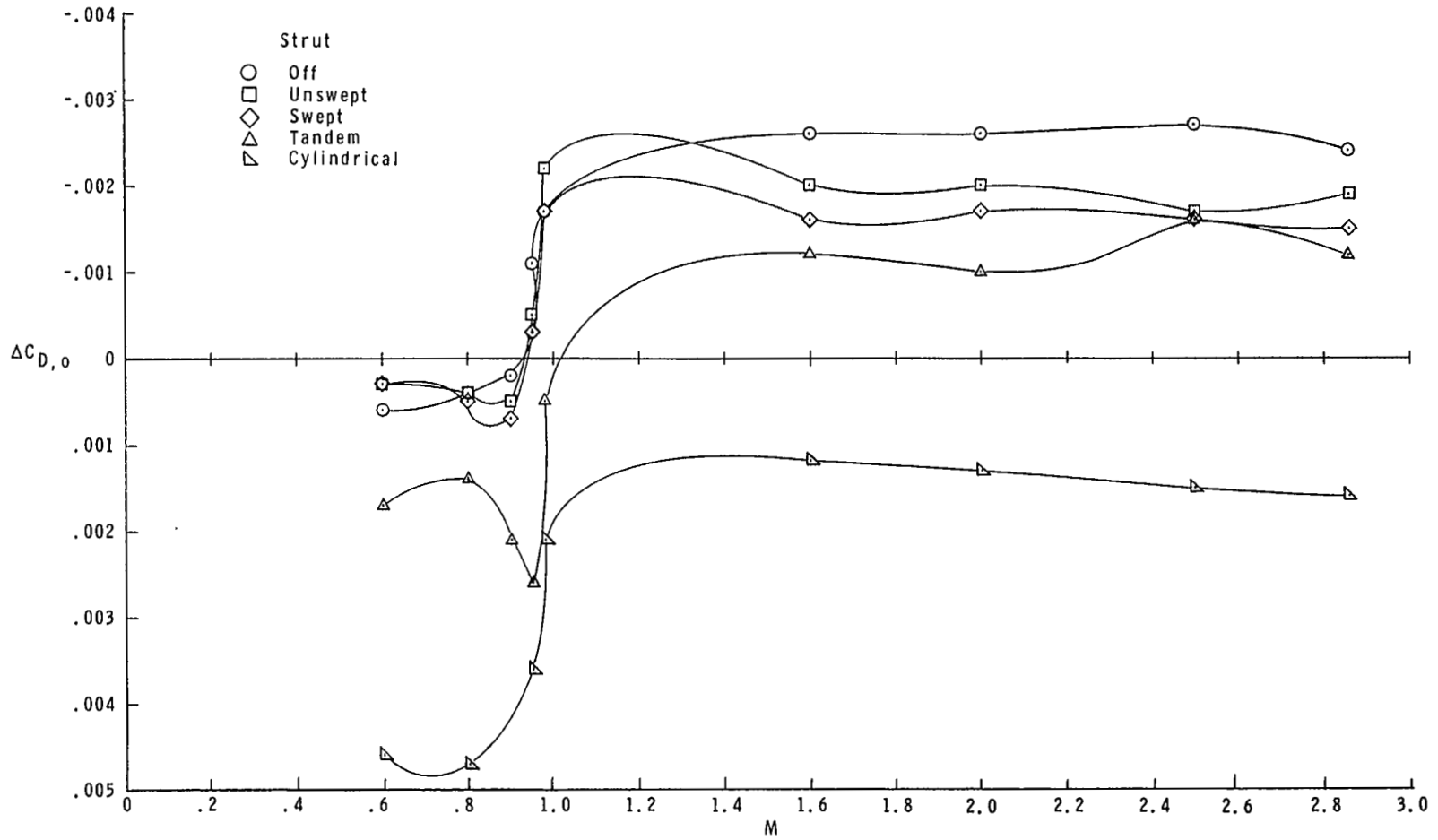
(j) Concluded.

Figure 11.- Concluded.

Figure 12.- Summary of experimental zero-lift drag coefficient increments for strut configurations relative to base-line (thick-wing) configuration.
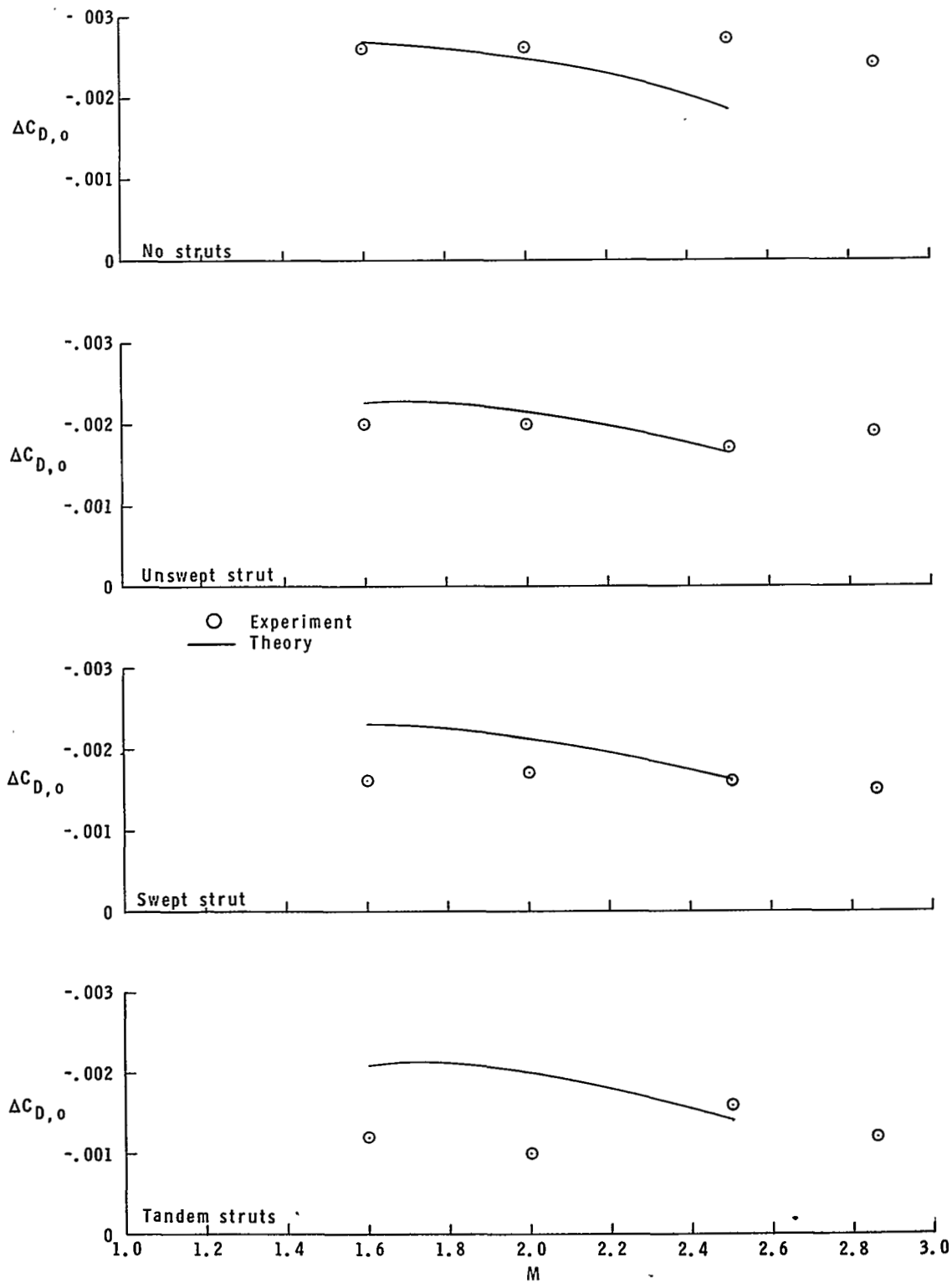
Figure 13.- Comparison of theoretical and experimental incremental drag coefficients.

1. Report No. NASA TP-1102	2. Government Accession No.	3. Recipient's Catalog No.
4. Title and Subtitle LONGITUDINAL AERODYNAMIC CHARACTERISTICS AT MACH 0.60 TO 2.86 OF A FIGHTER CONFIGURATION WITH STRUT BRACED WING		5. Report Date December 1977
		6. Performing Organization Code
7. Author(s) Samuel M. Dollyhigh, William J. Monta, and Giuliana Sangiorgio		8. Performing Organization Report No. L-11801
		10. Work Unit No. 505-11-21-03
9. Performing Organization Name and Address NASA Langley Research Center Hampton, VA 23665		11. Contract or Grant No.
		13. Type of Report and Period Covered Technical Paper
12. Sponsoring Agency Name and Address National Aeronautics and Space Administration Washington, DC 20546		
		14. Sponsoring Agency Code

15. Supplementary Notes

16. Abstract

An investigation has been made in the Mach number range from 0.60 to 2.86 to determine the effects on longitudinal aerodynamic characteristics of utilizing struts to brace the wing to allow the wing thickness to be reduced on the LFAX-8 fighter configuration. Structural and load analysis indicated that the maximum airfoil thickness could be reduced from 4.5 to 3.1 percent with the strut brace concept. Wave drag theory indicated that reducing the wing maximum thickness on the LFAX-8 from 4.5 percent to 3.1 percent would yield a significant reduction in zero-lift wave drag of about 28 percent at the design Mach number of 1.60. Three strut arrangements were designed and tested: a single straight strut, a single swept strut, and a set of tandem straight struts. In addition, a wire of approximately the same cross-sectional area replaced the single straight strut on one series of runs. Also, the original LFAX-8 with the 4.5-percent-thick wing was retested to serve as a base line for this investigation.

17. Key Words (Suggested by Author(s)) Struts Wave drag Wind-tunnel tests	18. Distribution Statement Unclassified — Unlimited Subject Category 02

19. Security Classif. (of this report) Unclassified	20. Security Classif. (of this page) Unclassified	21. No. of Pages 147	22. Price* $7.25

NASA-Langley, 1977

National Aeronautics and
Space Administration

Washington, D.C.
20546

Official Business
Penalty for Private Use, $300

THIRD-CLASS BULK RATE

U.S.MAIL

```
  2   1 1U,A,        113077 S00903DS
DEPT OF THE AIR FORCE
AF WEAPONS LABORATORY
ATTN: TECHNICAL LIBRARY (SUL)
KIRTLAND AFB NM 87117
```

NASA